Intercollegiate Faculty
of Biotechnology
University of Gdańsk
and Medical University of Gdańsk

DOCTORAL DISSERTATION

*Beata Agnieszka Kruszewska-Naczk, MSc*

# Genetic basis of bacterial responses to antimicrobial blue light: implications for safety and resistance development

## Genetyczne podstawy odpowiedzi bakterii na przeciwbakteryjne światło niebieskie: implikacje dla bezpieczeństwa i rozwoju oporności

Thesis submitted to the Board of the Discipline of Biotechnology
of the University of Gdańsk in order to be awarded a doctoral degree in the field
of exact and natural sciences in the discipline of biotechnological sciences

**Supervisor:** Dr. hab. Mariusz Grinholc, prof UG
Intercollegiate Faculty of Biotechnology, UG and MUG
Laboratory of Photobiology and Molecular Diagnostics

**Auxiliary supervisor:** Dr. Aleksandra Rapacka-Zdończyk
Intercollegiate Faculty of Biotechnology, UG and MUG
Laboratory of Photobiology and Molecular Diagnostics

GDAŃSK 2026

This work obtained financial support from the following sources:

National Science Centre in Poland:

NCN SONATINA 2020/36/C/NZ7/00061


University of Gdańsk:

UGrants-start 533-BGB0-GS52-24

*Pragnę serdecznie podziękować osobom, które przyczyniły się do powstania tej pracy:*

*Dr Aleksandrze Rapackiej-Zdończyk za bycie wspaniałą promotorką i mentorką na naukowej drodze pełnej wątpliwości i wielu niepowodzeń, ale też wielu wspólnych sukcesów. Dziękuję za wspólną przygodę, zaufanie i przyjęcie mnie pod swoje skrzydła.*

*Prof. UG. dr hab. Mariuszowi Grinholcowi za dzielenie się swoją ogromną wiedzą i doświadczeniem, wsparcie z uczelnianymi formalnościami oraz za profesjonalizm i spokój. Dzięki temu mogłam rozwijać swoją naukową ciekawość i przekazywać swoją wiedzę dalej.*

*Wszystkim pracownikom Zakładu Fotobiologii Diagnostyki Molekularnej, dr hab. Joannie Nakoniecznej prof. UG, dr Magdzie Rybickiej-Misiejko, dr Agnieszce Bernat-Wójtowskiej, dr Annie Wróblewskiej, dr Maciejowi Jaśkiewiczowi za bycie inspiracją na naukowej drodze oraz owocną współpracę i cenne rady.*

*Obecnym i byłym doktorantom ZFIDM: dr Agacie Wożniak-Pawlikowskiej – za życzliwość i troskliwą opiekę podczas realizowania pracowni magisterskiej, dr Patrycji Ogonowskiej, dr Michałowi Pierańskiemu, dr Klaudii Szymczak, mgr Natalii Burzyńskiej-Młotkowskiej, mgr Natalii Pawlik, mgr Dominice Goik za tworzenie fantastycznej atmosfery w laboratorium i na wyjazdach oraz za wszystkie naukowe i nienaukowe dyskusje.*

*Wszystkim pracownikom MWB, dzięki którym realizacja badań nie byłaby możliwa. W szczególności Małgorzacie Świderskiej i Grażynie Achramowicz za pomoc administracyjną i techniczną.*

*Moim Kochanym Rodzicom Małgorzacie i Markowi oraz bratu Arturowi i przyjaciółkom Gosi i Magdzie za wsparcie i nieustanną wiarę we mnie. Dobrze, że jesteście!*

*Podziękowania, których nie da się ubrać w słowa, należą się mojemu mężowi Marcinowi za anielską cierpliwość, za motywowanie mnie w chwilach zwątpienia i za to, że zawsze mogę na nim polegać.*

# Table of contents

# 1. Abstract

Antimicrobial resistance (AMR) represents one of the biggest challenges affecting healthcare, agriculture, and industry. Most infections are nowadays caused by pathogens resistant to first-line antibiotics. Additionally, an increasing number of strains are developing resistance to last-resort antibiotics and are exhibiting tolerance to disinfectants, significantly limiting available treatment options.

One of the most promising antibiotic alternatives to combat these infections is antimicrobial Blue Light (aBL). This strategy is based on the presence of endogenous photosensitizers in bacteria, which are activated by light of a specific wavelength in the blue spectrum. In the presence of oxygen, activated photosensitizers generate reactive oxygen species (ROS), damaging cellular structures and eventually leading to bacterial cell death. The detailed mechanism of aBL action remains poorly elucidated, which impacts the rare application of this method in routine practice. The gap in understanding the genetic basis of bacterial protection against aBL limits the development of safe treatment protocols that minimize the risk of resistance or other adaptations to aBL.

This study aims to identify genes involved in the bacterial response to aBL, to evaluate the risk of aBL resistance developing, and to assess the implications for the safety of this method. This doctoral dissertation is based on five publications. The first is a review of the current state of knowledge and identification of its research gaps. The remaining four research articles address the main and specific aims of this study.

The Keio collection of single-gene *Escherichia coli* BW25113 mutants was screened to identify mutants hypersensitive to aBL in comparison to the wild-type strain. Sixty-four mutants were selected, and the functions of deleted genes were identified. These genes are involved in essential cellular processes such as DNA repair, energy production, metabolism regulation, and stress response. To confirm the role of the identified genes in the bacterial response to aBL, complementation of the mutations was performed for several mutants. Complementation of selected knockout mutants restored wild-type aBL susceptibility or rendered mutants even less susceptible to aBL, confirming the protective role of the identified genes against aBL. The expression levels of the selected genes following aBL exposure were additionally

evaluated in the wild-type *E. coli* strain, with a comparative analysis of the effects of two wavelengths, 409 nm and 415 nm. The gene *ihfB* was selected as the reference gene due to its stable expression post-aBL exposure. Quantitative PCR (qPCR) analysis revealed significantly elevated expression levels in irradiated samples relative to non-irradiated controls for five of the seventeen genes examined: *dacA, fabH, rbfA, umuD*, and *yihE*, across both wavelengths. Additionally, the genes *purA* and *rfaC* demonstrated increased expression exclusively at 409 nm. Analysis results indicate that not all aBL protective gene products are engaged in the aBL response simultaneously, and this depends on irradiation parameters such as aBL wavelength and dose. Next, all mutants were exposed to aBL-generated single stressors, and their growth defects were assessed to evaluate the role of protective genes in response to a specific stress condition. Most of the mutants were sensitive to hydroxyl radicals (•OH) and oxygen radicals ($O^{2-}$), suggesting that most of the identified genes protect bacteria against these aBL-generated stressors. Notably, no correlation was observed between sensitivity to aBL and to aBL-generated single stressors. This emphasizes that the antibacterial mode of aBL's action is the effect of the combined action of stressors rather than the effect of a single one.

The last publications present findings regarding the safety implications of aBL application in the food industry, utilizing *E. coli* as a representative foodborne pathogen. A phenotypically stable tolerance to heat and aBL has developed. Importantly, the antibiotic susceptibility of both tolerant populations remained unaffected. The potential for cross-stress tolerance development between these two treatments was thoroughly evaluated. The analysis demonstrated that bacterial populations tolerant to aBL exhibited increased heat tolerance, whereas the susceptibility of heat-tolerant populations to aBL did not significantly change. Additionally, short-term and long-term heat preexposure diminished the aBL susceptibility of the tested strain. Eleven genes potentially involved in cross-stress adaptation were identified, and a potential mechanism was proposed.

All sixty-four identified genes could potentially contribute to resistance development. However, no specific genes have been identified whose knockouts confer definitive resistance to aBL, supporting its safety as an alternative to antibiotics.

Nevertheless, ongoing monitoring of all sixty-four aBL-protective genes is essential to detect any signs of adaptation. Additionally, potential risks should be carefully assessed when developing suitable aBL treatment protocols.

# 2. Streszczenie

Oporność mikroorganizmów na antybiotyki stanowi jedno z największych wyzwań dla sektorów opieki zdrowotnej, rolnictwa oraz przemysłu. Większość infekcji wywoływana jest przez patogeny oporne na antybiotyki pierwszego wyboru. Rosnąca liczba szczepów rozwija oporność na antybiotyki tzw. ostatniej szansy oraz staje się tolerancyjna na środki dezynfekcyjne, co ogranicza dostępne opcje leczenia. Jedną z najbardziej obiecujących alternatyw w zwalczaniu tych infekcji jest przeciwdrobnoustrojowe światło niebieskie (ang. *antimicrobial Blue Light* – aBL). Strategia ta opiera się na obecności w komórkach bakteryjnych endogennych fotosensybilizatorów, które są aktywowane przez światło o określonej długości fali w spektrum światła niebieskiego. W obecności tlenu aktywowane fotosensybilizatory generują reaktywne formy tlenu (RFT, ang. *reactive oxygen species* – ROS), uszkadzając struktury komórkowe i ostatecznie prowadząc do śmierci komórek bakteryjnych. Szczegółowy mechanizm działania aBL wciąż pozostaje słabo poznany, co wpływa na rzadsze zastosowanie tej metody w rutynowej praktyce klinicznej. Brak pełnego zrozumienia podstaw genetycznych odpowiedzi bakterii na aBL ogranicza możliwość opracowania bezpiecznych protokołów terapeutycznych, które minimalizowałyby ryzyko powstania oporności lub innych form adaptacji na tę terapię.

Niniejsza praca doktorska miała na celu identyfikację genów zaangażowanych w odpowiedź bakterii na aBL, ocenę ryzyka potencjalnego rozwoju oporności na aBL oraz analizę jej implikacji dla bezpieczeństwa stosowania tej metody. Praca doktorska opiera się na pięciu publikacjach. Pierwsza z nich stanowi przegląd aktualnego stanu wiedzy oraz identyfikuje luki badawcze, natomiast pozostałe cztery artykuły naukowe odnoszą się do głównych i szczegółowych celów opisanych w niniejszej pracy.

Przeprowadzono badanie przesiewowe z użyciem kolekcji mutantów Keio w pojedynczych genach *Escherichia coli* BW25113 w celu identyfikacji mutantów hiperwrażliwych na aBL w porównaniu z dzikim typem. Wyselekcjonowano sześćdziesiąt cztery mutanty i zidentyfikowano funkcje usuniętych z nich genów. Geny te biorą udział w kluczowych procesach komórkowych, takich jak naprawa DNA, produkcja energii, regulacja metabolizmu oraz odpowiedź na stres. Aby potwierdzić rolę zidentyfikowanych genów w odpowiedzi bakterii na aBL, przeprowadzono

komplementację mutacji dla wybranych mutantów. Komplementacja mutacji skutkowała przywróceniem wrażliwości na aBL do poziomu wrażliwości dzikiego typu lub zmniejszeniem wrażliwości na aBL poniżej tego poziomu, co potwierdza ochronną rolę badanych genów wobec aBL. Dodatkowo sprawdzono poziom ekspresji wybranych genów po ekspozycji na aBL w dzikim typie *E. coli*, porównując dwie różne długości fal światła niebieskiego: 409 nm i 415 nm. Gen *ihfB* wybrano jako referencyjny, ponieważ zachowywał stabilny poziom ekspresji po naświetlaniu. Analiza qPCR wykazała zwiększony poziom ekspresji w próbkach poddanych działaniu aBL w porównaniu z kontrolami nienaświetlanymi dla pięciu spośród siedemnastu badanych genów: *dacA, fabH, rbfA, umuD* i *yihE*, dla obu długości fal. Dodatkowo geny *purA* i *rfaC* wykazały zwiększoną ekspresję wyłącznie przy 409 nm. Wyniki te sugerują, że nie wszystkie produkty genów chroniących przed aBL są zaangażowane w odpowiedź na aBL jednocześnie, a ich udział zależy od parametrów naświetlania, takich jak długość fali i dawka aBL. Następnie wszystkie mutanty zostały poddane działaniu pojedynczych stresorów generowanych przez aBL, a ich defekty wzrostu oceniono w celu wykazania potencjalnej roli ochronnej produktów usuniętych genów w odpowiedzi na określony warunek stresowy. Większość mutantów była najbardziej wrażliwa na rodniki hydroksylowe (•OH) oraz anion ponadtlenkowy ($O^{2-}$), co sugeruje, że większość zidentyfikowanych genów chroni bakterie głównie przed tymi stresorami. Co istotne, nie zaobserwowano korelacji między wrażliwością na aBL a na pojedyncze stresory generowane przez aBL. Podkreśla to, że antybakteryjne działanie aBL wynika z łącznego efektu wielu czynników, a nie pojedynczego stresora.

W ostatniej publikacji przedstawiono wyniki dotyczące bezpieczeństwa stosowania aBL w przemyśle spożywczym z wykorzystaniem *E. coli* jako modelu patogenu przenoszonego przez żywność. Uzyskano populacje z fenotypowo stabilną tolerancją na ciepło i aBL. Co ważne, wrażliwość na antybiotyki obu populacji tolerancyjnych nie uległa zmianom. Przeanalizowano także możliwość rozwoju tolerancji krzyżowej między tymi dwoma metodami inaktywacji drobnoustrojów. Analiza wykazała, że populacje bakteryjne tolerancyjne na aBL wykazują zwiększoną tolerancję na ciepło, ale wrażliwość na aBL u populacji tolerancyjnych na ciepło pozostała bez zmian. Dodatkowo krótkoterminowa i długoterminowa wstępna ekspozycja na ciepło zmniejszała

wrażliwość badanego szczepu na aBL. Zidentyfikowano jedenaście genów potencjalnie zaangażowanych w adaptację krzyżową i zaproponowano jej możliwy mechanizm.

Podsumowując, wszystkie sześćdziesiąt cztery zidentyfikowane geny mogą potencjalnie przyczyniać się do rozwoju oporności. Nie zidentyfikowano jednak żadnych pojedynczych genów, których usunięcie mogłoby powodować oporność na aBL, co sugeruje, że aBL ma wysoki potencjał jako bezpieczna alternatywa dla antybiotyków. Jednakże ważne jest, aby nadal monitorować wszystkie sześćdziesiąt cztery geny zaangażowane w ochronę komórek przed aBL, by móc odpowiednio wcześnie wykryć ewentualne oznaki adaptacji. Aspekt ten powinien być uwzględniony przy tworzeniu odpowiednich protokołów stosowania aBL.

# 3. List of abbreviations

aBL – antimicrobial Blue Light

AMR – antimicrobial resistance

aPDI – antimicrobial Photodynamic Inactivation

aPDT – antimicrobial Photodynamic Therapy

DAEC – diffusely-adherent *E. coli*

EAEC – enteroaggregative *E. coli*

EHEC – enterohemorrhagic *E. coli*

EIEC – enteroinvasive *E. coli*

EPEC – enteropathogenic *E. coli*

ETEC – enterotoxigenic *E. coli*

HSP – heat shock proteins

HSR – heat shock response

LPS – lipopolysaccharide

$MDK_{99.9}$ – the minimal duration of the killing of 99% of the cells

MIC – minimal inhibitory concentration

PACT – Photodynamic antimicrobial chemotherapy

PCA – Principal Component Analysis

qPCR – quantitative Polymerase Chain Reaction

ROS – Reactive Oxygen Species

WHO – World Health Organization

WSS – Within-Cluster Sum of Squares

# 4. Introduction

Antimicrobial resistance (AMR) constitutes a significant and escalating global concern, affecting various sectors such as healthcare, veterinary medicine, agriculture, and food safety. The most recent report by the World Health Organization (WHO) reveals that approximately one in six laboratory-confirmed bacterial infections was caused by pathogens resistant to routinely used antibiotics. Notably, Gram-negative bacteria have been recognized as an increasing threat, with *E. coli* being the predominant pathogen. Many isolates demonstrate resistance to first-choice treatments such as beta-lactams and third-generation cephalosporins. Furthermore, the number of isolates resistant to last-resort therapies is increasing rapidly, thereby limiting available therapeutic options (WHO, 2025). This poses a serious risk, particularly to infants, children, pregnant women, elderly individuals, and immunocompromised patients (DeNegre et al., 2019).

The development of bacterial resistance is a natural evolutionary adaptation; however, the improper use of antibiotics accelerates this process, leading to bacteria becoming resistant to factors to which they are most frequently exposed. The misuse of antibiotics is often caused by inadequate diagnostic procedures. Apart from increasing the fatality rate caused by antimicrobial-resistant (AMR) pathogens, the consequences of AMR are also profoundly impactful on the economy, incurring substantial costs and hindering development, especially in low- and middle-income countries. In simulations conducted by the World Bank, a high level of AMR could lead to global output losses of $6.1 trillion annually by 2050 (World Bank, 2017). Additionally, AMR affects crops and livestock by increasing mortality and morbidity (Anomaly, J. 2020), impacts the environment by reducing microbial diversity (Han et al., 2018), and compromises food safety (Perreten et al., 1997).

Food constitutes one of the pathways by which AMR strains spread in the environment through agriculture and hospital wastewater, subsequently posing a direct risk of transmission to human populations (Founou et al., 2016; Das et al., 2025). Despite the implementation of routine surveillance and the utilization of advanced technological methodologies, the most prevalent sources of AMR bacteria are often food products contaminated during processing or originating from raw products.

Antibiotic-resistant foodborne pathogens such as *Clostridium perfringens, E. coli, Listeria monocytogenes, Campylobacter* sp., and *Salmonella* sp. pose a serious threat to human health due to limited therapeutic options for infections, many of which could be preventable (Moawad et al., 2017; Sołtysiuk et al., 2025; Maćkiw et al., 2020). Particularly, highly virulent *E. coli* pathotypes, including EHEC, ETEC, EPEC, EAEC, EIEC, and DAEC, can cause diarrhea and serve as etiological factors in septicemia, mastitis, peritonitis, and meningitis. Due to the aforementioned reasons, ensuring food safety is of utmost importance (Ekici, G., & Dümen, E., 2019).

AMR is addressed worldwide through the prevention and surveillance of infections, monitoring and controlling antimicrobial use, strengthening and ensuring access to accurate diagnosis, and developing new antibiotics. However, the risk of developing resistance to new antimicrobials remains; that's why safe alternatives to antibiotics are being intensively sought.

The method described in this dissertation was first reported in the early 20th century, prior to the discovery of penicillin in 1928. It was described by Jodlbauer and von Tappeiner in 1904 and by Huber in 1905, based on Raab's observation of the phototoxic effects of light-activated dyes, which led to the inactivation of *Paramecium caudatum* (Fleming, 1929; Wainwright et al., 2017). Only after several decades did photodynamic inactivation become intensively studied and applied in dermatology, blood disinfection, and other areas (Wanwright, 1998), especially at the end of the 'golden antibiotic era' in the 1970s, when AMR phenomena were observed (Aminov, 2010). Photodynamic antimicrobial chemotherapy (PACT), in the current literature known as antimicrobial Photodynamic Therapy (aPDT) and antimicrobial Photodynamic Inactivation (aPDI), is based on three elements: a nontoxic molecule of photosensitizer which accumulates in bacteria, light from the visible spectrum, and molecular oxygen present in bacterial cells (Wanwright, 1998).

A specific type of aPDI is antimicrobial Blue Light (aBL), in which the applied light spectrum lies between 405 and 490 nm. Furthermore, aBL does not necessitate the administration of an external photosensitizer, thereby reducing the overall duration of bacterial inactivation and reducing therapeutic costs. This benefit is attributable to the presence of endogenous photosensitizers in bacteria, such as porphyrins and flavins, as

well as other light-activated chromophores that exhibit absorption peaks in the blue spectral range (Ashkenazi et al., 2003; Hamblin et al., 2005).

Its antimicrobial effect is based on the toxic properties of reactive oxygen species (ROS) generated through the photoreaction of photosensitizer molecules with oxygen, which are activated by light of a specific wavelength. Bacterial cells exposed to high oxidative stress accumulate damage, which, in consequence, leads to cellular death (Cieplik et al., 2018). To date, membrane disruption, DNA damage, lipid oxidation, damage to the glucose uptake system, efflux pump dysfunction, and protein degradation have been reported (Grinholc et al, 2015; Kim & Yuk, 2017; Leanse et al., 2022; Dos Anjos et al., 2023). Interestingly, aBL also induces metabolic reprogramming and oxidative stress response pathways depending on the species and strain-specific ROS profiles (Cong et al., 2025).

A major advantage of aBL is its high specificity for killing bacterial cells, due to higher porphyrin levels in bacteria than in mammalian cells (Leanse et al., 2022). aBL is a broad-spectrum antimicrobial effective against many bacterial species, especially those with high cellular porphyrin levels (Wang et al., 2017). The next significant advantage that makes aBL a promising tool in infection control is its low risk of resistance development due to its multitarget mode of action and its lower mutagenic effect compared with UV (Dai et al., 2013; Wang et al., 2017). To date, no resistance to aBL has been observed; however, phenomena such as tolerance and other adaptation strategies have been reported for both Gram-negative and Gram-positive bacterial species. Notably, bacterial populations exhibiting tolerance to specific factors could still be eradicated through increased dosages or prolonged exposure to these factors (Rapacka-Zdonczyk et al., 2019; 2021; Pieranski et al., 2020; Nikinmaa, 2020). Moreover, a high level of efficacy in reducing bacterial counts has also been reported for strains resistant to antibiotics (Ma et al., 2018; dos Anjos et al., 2020).

This context emphasizes the critical significance of studies such as this one, which focus on elucidating the genetic background of bacterial responses to aBL to evaluate its safety and the potential risk of resistance development, thereby facilitating the broader application of this undervalued method.

# 5. Hypothesis and aims of the work

**Hypothesis:**

Bacterial response to aBL is a complex process mediated by multiple genes involved in DNA repair, oxidative stress response, and cell envelope maintenance. These genes determine bacterial susceptibility to aBL and may influence the potential risk of resistance development.

Therefore, **the main aim** of this doctoral dissertation was to **identify genes required for the bacterial response to aBL and to characterize their roles in cellular protection mechanisms and implications for potential resistance development.**

**Specific aims** were also formulated:

1. Identification of genes required for the aBL response in *E. coli* by screening the Keio single-gene mutant collection and selecting aBL-hypersensitive mutants.
2. Evaluation of the role of aBL protective genes in response to aBL-generated single stressors by determining growth defects in mutants lacking these genes when exposed to specific stress conditions.
3. Determination of changes in expression levels of selected genes after aBL exposure using qPCR analysis.
4. Assessment of which genes can be involved in the potential risk of aBL resistance development in *E. coli.*
5. Evaluation of the potential risk of aBL and heat cross-tolerance development in food safety applications.

# 6. Overview of publications

This doctoral dissertation is founded upon five previously published, peer-reviewed articles listed below:

Publication no. 1. Kruszewska-Naczk, B., Burzyńska, N., Goik, D., Grinholc, M., Nakonieczna, J., Pawlik, N., Pierański, M. K., Woźniak-Pawlikowska, A., Rapacka-Zdończyk, A. & Dai, T. (2026). Mechanisms and determinants of bacterial susceptibility to antimicrobial Blue Light: from chromophores to transcriptomes. *Drug Resistance Updates*, 101391. doi.org/10.1016/j.drup.2026.101391

Publication no. 2. Kruszewska-Naczk, B., Grinholc, M., Waleron, K., Bandow, J. E., & Rapacka-Zdończyk, A. (2024). Can antimicrobial blue light contribute to resistance development? Genome-wide analysis revealed aBL-protective genes in *Escherichia coli*. *Microbiology spectrum*, *12*(1), e02490-23. doi.org/10.1128/spectrum.02490-23

Publication no. 3. Kruszewska-Naczk, B., Grinholc, M., & Rapacka-Zdonczyk, A. (2024). Mimicking the Effects of Antimicrobial Blue Light: Exploring Single Stressors and Their Impact on Microbial Growth. *Antioxidants*, *13*(12), 1583. doi.org/10.3390/antiox13121583

Publication no. 4. Kruszewska-Naczk, B., Grinholc, M., & Rapacka-Zdonczyk, A. (2025). Identification and validation of reference genes for quantitative gene expression analysis under 409 and 415 nm antimicrobial blue light treatment. *Frontiers in Molecular Biosciences*, *11*, 1467726. doi: 10.3389/fmolb.2024.1467726

Publication no. 5. Kruszewska-Naczk, B., Pikulik-Arif, P., Grinholc, M., & Rapacka-Zdonczyk, A. (2024). Antibacterial blue light is a promising tool for inactivating *Escherichia coli* in the food sector due to its low risk of cross-stress tolerance. *Chemical and Biological Technologies in Agriculture*, *11*(1), 126. doi.org/10.1186/s40538-024-00658-x

Publication no. 1 is a review article on the current state of knowledge regarding the mechanisms of aBL action and the factors influencing aBL susceptibility, highlighting research gaps and establishing the theoretical foundation for the experimental studies in this dissertation. The theoretical introduction of the dissertation expands upon the information presented in Publication 1.

Publications no. 2–5 present the results of studies conducted as part of the dissertation and address the research objectives and the main and specific aims defined therein. Publication no. 2 constitutes the core of the dissertation and presents key research aimed at identifying the genetic basis of bacterial response mechanisms to aBL (aim 1). The studies described in Publication no. 3 examine the effects of individual stressors on the growth of aBL hypersensitive *E. coli* mutants (aim 2). Publication no. 4 presents the results of validation studies on the expression of selected genes following exposure to aBL, as well as on the establishment of a reference gene with a stable expression level after irradiation (aim 3). Publication no. 5 investigates one of the practical applications of aBL in food production and evaluates its safety by assessing potential resistance and tolerance development, as well as cross-stress adaptation between aBL and heat as food disinfection methods (aim 5). Moreover, publications no. 2-5 assess potential gene candidates for aBL resistance development (aim 4).

The full texts of all publications with supplementary materials are attached at the end of the dissertation.

# 6.1. Publication no. 1.

Kruszewska-Naczk, B., Burzyńska, N., Goik, D., Grinholc, M., Nakonieczna, J., Pawlik, N., Pierański, M. K., Woźniak-Pawlikowska, A., Rapacka-Zdończyk, A. & Dai, T. (2026). Mechanisms and determinants of bacterial susceptibility to antimicrobial Blue Light: from chromophores to transcriptomes. *Drug Resistance Updates*, 101391.

This review article synthesizes research on aBL published up to February 2026 in the PubMed, Scopus, and Web of Science databases, incorporating contemporary understanding of its mechanistic aspects and providing comprehensive coverage of both historical and recent contributions in this domain.

The review summarizes evidence on endogenous porphyrins (including coproporphyrins, protoporphyrins, and uroporphyrins), flavines, staphyloxanthin, granadaene, and other pigments activated by aBL. The cellular levels of these compounds determine the effectiveness of aBL and strain-dependent susceptibility. It highlights bacterial species that do not produce porphyrins, flavins, or other compounds that can act as endogenous porphyrins, a point discussed in particular for the *genera Streptococcus and Enterococcus*. Also, describe the multiple molecular targets of ROS generated by aBL (singlet oxygen $^1O_2$, superoxide anions $O_2^-$, hydrogen peroxide $H_2O_2$, and hydroxyl radicals •OH): such as DNA, proteins, lipids and membranes, metabolic pathways, and efflux pumps, highlighting the complex mode of action of this antimicrobial approach. It was reported that aBL causes a series of cellular damages that eventually lead to cellular death: lipid peroxidation, membrane disruption, ion leakage, reduction of transmembrane potential, genetic instability, oxidative DNA lesions, disruption of replication or transcription and translation, protein oxidation and carbonylation, enzymatic failure, and accumulation of protein aggregates.

Furthermore, the genetic determinants influencing cellular responses to aBL are discussed, including genes involved in porphyrin biosynthesis, cell exterior structures, regulation mechanisms, as well as components of the SOS response, DNA repair, and oxidative stress response genes. Transcriptomic analyses have also revealed changes in gene expression profiles related to stress responses. Notably, transcriptomic

modifications induced by aBL extend beyond conventional stress response pathways. This review emphasizes significant transcriptomic shifts under aBL stress, concentrating on five principal adaptive mechanisms: the suppression of motility as an energy-conserving measure; metabolic reprogramming through the upregulation of ATP-producing pathways and the downregulation of non-essential processes; remodeling of the membrane and cell envelope, including efflux mechanisms and the modulation of membrane permeability; regulation of metal ions via upregulation of ion metabolism genes; and modulation of virulence, which may potentially attenuate pathogenicity.

Furthermore, additional bacterial determinants, including virulence factors, biofilm formation, and antibiotic resistance profiles, can modulate bacterial sensitivity to aBL and impact inactivation kinetics. Importantly, the aBL response is also species and strain-specific, with limited variability within species and broader variability among genera. Environmental and physiological factors are also important: inoculum density limiting light penetration; temperature impacting the rate of bacterial metabolism; medium with iron content and oxygen availability, medium pH; light source; aBL wavelength and irradiance. It was reported that the most effective aBL wavelength for killing bacteria is 405 nm, which corresponds to the absorption spectrum of porphyrins and the highest rate of ROS production. Generally, bacteria in the growth phase, with elevated metabolic activity, are more susceptible to aBL, whereas those in the stationary phase, characterized by reduced metabolic activity, are less susceptible.

In summary, the review underscores that the efficacy of aBL is influenced by complex interactions among cellular chromophore availability, the bacterial genetic background, the cell's physiological state, and other external conditions. Research indicates that optimizing these conditions can significantly improve the efficacy of aBL while reducing potential cytotoxic effects. The review outlines the key gaps and factors that determine bacterial susceptibility to aBL, as well as areas that still require investigation. Optimizing clinical and industrial procedures and developing portable, cost-effective devices for therapeutic and environmental disinfection applications are paramount to achieving the safest and most effective protocols. Furthermore, comprehensive long-term safety evaluations are essential for assessing the effects of repeated aBL exposure. More clinical investigations using standardized protocols for

irradiation parameters are needed to support the routine use of aBL. To fully realize the potential of aBL as an antimicrobial strategy to combat antimicrobial-resistant infections, interdisciplinary efforts encompassing microbiology, photophysics, and clinical practice are necessary.

# 6.2. Publication no. 2.

Kruszewska-Naczk, B., Grinholc, M., Waleron, K., Bandow, J. E., & Rapacka-Zdończyk, A. (2024). Can antimicrobial blue light contribute to resistance development? Genome-wide analysis revealed aBL-protective genes in *Escherichia coli.* *Microbiology spectrum*, *12*(1), e02490-23.

It was the first study analyzing the genome-wide mutant response to aBL in the context of potential resistance or tolerance development. The main aim of this investigation was to describe the genetic background of the response of *E. coli* to aBL by identifying the genes required for bacterial protection against aBL. To achieve this goal, the Keio knockout collection of *E. coli* was screened to identify aBL-hypersensitive mutants. The Keio collection comprises 3,985 well-described single-gene knockout mutants of non-essential genes in the *E. coli* BW25113 strain background and is often used for genome-wide analysis of bacterial responses to various stresses. In the experiment, each mutant was screened using an LED light source ($\lambda_{max}$ 415 nm, irradiance 25 mW/cm$^2$) in three biological repetitions, at a sublethal dose ($MDK_{99.9}$) for the wild-type strain but lethal for potentially aBL-sensitive mutants ($\geq MDK_{99.9}$). No growth after aBL treatment in 2 of 3 repetitions qualified the mutant as aBL-hypersensitive. As a result, sixty-four single-gene mutants with an aBL-hypersensitive phenotype were identified, and their quantitative survival rates after aBL exposure were compared. Most mutants exhibit higher aBL sensitivity in comparison to the wild-type strain, except, i.e., *ΔnarL, ΔpriA, ΔubiC*, and *ΔyfgL*, with similar response, and *ΔnuoN, Δppc, ΔpurA, Δrpe*, and *Δsst* with lower aBL sensitivity than a wild-type strain. Moreover, it was demonstrated that the phase of bacterial growth was also important for establishing aBL sensitivity. Mutants in the exponential growth phase (2 h) were more susceptible to aBL than those in the stationary growth phase (16 h), where bacterial metabolism is reduced.

Then, the functions of the deleted genes were identified using UniProt, BioCyc, and the Omics Dashboard. These genes are involved in multiple cellular processes, including metabolism, biosynthesis, regulation, DNA repair, stress response, and others. 12.5% of

the sixty-four identified genes (eight genes; i.e., *umuD, rnt, rbfA, priA, oxyR, purA, fimB*, and *deoB*) are associated with the bacterial response to DNA damage. Importantly, these genes are not homologous and are regulated by various pathways. Almost half (48%) of the identified gene products are localized to the cell exterior: 36% at the plasma membrane, 7.8% in lipopolysaccharide, and 4.7% in the outer membrane. For this reason, the bacterial envelope could be an important part of cellular protection against aBL, serving as the first line of defense. According to the Omics Dashboard, more genes are engaged in RNA metabolism than in DNA and protein metabolism, suggesting that the cellular response to aBL can be mainly regulated at the RNA level. Bacterial aBL protection can be an active process that requires intense ATP production because mutants lacking ATP synthase subunits are especially sensitive to aBL.

Next, complementation of deleted genes was performed using the ASKA plasmid library for selected mutants (i.e., Δ*rbfA*, Δ*oxyR*, Δ*dnaK*, Δ*dnaJ*, Δ*purA*, Δ*fimB*, Δ*yihE*, Δ*ydcX*, Δ*umuD,* Δ*pgi,* Δ*cpxA*, and Δ*deoB*), and their aBL sensitivity profiles were compared with those of knockout mutants and the wild-type strain. In most cases, complementation of mutations restored the wild-type phenotype, and some complemented mutants were even more tolerant to aBL than the parental strain (*oxyR*, *ydcX*, *yihE*, *rbfA*, *fimB*, *umuD*, and *deoB)*. It may confirm the crucial role of deleted genes in the mechanism by which bacterial cells protect against the bactericidal effect of aBL. One of them, the *oxyR* gene encoding the OxyR protein, called "oxidative stress regulator," protects bacteria against the toxic effects of ROS generated upon aBL irradiation. It also regulates the expression of other genes engaged in the cellular response to oxidative stress (i.e. *metR*).

To conclude, the bacterial response to aBL depends on multiple factors, making it hardly possible to identify a predominant mechanism of action or a single potential way in which bacteria can develop resistance or tolerance to aBL. A potential adaptation would result from genetic alternation leading to the overexpression of identified aBL protective genes, or from the combination of complex genetic changes in the bacterial genome. These significantly lower the risk of its development compared to one-target antimicrobial approaches. It makes aBL a promising and safe alternative to antibiotics.

# 6.3. Publication no. 3.

## Kruszewska-Naczk, B., Grinholc, M., & Rapacka-Zdonczyk, A. (2024). Mimicking the Effects of Antimicrobial Blue Light: Exploring Single Stressors and Their Impact on Microbial Growth. *Antioxidants*, *13*(12), 1583.

It has previously been demonstrated that aBL, unlike one-target antibiotics, simultaneously affects multiple cellular targets through ROS generation. During aBL exposure, species such as singlet oxygen ($^1O_2$), superoxide anions ($O_2^-$), hydroxyl radicals (•OH), and hydrogen peroxide ($H_2O_2$) are generated and cause widespread damage, leading to cellular death. Nitric oxide (NO•) is not directly produced during photoinactivation; however, there are reports of nitric oxide release from nitrosated proteins upon aBL irradiation. Additionally, the pH of the environment can significantly affect the effectiveness of aBL, especially in acidic environments, promoting ROS accumulation. Another form of stress affecting bacteria when exposed to aBL is membrane stress, which results from lipid peroxidation and compromises cell membrane integrity by increasing permeability.

This investigation aimed to elucidate the role of aBL protective genes in response to aBL-generated single stressors, thereby contributing to understanding the aBL mode of action in bacteria. To achieve this, the previously described sixty-four-aBL hypersensitive mutants were cultured under conditions mimicking aBL-generated single-species, and their growth defects were compared with the wild-type strain's response to elevated stress conditions.

Mutants were incubated for 16 h at 37°C with shaking in the presence of the following stressors: $H_2O_2$, $O^{2-}$, NO•, HCl (acidic pH), membrane stress, and •OH, at doses that reduced the growth of the wild-type strain by 30-40%. The experiment was performed in five biological replicates. Then, $\Delta OD_{600}$ values were determined, and the growth defect was calculated using the formula provided in the publication methodology. The higher the growth defect value, the greater the single-gene mutant's sensitivity to specific stress conditions. Strains exhibiting a growth defect of 20% or more were classified as ‘sensitive’ to that stressor.

This research indicates that, excluding singlet oxygen, which was not studied herein, the most significant individual stressors in the bacterial response to aBL are •OH and $O^{2-}$. This conclusion is supported by the observation that the highest number of aBL-hypersensitive mutants (45) treated with these stressors exhibit a growth defect exceeding 20% in comparison to the wild-type strain.

The subsequent stressors that most significantly impacted mutant growth were NO• (36), membrane stress (9), and $H_2O_2$ (7). No mutant's growth was affected by acidic pH, which may suggest that acidic pH, when applied as a single stressor, does not substantially influence the growth of *E. coli* mutants. Although acidic pH alone is insufficient to induce growth inhibition, it may predispose bacteria to oxidative stress from reactive oxygen species generated during aBL exposure.

Mutants Δ*atpC*, Δ*gmhB*, Δ*rfaD*, and Δ*yccM* were susceptible to four stressors. The absence of *atpC*, which encodes the ATP synthase subunit, may result in inadequate energy production and hinder the bacterial capacity to withstand oxidative stress. Nonfunctional *gmhB* and *rfaD*, involved in lipopolysaccharide (LPS) biosynthesis, may elevate membrane permeability, thereby escalating stress susceptibility. Two mutants, Δ*atpD* and Δ*ydcX*, exhibited no sensitivity to any stressors. This could be due to bacteria lacking these genes being sensitive to other stressors produced by aBL, such as singlet oxygen, which was not tested here, or to the possibility that only the combination of single stressors causes the growth defect of these mutants.

In the next step, the statistical analysis was performed at the $\alpha = 0.05$ significance level. To check the correlation between mutants' sensitivity to aBL and each stressor, the ρ-Spearman correlation coefficient was calculated. Results show a negative, statistically significant correlation between aBL and $H_2O_2$ ($\rho = -0.45$, $p < 0.001$) and between aBL and membrane stress ($\rho = -0.31$, $p < 0.05$), as shown in the correlograms. No significant correlation was observed for other stressors.

No positive correlation was observed between the mutants' sensitivity to individual stressors and aBL. These findings suggest that the bactericidal effect of aBL results from the combined impact of multiple stressors, rather than a single one. The additive or synergistic toxic effects of stressors generated by aBL, particularly when localized near different cellular components, are most effective in eradicating bacteria.

Additionally, during aBL irradiation, ROS are generated mainly in bacteria near key cellular components such as membranes, nucleic acids, and enzymes, whereas in the experiment, stressors were administered externally, which may have affected the results.

Subsequently, mutants were categorized based on their sensitivity profiles utilizing Principal Component Analysis (PCA) and the k-means++ algorithm with cosine distances. The findings were subsequently displayed on a distance map. Then, mutants were grouped into three clusters based on their sensitivity profiles using the WSS (Within-Cluster Sum of Squares) index and the Silhouette statistics. In the next step, the Mann–Whitney U test was used to characterize the clusters and assess differences in stressors across clusters by calculating the statistical significance of median differences. Gene co-expression and protein–protein interaction networks within clusters were analyzed using the STRING database. The analysis shows multiple relationships between genes, including gene neighborhoods, gene fusions, gene co-occurrence, co-expression, protein homology, and protein–protein interactions.

Cluster 1 comprises genes predominantly engaged in fundamental cellular processes, such as energy metabolism, oxidative stress response and adaptation, regulatory functions, maintenance of cell wall and membrane integrity, DNA replication and repair, as well as nitrogen metabolism. It is also associated with significantly higher sensitivity to $O^{2-}$ and NO• within this cluster compared with clusters 2 and 3.

Cluster 2 predominantly comprises genes associated with energy production, environmental adaptation, stress response, detoxification, and fatty acid biosynthesis. Mutants within this cluster demonstrate a significantly heightened sensitivity to $H_2O_2$ and •OH stressors, as well as the least growth impairment in response to NO•, when compared to mutants from other clusters.

The smallest cluster, 3, is primarily concentrated on protein quality control, intermediary metabolism, and cellular nucleotide synthesis, with individual genes associated with DNA repair and genome stability under conditions of stress or damage. This may also elucidate the minimal growth defects observed in this cluster compared to those in other clusters.

Interestingly, some cross-cluster functional integration is evident: energy metabolism and stress response genes (*atp, dnaK, cpxA*) span clusters, underscoring their importance to bacterial survival. Moreover, stress response regulators (*oxyR, cpxA, dnaJ*) link various metabolic pathways, which may contribute to the development of coordinated adaptation to aBL.

To sum up, no positive correlation between mutants' sensitivity to aBL and to single stressors was observed, indicating that the effectiveness of aBL results from the complex interplay of the various stressors' actions, which cause multitargeted damage in bacterial cells. Moreover, no specific genes were identified whose knockout determines the development of a definite resistance to stressors. Understanding bacterial responses to single stressors and combinations of them in aBL may lead to better experimental design, especially for less-oxidative-susceptible bacteria in clinical and industrial applications.

# 6.4. Publication no. 4.

Kruszewska-Naczk, B., Grinholc, M., & Rapacka-Zdonczyk, A. (2025). Identification and validation of reference genes for quantitative gene expression analysis under 409 and 415 nm antimicrobial blue light treatment. *Frontiers in Molecular Biosciences*, *11*, 1467726.

The following investigations were performed to compare the expression levels of selected genes involved in bacterial protection against aBL before and after exposure. The second goal of this study was to compare gene expression profiles after aBL application at two wavelengths, 409 and 415 nm. To achieve this, the first crucial step was to establish a reference gene with stable expression after aBL irradiation. 10 genes involved in essential cellular processes were selected as potential reference gene candidates: *arcA, cysG, gyrA, hcaT, idnT, ihfB, rpoA, rssA, uidA,* and *uxuR*. qPCR results were analyzed using 4 programs: BestKeeper, geNorm, NormFinder, and RefFinder. For both aBL wavelengths, the gene with the most stable expression after aBL irradiation was *ihfB*, encoding the integration host factor β subunit. The next-best reference gene candidates were *cysG, uidA*, and *gyrA*, and the best gene combination was *cysG-gyrA.*

Additionally, 17 genes were selected to assess their expression after aBL irradiation. 11 of them were identified in prior studies, and their deletion results in aBL hypersensitivity: *cpxA, deoB, dnaK, dnaJ, oxyR, pgi, purA, rbfA, umuD, ydcX,* and *yihE* (Kruszewska-Naczk et al., 2024). The other 6 genes potentially associated with bacterial protection against aBL were also tested in wild-type *E. coli: rfaC, rfaD, dacA, fabH, gmhB*, and *hldE*. Results comparing the expression profiles of the tested genes after irradiation with aBL at 409 and 415 nm showed no statistically significant difference between the two wavelengths. The only exception was *oxyR*, which was overexpressed after 409 nm irradiation, probably because more ROS were generated at 409 nm aBL, and more *oxyR* products, which are involved in oxidative stress, are essential for bacterial protection. For both wavelengths, significantly higher expression after irradiation compared with non-irradiated bacteria was observed for 5 of 17 tested genes: *dacA, fabH, rbfA, umuD*, and *yihE*. Two genes, *purA* and *rfaC*, exhibited higher

expression levels only at 409 nm. No significant increase in expression was noted for the remaining 10 genes: cpxA*, deoB, dnaJ, dnaK, gmhB, hldE, oxyR, pgi, rfaD*, and *ydcX*.

Main conclusions based on the functions of genes with higher expression level:

- *dacA* and *rfaC* are responsible for peptidoglycan synthesis and maintenance of cell shape and may be involved in the repair of cell wall deformation induced by aBL.
- *fabH* – involved in fatty acids biosynthesis, which are also signal molecules, components of cell membranes, and an energy reservoir. During aBL irradiation, bacteria can use fatty acids as signaling molecules to activate protective pathways. Moreover, aBL protection is an active process, and fatty acid-derived energy may be used during the cellular response to aBL. Rebuilding energy reserves may require increased expression of genes involved in fatty acid biosynthesis. Additionally, aBL causes membrane damage through fatty acid oxidation and changes in the cellular fatty acid profile.
- *rbfA, purA* – involved in the response to DNA damage. Not all investigated genes involved in DNA repair were highly expressed, suggesting that bacteria activate only beneficial repair systems at certain doses of aBL, and that this may vary with time and dose of irradiation. The aBL cellular protection system involves gene products from various DNA repair pathways that are not genetically homologous.
- *umuD* – the main component of bacterial SOS response, UmuD′$_2$C is known to function as a DNA damage checkpoint system, controlling the timing and level of DNA synthesis in bacteria experiencing DNA damage stress.
- *yihE* – encoded stress response kinase A (SrKA), which is also regulated by the CpxR system – the response to many kinds of environmental stress. aBL generates stress in bacteria.

It was the first report on the establishment of genes with stable expression after aBL irradiation in *E. coli*.

# 6.5. Publication no. 5.

Kruszewska-Naczk, B., Pikulik-Arif, P., Grinholc, M., & Rapacka-Zdonczyk, A. (2024). Antibacterial blue light is a promising tool for inactivating *Escherichia coli* in the food sector due to its low risk of cross-stress tolerance. *Chemical and Biological Technologies in Agriculture*, *11*(1), 126.

The study conducted by our research team in 2021, which I also participated in, was the first report on tolerance to aBL in Gram-negative bacteria such as *E. coli*, *Klebsiella pneumoniae,* and *Pseudomonas aeruginosa*. (This publication is not part of this dissertation.) (Rapacka-Zdończyk et al. 2021). The report underscored that, after repeated exposure to a sublethal dose of aBL, bacteria develop tolerance to this factor but can still be eradicated with higher photoinactivation doses. To date, resistance to aPDI and aBL has not been observed. These studies marked the beginning of further exploration of mechanisms underlying tolerance. The idea of linking this topic to practical applications emerged during the investigation of the single stressors and the presence of Gram-negative bacteria among food-borne pathogens, such as *E. coli, Salmonella* sp., and *Campylobacter* sp. In aBL, it is essential to control the temperature during irradiation, especially for longer exposures and higher light doses, to avoid thermal effects. High temperatures are commonly used for food preservation, with many advantages but also drawbacks, such as loss of food physicochemical quality and the potential risk of heat tolerance development in foodborne pathogens. The combination of heat and aBL as a food preservation method would provide a safe alternative for ensuring food safety. Those revealed the need to assess the potential for cross-stress tolerance development in bacteria to heat and aBL.

The studies reported that *E. coli* developed a phenotypically stable tolerance to aBL and to high temperature (52 °C) after 5 days of repeated selective pressure, compared with the untreated control. The temperature-tolerant population has not developed increased aBL-sensitivity. Analyzing the aBL-sensitivity profile of temperature-tolerant populations reveals no stable pattern. However, aBL-tolerant populations were less susceptible to high temperatures (52-56°C) than controls but remained more thermally

susceptible than temperature-tolerant populations. Therefore, the order of exposure to disinfection methods is crucial for the development of potential cross-stress tolerance in the food-processing sector.

Also, short- and long-term preincubation before aBL irradiation was tested for the wild-type strain. Both preincubations exhibited significantly reduced aBL sensitivity. The highest tolerance was observed with preincubation at 50 °C for 10 min, likely related to the immediate heat shock response (HSR) and the transcription of heat shock proteins (HSPs), which accumulate in sufficient amounts to increase aBL tolerance. Higher aBL sensitivity after 20 min of incubation likely reflects increasing accumulation of cellular damage. Bacteria with long-term overnight preincubation in 42°C were less sensitive to aBL in a certain range of aBL doses. To conclude, high temperatures significantly affect bacterial response to aBL treatment. Moreover, tolerance to aBL and temperature does not significantly change antibiotic MICs relative to the wild-type strain. The largest MIC difference was observed for ciprofloxacin in the aBL-tolerant population, but the categorization of susceptibility to this antimicrobial has not changed. The possible involvement of shared genes in aBL and the temperature response was assessed by incubating single-gene mutants lacking genes encoding proteins involved in bacterial aBL protection for 16 h under heat shock conditions. The growth defect in certain mutants suggests that missing genes are important for cellular protection against both temperature and aBL stress and may be involved in cross-adaptation to both stressors. For 11 of 64 mutants, the growth defect was observed for: ***yncA/mnaT*** (l-amino acid *N*-acyltransferase), ***yfgL/bamB*** (outer membrane protein assembly factor BamB), ***ydcX*** (orphan toxin OrtT), ), ***ydcE***/***pptA*** (tautomerase PptA), ***yccM*** (putative electron transport protein YccM), ***tolA*** (Tol–Pal system protein TolA, ***nuoN*** (NADH: quinone oxidoreductase subunit N), ***dnaJ*** (chaperone protein DnaJ), ***atpH*** (ATP synthase F1 complex subunit δ), ***atpG*** (ATP synthase F1 complex subunit γ), ***atpE*** (ATP synthase Fo complex—subunit c). Interestingly, most of these genes were plasma membrane proteins, suggesting the important role of this cellular component in bacterial protection. In a publication, the possible mechanism of cross-adaptation for aBL and heat was proposed in Figure 8 in the publication. The common part of both kinds of adaptation is ROS generation, the main mode of aBL action, and a result of cell membrane disruption and ion leakage

caused by heat stress. Overexpression of genes involved in the bacterial response to aBL and heat can lead to cross-stress tolerance to both factors. It is important to note that, despite the common elements of protection strategies, bacteria can also respond to stressors in other ways. 53 of 64 single-gene mutants were hypersensitive to aBL, not to heat.

This shows multiple ways of heat and aBL action in bacteria and the promising potential of combining these factors as a disinfection method in the food sector. The studies underscored the need to optimize protocols to account for adaptation and coselection, ensuring safe food-preservation methods, and minimizing the risk of spreading foodborne pathogens.

# 7. Summary and conclusions

To summarize the key results, the analysis of the single-gene Keio mutant collections revealed sixty-four aBL-hypersensitive mutants, suggesting that sixty-four genes participate in *E. coli's* cellular response to aBL (Aim 1). Identified aBL-protective genes are responsible for multiple important cellular processes. The analysis reveals multiple complex networks among aBL-protective genes, including gene neighborhoods, gene fusions, gene co-occurrence, co-expression, protein homology, and protein–protein interactions. Importantly, the bactericidal effect of aBL results from the combined action of stressors generated by aBL, which is supported by the lack of observed correlation between mutants' sensitivity to individual stressors and their sensitivity to aBL. Most aBL-protective genes are primarily involved in defending against hydroxyl radicals (•OH) and oxygen radicals ($O^{2-}$) (Aim 2). This study included only non-essential genes; therefore, it cannot be ruled out that untested genes in the essential group also participate in bacterial defense against aBL, which represents a limitation of the methodology employed in this study.

The gene expression analysis revealed that not all tested genes previously found to be aBL-protective are expressed simultaneously. Their expression levels depend on the wavelength, irradiation time, and dose of applied aBL; optimizing these parameters can increase eradication efficacy (Aim 3). All sixty-four identified genes may contribute to the risk of resistance development. However, no specific genes were identified whose knockout determines the development of a definitive resistance to aBL-generated single stressors, making aBL a safe alternative to antibiotics. Unlike antibiotic resistance, which is caused mainly by a single-gene mutation, in developing aBL resistance, many changes in the genome or gene expression patterns must occur (Aim 4).

Furthermore, the studies have assessed the safety of aBL as an antimicrobial method in the food industry. aBL may serve as a supplementary method to heat treatment without affecting antibiotic susceptibility and with a low risk of resistance development. Nonetheless, the potential for cross-stress tolerance development warrants consideration when devising protocols, as elevated temperatures can markedly influence bacterial susceptibility to aBL (Aim 5).

In conclusion, the bacterial response to aBL involves a complex interaction of genetic networks that connect multiple protective genes and their regulons, which modulate specific expression patterns in response to different aBL exposure conditions. The results of this study confirmed the hypothesis of this doctoral dissertation: bacterial response to aBL is a complex process mediated by multiple genes involved in DNA repair, oxidative stress response, and cell envelope maintenance. These genes determine bacterial susceptibility to aBL and may influence the potential risk of resistance development. Moreover, the main aim of this study, along with its specific aims, was achieved.

This doctoral dissertation is the first study to provide comprehensive insights into the genetic basis of bacterial responses to aBL that influence bacterial susceptibility to aBL and may contribute to the development of resistance, and additionally provides implications for application in the food sector. Therefore, considering all aBL limitations, I conclude that aBL could be applied as a safe alternative to antibiotics or as an additional treatment in combination with other antimicrobial strategies.

Future research priorities should focus on translating the promising potential of aBL into optimized standards and protocols for reliable antimicrobial interventions in clinical and food industry contexts. This involves evaluating treatment frameworks tailored to specific species and strains, conducting more comprehensive mechanistic investigations into the dynamics of aBL-generated single stressors under biologically relevant conditions, thoroughly assessing reproducibility across various experimental platforms, and implementing safe practices to mitigate the risk of resistance development to aBL.

# 8. Attachments – Publications being the subject of this doctoral dissertation

## 8.1. Publication no. 1.

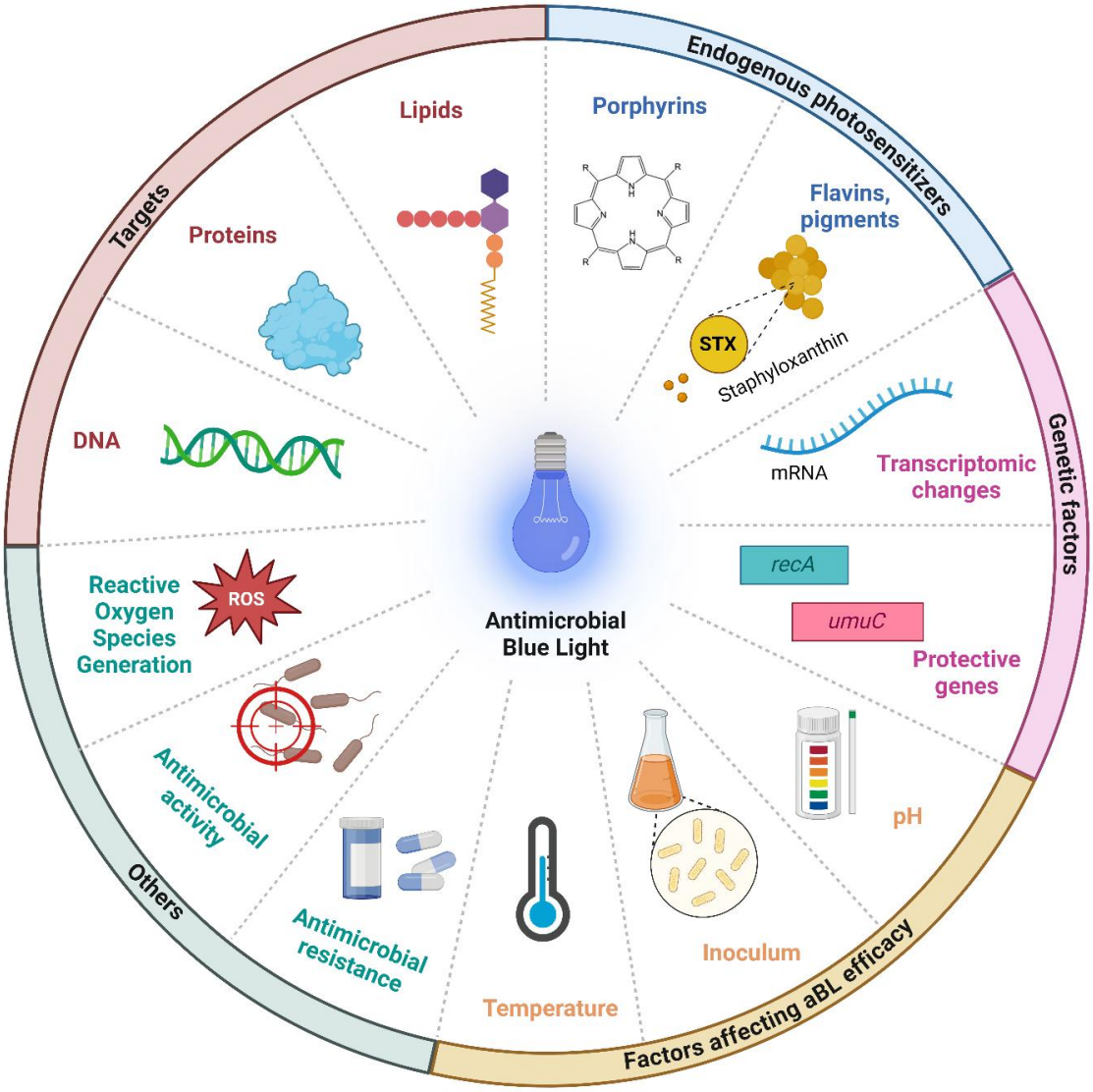


Figure 1. Graphical abstract of Publication no. 1.

Drug Resistance Updates 86 (2026) 101391

Contents lists available at ScienceDirect

Drug Resistance Updates

journal homepage: www.elsevier.com/locate/drup

# Mechanisms and determinants of bacterial susceptibility to antimicrobial Blue Light: From chromophores to transcriptomes

Beata Kruszewska-Naczk [a], Natalia Burzyńska [a], Dominika Goik [a], Mariusz Grinholc [a], Joanna Nakonieczna [a], Natalia Pawlik [a], Michał K. Pieranski [b], Agata Wozniak-Pawlikowska [a], Aleksandra Rapacka-Zdonczyk [a,*], Tianhong Dai [c,*]

[a] Laboratory of Photobiology and Molecular Diagnostics, Intercollegiate Faculty of Biotechnology, University of Gdansk and Medical University of Gdansk, Poland
[b] Department of Pharmaceutical Technology and Biochemistry, Faculty of Chemistry, Gdansk University of Technology, Poland
[c] Wellman Center for Photomedicine, Massachusetts General Hospital, Harvard Medical School, Boston, USA

ARTICLE INFO

*Keywords:*
Antimicrobial blue light (aBL)
Reactive oxygen species (ROS)
Endogenous photosensitizers
Porphyrins
Flavins
Oxidative stress

ABSTRACT

Antimicrobial blue light (aBL) is emerging as a promising non-pharmacological antimicrobial strategy with multitarget activity and a low risk of resistance development. Its effects are primarily mediated by endogenous porphyrins, but additional chromophores such as flavins and bacterial pigments can also contribute. In this review, we summarize current evidence on these photosensitizers and discuss how their diversity underlies species-dependent susceptibility, with special emphasis on the variable responses of *Streptococcus* and *Enterococcus* spp. At the molecular level, aBL-induced reactive oxygen species (ROS) damage DNA, proteins, and membranes, disrupting metabolic pathways, efflux pumps, and membrane integrity. Genetic determinants, including porphyrin biosynthesis genes, cell envelope regulators, and components of the SOS and oxidative stress responses, further influence susceptibility. Transcriptomic studies reveal global shifts affecting stress responses, energy metabolism, motility, membrane remodeling, metal ion regulation, and virulence-associated functions. Additional microbial determinants, such as biofilm formation, virulence factors, and antibiotic resistance profiles, modulate treatment outcomes, while environmental and physiological parameters (growth phase, inoculum density, temperature, wavelength, and irradiance) strongly impact efficacy. Altogether, these findings indicate that aBL efficacy is shaped by a complex interplay of chromophore availability, genetic background, physiological state, and external conditions. Clarifying these mechanisms is essential to optimize aBL for clinical and industrial applications. In summary, this review provides a comprehensive overview of the molecular and physiological bases of bacterial susceptibility to aBL and outlines key gaps that must be addressed to translate this modality into routine antimicrobial practice.

## 1. Introduction

The emergence of antimicrobial resistance (AMR) ranks among the most significant threats to public health and development worldwide. Moreover, the COVID-19 pandemic has had a substantial impact on exacerbating antibiotic resistance. According to a meta-analysis, the majority of patients with laboratory-confirmed SARS-CoV-2 in the United States (71.8%) were treated with antibiotics. However, bacterial coinfection was reported in only 6.9% of these patients (Langford et al., 2020). Additionally, patients with prolonged hospitalization were more prone to bacterial infections. During the pandemic, many infections caused by carbapenem-resistant strains were reported, including New Delhi metallo-β-lactamase (NDM)-producing *Enterobacter cloacae* and *Escherichia coli,* carbapenemase (KPC)-producing *K. pneumoniae*, carbapenem-resistant *Acinetobacter baumannii* (CRAB), penicillin and macrolide-resistant *Streptococcus pneumoniae,* and more (Nori et al., 2020; Perez, 2020; Arcari et al., 2021; Gomez-Simmonds et al., 2021; Kovacevic et al., 2024). Many individuals are working together to combat this serious issue, including researchers, healthcare professionals, world organizations, and bioinformaticians/programmers, using artificial intelligence tools for infection and treatment control and educational support to optimize the drug development process (Abavisani et al., 2024).

In the antibiotic resistance era, antimicrobial blue light (aBL) has

* Corresponding authors.
*E-mail addresses:* aleksandra.rapacka-zdonczyk@ug.edu.pl (A. Rapacka-Zdonczyk), TDAI@MGH.HARVARD.EDU (T. Dai).

https://doi.org/10.1016/j.drup.2026.101391
Received 3 December 2025; Received in revised form 17 February 2026; Accepted 13 March 2026
Available online 17 March 2026

gained much attention as a promising alternative therapeutic approach to conventional antibiotic therapy. aBL should be clearly distinguished from ultraviolet (UV) radiation, despite both being light-based antimicrobial strategies. aBL refers to visible light, typically in the range of approximately 400–470 nm, whereas UV irradiation comprises shorter wavelengths below 400 nm, including UV-B and UV-C (Dai et al., 2012; Maclean et al., 2008). These two modalities differ fundamentally in their primary molecular targets and mechanisms of action. UV light exerts its antimicrobial effect predominantly through direct absorption by nucleic acids, resulting in DNA damage such as pyrimidine dimer formation and strand breaks, which are strongly associated with mutagenesis and cell death (Friedberg et al., 2005; Cadet & Wagner, 2013).

In contrast, aBL does not require the involvement of exogenous photosensitization but instead exploits the presence of naturally occurring endogenous chromophores, such as porphyrins and flavins, which absorb visible blue light and trigger intracellular reactive oxygen species (ROS) generation upon irradiation (Ashkenazi et al., 2003; Maclean et al., 2009). The resulting oxidative stress affects multiple cellular targets, including membranes, proteins, and metabolic pathways, rather than inducing direct DNA photodamage. Consistent with this mechanism, aBL induces complex stress-response pathways and metabolic reprogramming rather than canonical UV-associated SOS responses (Dos Anjos et al., 2023; Seo & Dai, 2026).

As a consequence, aBL exhibits species- and strain-dependent antimicrobial efficacy, reflecting differences in chromophore content, cellular redox balance, and stress-response capacity (Guffey & Wilborn, 2006). Moreover, unlike UV irradiation, aBL is non-ionizing and substantially less mutagenic, which has important implications for safety, resistance development, and potential clinical applicability (Dai et al., 2013). These mechanistic distinctions underscore that aBL is not a variant of UV irradiation but a fundamentally different antimicrobial modality with unique determinants of bacterial susceptibility and adaptive response.

aBL is characterized by a multitarget mode of action. The prevailing hypothesis is that aBL irradiation of microorganisms leads to the generation of ROS, which are toxic to bacteria at high concentrations (Tardu et al., 2017; Wu et al., 2018; Hamblin & Abrahamse, 2020; Vatansever et al., 2013). The blue light in the 400–470 spectrum is absorbed by endogenous photosensitizers (Ashkenazi et al., 2003; Hamblin et al., 2005). Two major photochemical mechanisms are recognized: Type I, involving electron or hydrogen transfer that produces superoxide anion ($O_2\bullet^-$), hydrogen peroxide ($H_2O_2$), and hydroxyl radicals (•OH); and Type II, involving energy transfer to molecular oxygen, resulting in singlet oxygen ($^1O_2$) generation. Importantly, singlet oxygen is considered fundamentally non-resisted. Owing to its microsecond lifetime and nanometer-scale diffusion range, no specific enzymatic systems have been identified that directly neutralize $^1O_2$, in contrast to superoxide or peroxides, which are scavenged by bacterial antioxidant enzymes (Moan & Berg, 1991; Ogilby, 2010). Recent work demonstrates that aBL induces a dynamic and species-dependent ROS profile, which triggers specific oxidative stress response pathways and metabolic reprogramming rather than uniform bactericidal damage. Importantly, these findings support the view that ROS generated under aBL acts not only as cytotoxic agents but also as regulatory signals shaping heterogeneous cellular responses under sublethal conditions (Cong et al., 2025).

ROS can oxidize cell structures and cause DNA damage (Grinholc et al., 2015; Kim & Yuk, 2017), cell membrane degradation or loss of membrane integrity (Kim et al., 2017; Hoenes et al., 2021a), lipidomic remodeling and oxidative alterations of membrane composition under sublethal exposure (Wu et al., 2025), ion leakage (Wu et al., 2018), alterations in transmembrane potential (Biener et al., 2017), damage to the glucose uptake system, efflux pump dysfunction (Kim & Yuk, 2017) and other processes that lead to cell death. The photochemical basis of these reactions has been extensively characterized in the field of photodynamic therapy and photochemistry (Foote, 1968; Foote, 1991; Moan & Berg, 1991; Jori, 1996; Dougherty et al., 1998; Schmidt-Erfurth & Hasan, 2000; Ogilby, 2010; Arnaut, 2011; Jori et al., 2006; Plaetzer et al., 2009; Allison & Moghissi, 2013; Dąbrowski & Arnaut, 2015; Halliwell & Gutteridge, 2015; Baptista et al., 2017), providing the conceptual foundation for understanding aBL. Importantly, recent studies demonstrate that radiometric parameters such as irradiance and light delivery mode (pulsed versus continuous) critically shape aBL efficacy, highlighting the need to consider ROS generation kinetics rather than fluence alone (Bolognese et al., 2025).

In addition to the well-established Type I and Type II photochemical pathways, a hypothetical Type III pathway has been proposed, referring to oxygen-independent photochemical damage mediated directly by activated photosensitizers (Hamblin & Abrahamse, 2020). Experimental observations consistent with oxygen-independent effects have been reported primarily for exogenous photosensitizers. For example, photoactivated tetracyclines retain substantial antibacterial activity under oxygen-depleted conditions and in the presence of singlet oxygen quenchers, indicating that mechanisms other than classical Type II photochemistry may contribute (Xuan et al., 2018). Likewise, psoralen photochemistry involves direct DNA adduct and crosslink formation that does not strictly depend on molecular oxygen (Bianchi et al., 1996). However, whether these oxygen-independent reactions constitute a distinct pathway remains a matter of conceptual interpretation. Importantly, robust experimental evidence supporting such a mechanism in the context of endogenous chromophore-mediated aBL remains limited.

Understanding the precise mechanisms of aBL is essential not only from a fundamental photobiological perspective but also in the context of antimicrobial resistance. Unlike conventional antibiotics that act on single molecular targets and rapidly select for resistant mutants, aBL involves a multitarget oxidative mode of action that has so far shown a low risk of resistance development. Clarifying the molecular pathways behind these effects is therefore critical to validate aBL as a robust antimicrobial strategy and to guide its safe translation into clinical and industrial practice.

Finally, many studies have pointed to the promising potential of aBL in the food, medical, and other industries, although its clinical and industrial implementation is still limited. All aBL applications and the current knowledge about aBL have been summarized in several review articles (Dai et al., 2012; Gwynne and Gallagher, 2018; Hadi et al., 2020, 2021; Huang et al., 2023; Leanse et al., 2022; Ozdemir et al., 2025; Ruiz-Arellano and Araque, 2026; Tomb et al., 2018; Wang et al., 2017a; Yin et al., 2013; Burzyńska et al., 2026). Despite many potential applications of aBL in various industries, the detailed mechanism of action of aBL is not fully understood (Wang et al., 2017b). This can be a factor limiting the implementation of aBL to routine antimicrobial procedures. At present, aBL treatment is not common and is limited to the treatment of infections caused by *Cutibacterium acnes* (formerly *Propionibacterium acnes*) (Dai et al., 2012). In addition, recent studies (Gigante et al., 2024; Negri et al., 2025; Gonçalves et al., 2025; Kruszewska-Naczk et al., 2024) have extended the evidence for biofilm applications, combinational therapies, and food industry usage, but still highlight gaps in understanding of the underlying molecular and genetic responses. Therefore, it is necessary to investigate the mode of action of aBL and the benefits and possible risks of using this promising approach. This publication aims to summarize the current literature on the mechanism of action of aBL. We described the roles of endogenous porphyrins and other chromophores, aBL targets, genetic factors in aBL treatment efficacy, transcriptomic changes after aBL exposure, the impact of aBL on antibiotic resistance, and other factors affecting aBL. In this review, 'ROS generation' refers to the photochemical formation of reactive species ($O_2\bullet^-$, $H_2O_2$, •OH, $^1O_2$), while 'oxidative stress' refers to the subsequent cellular responses triggered by their accumulation.

Beyond bacteria, blue light (either alone or in combination with exogenous photosensitizers) has been reported to be effective against fungi (Dai & Hamblin, 2017), actinomycetes (Voronkina et al., 2024), and viruses (Marchi et al., 2025; Amodeo et al., 2025); however,

differences in cellular organization and photochemical targets justify their exclusion from the present bacteria-centered mechanistic analysis.

## 2. Endogenous porphyrins as primary photosensitizers in aBL

### 2.1. Photophysical properties of porphyrins

Endogenous porphyrins are heterocyclic macrocycles composed of pyrrole ring molecules that can absorb light strongly in Soret bands near 400 nm and weakly in four Q bands with decreasing intensities ranging from 450 to 700 nm (Aihara, 2008; Fernandez et al., 1997; Giovannetti, 2012). Moreover, they can be easily detected because of their intense fluorescence in the range of 600–730 nm (Ashkenazi et al., 2003; Quiroz-Segoviano et al., 2014).

### 2.2. Porphyrins and aBL wavelength dependency

Among microorganisms, we can distinguish coproporphyrins, protoporphyrins, and uroporphyrins (Fig. 2) as the most abundant metal-free tetrapyrroles that are capable of absorbing light, leading to the photochemical generation of ROS (Plavskii et al., 2018; Fontana et al., 2015; Fyrestam et al., 2015). aBL efficacy strongly depends on its wavelength; a literature review of both gram-positive and gram-negative bacteria indicated that the highest efficiency of aBL occurred at approximately 405 nm and decreased toward 450 nm, which corresponds with the porphyrin absorption spectra (Hessling et al., 2017). In addition, other studies independently compared the effectiveness of 405- and 520-nm photoinactivation and revealed that 405-nm LEDs exhibit better antibacterial effects than do 520-nm LEDs at much lower doses (Kumar et al., 2015; Kumar et al., 2016), which aligns with the range of absorption of porphyrins. Porphyrins are proposed to contribute to aBL efficacy by producing ROS via energy absorption from visible light. aBL has been widely studied among different species of bacteria such as *Acinetobacter baumannii* (Zhang et al., 2014), *Escherichia coli* (Plavskii et al., 2018; Walker, 2022; Dos Anjos et al., 2023), *Neisseria gonorrheae* (Wang et al., 2019), *Pseudomonas aeruginosa* (Dai et al., 2013; Wang et al., 2016; Amin et al., 2016; Fila et al., 2018; Dos Anjos et al., 2023), *Staphylococcus aureus* (Plavskii et al., 2018; Dos Anjos et al., 2023), *Salmonella* spp. (Kim and Yuk, 2017; Kim et al., 2017), *Vibrio vulnificus* (Dos Anjos et al., 2022), and periodontal pathogens (Cieplik et al., 2014; Fontana et al., 2015; Yoshida et al., 2017). All of the abovementioned studies led to the conclusion that the involvement of porphyrins in photoinactivation is mediated by blue light. Along with these findings, Wu et al. (2018) reported a decrease in coproporphyrin levels in *S. aureus* before and after irradiation, which suggests its engagement and consumption during aBL treatment (Wu et al., 2018).

### 2.3. Genetic evidence and strain-specific variability

aBL susceptibility testing was carried out on *S. aureus* wild-type strain and a *hemB* mutant strain with impaired porphyrin production (Grinholc et al., 2015). In the study, the wild-type strain showed a significant reduction in viability following 405 nm aBL treatment, particularly when preincubated with novobiocin. In contrast, the mutant strain displayed no decrease in viability, supporting the requirement for endogenously produced porphyrins for the bactericidal effects of light treatment at 405 nm (Grinholc et al., 2015). However, the effects of porphyrin contents on aBL treatment effectiveness remain unclear. For example, comparative studies with *Campylobacter jejuni* and *E. coli* revealed that *C. jejuni* is more susceptible to 405 nm aBL, which is associated with a greater abundance of protoporphyrin IX (PPIX) and correlates with an increase in ROS generation (Walker et al., 2022). Dos Anjos et al. (2023) reported a similar effect on *P. aeruginosa,* with the highest concentration of intracellular porphyrins and aBL sensitivity, in comparison with *S. aureus* and *E. coli*, which have much lower porphyrin contents and a decreased response to photoinactivation (Dos Anjos et al., 2023). Supplementation with exogenous porphyrins (PpIX or CPIII) rendered non-porphyrin-producing *S. agalactiae* susceptible to aBL in the study by Bumah et al. (2020). Importantly, the absorption spectra show that both porphyrins absorb strongly in the 405–415 nm range, whereas absorption at 450 nm is minimal. This indicates that the observed bactericidal effect was most likely driven by shorter-wavelength components within the emission spectrum of the light source, rather than by direct excitation at 450 nm (Bumah et al., 2020). In *Helicobacter pylori*,

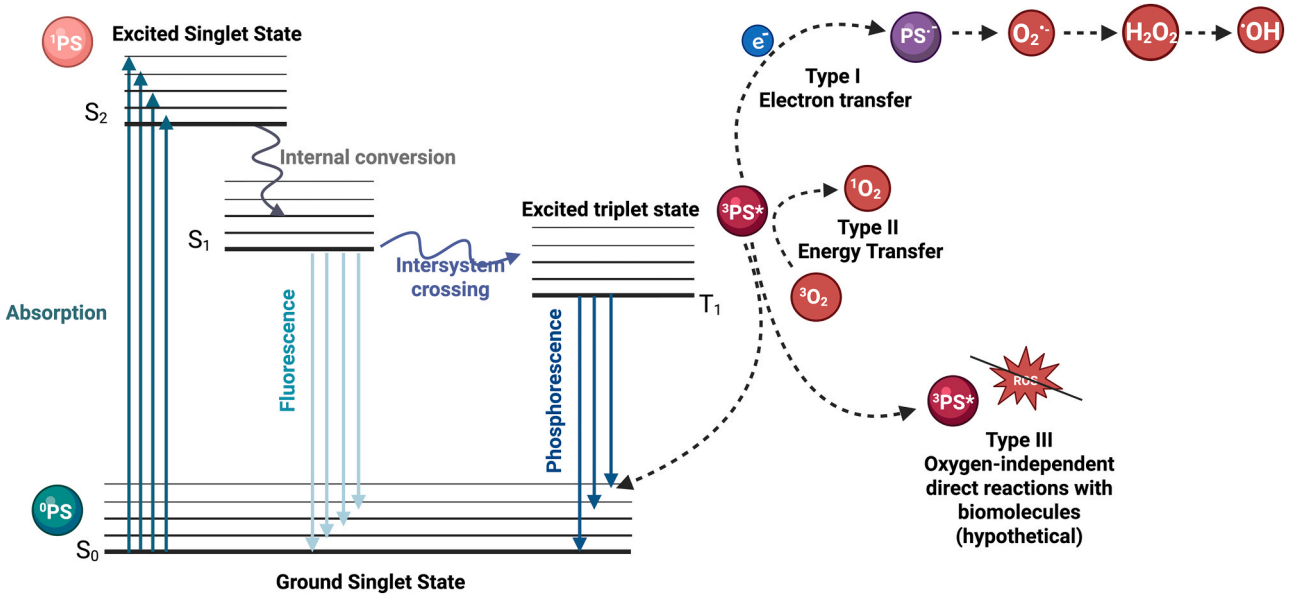


**Fig. 1.** Simplified Jablonski diagram illustrating photophysical processes and proposed phototreatment mechanisms. Upon excitation by blue light (400–470 nm), endogenous photosensitizers (PS) absorb photons and transition from the ground state ($S_0$) to excited singlet states ($S_1$, $S_2$). Relaxation may occur via internal conversion (IC), fluorescence, or intersystem crossing (ISC) to the triplet state ($^3PS^*$). From $^3PS^*$, three pathways are possible: Type I, electron or hydrogen transfer leading to sequential formation of superoxide anion ($O_2^{\bullet-}$), hydrogen peroxide ($H_2O_2$), and hydroxyl radicals ($\bullet OH$); Type II, energy transfer to molecular oxygen ($^3O_2$) producing singlet oxygen ($^1O_2$); and Type III, oxygen-independent direct interactions of $^3PS^*$ with biomolecules, proposed as a hypothetical mechanism for aBL (Hamblin and Abrahamse, 2020).

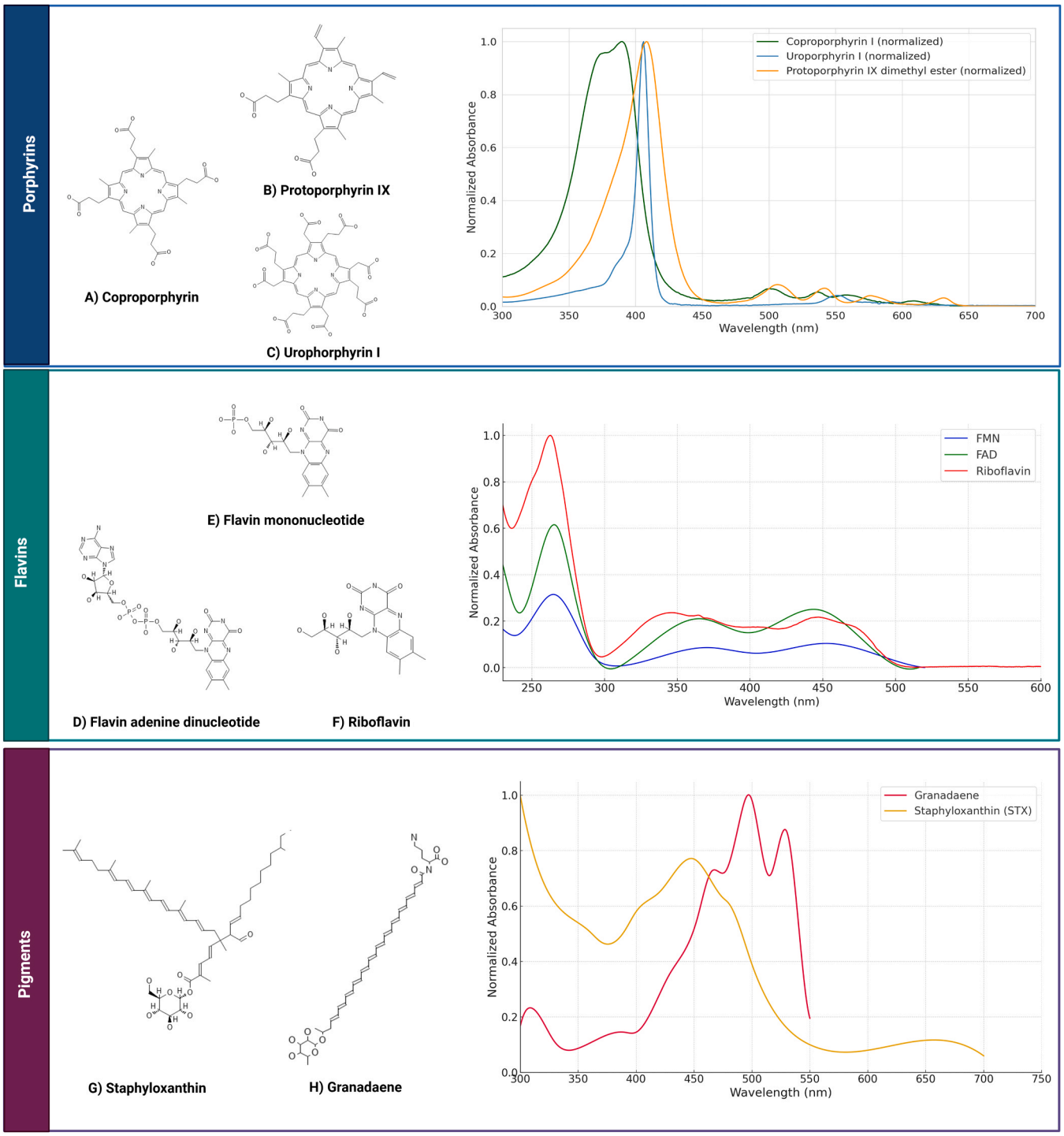


**Fig. 2.** Structures of endogenous PSs. A) Coproporphyrin, B) Protoporphyrin IX, C) Uroporphyrin I, D) Flavin mononucleotide, E) Flavin adenine dinucleotide, F) Riboflavin, G) Staphyloxanthin, H) Granadaene. The porphyrin spectra were constructed based on data from the PhotochemCAD spectral database (www.photochemcad.com), including absorption spectra of protoporphyrin IX dimethyl ester, uroporphyrin I (in 1 N aqueous HCl), and coproporphyrin I (in 0.1 M phosphate buffer). To generate the flavin spectra, the following sources were utilized: Fig. 1 (Normalized UV-Vis absorption spectrum of FMN in ion-exchanged water) from Turunen et al# (2011), Fig. 1 (Absorption spectra of FAD in phosphate buffer) from Kowalska et al# (2007), and the riboflavin spectrum available in the PhotochemCAD database. For bacterial pigments, spectra were based on Fig. 2B (Absorption spectrum of pigment dissolved in DMSO with 0.1% TFA) from Vanberg et al# (2007) and Fig. 1A (Absorption spectrum of isolated and concentrated staphyloxanthin in methanol) from Jusuf et al# (2019). The OpenAI ChatGPT model was used to assist in plotting and visual formatting of these spectra based on the authors' manually extracted numerical data.

where the accumulation of PpIX and CPIII correlated strongly with enhanced photoinactivation under 400–425 nm aBL, despite comparable total porphyrin levels across strains (Hamblin et al., 2005). Together, these observations underscore that the porphyrin profile determines phototoxic responsiveness.

Notably, different porphyrins exhibit varying quantum yields of singlet oxygen production, which directly influences their phototoxic efficacy upon aBL excitation (Akbar et al., 2023).

### 2.4. Limitations of porphyrins as a universal aBL target

Although porphyrins play a well-established role in antimicrobial photoinactivation, some studies have reported that differences in porphyrin content do not necessarily correlate with aBL susceptibility (Fontana et al., 2015; Kim & Yuk, 2017; Kumar et al., 2015). Despite the well-documented role of porphyrins in antimicrobial photoinactivation, they are not universally present across all bacterial species (Frankenberg et al. 2002; Ramsey et al., 2014), and their phototoxic potential may vary depending on cellular localization, concentration, and spectral compatibility with the applied light. Moreover, the antioxidant capacity of bacteria can significantly influence the effectiveness of aBL. Bacteria equipped with efficient ROS-neutralizing mechanisms, such as catalase (katA), superoxide dismutase, or carotenoid pigments like staphyloxanthin, are able to counteract oxidative stress even when photoactive porphyrins are present. As a result, their susceptibility to aBL may be considerably reduced (Hadi et al., 2021; Orlandi et al., 2018; Leanse et al., 2020).

### 2.5. Unresolved questions and the role of alternative chromophores

It remains unclear which intracellular chromophore plays the most critical role in the phototoxic process. A molecule present in small amounts but excited in a photoreactive site may exert a stronger bactericidal effect than one produced abundantly yet located in less responsive areas of the cell (Walter et al., 2020; Ashkenazi et al., 2003; Dos Anjos et al., 2023). This uncertainty prompts the need to consider other endogenous chromophores, such as flavins, which are nearly ubiquitous in bacteria and may play a complementary or even dominant role in aBL-mediated inactivation under certain conditions (Plavskii et al., 2018; Hoenes et al., 2021a; Edwards, 2014).

## 3. Other endogenous photosensitizing chromophores

### 3.1. Flavins as endogenous photosensitizers

#### 3.1.1. Chemical nature and photoreactivity of flavins

Flavins are organic compounds that contain isoalloxazine. In living organisms, flavins include riboflavin (RF, vitamin $B_2$) and its metabolically active derivatives, flavin mononucleotide (FMN) and flavin adenine dinucleotide (FAD) (Fig. 2). FMN and FAD participate in a range of redox reactions and are part of complex redox centers in proton pumps and large protein complexes involved in oxidation processes, serving as cofactors for biological processes such as radical scavenging, photosynthesis, and DNA repair. Flavins absorb light at maximum wavelengths of 375 and 450 nm (Eley et al., 1970; Heelis, 1982; Song et al., 2007; Cardoso et al., 2012; Plavskii et al., 2018) and exhibit fluorescence in the range of 520–536 nm (Kotaki & Yagi, 1970; Heelis, 1982; Plavskii et al., 2018). Upon irradiation, flavins undergo photochemical reactions that generate ROS, which in turn can cause deoxyribose degradation and DNA strand breaks (Huang et al., 2004; Liang et al., 2013; Liang et al., 2015).

#### 3.1.2. Flavins as endogenous PSs

Although flavins participate in redox reactions and can contribute to radical scavenging, under certain conditions, they can act as photosensitizers. Upon exposure to aBL, flavins transit into an excited state, leading to triplet state formation and initiating photodynamic reactions. This process results in the production of singlet oxygen and other ROS (Liang et al., 2015). It is also important to note that in experimental settings, where higher light doses are applied compared to typical biological conditions, the photogeneration of ROS is more pronounced, making flavins effective agents for microbial photoinactivation (Liang et al., 2015; Plavskii et al., 2018; Eichner et al., 2015; Hoenes et al., 2021a). Blue light (462 nm) had the greatest effect on riboflavin and FMN photoinactivation (Liang et al., 2015). Interestingly, FMN photoinactivation results in the production of more ROS than RF photoactivation does (Liang et al., 2015). Moreover, studies have revealed that exogenously administered flavins such as FMN via the use of light-activated derivatives of RF could reduce the survival of *E. coli* (Plavskii et al., 2018; Liang et al., 2015) or inactivate *Bacillus atrophaeus* spores (Eichner et al., 2015). Additionally, the role of flavins as endogenous PSs in aBL among various bacterial species has been investigated in many studies. Several bacterial species, such as *A. baumannii* (Hoenes et al., 2021b), *Aggregatibacter actinomycetemcomitans* (Cieplik et al., 2014), *Enterococcus moraviensis* (Hoenes et al., 2021a, Hessling et al., 2020), *E. coli* (Hoenes et al., 2021a, Plavskii et al., 2018), *Legionella rubrilucens* (Schmid et al., 2019), *P. aeruginosa* (de Lucca et al., 2012; Hoenes et al., 2021a), *Salmonella enterica* (Bumah et al., 2015), *S. aureus* (Hoenes et al., 2021a; Plavskii et al., 2018; Bumah et al., 2015; Enwemeka et al., 2009), *Staphylococcus carnocus* (Hoenes et al., 2020; Hoenes et al., 2021a) and *Streptococcus mutans* (Mohamad et al., 2023), have been investigated. In all the above-mentioned studies, aBL at a wavelength of 450–460 nm significantly reduced bacterial survival; however, a higher dose of irradiation had to be used at 450–460 nm than at 405 nm to obtain similar antimicrobial efficiency. The data in the literature differ regarding the doses that cause effective inactivation of bacteria. The reason may be that different strains of bacteria were used in the experiments, and different strains may have different contents of endogenous photosensitizing chromophores. In the context of wavelengths of 450–460 nm, most authors consider flavins to be the PSs responsible for the photoinactivation effect. The absorbance measurements of the bacterial lysates revealed peaks characteristic of flavins, which confirms the presence of these compounds in the tested bacterial species (Plavskii et al., 2018; Cieplik et al., 2014; Hessling et al., 2020; Hoenes et al., 2020; Hoenes et al., 2021a; Mohamad et al., 2023).

#### 3.1.3. Advantages of targeting flavins with aBL

Although the use of wavelengths ranging from 450 to 460 nm requires a higher irradiation dose, this method can have a wider range of applications than those using shorter wavelengths because most bacteria should be somewhat sensitive to aBL irradiation as a result of their ubiquitous flavin content (Edwards, 2014), in contrast to porphyrins, which are not produced by all bacterial species. For example, Enterococci are not capable of synthesizing porphyrins (Frankenberg et al. 2002; Ramsey et al., 2014).

#### 3.1.4. Flavins in blue-light sensing systems

Along with porphyrin sensitizers, flavin compounds can act as acceptors of light from the blue spectral region, leading to the photoinactivation of microbial cells and the inhibition of their growth. Among these photoreceptors are blue light-sensing flavin adenine diphosphate (BLUF) proteins, which undergo structural changes that affect bacterial surface attachment, biofilm formation, and bacterial motility upon blue light exposure (Braatsch and Klug, 2004). It has been reported that the BLUF-associated protein YcgF reduces the synthesis of curli fibers while regulating biofilm formation in *E. coli* (Tschowri et al., 2009; Tschowri et al., 2012). Mussi et al. (2010) reported that *A. baumannii* is not able to form biofilms after aBL irradiation. However, mutants lacking the functional *blsA* gene encoding BLUF-containing photoreceptors can form biofilms upon blue light (462 nm) treatment, which confirms the crucial role of this gene in blocking biofilm formation after aBL treatment. While aBL did not affect the survival of either the wild-type or the mutant strains, it inhibited bacterial motility and pellicle formation (Mussi et al., 2010).

#### 3.1.5. Summary

In summary, flavins, along with porphyrins, are important aBL targets. Flavins are typically excited with blue light at wavelengths ranging from 450 to 460 nm, which can be used to eradicate bacteria that do not contain porphyrins. However, few reports exist concerning flavins, and

broader studies are needed to address this issue. To better and more accurately compare studies conducted by different research groups and ensure more reproducible standardized procedures for testing different wavelengths of visible light for bacterial inactivation, additional protocols should be developed.

### 3.2. Pigments with photoprotective or photosensitizing properties

In this section, we define pigments as endogenous molecules primarily responsible for coloration and light absorption in bacterial cells. While porphyrins and flavins exhibit strong absorption in the visible spectrum, they are discussed in the context of their roles as cofactors and photosensitizers rather than structural pigments. Pigments produced by several bacterial species can also act as endogenous PSs.

#### 3.2.1. Staphyloxanthin in Staphylococcus aureus

*S. aureus*, including methicillin-resistant *S. aureus* (MRSA), produces the characteristic golden yellow pigment staphyloxanthin (STX), which is important for maintaining structural membrane stability and defending against oxidative stress and immune cell evasion (Valliammai et al., 2021; Clauditz et al., 2006; Liu et al., 2005). It has been reported that STX displays a prominent absorbance peak at 460 nm. A comprehensive analysis employing both Raman spectroscopy and mass spectrometry revealed that exposing isolated STX to aBL at a wavelength of 460 nm leads to the cleavage of its conjugated C═C double bonds and its photolysis. Moreover, STX photolysis also contributes to increased hydrogen peroxide entry into bacterial cells (Marshall & Wilmoth, 1981; Dong et al., 2019). However, an analysis performed by Dong et al. (2019) revealed that STX photolysis alone is not sufficient to eradicate MRSA.

#### 3.2.2. Granadaene in Streptococcus agalactiae

*S. agalactiae* is a beta-hemolytic agent and one of the leading causes of delayed wound healing and infection within cutaneous wounds, alongside *S. aureus* and *P. aeruginosa* (Rosa-Fraile et al., 2006; Angel et al., 2011; Armistead et al., 2020). It produces the red–orange pigment granadaene, which plays a dual role: it contributes to hemolytic activity and provides protection against cellular oxidative stress (Whidbey et al., 2013; Liu et al., 2004). Notably, granadaene has been described both as an antioxidant and a photosensitizer susceptible to degradation upon light exposure (Jusuf et al., 2021). Although these roles may appear contradictory, they are likely dependent on environmental factors such as oxygen levels and light availability. Like most pigments, granadaene contains a highly conjugated C═C system that renders it photosensitive, and similar to the role of STX in *S. aureus*, granadaene contributes to the survival and virulence of *S. agalactiae* (Rosa-Fraile et al., 2006; Armistead et al., 2020). Investigations into the role of granadaene have indicated that the pigment plays a role as an antioxidant that protects *S. agalactiae* from oxidative damage and is involved in its hemolytic activity (Whidbey et al., 2013; Liu et al., 2004). An examination of the effects of three wavelengths of light (430 nm, 460 nm, and 490 nm) on granadaene pigment demonstrated that light at a wavelength of 430 nm caused the greatest photodegradation of granadaene. Moreover, photobleaching of granadaene by light at 430 nm markedly diminished the hemolytic activity of *S. agalactiae* by almost 50%, providing additional evidence of the substantial involvement of this pigment in the hemolytic activity of this pathogen. Moreover, photobleaching of granadaene can greatly diminish the antioxidant activity of *S. agalactiae*, significantly depleting its ability to resist oxidative stress (Jusuf et al., 2021).

#### 3.2.3. Conclusions

In conclusion, pigments such as staphyloxanthin and granadaene represent a distinct group of endogenous chromophores that contribute to both the defense and vulnerability of bacterial cells under aBL exposure. Their highly conjugated structures enable light absorption, which under certain conditions can lead to photodegradation and enhanced susceptibility to oxidative damage. While these pigments primarily serve protective roles, such as membrane stabilization or antioxidative defense, they can also act as photosensitizers that mediate ROS generation through photochemical reactions upon aBL exposure. The dual functionality of these molecules highlights the context-dependent nature of their effects and underscores the importance of environmental factors, such as light wavelength and oxygen availability. Understanding the photoreactivity and biological roles of bacterial pigments may offer new insights into species-specific responses to aBL and guide the development of targeted photoinactivation strategies.

The key endogenous photosensitizers proposed to mediate aBL effects include porphyrins (coproporphyrin, protoporphyrin IX, uroporphyrin I), flavins (FMN, FAD, riboflavin), and bacterial pigments such as staphyloxanthin and granadaene. Their chemical structures and absorption spectra are summarized in Fig. 2, which highlights their absorption maxima within the blue-light region (400–470 nm). Notably, porphyrins and flavins absorb strongly in this spectral window, whereas pigments such as staphyloxanthin and granadaene exhibit broader absorption profiles that may contribute to both photoprotection and photosensitization, depending on the cellular context.

Although porphyrins, flavins, and other endogenous pigments are often studied as distinct contributors to aBL activity, establishing a universal or quantitative ranking of their relative contributions remains challenging. Their impact is highly context-dependent and shaped by wavelength, oxygen availability, and bacterial physiology. Porphyrins, owing to their strong absorption in the near-UV/blue range and high singlet oxygen yield, tend to dominate aBL-mediated photoinactivation in porphyrin-producing bacteria under aerobic conditions. In contrast, flavins and flavin-derived photoproducts may contribute more prominently at longer blue wavelengths or in organisms with limited porphyrin biosynthesis, where redox cycling and type I pathway become relatively more important. This context-dependent interplay highlights that aBL efficacy arises from multiple photochemical pathways rather than from a single universally dominant chromophore class. To facilitate this comparison, a conceptual summary table is provided below that contrasts porphyrins, flavins, and other selected bacterial pigments across absorption wavelengths, photochemical pathways, and representative bacterial contexts (Table 1).

## 4. Susceptibility of *Streptococcus* and *Enterococcus* to aBL

Despite the crucial role of endogenous porphyrins in mediating aBL efficacy, bacteria from the *Streptococcus* and *Enterococcus genera* lack porphyrin biosynthesis pathways. This biochemical limitation has raised questions about their susceptibility to aBL. This section summarizes current knowledge on aBL activity against representative *Streptococcus* and *Enterococcus* species, highlighting strain-specific differences, potential alternative photosensitizers, and emerging insights into the underlying mechanisms.

### 4.1. General characteristics of lactic acid bacteria and aBL susceptibility

The focus on *Streptococcus* and *Enterococcus* species in this section is intentional and reflects their value as informative case studies for understanding species-dependent susceptibility to aBL. Unlike UV radiation, which exerts largely species-independent antimicrobial effects through direct DNA damage, aBL efficacy is strongly influenced by the presence, type, and abundance of endogenous chromophores. Lactic acid bacteria (LAB), including *Streptococcus* and *Enterococcus*, lack canonical porphyrin biosynthesis pathways (König & Fröhlich, 2017). As a consequence, these bacteria are intrinsically less susceptible to aBL and therefore particularly useful models for dissecting chromophore-independent or alternative mechanisms of aBL action. Therefore, this section emphasizes bacterial taxa that challenge the conventional porphyrin-centered paradigm of aBL, rather than aiming to provide a comprehensive comparison across all microbial domains.

**Table 1**
Conceptual comparison of endogenous chromophores contributing to aBL activity.

| Chromophore class | Representative molecules | Major absorption range (nm) | Dominant photochemical pathway | Typical bacterial taxa | Contexts of dominant contribution | Key limitations | References |
|---|---|---|---|---|---|---|---|
| **Porphyrins** | Coproporphyrin, Protoporphyrin IX, Uroporphyrin I | ~400–415 (Soret band) | Type II (singlet oxygen, $^1O_2$) | Porphyrin-producing Gram+ and Gram− | Shorter blue wavelengths (~405 nm); high phototoxic efficiency | Absent in many taxa; activity modulated by localization and antioxidant defenses | Plavskii et al., 2018; Kumar et al., 2015; Frankenberg et al. 2002; Aihara, 2008 |
| **Flavins** | FMN, FAD, riboflavin | ~375 and 450–460 | Type I / mixed ROS pathways | Broadly distributed across bacteria, incl. porphyrin-deficient species | Longer blue wavelengths (450–460 nm); higher doses; redox-active environments | Lower phototoxic efficiency per photon; requires higher fluence | Eley et al., 1970; Plavskii et al., 2018; Liang et al., 2015; Edwards, 2014; |
| **Pigments** | Staphyloxanthin, granadaene | Broad, ~430–490 | Mixed (photobleaching, indirect ROS effects) | Pigment-producing pathogens (*S. aureus*, *S. agalactiae*) | Species-specific; modulation of virulence and oxidative stress responses | Often photoprotective; photolysis alone rarely bactericidal | Dong et al., 2019; Jusuf et al., 2021; Liu et al., 2004 |

Note: Relative contributions are context-dependent and cannot be universally ranked; dominance reflects experimental and physiological conditions rather than intrinsic chromophore potency.

Although porphyrins are considered the main endogenous PSs allowing effective aBL inactivation, multiple studies have examined the susceptibility of *Streptococcus* and *Enterococcus* species to aBL.

### 4.2. *Streptococcus mutans*

Most of the research on *Streptococci* has been performed on *Streptococcus mutans*. None of the researchers using light at 450 nm or higher wavelengths, regardless of the light dose (18–206 J/cm$^2$), reported greater viability reductions than 0.2 $\log_{10}$ units for both planktonic and biofilm cultures (Feuerstein et al., 2004; Paschoal et al., 2013; Pereira et al., 2013; Kim et al., 2018; Shiotsu-Ogura et al., 2019). Additionally, irradiation doses between 9.26 and 831 J/cm$^2$ at 405 nm reduced the viability from 0 to 1 $\log_{10}$ units for both the biofilm and planktonic cultures (Maisch et al., 2009; Paschoal et al., 2015; Gomez et al., 2016; Merigo et al., 2019; Felix Gomez et al., 2019; Nikinmaa et al., 2020; Mohamad et al., 2021). Even though aBL had no significant effect on *S. mutans* biofilm viability, Lins de Sousa et al., 2015 reported that the insoluble exopolysaccharide (EPS) level and bacterial dry weight were reduced and that the biofilm morphology was altered (Lins de Sousa et al., 2015). On the other hand, Cohen-Berneron et al. (2016) reported that after aBL treatment, biofilm growth increased; however, reduced acid and polysaccharide production was also reported in this study (Cohen-Berneron et al., 2016). This paradoxical outcome likely reflects a dose-dependent phenomenon. At sublethal fluences, aBL may not trigger bactericidal effects but rather photobiomodulation (PBM), a response involving mild oxidative signaling, transient metabolic activation, and altered gene expression. PBM-like effects have been documented in bacteria and other non-mammalian systems, where low-intensity light can stimulate metabolism and growth (Dai et al., 2012; Hamblin et al., 2019; Yin et al., 2013). Thus, the outcome of aBL exposure in *S. mutans* biofilms may depend on the balance between photobiomodulatory signaling and oxidative stress. In complex microbial communities, this balance may shift through interspecies interactions or the presence of exogenous chromophores, which alter local light absorption and ROS dynamics. Chebath-Taub et al. (2012) reported a reduced number of *S. mutans* cells in a biofilm regrown after aBL irradiation (Chebath-Taub et al., 2012). *S. mutans* was also more sensitive to other treatments, such as fluoride or hydrogen peroxide, after exposure to aBL (Steinberg et al., 2008; Tsutsumi-Arai et al., 2022). Interestingly, Tsutsumi-Arai et al. (2022) reported that after 405 nm aBL irradiation of *S. mutans* and *Candida albicans* dual-species biofilms (379.7 J/cm$^2$), *S. mutans* viability was reduced by more than 4 $\log_{10}$ units. The same researchers demonstrated the presence of coproporphyrin and protoporphyrin in *S. mutans* cells and determined that their concentrations were approximately 10-fold lower than those in *C. albicans* cells. This raises the question of whether the surprisingly high effectiveness of aBL against *S. mutans* in dual-species biofilms may be the result of the absorption of porphyrins produced by *C. albicans* (Tsutsumi-Arai et al., 2022).

### 4.3. *Other Streptococcus species*

For biofilm cultures of *S. sanguinis,* regardless of the light source and light dose (95–146 J/cm$^2$), the reduction in viability did not exceed 0.2 $\log_{10}$ units (Pereira et al., 2013; Shany-Kdoshim et al., 2019). Roh et al. (2016) reported a reduction in the viability of planktonic cultures of *S. iniae* and *S. parauberis* ranging between 2.9 and 3.5 $\log_{10}$ units for both 405 nm and 465 nm wavelengths, but the time required to obtain such an effect was 6–24 h of irradiation. The low irradiance applied (7.4 mW cm$^{-2}$ at 405 nm and 13.3 mW cm$^{-2}$ at 465 nm) likely explains the extended exposure times required for effective inactivation. (Roh et al., 2016). Bumah et al. reported that irradiation of *S. agalactiae* planktonic cultures with three pulses of light at a wavelength of 450 nm and a dose of 7.6 J/cm$^2$ did not reduce viability. The addition of exogenous PpIX or coproporphyrin resulted in a reduction in the viability of up to 9.54 $\log_{10}$ units, but the addition of FMN, FAD, nicotinamide adenine dinucleotide (NAD) or NADH did not result in a significant reduction in viability. They concluded that porphyrins are necessary for the efficacy of aBL against *S. agalactiae* (Bumah et al., 2020; Bumah et al., 2021). Interestingly, both PpIX and coproporphyrin exhibit only weak absorption around 450 nm (Kolarova et al., 2008; Glowacka-Sobotta et al., 2024), which suggests that the pronounced effect observed by Bumah et al. may involve indirect excitation pathways or secondary photochemical reactions leading to enhanced ROS generation. Consistent with this, Jusuf et al. (2021) demonstrated that although exposure of *S. agalactiae* to 430 nm aBL alone did not reduce viability, it increased its susceptibility to hydrogen peroxide and daptomycin. This response was associated with the photobleaching of granadaene, which suggests photolytic degradation and loss of its ROS-scavenging function (Jusuf et al., 2021).

Surprisingly, two independent studies demonstrated high susceptibility of *Streptococcus pyogenes* to aBL (405 nm). Maclean et al. (2009) reported a ~5 $\log_{10}$ CFU reduction in planktonic cultures exposed to aBL exposures of 32 and 54 J cm$^{-2}$ (10 mW cm$^{-2}$), while Shehatou et al. (2019) achieved eradication ($\geq$ 8 $\log_{10}$ CFU reduction) of *S. pyogenes* at light doses of up to 36 J cm$^{-2}$ (5–25 mW cm$^{-2}$) (Maclean et al., 2009; Shehatou et al., 2019). *S. pyogenes* is the only *Streptococcus* in which a dedicated heme uptake system similar to that present in other gram-positive bacteria has been identified thus far (Baureder & Hederstedt, 2013). The high efficacy of heme acquisition from the

environment in *S. pyogenes* may be the cause of its greater susceptibility to aBL than other Streptococci species.

### 4.4. Enterococcus faecalis and E. faecium

For the *Enterococcus* group, the irradiation of *E. faecalis* with aBL for 8 min or less with doses ranging from 19.3 to 206 J/cm$^2$ led to reductions in viability of less than 1 $\log_{10}$ units, regardless of the light wavelength used and whether the cells were planktonic or sessile within a biofilm (Feuerstein et al., 2004; Maisch et al., 2009; Pileggi et al., 2013; Ferrer-Espada et al., 2020; Borba et al., 2017; Chiniforush et al., 2020; Sampaio et al., 2020; Moradi et al., 2022).

Under more prolonged exposures, however, measurable photoinactivation was observed. Irradiation of *E. faecalis* planktonic cultures with 405 nm aBL at an irradiance of 10 mW/cm$^2$ and a total fluence of 216 J/cm$^2$ led to a 2.6 $\log_{10}$ CFU reduction after 6 h, whereas biofilm cultures exposed to 60 mW/cm$^2$ for 60 min (216 J/cm$^2$) showed only a 0.84 $\log_{10}$ CFU reduction (Maclean et al., 2009; Ferrer-Espada et al., 2020). Interestingly, both studies achieved comparable reductions (~0.8 $\log_{10}$) at the same radiant exposure (216 J/cm$^2$) despite a sixfold difference in irradiance, suggesting that *E. faecalis* tolerance to aBL is determined not by light dose alone but by intrinsic biological factors, including its low porphyrin content, strong antioxidant defenses, and the protective architecture of its biofilm (Maclean et al., 2009; Ferrer-Espada et al., 2020). At even higher aBL doses, the extent of inactivation increased substantially. Exposure to 405 nm at 432–885 J/cm$^2$ reduced the viability of *E. faecalis* planktonic cultures by 4.7–5 $\log_{10}$ units (Zhang et al., 2020; Gupta et al., 2015).

Additionally, Pourhajibagher et al. (2024) demonstrated that the use of aBL at 450 nm against *E. faecalis* reduced the regrowth potential of *E. faecalis* biofilms (Pourhajibagher et al., 2024). In contrast, the irradiation of *E. faecium* with 405 nm light doses of up to 530 J/cm$^2$ did not lead to any reduction in viability (Shehatou et al., 2019; Bauer et al., 2021; Cong et al., 2023). The use of even higher light doses at either 405 or 450 nm wavelengths (648–1000 J/cm$^2$) reduced the viability of *E. faecium* planktonic cultures to between 1.86 and 3.06 $\log_{10}$ units (Halstead et al., 2016; Hoenes et al., 2021b; Bauer et al., 2021).

### 4.5. Other Enterococcus species

A similar viability reduction to that observed for *E. faecium* (~ 3 $\log_{10}$ CFU) was reported when a 1296 J/cm$^2$ dose of 405 nm light was applied against *Enterococcus moraviensis* (Hoenes et al., 2021b). The same research group reported that *E. moraviensis* is more susceptible to inactivation with aBL at 405 nm than with aBL at 450 nm, and the authors suggested that NADH and lumichrome are most likely involved as photosensitizing agents (Hessling et al., 2020). Since lumichrome is a photodegradation product of flavins, its involvement could explain why only high total light exposures (J/cm$^2$), rather than merely long irradiation times, very long irradiation periods are effective against *Enterococcus* and most *Streptococcus* species.

The generally low susceptibility of *Streptococcus* and *Enterococcus* to aBL can be interpreted in the context of an integrated physiological framework combining limited endogenous chromophore availability, distinctive membrane architecture, and a fermentative metabolic state. As LAB, these organisms lack canonical porphyrin biosynthesis and rely primarily on glycolysis, resulting in altered intracellular redox balance and reduced electron transport activity (Abranches et al., 2018). At the same time, streptococci possess highly effective ROS detoxification and repair systems, including SodA-, AhpC-, and GpoA-mediated pathways, which have evolved to counter oxidative stress encountered during host infection (Henningham et al., 2015). Within this context, aBL-induced ROS are more likely to elicit sublethal oxidative signaling or photobiomodulatory responses rather than direct bactericidal effects, unless unusually high radiant exposures or auxiliary photosensitizing factors are present.

Altogether, the evidence discussed above highlights that LAB genera such as *Streptococcus* and *Enterococcus* generally display low susceptibility to aBL, likely due to the absence of endogenous porphyrins. However, exceptions exist (*S. pyogenes*, *E. moraviensis*), possibly due to alternative photosensitizers or heme uptake systems. The exact mechanisms underlying aBL sensitivity in LAB remain to be fully elucidated.

The bacterial effect of aBL on LAB representatives is presented in Fig. 3.

The consistently low susceptibility of most *Streptococcus* and *Enterococcus* species to aBL, in contrast to porphyrin-producing bacteria, provides indirect evidence that endogenous porphyrins are the primary photosensitizers mediating the photodynamic effect of aBL. At the same time, these observations highlight that aBL is not uniformly robust across bacterial taxa and that, in certain physiological contexts such as porphyrin-deficient LAB, its efficacy may be inherently limited despite the presence of oxidative stress. Recent mechanistic studies further support this view, demonstrating that ROS generation alone does not guarantee bactericidal outcomes and that membrane composition, redox buffering capacity, and metabolic state critically shape the effectiveness of light-induced oxidative damage (Rapacka-Zdonczyk, 2025; 2026).

## 5. Molecular targets and lethal mechanisms of aBL

The bactericidal effects of aBL are primarily mediated through the photochemical generation of ROS, which subsequently induce oxidative stress responses within bacterial cells. It has been established that endogenously produced chromophores such as porphyrins and flavins (as discussed earlier) within bacterial cells can absorb blue light, leading to the excitation of these molecules and the transfer of energy to molecular oxygen. This process generates various ROS, including singlet oxygen ($^1O_2$), superoxide anions ($O_2^{\bullet -}$), hydrogen peroxide ($H_2O_2$), and hydroxyl radicals (•OH). These ROS induce oxidative damage to critical cellular components.

Numerous studies have investigated the mechanisms of aBL-induced bacterial cell death, and the most commonly observed effects include DNA damage, membrane depolarization, protein carbonylation, and cell wall damage (Leanse et al., 2022). To date, which structures are most important in aBL-mediated photokilling of bacterial cells has been the subject of many studies. Most of the information on damage to cellular biomolecules under the influence of the photodynamic reaction, including that generated by aBL, comes from in vitro studies. These studies show that virtually all biomolecules (proteins, DNA, lipids, sugars) can undergo oxidative damage (Fig. 4). However, the direct cause of bacterial cell death remains unknown.

### 5.1. Membrane disruption and lipid peroxidation

Lipid is important to the physiology of a bacterial cell, as it is a major structural component of the cytoplasmic membrane that maintains the integrity of the cell and ensures normal transmembrane potential. Lipid and membrane damage can directly lead to cell death (Ayala et al., 2014). If highly reactive radicals or singlet oxygen are generated near key lipids such as cell membrane phospholipids, a radical chain reaction phenomenon can occur. This reaction propagates along the surface of the membrane, reducing its fluidity and consequently disrupting its proper function. As a result of ROS overproduction, the proton potential can be disrupted, and ultimately, the membrane can rupture, and ions can leak outside the cell, leading to cell death. Recently, aBL-mediated lipid peroxidation has been experimentally demonstrated in living cells of both gram-positive and gram-negative species (Dos Anjos et al., 2023). Membrane damage is detrimental to the physiology of a bacterial cell, as leakage of cell contents leads directly to cell death. Increased membrane permeability under the influence of aBL has been reported in several studies, but the exact mechanism has not yet been elucidated (Wu et al., 2018; Kim et al., 2016; Chu et al., 2019). Interestingly, a recent study revealed that after aBL treatment, the transmembrane

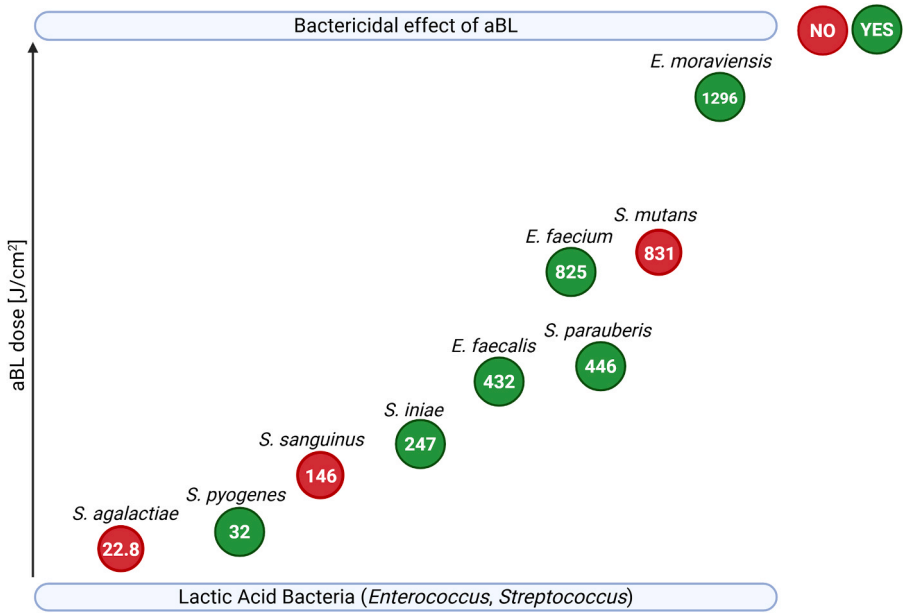


**Fig. 3.** Effect of aBL on representatives of the *Streptococcus* and *Enterococcus* species. The aBL dose used for a particular strain is described in the center of the circles. The red circles represent no or weak inactivation effects, and the green circles represent the inactivation effects of aBL. It should be noted that the light exposures reported in different studies are not directly comparable because of variations in experimental setups, irradiance levels, and biological models. Nevertheless, this compilation provides a general overview of the relative aBL susceptibility trends among *Streptococcus* and *Enterococcus* species.

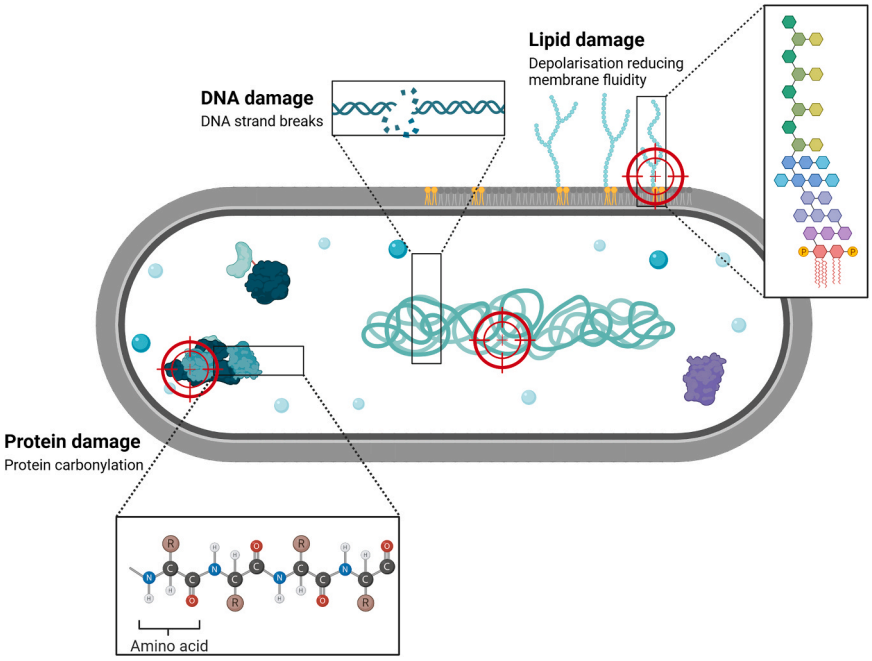


**Fig. 4.** aBL targets. aBL irradiation causes numerous toxic effects, including DNA damage, membrane depolarization, protein carbonylation, and cell wall damage.

potential of bacterial cells is reduced, which correlates with rapid cell death. The authors observed the rapid effect of aBL on cell viability but not on the induction of mutations that reduce bacterial cell viability in the long term (Hoenes et al., 2021a). In contrast, studies conducted on a *Salmonella* model indicate that aBL does not cause damage to the membrane but rather to membrane-anchored proteins such as glucose transporters or efflux systems (Kim & Yuk, 2017). Other authors have reported that aBL can generate ROS via cytochromes containing a heme prosthetic group in their structure. Bacterial cytochromes are anchored to the cytoplasmic membrane, so there is a possibility of aBL-mediated ROS generation on the basis of the heme moiety and damage localized near the cell membrane (Fraikin et al., 1996).

### 5.2. Genetic instability and oxidative DNA lesions

DNA damage deserves special attention because its formation can result in new mutations. Among the ROS produced during aBL treatment, the hydroxyl radical poses the greatest threat to DNA, mainly because of the variety of types of reactions in which it can participate as well as its high oxidative potential (Halliwell et al., 2021). DNA damage generated by the action of the hydroxyl radical can lead to strand breaks, the formation of cross-links between proteins and DNA, or cross-links

between DNA strands. Consequently, this can lead to the disruption of replication, transcription, and translation processes and ultimately to cell death. To date, however, there is a lack of direct data on the effects of the ROS generated during aBL treatment on the aforementioned processes. Nevertheless, aBL, similar to aPDT, is generally considered a multi-target approach, in which DNA represents one of several potential intracellular targets. However, aBL can induce DNA damage in some bacterial species, especially at relatively high levels of exposure, as indicated by measured levels of 8-oxo-D-guanine (8-OHdG) (Kim et al., 2017; Yoshida et al., 2017). A study by Grinholc et al. (2015) revealed that aBL induces DNA damage in living cells and the production of the repair protein RecA indirectly through the formation of single-strand DNA (ssDNA), but importantly, this response was not associated with mutagenesis. In contrast, other authors reported no DNA damage after aBL treatment (Kim et al., 2016), suggesting that a threshold level of light exposure may be required to trigger DNA lesions. Studies conducted on microorganisms sensitive and resistant to electromagnetic radiation revealed that severe death from exposure to oxidative stress was directly caused by protein damage, not DNA damage (Daly et al., 2007). Thus, determining whether DNA damage is the cause of aBL-induced cell death requires further investigation.

### 5.3. Protein oxidation and enzymatic failure

The damage to proteins that occurs in cells after aBL treatment-mediated ROS production seems to contribute the most to the cytotoxic effect of aBL treatment. This is primarily because proteins are the most accessible biomolecules, and most of them are present in any cell (Feijó Delgado et al., 2013). Proteins are localized throughout the cellular space, so regardless of where endogenous PSs are formed, they are in contact with them. Moreover, proteins, especially enzymatic proteins, are responsible for all metabolic processes occurring in bacterial cells. Both hydroxyl radicals and singlet oxygen can lead to protein carbonylation, which is an irreversible process (Maisonneuve et al., 2008). Importantly, even damage to a single amino acid residue in the structure of a protein can cause structural modifications and loss of function. Proteins that lose their normal structure are directed toward proteolytic cleavage or are deposited in cells in the form of aggregates. The accumulation of aggregates in the cell leads to severe toxicity. Moreover, reports are beginning to describe aBL-induced direct damage to bacterial proteins involved in basic cell metabolism, such as cellular respiration and proper protein folding (St. Denis et al., 2011; Walker et al., 2022).

Despite clear evidence of oxidative damage to multiple biomolecular targets, including lipids, DNA, and proteins, the exact sequence of events leading to bacterial cell death after aBL treatment remains incompletely defined. Protein damage appears to play a dominant role, while membrane destabilization and DNA damage may contribute in species-specific or dose-dependent contexts. Understanding which cellular components are most vulnerable to aBL-induced ROS will be essential for optimizing this modality as a targeted antimicrobial strategy.

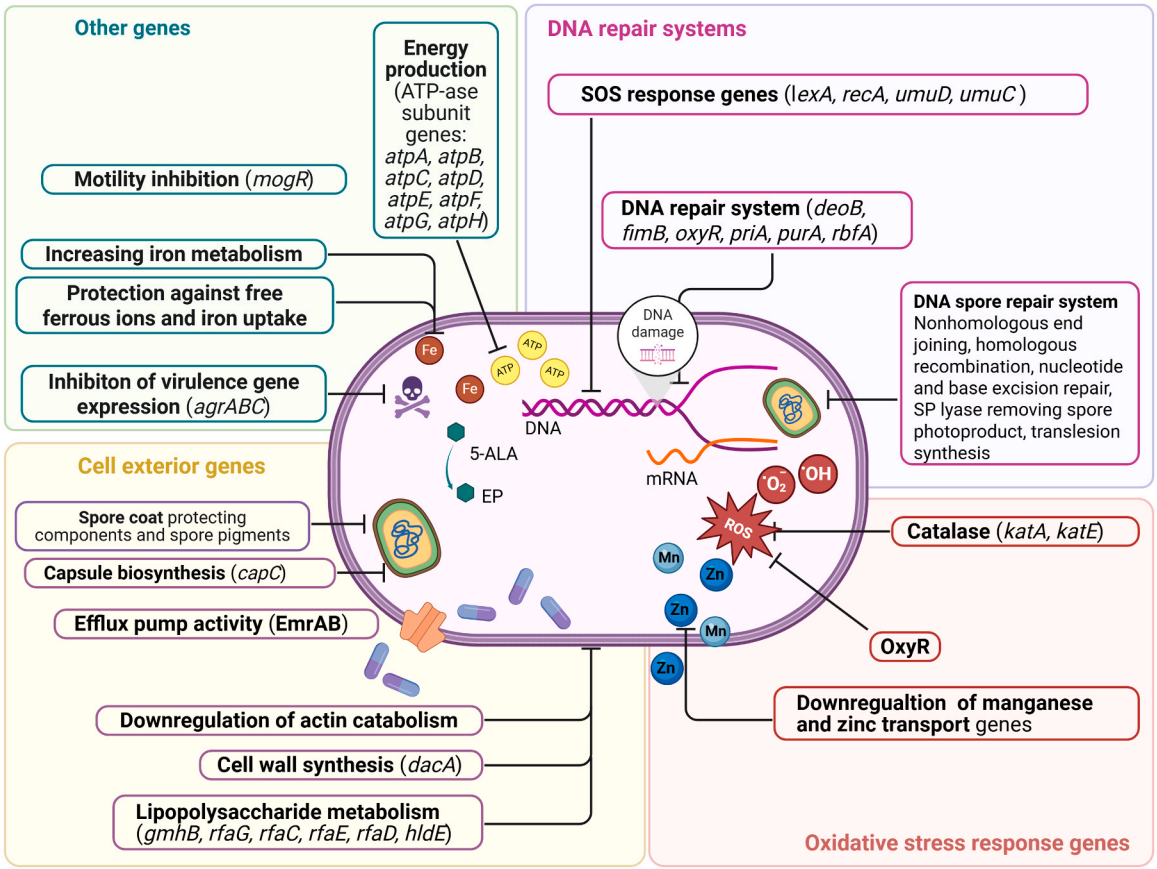


**Fig. 5.** Genetic and physiological determinants associated with bacterial response to aBL. The schematic highlights DNA repair systems, oxidative stress response genes, cell exterior genes, and other genetic pathways modulating susceptibility. Abbreviations: 5-ALA, 5-aminolevulinic acid; EP, exogenous photosensitizer; ROS, reactive oxygen species; $^1O_2$, singlet oxygen; •OH, hydroxyl radical; ATP, adenosine triphosphate; ATP-ase, adenosine triphosphatase; SOS (*lexA*, *recA*, *umuD*, *umuC*), bacterial DNA damage repair regulon; EmrAB, multidrug efflux pump; *dacA*, gene involved in peptidoglycan biosynthesis; *capC*, capsule biosynthesis gene; *gmhB*, *rfaG*, *rfaC*, *rfaE*, *rfaD*, *hldE*, genes involved in lipopolysaccharide biosynthesis; *katA/katE*, catalase isoenzymes; OxyR, transcriptional regulator of oxidative stress response; Mn, manganese; Zn, zinc.

## 6. Genetic factors influencing bacterial susceptibility to aBL

The genetic response of bacteria to aBL is complex and involves multiple interconnected cellular pathways. However, the specific genetic determinants underlying this response, including those influencing susceptibility, remain largely unexplored. It is likely that additional, yet unidentified genes contribute to bacterial sensitivity to aBL, but current data are limited to a few preliminary studies. The latest findings have grouped genes of interest into four categories: cell envelope-associated genes, genes involved in DNA damage response and repair, oxidative stress response genes and other genes, which are summarized in Fig. 5. Although genes involved in endogenous porphyrin/heme biosynthesis (e.g., *hemA–hemH*) are known to modulate intracellular photosensitizer levels in *E. coli* and thus influence sensitivity to photo-oxidative stress, their direct involvement in the genetic response to aBL has not yet been confirmed experimentally (no hem-gene hits in genome-wide aBL sensitivity screens).

### 6.1. Cell envelope-associated genes

Exposure to aBL triggers the expression of genes that enhance the structural and functional integrity of the bacterial cell envelope, limiting ROS penetration and cellular damage. Screening of single-gene mutants collected from nonessential *E. coli* genes revealed 64-aBL-hypersensitive mutants, almost 50% of which encode proteins localized in the outer part of the cell. These include proteins involved in cell wall biosynthesis (*dacA*) and lipopolysaccharide metabolism (*gmhB, rfaG, rfaC, rfaE, rfaD, hldE*) (Kruszewska-Naczk et al., 2024). Additionally, Hu et al. (2021) reported a crucial role of the *rfaC* gene in aBL sensitivity after observing increased sensitivity of the Δ*rfaC* mutant strain to aBL. The protein encoded by this gene is important in linking the core region of LPS to lipid A, and mutation leads to changes in the fatty acid profiles of the cell membrane. Researchers have concluded that these changes lead to increased membrane permeability of the mutant strains following aBL irradiation compared with that of the wild-type strain, which may also confer sensitization to aBL (Hu et al., 2021). Wan et al. (2022) reported that antiholin-like protein (LrgA), which is involved in biofilm modulation and autolysis due to alternations in murein hydrolase activity, also plays an important role in modulating photokilling efficiency. A mutant with constitutively expressed *lrgA* was more sensitive to phototherapy (Wan et al., 2022). A later report indicated that the *lrgA* gene can modulate the response of *S. aureus* to aBL (460 nm) via modulation of the antioxidant response and autolysis (Yang et al., 2024).

### 6.2. Genes involved in DNA damage response and repair

A key genetic pathway implicated in the bacterial response to aBL is the SOS response system, which reacts to ROS-induced DNA damage. The two main regulators of this system are LexA and RecA. RecA is essential for the bacterial response to phototreatment, as a lack of RecA increases the level of light-induced DNA damage (Grinholc et al., 2015). Moreover, a mutant lacking *recA* was unable to develop tolerance to aBL (411 nm) (Rapacka-Zdonczyk et al., 2021). Interestingly, blocking RecA with dedicated inhibitors did not increase the bactericidal activity of aBL (Metzger et al., 2022). This may indicate that RecA-mediated repair represents only one component of a multilayered stress response network. Redundant DNA repair and antioxidant systems could compensate for its inhibition, preventing further enhancement of aBL lethality.

RecA also plays a crucial role in the development of resistance to the ROS-generating antibiotics amoxicillin and enrofloxacin (Händel et al., 2016). This finding is consistent with previously published studies indicating that the ROS generated during aPDI and aBL treatment, such as hydrogen peroxide and singlet oxygen, can cause oxidative DNA damage and activate the SOS response (Goerlich et al., 1989). Another component of the SOS system, *umuD* and *umuC* (encoding error-prone DNA polymerase V), which are regulated by *recA*, is important in the development of tolerance to aBL (411 nm) in gram-negative bacteria, as mutants lacking these genes do not develop tolerance to photoinactivation (Rapacka-Zdonczyk et al., 2021). The single-gene mutant lacking *umuD* was also reported to be aBL hypersensitive, and complementation of this gene restored the wild-type phenotype (Kruszewska-Naczk et al., 2024).

The role of various protection and DNA repair systems in *Bacillus subtilis* spores was investigated by comparing the sensitivity of spores of the wild-type strain and spores of mutants established by knocking out genes involved in the response to aBL at 400 nm (Djouiai et al., 2018). Compared with the wild-type strain, mutants lacking the spore coat-protecting components *sspA-sspB, dacB, cotE, cotA, cotE-gerE, and cotE-sspA-sspB* were more sensitive to aBL. The proteins encoded by the deleted genes are spore coat and pigment proteins; acid-soluble spore proteins (SASP), which protect the DNA from damage; and proteins involved in the regulation of the spore water content. Additionally, almost all of the tested mutants with aberrant DNA repair systems were more sensitive to aBL than were the wild-type strains. The genes that were deleted are responsible for nonhomologous end joining (NHEJ), homologous recombination (HR), nucleotide excision repair (NER), base excision repair (BER), SP lyase (SPL) removal of the spore photoproduct (SP), and translesion synthesis (TLS). Interestingly, the spores of the strains lacking RecA, a protein that is involved in, among other processes, the SOS response, were not significantly more sensitive than the wild-type strain spores were. All of these findings suggest the complexity of the spore response to aBL and the engagement of many DNA repair systems and spore exterior protective systems against aBL (Djouiai et al., 2018).

The use of different DNA repair systems was also confirmed in *E. coli,* where single-gene mutants lacking *deoB, fimB, oxyR, priA, purA, rbfA, rnt,* and *umuD* were more susceptible to aBL than the wild-type strain was. The important role of these genes in the aBL response was confirmed following the restoration of the aBL sensitivity profile via the complementation of the *deoB, fimB, oxyR, purA, rbfA,* and *umuD* genes. In addition to canonical DNA repair genes, several energy-related genes appear to modulate the bacterial response to aBL. Notably, mutants lacking subunits of the ATP synthase complex (*atpA*, *atpB*, *atpC*, *atpD*, *atpE*, *atpF*, *atpG*, and *atpH*) exhibited increased sensitivity to aBL. Although these genes are not directly involved in DNA repair, the energetic demands of repair systems under oxidative stress likely render ATP availability a critical factor in maintaining cellular tolerance to photoinactivation (Kruszewska-Naczk et al., 2024).

### 6.3. Oxidative stress response genes

During aBL irradiation, bacteria are exposed to ROS generated through photochemical reactions. To counteract the resulting oxidative stress, they employ antioxidant strategies. One is the activation of catalase, which scavenges $H_2O_2$ and protects bacteria against the toxic effects of the ROS generated during photoinactivation. Orlandi et al. (2018) reported that a *Pseudomonas aeruginosa* PAO1 mutant lacking *katA* (encoding catalase) was significantly more sensitive to aBL (464 nm) than the wild-type strain was. Moreover, complementation of the mutation restored the wild-type phenotype, suggesting the protective role of KatA in the cellular response to aBL. Interestingly, the overexpression of *katA* did not affect the sensitivity of *P. aeruginosa* to aBL (Orlandi et al., 2018). The lack of additional protection upon *katA* overexpression might indicate that catalase activity is not the limiting factor under aBL exposure, or that other types of ROS, such as singlet oxygen, play a more dominant role.

Other studies have demonstrated that aBL (approximately 465–470 nm) modulates many cellular processes in *Acinetobacter baumanii*. One of them may be an oxidative stress response, including KatE catalase activity regulated by the BlsA enzyme (Müller et al., 2017; Squire et al., 2022). Compared with the wild-type strain in the dark, the

*blsA*-lacking mutant presented no significant difference in catalase activity. However, complementation of the mutation resulted in greater catalase activity in the light than in the dark. Moreover, *S. aureus* has been reported to have reduced $H_2O_2$ susceptibility after aBL irradiation (Tomb et al., 2017; Rapacka-Zdonczyk et al., 2019). In response to aBL-induced oxidative stress, bacteria can increase the expression of the *katA* gene, which encodes the $H_2O_2$-scavenging catalase protein, thus resulting in greater tolerance to $H_2O_2$ (Dosselli et al., 2012). However, another study conducted by Dong et al. (2022) reported that catalase can be inactivated by aBL via heme ring dissociation. Interestingly, high-peak power pulsed light inactivates this enzyme more effectively than does continuous light at the same wavelength (Dong et al., 2022). These seemingly opposite findings likely reflect differences in experimental conditions and light regimens. Under low-intensity exposure, aBL can trigger the expression of antioxidant enzymes such as catalase, whereas higher intensities or pulsed irradiation may promote direct photoinactivation of heme-containing enzymes. Thus, aBL may both induce and impair antioxidant defenses, depending on the species, light dose, and physiological state of the cells.

One of the main regulators of the oxidative stress response in *E. coli* is OxyR, which is activated in response to ROS accumulation and oxidative stress. A mutant lacking *oxyR* was also found to be aBL-hypersensitive. Interestingly, complementation of this gene led to increased tolerance to aBL compared with the wild-type strain (*E. coli* BW25113), which also supports the hypothesis of the toxic effect of ROS during aBL irradiation (Kruszewska-Naczk et al., 2024).

Two major regulators of the response to ROS generated by environmental blue light have been described in *Vibrio cholerae*: the anti-sigma factor (ChrR) and the putative metalloregulatory-like protein (MerR). The gene expression patterns in the Δ*chrR* and Δ*chrR*Δ*merR* knockout mutants after irradiation differed from those in the wild type strain, which may suggest that these genes separately or together regulate the effects of ROS on *V. cholerae* gene expression (Tardu et al., 2017).

## 7. Transcriptomic responses to aBL-induced oxidative stress

aBL irradiation is associated with genome-wide alterations in gene expression in both gram-negative and gram-positive bacteria (Tardu et al., 2017; Amin et al., 2016; Walker et al., 2022; Müller et al., 2017; Adair & Drum, 2016; Dorey et al., 2019; Santamaría-Hernando et al., 2020). Key genes regulated by aBL encode proteins involved in the oxidative stress response and chaperone proteins involved in protein refolding in response to ROS (Tardu et al., 2017; Amin et al., 2016; Walker et al., 2022; Chu et al., 2019; Luo et al., 2022; Müller et al., 2017; Adair & Drum, 2016; Dorey et al., 2019; Santamaría-Hernando et al., 2020). However, aBL-induced transcriptomic remodeling extends beyond classical stress pathways. Importantly, recent time-resolved comparative transcriptomic profiling across multiple mechanistically distinct photodynamic modalities has revealed that these responses are not random or treatment-specific artifacts, but rather converge on a conserved ROS-driven regulatory architecture. Despite differences in chromophore chemistry (Type I versus Type II photochemical pathways), short-term exposure to both aBL and exogenous photosensitizer-based aPDI triggered a coordinated induction of oxidative defense and sulfur metabolism pathways, accompanied by a global downshift in biosynthesis and energy-generating processes, affecting up to ~58% of the transcriptome. This convergence suggests that chromophore excitation funnels into shared oxidative signaling nodes, rather than generating modality-specific transcriptomic chaos. In contrast, prolonged exposure resulted in more restrained but treatment-specific metabolic rewiring, indicating that while acute responses reflect universal ROS pressure, long-term adaptation follows modality-dependent trajectories (Burzynska et al., 2026).

At a functional level, this conserved ROS-driven architecture manifests as regulatory changes affecting bacterial motility, central carbon metabolism, membrane composition, metal ion homeostasis, and virulence-associated functions. The following sections highlight the major transcriptomic shifts observed under aBL stress, focusing on five key adaptive processes: motility suppression, metabolic reprogramming, membrane and cell envelope remodeling, metal ion regulation, and virulence modulation.

### 7.1. Motility suppression

As an early adaptive response, bacteria often reprogram motility genes to conserve energy under aBL–induced oxidative stress. Dorey et al. (2019) demonstrated that in *Listeria monocytogenes*, genes regulated by the σB regulon, a key component of the general stress response, were upregulated after aBL irradiation. When upregulated, the sigma factor σB, located upstream of MogR (which represses motility genes), increases MogR levels, inhibiting bacterial cell motility (Dorey et al., 2019). Genes involved in chemotaxis and mobility were also found to be downregulated in *Vibrio cholerae* after aBL irradiation (Tardu et al., 2017; Müller et al., 2017). This is considered an energy-saving strategy since the general stress response is energy-consuming, and maintaining two energy-intensive processes simultaneously is burdensome for bacterial cells (Dorey et al., 2019).

### 7.2. Energy metabolism reprogramming

Although acute transcriptomic profiling reveals a global downshift in energy-intensive processes, species-specific studies indicate that selected ATP-generating pathways may be transiently upregulated to support immediate stress adaptation. To survive the oxidative challenge posed by aBL, bacteria upregulate ATP-generating pathways while downregulating nonessential processes. This energy-saving strategy may also explain the upregulation of pathways involved in energy generation (Adair & Drum, 2016), such as the citrate cycle (TCA cycle), oxidative phosphorylation, carbon metabolism (Tardu et al., 2017), carbohydrate and organic acid metabolism and transport (Santamaría-Hernando et al., 2020), and glycolysis/gluconeogenesis (Yang et al., 2024). In *Acinetobacter baumannii*, aBL induced the expression of genes involved in actin catabolism by binding the blue light-sensing protein BlsA to its repressor AcoN (Tuttobene et al., 2019).

### 7.3. Membrane and cell envelope remodeling

Since the cell envelope is a frontline defense for bacteria, aBL treatment induces transcriptomic shifts that alter membrane structure and transporter activity.

#### 7.3.1. Efflux and membrane permeability modulation

Transcriptomic analyses have revealed that aBL irradiation modulates membrane transporters and porins, contributing to drug susceptibility and oxidative defense changes. Müller et al. (2017) previously reported aBL-induced membrane alterations in *A. baumannii*, including increased EmrAB efflux pump activity, which contributes to minocycline and tigecycline susceptibility, and genes related to non-inherited fluoroquinolone tolerance (Müller et al., 2017). Moreover, the blue light sensor BlsA was shown to interact with the transcriptional regulator bipA, inducing OmpA expression, which alters membrane permeability and facilitates antibiotic uptake under photostress (Yang et al., 2023). Notably, available global transcriptomic datasets, including recent time-resolved analyses, do not indicate coordinated activation of canonical multidrug resistance regulons (e.g., mar/sox/rob systems) under aBL stress, but rather reflect oxidative stress-centered regulatory responses (Burzynska et al., 2026). This distinction is important, as modulation of membrane transporters under oxidative stress does not necessarily equate to induction of antibiotic resistance programs.

#### 7.3.2. Lipid remodeling and stress adaptation

Modifications in lipid biosynthesis pathways have also been associated with aBL adaptation. Notably, genes involved in cyclopropanation of fatty acids—a process enhancing membrane rigidity and ROS resistance—are upregulated in *Vibrio cholerae* upon exposure to aBL (Tardu et al., 2017). In *Campylobacter jejuni*, a reduction in the expression of lipid metabolism genes has been reported, possibly contributing to a decrease in membrane fluidity and affecting cellular homeostasis (Walker et al., 2022).

#### 7.3.3. Cell wall biosynthesis and capsule regulation

aBL also alters the transcription of genes involved in peptidoglycan (PG) metabolism. In MRSA strains, repeated aBL exposure resulted in upregulation of PG biosynthesis genes. In contrast, genes involved in PG hydrolysis were downregulated, leading to a thicker and more resilient cell wall structure (Luo et al., 2022). In *Cronobacter sakazakii*, aBL induced expression of CapC, which is associated with capsule biosynthesis, and similar effects were observed in *Staphylococcus aureus* (Adair &Drum, 2016; Yang et al., 2017). These envelope adaptations may contribute to increased survival under recurrent oxidative stress.

#### 7.3.4. Envelope biosynthesis inhibition and growth arrest

In contrast, some species show transcriptional repression of envelope-related genes in response to aBL. For instance, *C. jejuni* exhibits downregulation of genes involved in cell wall and membrane biosynthesis, suggesting a stress-induced arrest in cellular proliferation (Walker et al., 2022). Similarly, *Porphyromonas gingivalis* displayed downregulation of genes linked to DNA replication and cell cycle control, indicating a bacteriostatic effect under aBL treatment (Chui et al., 2012).

### 7.4. Metal ion regulation

Tight regulations of metal ions by bacteria are vital in fuelling defence enzymes and minimizing Fenton chemistry under light-induced oxidative conditions. Yuan et al. (2023) reported that aBL induces the upregulation of genes involved in protection against free ferrous ions and iron uptake, leading to increased heme-derived endogenous PS production and cell death. They also noted the downregulation of genes involved in manganese and zinc transport, decreasing the ability of *P. gingivalis* to eliminate ROS (Yuan et al., 2023). Genes involved in iron metabolism were similarly upregulated in *A. baumannii* (Müller et al., 2017), *S. aureus* (Yang et al., 2017), and *Pseudomonas syringae* pv. tomato (Santamaría-Hernando et al., 2020). These findings are particularly relevant because dysregulation of intracellular metal homeostasis can potentiate aBL-induced killing. Increased availability of ferrous ions promotes Fenton-type reactions and amplifies ROS formation, while reduced manganese and zinc uptake weakens antioxidant defenses, collectively enhancing the oxidative burden under blue-light stress (Imlay, 2013; Anjem et al., 2009; Wei et al., 2012; Touati, 2000).

### 7.5. Virulence modulation and prophage activation

aBL also impacts the expression of virulence determinants, potentially reducing bacterial pathogenicity and biofilm formation. The final group of genes altered by light irradiation at 400–450 nm is related to virulence, influencing the LrgA-AtlA axis, which is responsible for biofilm formation in *S. aureus* (Yang et al., 2024); trehalose production; the type 6 secretion system; the OB-fold protein in *A. baumannii* (Müller et al., 2017); and the MCP and type 3 secretion system in *P. syringae* pv. tomato (Santamaría-Hernando et al., 2020), with downregulation of *agrABC* in *S. aureus* (Yang et al., 2024). Moreover, Yang's group observed prophage gene activation upon aBL treatment, confirming that this is part of the MRSA eradication process (Yang et al., 2024).

Current transcriptomic evidence indicates that aBL does not induce coordinated antibiotic-like resistance regulons, but instead elicits a conserved oxidative stress architecture followed by adaptive remodeling.

## 8. Microbial determinants of susceptibility to aBL

While aBL has been shown to effectively inactivate a broad spectrum of bacterial pathogens, its efficacy is not uniform across all bacterial taxa. Multiple studies have indicated that microbial characteristics, including species identity, strain-level variability, virulence traits, and antimicrobial resistance profiles, can influence the outcome of photoinactivation. This section explores how these factors affect aBL susceptibility. Understanding these relationships is crucial for optimizing aBL as a therapeutic and decontamination strategy.

### 8.1. Species- and strain-specific response to aBL

The heterogeneity of strains within a species leads to different responses to aBL. The response of microorganisms to aBL is species- and strain-dependent (Lacombe et al., 2016; Abana et al., 2017; Halstead et al., 2019; Wu et al., 2021; Hoenes et al., 2021; Wu et al., 2022). The mechanism underlying this phenomenon is not completely understood, and the genetic or physiological determinants responsible for these inter- and intraspecies differences remain to be elucidated. Hoenes et al. (2021) irradiated ESKAPE pathogens and their close nonpathogenic relatives with aBL at 405 and 450 nm to investigate differences in aBL response between pathogenic and nonpathogenic species of one genus. The research group examined the resistance profiles of vancomycin-resistant *Enterococcus* (VRE), MRSA, and extended-spectrum beta-lactamase (ESBL) strains, among others. They reported dose-dependent differences among different genera, but within the same genus, the pathogenic and nonpathogenic strains exhibited similar responses. Moreover, the authors noted that pathogenic strains were usually more susceptible to aBL irradiation at 405 nm than their nonpathogenic counterparts. A similar effect was observed with aBL at a wavelength of 450 nm. Only in the case of *E. coli* did the results contradict the observed trend (Hoenes et al., 2021b). However, Lacombe et al. (2016) did not observe significant differences in the response to aBL at 405 nm between nonpathogenic and pathogenic *E. coli* and virulent and avirulent *Salmonella* strains at high inoculation levels (Lacombe et al., 2016).

It is worth noting that other studies have reported considerable variability both among and within species of the *Acinetobacter calcoaceticus–baumannii* complex. Distinct *A. baumannii* strains differ markedly in their susceptibility to aBL and in light-induced oxidative stress responses (Müller et al., 2017; Squire et al., 2022). Moreover, Tuttobene et al. (2021) observed species-specific regulation of metabolic pathways such as phenylacetic acid and acetoin catabolism, with *A. nosocomialis* displaying light-dependent regulation absent in several *A. baumannii* strains. Such findings highlight the need for strain- and species-level analyses to identify the molecular determinants of aBL susceptibility, which may include differences in endogenous photosensitizer content, antioxidant capacity, and photoreceptor-mediated signaling. A deeper understanding of these light-responsive mechanisms could ultimately support the development of more effective blue-light-based infection control strategies.

### 8.2. Influence of phylogeny and pathotype

Abana et al. (2017) compared the efficacy of aBL at 455 nm between *E. coli* strains belonging to five phylogenetic groups (A, B1, B2, D, and E), which included both nonpathogenic strains and representatives of the UPEC (uropathogenic), ETEC (enterotoxigenic), and EHEC (enterohemorrhagic) pathotypes. The authors demonstrated that the UPEC strain EC958 (multidrug-resistant, extended-spectrum β-lactamase-producing) and the ETEC strain E9034A were the least sensitive to aBL at 455 nm; nonetheless, the nonpathogenic strain E343 also presented a

low response to irradiation (Abana et al., 2017)

### 8.3. Antibiotic resistance and aBL susceptibility

The relationship between antibiotic resistance and aBL susceptibility remains unclear and may vary across species. Some studies suggest no consistent correlation between resistance phenotype and photoinactivation efficiency. Ma et al. (2018) demonstrated high aBL efficacy against eleven *Helicobacter pylori* strains, including ten multidrug-resistant strains and one sensitive strain. The authors reported a high efficiency of aBL irradiation against all eleven strains. The authors also noted the anti-proliferative effect of aBL, particularly in the case of various antibiotic-resistant *H. pylori* strains (Ma et al., 2018). In contrast, Dos Anjos et al., 2020a reported that β–lactamase–producing *Klebsiella pneumoniae* strains required longer irradiation times at 410 nm than the reference strain (ATCC). Moreover, the authors reported that aBL at 410 nm inhibited several β-lactamases, including KPC-2, IMP-1, ESBLs, and OXA-2 class D enzymes (Dos Anjos et al., 2020a).

### 8.4. Effects on virulence-associated phenotypes

In the second study by Dos Anjos et al., 2020b, the efficacy of aBL at 410 nm against hypermucoviscous (hmKp) and hypervirulent *K. pneumoniae* (hvKp) strains was examined and compared with that of nonhypermucoviscous and nonhypervirulent (nonhmKp/nonhvKp) control strains. All hvKp/hmKp strains were effectively inactivated by aBL irradiation. However, different inactivation kinetics were observed. Specifically, hypermucoviscous isolates required longer exposure times to achieve equivalent CFU reductions, indicating a greater tolerance factor toward aBL despite overall susceptibility (Dos Anjos et al., 2020b). In a broader study, Dos Anjos et al., 2024 examined the efficacy of aBL at 410 nm against β-lactamase-carrying bacteria (*P. aeruginosa*, *E. coli*, and *K. pneumoniae*) and the effect of aBL on the activity of β-lactamases. This study revealed that aBL was effective against both β-lactamase–expressing and antimicrobial-sensitive strains. Significant differences in sensitivity to aBL were observed between different species; however, there was no significant difference between strains of the same species. *K. pneumoniae* was the most tolerant species to aBL (341 J/cm$^2$ to 4-log$_{10}$ CFU/ml reduction), followed by *E. coli* (204 J/cm$^2$) and *P. aeruginosa* (68.2 J/cm$^2$). Moreover, aBL reduced β-lactamase activity in all the tested strains (Dos Anjos et al., 2024). In summary, bacteria may exhibit structural features that influence aBL efficacy, and the virulence factors they possess, such as toxins or enzymes, may also modulate but not determine aBL efficacy. However, aBL remains broadly effective against a range of bacterial pathogens, with species-specific variations in susceptibility. Effects of microbial factors on the effectiveness of aBL were summarized in Fig. 6.

## 9. Environmental and physiological factors affecting aBL efficacy

Many scientific studies have attempted to clarify the effects of various aBL parameters on the bactericidal efficacy of aBL. The complexity of these parameters and the fact that we do not have a standardized experimental protocol to ensure that aBL studies are conducted under homogeneous test conditions make it extremely difficult to

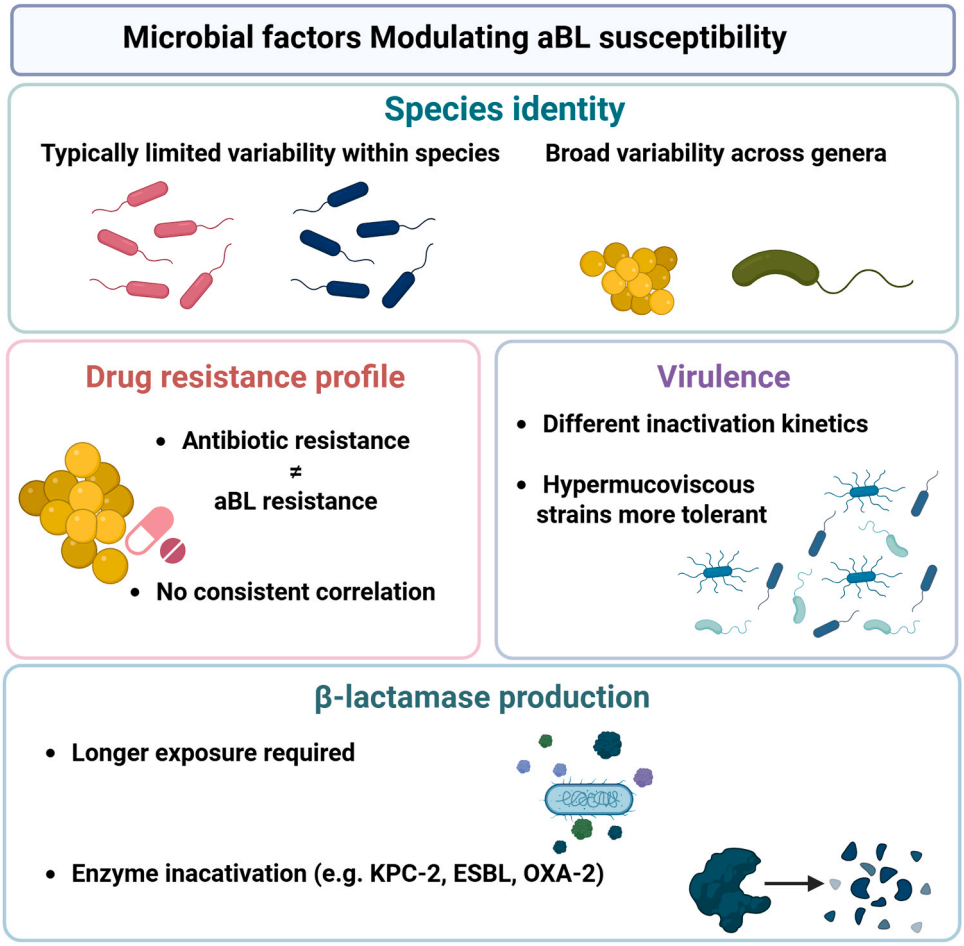


**Fig. 6.** Microbial factors modulating susceptibility to aBL. The scheme summarizes key microbial traits that may influence the response of microbes to aBL. While intra-species variability is generally lower than inter-genus differences, notable exceptions have been reported (Müller et al., 2017; Squire et al., 2022).

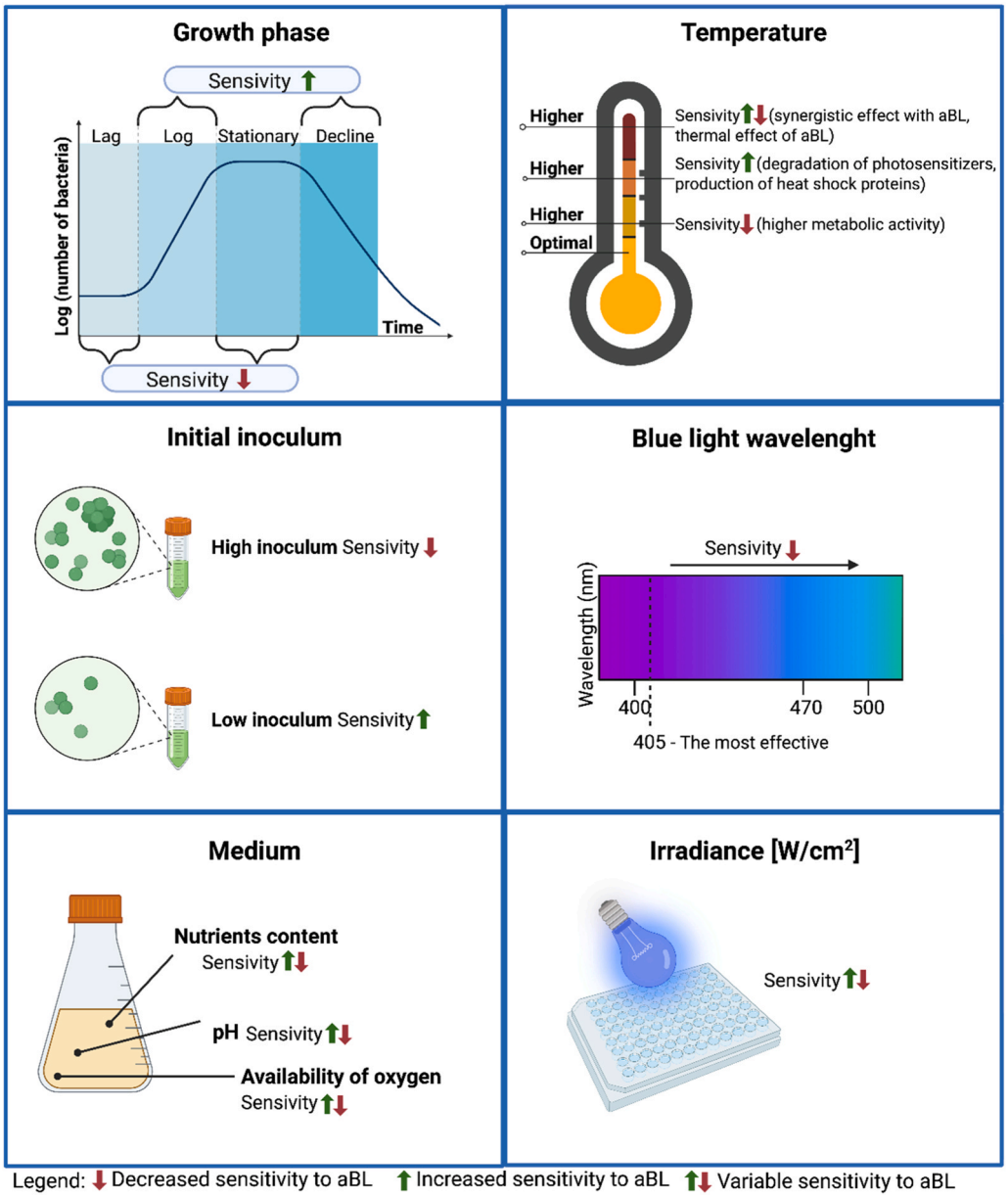


**Fig. 7.** Environmental and physiological factors affecting aBL efficacy. Sensitivity to aBL varies depending on: (i) growth phase, with higher susceptibility in logarithmic phase and lower in stationary/decline; (ii) temperature, where synergistic or antagonistic effects may occur depending on metabolic activity, photosensitizer degradation, or induction of heat shock proteins; (iii) initial inoculum, where lower inoculum generally increases sensitivity; (iv) blue light wavelength, with 405 nm being the most effective range; (v) medium composition, including nutrient content, pH, and oxygen availability; and (vi) irradiance, which can modulate bacterial inactivation efficiency depending on exposure time and light delivery mode.

draw clear conclusions. The following are the most important variables in the experimental process related to the bactericidal efficacy of aBL.

### 9.1. *Effect of growth phase on aBL efficacy*

The growth phase of bacteria is an important determinant of the effectiveness of aBL (Abana et al., 2017). During the lag phase, bacteria adapt to new environmental conditions, which is associated with lower metabolic activity and reduced DNA replication. It may be assumed that during the lag phase, bacteria may be less susceptible to aBL due to lower metabolic activity, leading to less production of endogenous porphyrins and ROS, which are key to aBL efficacy. In the log phase, bacteria divide rapidly, and their metabolic activity is at its highest level, which may promote the production of porphyrins and other chromophores, resulting in increased ROS production upon aBL exposure and subsequent enhanced bacterial killing. In the stationary phase, bacterial growth stops because of nutrient depletion and the accumulation of waste products, and their metabolic activity is reduced. On the other hand, bacteria in the stationary phase may be less susceptible to aBL (Wang et al., 2024). Reduced metabolic activity may lead to less production of porphyrins and ROS, which reduces the effectiveness of aBL in killing bacteria. In the declining phase, the number of viable bacterial cells decreases as they die from a lack of nutrients and toxic waste products. Due to weakened defense mechanisms, cells may be more susceptible to aBL. Hamblin et al. (2005) suggested that bacteria may be more susceptible to aBL during this phase. When cells are weakened and less able to neutralize ROS, the aBL efficacy is greater (Hamblin et al., 2005).

### 9.2. Effect of temperature on aBL

The effect of temperature on the effectiveness of aBL may be an important factor that can significantly affect treatment outcomes (Kumar et al., 2016; Hyun et al., 2021). Temperature directly affects the metabolic activity of bacteria, which can, in turn, affect the effectiveness of aBL. Elevated, non-cytotoxic temperatures enhance ALA-induced porphyrin production in *C. acnes* (Ramstad et al., 2006), which may, in principle, increase photosensitization and thereby improve the effectiveness of aBL. Conversely, heat stress can induce protective mechanisms, such as the synthesis of heat shock proteins (HSPs; e.g., DnaK, GroEL, etc.), which stabilize cellular components and mitigate ROS toxicity (Vanbogelen et al., 1987; St. Denis et al., 2011). In addition, bacteria may develop adaptive mechanisms in response to varying temperature conditions, which may affect their susceptibility to aBL. Kruszewska-Naczk et al. (2024) demonstrated an asymmetric cross-tolerance between these stressors: *E. coli* populations adapted to aBL exhibited increased thermotolerance, whereas heat-adapted populations showed unchanged aBL susceptibility. Moreover, short-term pre-incubation at elevated temperatures significantly increased aBL tolerance, highlighting that temperature can modulate photooxidative outcomes.

### 9.3. Effect of initial inoculum density on the efficacy of aBL

The initial number of bacteria, or inoculum density, affects the efficacy of aBL (Bumah et al., 2013; Maclean et al., 2009). A relatively high bacterial cell density may reduce the effectiveness of aBL because of limited light penetration into the inner layers of bacterial cells. In the case of a high inoculum, the outer cell layers may act as a barrier, protecting the inner cells from light exposure. When the inoculum concentration is low, the bacteria are more dispersed, allowing for more uniform light penetration and more efficient ROS generation.

### 9.4. Effect of blue light wavelength on aBL efficacy

The blue light wavelength is a key determinant of aBL effectiveness. Blue light, which is used for its antimicrobial effect, covers the wavelength range from approximately 400 nm to 470 nm. Different wavelengths in this range have different efficacies in killing bacteria. Maclean et al. (2008) reported that wavelengths in the 405 nm range are most effective in generating ROS and subsequently killing bacteria. Light at 405 nm was able to effectively eliminate bacteria, such as *Staphylococcus aureus*, by inducing photodynamic oxidative stress (Maclean et al., 2008a). Hamblin et al. (2005) reported that bacteria accumulate endogenous PSs such as porphyrins, which are most efficiently stimulated by light at approximately 405 nm, leading to ROS production and bacterial death (Hamblin et al., 2005). Different wavelengths in the blue light range have different abilities to generate ROS and penetrate tissue. The effectiveness of light decreases with increasing wavelength, which is related to lower photon energy and reduced absorption by endogenous chromophores. Importantly, the wavelength dependence also reflects the absorption spectra of targeted PSs: porphyrins exhibit strong absorption bands near 400–420 nm but minimal absorption beyond 460–470 nm, whereas flavins and NADH absorb more efficiently in the 440–470 nm region (Plavskii et al., 2018; Plattfaut et al., 2021). The optimal wavelength of blue light for antibacterial action is approximately 405 nm, which has been confirmed by numerous scientific studies (Wang et al., 2024).

### 9.5. Influence of medium on aBL efficacy

Culture medium used for bacteria can significantly affect the effectiveness of aBL. The environment in which bacteria are located can affect the effectiveness of aBL through changes in nutrient availability, pH, and the presence of medium-derived PSs. Another key factor affecting the aBL effectiveness is the availability of oxygen in the medium, as oxygen is necessary for the generation of ROS (Maclean et al., 2008b). Moreover, the composition of culture medium, especially its iron levels, may significantly affect the aBL outcome (Wang et al., 2024).

### 9.6. Effect of irradiance on aBL efficacy

It is generally believed that the radiant exposure expressed in $J/cm^2$ is the dominant parameter determining the effectiveness of aBL. Nevertheless, some studies have shown that irradiance can also, albeit to a lesser extent, affect the final outcome of this method. Numerous studies have shown that using the same light dose but delivered at different irradiances with different treatment times can affect the microbial response to aBL to varying degrees (Sommers et al., 2017; Lang et al., 2022; Prates et al., 2008). Although the effect of irradiance on the bactericidal efficiency of aBL does not seem to be as significant as radiant exposure, we are convinced that the variable of irradiance cannot be ignored.

## 10. Conclusions and future perspectives

### 10.1. Overall conclusions

aBL is gaining increasing recognition as a non-invasive strategy for combating bacterial infections, especially in the era of rising antibiotic resistance. The mechanism of aBL is based on the photoactivation of endogenous photosensitizers, primarily porphyrins and flavins, leading to the production of ROS that cause oxidative damage to bacterial cells. However, the effectiveness of aBL varies significantly depending However, the effectiveness of aBL varies significantly among bacterial species, which differ in their endogenous chromophore composition and in their environmental responses.

Recent studies have highlighted the role of bacterial porphyrins and other photosensitizing pigments in determining sensitivity to aBL. *Streptococcus* and *Enterococcus* species, key bacterial genera in human infections, exhibit variability in aBL susceptibility due to differences in chromophore content and cellular defense mechanisms. Additionally, transcriptomic analyses have provided valuable insights into bacterial stress responses to aBL, revealing the activation of oxidative stress response pathways, SOS repair systems, and gene expression changes that may influence bacterial survival. Understanding these genetic and physiological factors is critical for optimizing aBL applications. The bactericidal effects of aBL are further influenced by growth phase, temperature, inoculum density, and light parameters such as wavelength, irradiance, and exposure time. Studies suggest that optimizing these conditions can significantly enhance aBL efficacy while minimizing potential cytotoxic effects. Furthermore, the interaction between aBL and bacterial pathogenicity or antibiotic resistance profiles remains an area of ongoing research. Current data suggest that multidrug-resistant strains are not necessarily less susceptible to aBL, likely because its mechanism bypasses conventional antibiotic targets. These observations underscore the importance of physiological context in determining aBL efficacy.

### 10.2. Key bottlenecks limiting translation

Despite its growing translational appeal, the implementation of aBL remains constrained by several unresolved biological and technical challenges. A central bottleneck lies in the pronounced context dependence of aBL efficacy, which is shaped by bacterial physiology, chromophore availability, and environmental conditions. In particular, reduced susceptibility in porphyrin-deficient organisms highlights intrinsic biological limits that cannot be overcome by dose escalation alone.

In parallel, the limited penetration depth of aBL in biological tissues restricts current applications largely to superficial, surface-associated,

or device-related infections if topically delivered. Translation is further complicated by the strong dependence of treatment outcomes on irradiation parameters, including wavelength, irradiance, and exposure time, as well as by the lack of standardized protocols, which hampers cross-study comparisons and reproducibility.

Importantly, although aBL does not appear to readily select for stable genetic resistance, several studies have documented adaptive responses following sublethal or repeated exposure, including enhanced oxidative stress buffering, cell envelope remodeling, and tolerance phenotypes (Rapacka-Zdonczyk et al., 2019; 2021; Pieranski et al., 2020; Nikinmaa, 2020; Snell et al., 2021; Metzger et al., 2022; Luo et al., 2022). These observations suggest that while durable resistance remains unlikely based on current evidence, physiological plasticity may influence short-term robustness under specific experimental or environmental conditions.

Beyond these biological and technical constraints, practical and regulatory considerations also represent significant bottlenecks. Most available evidence is derived from in vitro or animal models, and robust clinical data supporting routine implementation remain limited. In addition, long-term safety assessments, regulatory approval pathways, and the influence of biological matrices or fluids on treatment efficacy require further systematic investigation before aBL can be reliably integrated into antimicrobial management.

### *10.3. Enabling strategies to overcome current limitations*

From a translational perspective, several enabling strategies are emerging that may help mitigate these constraints. Advances in light-delivery technologies, including optimized irradiance profiles (Walter et al., 2020), pulsed illumination strategies (Gillespie et al., 2017), surface-adapted (Sarkar & Jana, 2025) or fiber-based systems (Chen et al., 2011; Goh et al., 2025), optical clearing of biological tissue (Genina et al., 2010; Oliveira & Tuchin, 2019) and ultrasound-assisted light delivery (Wang et al., 2022), offer opportunities to enhance local ROS effectiveness while minimizing collateral effects. Combination approaches integrating aBL with antimicrobial agents (Wozniak & Grinholc, 2018) or physicochemical adjuvants (Hamblin & Abrahamse, 2018) represent a promising avenue for extending efficacy in low-susceptibility systems. In parallel, broader phototherapeutic platforms are being developed to enhance biofilm eradication and overcome antibiotic-refractory infections. These include NIR-II–activated nanoplatforms, responsive photosensitizer systems, and precision PTT/PDT-based strategies designed to achieve spatiotemporal control and multimodal antimicrobial effects (Ding et al., 2025a; 2025b; 2026). While mechanistically distinct from endogenous chromophore-driven aBL, such approaches reflect a converging effort to exploit light-induced oxidative and thermal stress as an alternative to conventional antibiotic targeting. Crucially, such strategies require a mechanistic grounding that accounts for membrane properties, redox buffering capacity, and metabolic state, rather than relying on empirical optimization alone.

### *10.4. Research priorities for future studies*

Looking forward, future research should focus on establishing physiologically informed frameworks for aBL application. This includes systematic, species-specific optimization of treatment parameters, deeper mechanistic interrogation of ROS dynamics under biologically relevant conditions, and rigorous evaluation of reproducibility across experimental platforms. Equally critical is the generation of high-quality clinical evidence and the development of standardized reporting practices, which together will be essential for translating promising laboratory observations into reliable antimicrobial interventions. Addressing these priorities through interdisciplinary collaboration spanning microbiology, photophysics, engineering, and clinical research will ultimately define the realistic scope and long-term utility of aBL within antimicrobial management strategies.

## 11. Literature Search Strategy

This review is based on a comprehensive literature search conducted in PubMed, Scopus, and Web of Science databases up to March 2025. The search combined terms such as *"antimicrobial blue light"*, *"photoinactivation"*, *"photodynamic inactivation"*, *"endogenous porphyrins"*, *"reactive oxygen species"*, and *"oxidative stress"*. Reference lists of relevant articles and reviews were also screened to identify additional studies.

Eligibility criteria included peer-reviewed original articles, reviews, and book chapters written in English that addressed the mechanisms of action, targets, or bacterial responses to aBL. Studies focusing exclusively on ultraviolet irradiation or exogenous photosensitizers without direct connection to aBL were excluded. No restrictions were applied regarding publication date. Although not designed as a systematic review, this strategy aimed to ensure broad coverage of both historical and recent contributions.

## Declaration of Generative AI and AI-assisted technologies in the manuscript preparation process

During the preparation of this work, the authors used ChatGPT 5 (OpenAI) to assist in language editing and improving the clarity of selected paragraphs, as well as to help prepare one absorption plot by visualizing numerical data manually extracted by the authors from published sources. No images or artwork were generated or altered using AI tools; the plot was created solely through visualization of manually extracted data. After using this tool, the authors reviewed, verified, and edited all content as needed and take full responsibility for the content of the published article.

## CRediT authorship contribution statement

**Joanna Nakonieczna:** Writing – original draft. **Mariusz Grinholc:** Writing – review & editing, Writing – original draft. **Dominika Goik:** Writing – original draft. **Natalia Burzyńska:** Writing – original draft. **Beata Kruszewska-Naczk:** Writing – original draft, Conceptualization. **Aleksandra Rapacka-Zdonczyk:** Writing – review & editing, Writing – original draft, Funding acquisition, Conceptualization. **Tianhong Dai:** Writing – review & editing. **Agata Wozniak-Pawlikowska:** Visualization. **Michał K. Pieranski:** Writing – original draft. **Natalia Pawlik:** Writing – original draft.

## Funding

This work was supported by the National Science Centre under Grant No.2022/47/D/NZ7/01795 (A.R.-Z.).

## Declaration of Competing Interest

The authors declare that they have no known competing financial interests or personal relationships that could have appeared to influence the work reported in this paper.

## Acknowledgements

Figures were created with BioRender (accessed on 1 December 2025).

## Data availability

No datasets were generated or analysed during the current study.

## References


Abana, C.M., Brannon, J.R., Ebbott, R.A., Dunigan, T.L., Guckes, K.R., Fuseini, H., Hadjifrangiskou, M., 2017. Characterization of blue light irradiation effects on pathogenic and nonpathogenic *Escherichia coli*. Microbiologyopen 6 (4), e00466. https://doi.org/10.1002/mbo3.466.

Abavisani, M., Khoshrou, A., Foroushan, S.K., Sahebkar, A., 2024. Chatting with artificial intelligence to combat antibiotic resistance: opportunities and challenges. Curr. Res. Biotechnol., 100197 https://doi.org/10.1016/j.crbiot.2024.100197.

Abranches, J., Zeng, L., Kajfasz, J.K., Palmer, S.R., Chakraborty, B., Wen, Z.T., Lemos, J. A., 2018. Biology of oral streptococci. Microbiol. Spectr. 6 (5), 10–1128. https://doi.org/10.1128/9781683670131.ch26.

Adair, T.L., Drum, B.E., 2016. RNA-Seq reveals changes in the Staphylococcus aureus transcriptome following blue light illumination. Genom. Data 9, 4–6. https://doi.org/10.1016/j.gdata.2016.05.011.

Aihara, J.I., 2008. Macrocyclic conjugation pathways in porphyrins. J. Phys. Chem. A 112 (23), 5305–5311. https://doi.org/10.1021/jp8014996.

Akbar, A., Khan, S., Chatterjee, T., Ghosh, M., 2023. Unleashing the power of porphyrin photosensitizers: Illuminating breakthroughs in photodynamic therapy. J. Photochem. Photobiol. B Biol. 248, 112796. https://doi.org/10.1016/j.jphotobiol.2023.112796.

Allison, R.R., Moghissi, K., 2013. Photodynamic therapy (PDT): PDT mechanisms. Clin. Endosc. 46 (1), 24–29. https://doi.org/10.5946/ce.2013.46.1.24.

Amin, R.M., Bhayana, B., Hamblin, M.R., Dai, T., 2016. Antimicrobial blue light inactivation of Pseudomonas aeruginosa by photo-excitation of endogenous porphyrins: in vitro and in vivo studies. Lasers Surg. Med. 48 (5), 562–568. https://doi.org/10.1002/lsm.22474.

Amodeo, D., Marchi, S., Fiaschi, L., Raucci, L., Biba, C., Salvestroni, V., Messina, G., 2025. Analysis of the SARS-CoV-2 inactivation mechanism using violet-blue light (405 nm). Appl. Environ. Microbiol., e00403-25 https://doi.org/10.1128/aem.00403-25.

Angel, D.E., Lloyd, P., Carville, K., Santamaria, N., 2011. The clinical efficacy of two semi-quantitative wound-swabbing techniques in identifying the causative organism (s) in infected cutaneous wounds. Int. Wound J. 2011 (8), 176–185. https://doi.org/10.1111/j.1742-481x.2010.00765.x.

Anjem, A., Varghese, S., Imlay, J.A., 2009. Manganese import is a key element of the OxyR response to hydrogen peroxide in *Escherichia coli*. Mol. Microbiol. 72 (4), 844–858. https://doi.org/10.1111/j.1365-2958.2009.06699.x.

Arcari, G., Raponi, G., Sacco, F., Bibbolino, G., Di Lella, F.M., Alessandri, F., Carattoli, A., 2021. *Klebsiella pneumoniae* infections in COVID-19 patients: a 2-month retrospective analysis in an Italian hospital. Int. J. Antimicrob. Agents 57 (1), 106245. https://doi.org/10.1016/j.ijantimicag.2020.106245.

Armistead, B., Whidbey, C., Iyer, L.M., Herrero-Foncubierta, P., Quach, P., Haidour, A., Rajagopal, L., 2020. The cyl genes reveal the biosynthetic and evolutionary origins of the group B Streptococcus hemolytic lipid, granadaene. Front. Microbiol. 10, 3123. https://doi.org/10.3389/fmicb.2020.00325.

Arnaut, L.G., 2011. Design of porphyrin-based photosensitizers for photodynamic therapy. In: Advances in Inorganic Chemistry, 63. Academic Press, pp. 187–233. https://doi.org/10.1016/B978-0-12-385904-4.00006-8.

Ashkenazi, H., Malik, Z., Harth, Y., Nitzan, Y., 2003. Eradication of Propionibacterium acnes by its endogenic porphyrins after illumination with high intensity blue light. FEMS Immunol. Med. Microbiol. 35 (1), 17–24. https://doi.org/10.1016/s0928-8244(02)00423-6.

Ayala, A., Muñoz, M.F., Argüelles, S., 2014. Lipid peroxidation: production, metabolism, and signaling mechanisms of malondialdehyde and 4-hydroxy-2-nonenal. Oxid. Med. Cell. Longev. 2014 (1), 360438. https://doi.org/10.1155/2014/360438.

Baptista, M.S., Cadet, J., Di Mascio, P., Ghogare, A.A., Greer, A., Hamblin, M.R., Yoshimura, T.M., 2017. Type I and type II photosensitized oxidation reactions: guidelines and mechanistic pathways. Photochem. Photobiol. 93 (4), 912–919. https://doi.org/10.1111/php.12716.

Bauer, R., Hoenes, K., Meurle, T., Hessling, M., Spellerberg, B., 2021. The effects of violet and blue light irradiation on ESKAPE pathogens and human cells in presence of cell culture media. Sci. Rep. 11 (1), 24473. https://doi.org/10.1038/s41598-021-04202-x.

Baureder, M., Hederstedt, L., 2013. Heme proteins in lactic acid bacteria. In: Advances in microbial physiology, 62. Academic Press, pp. 1–43. https://doi.org/10.1016/b978-0-12-410515-7.00001-9.

Bianchi, L., Melli, R., Pizzala, R., Stivala, L.A., Rehak, L., Quarta, S., Vannini, V., 1996. Effects of β-carotene and α-tocopherol on photogenotoxicity induced by 8-methoxypsoralen: The role of oxygen. Mutat. Res. /Genet. Toxicol. 369 (3-4), 183–194.

Biener, G., Masson-Meyers, D.S., Bumah, V.V., Hussey, G., Stoneman, M.R., Enwemeka, C.S., Raicu, V., 2017. Blue/violet laser inactivates methicillin-resistant Staphylococcus aureus by altering its transmembrane potential. J. Photochem. Photobiol. B Biol. 170, 118–124. https://doi.org/10.1016/j.jphotobiol.2017.04.002.

Bolognese, F., Emashova, N., Baldelli, V., Landini, P., Orlandi, V.T., 2025. The "Irradiance Effect" Plays a Crucial Role in the Photosensitization of *Escherichia coli* by Blue Light. Molecules 30 (23), 4515. https://doi.org/10.3390/molecules30234515.

Borba, A.S.M., da Silva Pereira, S.M., Borba, M.C.M., Paschoal, M.A.B., de Jesus Tavarez, R.R., de Castro Rizzi, C., Maia Filho, E.M., 2017. Photodynamic therapy with high-power LED mediated by erythrosine eliminates *Enterococcus faecalis* in planktonic forms. Photo Photodyn. Ther. 19, 348–351. https://doi.org/10.1016/j.pdpdt.2017.07.007.

Braatsch, S., Klug, G., 2004. Blue Light Perception in Bacteria. Photosynth. Res. 79, 45–57. https://doi.org/10.1023/B:PRES.0000011924.89742.f9.

Bumah, V.V., Masson-Meyers, D.S., Cashin, S.E., Enwemeka, C.S., 2013. Wavelength and bacterial density influence the bactericidal effect of blue light on Methicillin-Resistant Staphylococcus aureus (MRSA). Lasers Surg. Med. 31 (11), 547–553. https://doi.org/10.1089/pho.2012.3461.

Bumah, V.V., Masson-Meyers, D.S., Enwemeka, C.S., 2015. Blue 470 nm light suppresses the growth of Salmonella enterica and methicillin-resistant Staphylococcus aureus (MRSA) in vitro. Lasers Surg. Med. 47 (7), 595–601.

Bumah, V.V., Morrow, B.N., Cortez, P.M., Bowman, C.R., Rojas, P., Masson-Meyers, D.S., Enwemeka, C.S., 2020. The importance of porphyrins in blue light suppression of *Streptococcus agalactiae*. J. Photochem. Photobiol. B Biol. 212, 111996. https://doi.org/10.1016/j.jphotobiol.2020.111996.

Bumah, V.V., Cortez, P.M., Morrow, B.N., Rojas, P., Bowman, C.R., Masson-Meyers, D.S., Enwemeka, C.S., 2021. Blue light absorbing pigment in *Streptococcus agalactiae* does not potentiate the antimicrobial effect of pulsed 450 nm light. J. Photochem. Photobiol. B Biol. 216, 112149. https://doi.org/10.1016/j.jphotobiol.2021.112149.

Burzynska, N., Szczesniak, M., Grinholc, M., 2026. Time-resolved transcriptomic mapping reveals conserved stress programs and metabolic rewiring in *Escherichia coli* under antimicrobial photodynamic and blue light exposure, 2026-02 bioRxiv. https://doi.org/10.64898/2026.02.02.703343.

Burzyńska, N., Woźniak-Pawlikowska, A., Rapacka-Zdończyk, A., Jaśkiewicz, M., Kruszewska-Naczk, B., Nakonieczna, J., Grinholc, M., 2026. Illuminating the mechanism: gene expression responses to antimicrobial photodynamic therapy. BMC genom.

Cadet, J., Wagner, J.R., 2013. DNA base damage by reactive oxygen species, oxidizing agents, and UV radiation. Cold Spring Harb. Perspect. Biol. 5 (2), a012559. https://doi.org/10.1101/cshperspect.a012559.

Cardoso, D.R., Libardi, S.H., Skibsted, L.H., 2012. Riboflavin as a photosensitizer. Effects on human health and food quality. Food Funct. 3 (5), 487–502. https://doi.org/10.1039/c2fo10246c.

Chebath-Taub, D., Steinberg, D., Featherstone, J.D., Feuerstein, O., 2012. Influence of blue light on Streptococcus mutans re-organization in biofilm. J. Photochem. Photobiol. B Biol. 116, 75–78. https://doi.org/10.1016/j.jphotobiol.2012.08.004.

Chen, J., Cesario, T.C., Rentzepis, P.M., 2011. Fiber based pathogen photoinactivating system. Rev. Sci. Instrum. 82 (1). https://doi.org/10.1063/1.3531983.

Chiniforush, N., Pourhajibagher, M., Parker, S., Benedicenti, S., Bahador, A., Sălăgean, T., Bordea, I.R., 2020. The effect of antimicrobial photodynamic therapy using chlorophyllin–Phycocyanin mixture on Enterococcus faecalis: The influence of different light sources. Appl. Sci. 10 (12), 4290. https://doi.org/10.3390/app10124290.

Chui, C., Hiratsuka, K., Aoki, A., Takeuchi, Y., Abiko, Y., Izumi, Y., 2012. Blue LED inhibits the growth of Porphyromonas gingivalis by suppressing the expression of genes associated with DNA replication and cell division. Lasers Surg. Med. 44 (10), 856–864. https://doi.org/10.1002/lsm.22090.

Chu, Z., Hu, X., Wang, X., Wu, J., Dai, T., Wang, X., 2019. Inactivation of *Cronobacter sakazakii* by blue light illumination and the resulting oxidative damage to fatty acids. Can. J. Microbiol. 65 (12), 922–929. https://doi.org/10.1139/cjm-2019-0054.

Cieplik, F., Späth, A., Leibl, C., Gollmer, A., Regensburger, J., Tabenski, L., Schmalz, G., 2014. Blue light kills Aggregatibacter actinomycetemcomitans due to its endogenous photosensitizers. Clin. Oral. Investig. 18, 1763–1769. https://doi.org/10.1007/s00784-013-1151-8.

Clauditz, A., Resch, A., Wieland, K.-P., Peschel, A., Götz, F., 2006. Staphyloxanthin plays a role in the fitness of Staphylococcus aureus and its ability to cope with oxidative stress. Infect. Immun. 2006 (74), 4950–4953. https://doi.org/10.1128/iai.00204-06.

Cohen-Berneron, J., Steinberg, D., Featherstone, J.D., Feuerstein, O., 2016. Sustained effects of blue light on Streptococcus mutans in regrown biofilm. Lasers Med. Sci. 31, 445–452. https://doi.org/10.1007/s10103-016-1873-3.

Cong, X., Krolla, P., Khan, U.Z., Savin, M., Schwartz, T., 2023. Antibiotic resistances from slaughterhouse effluents and enhanced antimicrobial blue light technology for wastewater decontamionation. Environ. Sci. Pollut. Res. 30 (50), 109315–109330. https://doi.org/10.1007/s11356-023-29972-x.

Cong, X., Hillert, J., Krolla, P., Schwartz, T., 2025. Cellular insights into reactive oxidative species (ROS) and bacterial stress responses induced by antimicrobial blue light (aBL) for inactivating antibiotic resistant bacteria (ARB) in wastewater. Sci. Total Environ. 1005, 180878. https://doi.org/10.1016/j.scitotenv.2025.180878.

Dai, T., Gupta, A., Murray, C.K., Vrahas, M.S., Tegos, G.P., Hamblin, M.R., 2012. Blue light for infectious diseases: Propionibacterium acnes, *Helicobacter pylori,* and beyond? Drug Resist. Updates 15 (4), 223–236. https://doi.org/10.1016/j.drup.2012.07.001.

Dai, T., Gupta, A., Huang, Y.Y., Yin, R., Murray, C.K., Vrahas, M.S., Hamblin, M.R., 2013. Blue light rescues mice from potentially fatal Pseudomonas aeruginosa burn infection: efficacy, safety, and mechanism of action. Antimicrob. Agents Chemother. 57 (3), 1238–1245. https://doi.org/10.1128/aac.01652-12.

Dai, T., Hamblin, M.R., 2017. Visible blue light is capable of inactivating Candida albicans and other fungal species. Photomed. Laser Surg. 35 (7), 345. https://doi.org/10.1089/pho.2017.4318.

Daly, M.J., Gaidamakova, E.K., Matrosova, V.Y., Vasilenko, A., Zhai, M., Leapman, R.D., Fredrickson, J.K., 2007. Protein oxidation implicated as the primary determinant of bacterial radioresistance. PLoS Biol. 5 (4), e92. https://doi.org/10.1371/journal.pbio.0050092.

Dąbrowski, J.M., Arnaut, L.G., 2015. Photodynamic therapy (PDT) of cancer: from local to systemic treatment. Photochem. & Photobiol. Sci. 14 (10), 1765–1780. https://doi.org/10.1039/C5PP00132C.

de Lucca, A.J., Carter-Wientjes, C., Williams, K.A., Bhatnagar, D., 2012. Blue light (470 nm) effectively inhibits bacterial and fungal growth. Lett. Appl. Microbiol. 55 (6), 460–466. https://doi.org/10.1111/lam.12002.

Ding, Q., Xie, Y., Xiong, K., Jia, H., Chen, L., Li, C., Tang, B.Z., 2025a. From light to cure: precision phototherapies for antibiotic-refractory biofilm infections. Angew. Chem. Int. Ed. 64 (43), e202510900. https://doi.org/10.1002/ange.202510900.
Ding, Q., Ding, L., Xiang, C., Li, C., Kim, E., Yoon, C., Kim, J.S., 2025b. pH-Responsive AIE Photosensitizers for Enhanced Antibacterial Therapy. Angew. Chem., e202506505 https://doi.org/10.1002/ange.202506505.
Ding, Q., Zhou, L., Xiong, T., Liu, J., Chen, L., Yoo, J., Kim, J.S., 2026. Sunlight PDT leveraging NIR-II nanospray: painless, hemostatic, anti-inflammatory therapy towards diabetic wound infections. Natl. Sci. Rev. 13 (2), nwaf554. https://doi.org/10.1093/nsr/nwaf554.
Djouiai, B., Thwaite, J.E., Laws, T.R., Commichau, F.M., Setlow, B., Setlow, P., Moeller, R., 2018. Role of DNA repair and protective components in Bacillus subtilis spore resistance to inactivation by 400-nm-wavelength blue light. Appl. Environ. Microbiol. 84 (19), e01604-18. https://doi.org/10.1128/aem.01604-18.
Dong, P.T., Mohammad, H., Hui, J., Leanse, L.G., Li, J., Liang, L., Cheng, J.X., 2019. Photolysis of Staphyloxanthin in methicillin-resistant Staphylococcus aureus potentiates killing by reactive oxygen species. Adv. Sci. 6 (11), 1900030. https://doi.org/10.1002/advs.201900030.
Dong, P.T., Jusuf, S., Hui, J., Zhan, Y., Zhu, Y., Liu, G.Y., Cheng, J.X., 2022. Photoinactivation of catalase sensitizes a wide range of bacteria to ROS-producing agents and immune cells. JCI Insight 7 (10). https://doi.org/10.1172/jci.insight.153079.
Dorey, A.L., Lee, B.-H., Rotter, B., O'Byrne, C.P., 2019. Blue Light Sensing in Listeria monocytogenes Is Temperature-Dependent and the Transcriptional Response to It Is Predominantly SigB-Dependent. Front. Microbiol. 10, 2497. https://doi.org/10.3389/fmicb.2019.02497.
Dos Anjos, C., Sellera, F.P., Ribeiro, M.S., Baptista, M.S., Pogliani, F.C., Lincopan, N., Sabino, C.P., 2020a. Antimicrobial blue light and photodynamic therapy inhibit clinically relevant β-lactamases with extended-spectrum (ESBL) and carbapenemase activity. Photo Photodyn. Ther. 32, 102086. https://doi.org/10.1016/j.pdpdt.2020.102086.
Dos Anjos, C., Sabino, C.P., Sellera, F.P., Esposito, F., Pogliani, F.C., Lincopan, N., 2020b. Hypervirulent and hypermucoviscous strains of *Klebsiella pneumoniae* challenged by antimicrobial strategies using visible light. Int. J. Antimicrob. Agents 56 (1), 106025. https://doi.org/10.1016/j.ijantimicag.2020.106025.
Dos Anjos, C., Leanse, L.G., Liu, X., Miranda, H.V., Anderson, R.R., Dai, T., 2022. Antimicrobial blue light for prevention and treatment of highly invasive *Vibrio vulnificus* burn infection in mice. Front. Microbiol. 13, 932466. https://doi.org/10.3389/fmicb.2022.932466.
Dos Anjos, C., Leanse, L.G., Ribeiro, M.S., Sellera, F.P., Dropa, M., Arana-Chavez, V.E., Sabino, C.P., 2023. New insights into the bacterial targets of antimicrobial blue light. Microbiol. Spectr. 11 (2), e02833-22. https://doi.org/10.1128/spectrum.02833-22.
Dos Anjos, C., Wang, Y., Truong-Bolduc, Q.C., Bolduc, P.K., Liu, M., Hooper, D.C., Leanse, L.G., 2024. Blue Light Compromises Bacterial β-Lactamases Activity to Overcome β-Lactam Resistance. Lasers Surg. Med. 56 (7), 673–681. https://doi.org/10.1002/lsm.23819.
Dosselli, R., Millioni, R., Puricelli, L., Tessari, P., Arrigoni, G., Franchin, C., Reddi, E., 2012. Molecular targets of antimicrobial photodynamic therapy identified by a proteomic approach. J. Proteom. 77, 329–343. https://doi.org/10.1016/j.jprot.2012.09.007.
Dougherty, T.J., Gomer, C.J., Henderson, B.W., Jori, G., Kessel, D., Korbelik, M., Peng, Q., 1998. Photodynamic therapy. J. Natl. Cancer Inst. 90 (12), 889–905. https://doi.org/10.1093/jnci/90.12.889.
Edwards, A.M., 2014. Structure and general properties of flavins. Methods Mol. Biol. 1146, 3–13. https://doi.org/10.1007/978-1-4939-0452-5_1.
Eichner, A., Gollmer, A., Späth, A., Bäumler, W., Regensburger, J., König, B., Maisch, T., 2015. Fast and effective inactivation of Bacillus atrophaeus endospores using light-activated derivatives of vitamin B2. Photochem. Photobiol. Sci. 14 (2), 387–396. https://doi.org/10.1039/c4pp00285g.
Eley, M., Lee, J., Lhoste, J., Lee, C.Y., Cormier, M.J., Hemmerich, P., Cormier, M.J., 1970. Bacterial Bioluminescence. Comparisons of Bioluminescence Emission Spectra, the Fluorescence of Luciferase Reaction Mixtures, and the Fluorescence of Flavin Cations* Í All inquiries should be sent to. Biochem. Biophys. Res. Commun. 16. ⟨https://pubs.acs.org/sharingguidelines⟩.
Enwemeka, C.S., Williams, D., Enwemeka, S.K., Hollosi, S., Yens, D., 2009. Blue 470-nm light kills Methicillin-Resistant Staphylococcus aureus (MRSA) in vitro. Photomed. Laser Surg. 27 (2), 221–226. https://doi.org/10.1089/pho.2008.2413.
Feijó Delgado, F., Cermak, N., Hecht, V.C., Son, S., Li, Y., Knudsen, S.M., Manalis, S.R., 2013. Intracellular water exchange for measuring the dry mass, water mass and changes in chemical composition of living cells. PloS One 8 (7), e67590. https://doi.org/10.1371/journal.pone.0067590.
Felix Gomez, G.G., Lippert, F., Ando, M., Zandona, A.F., Eckert, G.J., Gregory, R.L., 2019. Photoinhibition of Streptococcus mutans biofilm-induced lesions in human dentin by violet-blue light. Dent. J. 7 (4), 113. https://doi.org/10.3390/dj7040113.
Ferrer-Espada, R., Wang, Y., Goh, X.S., Dai, T., 2020. Antimicrobial blue light inactivation of microbial isolates in biofilms. Lasers Surg. Med. 52 (5), 472–478. https://doi.org/10.1002/lsm.23159.
Fernandez, J.M., Bilgin, M.D., Grossweiner, L.I., 1997. Singlet oxygen generation by photodynamic agents. J. Photochem. Photobiol. B Biol. 37 (1-2), 131–140. https://doi.org/10.1016/s1011-1344(96)07349-6.
Feuerstein, O., Persman, N., Weiss, E.I., 2004. Phototoxic Effect of Visible Light on Porphyromonas gingivalis and Fusobacterium nucleatum: An In Vitro Study¶. Photochem. Photobiol. 80 (3), 412–415. https://doi.org/10.1562/2004-06-13-ra-196.1.
Fila, G., Krychowiak, M., Rychlowski, M., Bielawski, K.P., Grinholc, M., 2018. Antimicrobial blue light photoinactivation of Pseudomonas aeruginosa: Quorum sensing signaling molecules, biofilm formation and pathogenicity. J. Biophotonics 11 (11), e201800079. https://doi.org/10.1002/jbio.201800079.
Fontana, C.R., Song, X., Polymeri, A., Goodson, J.M., Wang, X., Soukos, N.S., 2015. The effect of blue light on periodontal biofilm growth in vitro. Lasers Med. Sci. 30, 2077–2086. https://doi.org/10.1007/s10103-015-1724-7.
Foote, C.S., 1968. Mechanisms of photosensitized oxidation: there are several different types of photosensitized oxidation which may be important in biological systems. Science 162 (3857), 963–970. https://doi.org/10.1126/science.162.3857.963.
Foote, C.S., 1991. Definition of Type I and Type II Photosensitized Oxidation. Photochem. Photobio. 1991 54 (5), 659. https://doi.org/10.1111/j.1751-1097.1991.tb02071.x.
Fraikin, G.Y., Strakhovskaya, M.G., Rubin, A.B., 1996. The role of membrane-bound porphyrin-type compound as endogenous sensitizer in photodynamic damage to yeast plasma membranes. J. Photochem. Photobiol. B Biol. 34 (2-3), 129–135. https://doi.org/10.1016/1011-1344(96)07287-9.
Frankenberg, L., Brugna, M., Hederstedt, L., 2002. Enterococcus faecalis Heme-Dependent Catalase. J. Bacteriol. 184. https://doi.org/10.1128/jb.184.22.6351-6356.2002.
2005. Friedberg, E.C., Walker, G.C., Siede, W., & Wood, R.D. (Eds.). (2005). DNA repair and mutagenesis. American Society for Microbiology Press. https://doi.org/10.1128/9781555816704.
Fyrestam, J., Bjurshammar, N., Paulsson, E., Johannsen, A., Östman, C., 2015. Determination of porphyrins in oral bacteria by liquid chromatography electrospray ionization tandem mass spectrometry. Anal. Bioanal. Chem. 407, 7013–7023. https://doi.org/10.1007/s00216-015-8864-2.
Genina, E.A., Bashkatov, A.N., Larin, K.V., Tuchin, V.V., 2010. Light–tissue interaction at optical clearing. Laser Imaging Manip. Cell Biol. 113–164. https://doi.org/10.1002/9783527632053.ch7.
Gigante, A.M., Hadis, M.A., Secker, B., Shaw, S.C., Cooper, P.R., Palin, W.M., Atterbury, R.J., 2024. Exposure to blue light reduces antimicrobial resistant *Pseudomonas aeruginosa* isolated from dog ear infections. Front. Microbiol. 15, 1414412. https://doi.org/10.3389/fmicb.2024.1414412.
Gillespie, J.B., Maclean, M., Given, M.J., Wilson, M.P., Judd, M.D., Timoshkin, I.V., MacGregor, S.J., 2017. Efficacy of pulsed 405-nm light-emitting diodes for antimicrobial photodynamic inactivation: effects of intensity, frequency, and duty cycle. Photomed. Laser Surg. 35 (3), 150–156. https://doi.org/10.1089/pho.2016.4179.
Giovannetti, R., 2012. The use of spectrophotometry UV-Vis for the study of porphyrins. Macro Nano Spectrosc. 87–108. https://doi.org/10.5772/38797.
Glowacka-Sobotta, A., Czarczynska-Goslinska, B., Ziental, D., Wysocki, M., Michalak, M., Güzel, E., Sobotta, L., 2024. Versatile porphyrin arrangements for photodynamic therapy—A review. Nanomaterials 14 (23), 1879. https://doi.org/10.3390/nano14231879.
Goerlich, O., Quillardet, P., Hofnung, M., 1989. Induction of the SOS response by hydrogen peroxide in various Escherichia coli mutants with altered protection against oxidative DNA damage. J. Bacteriol. 171 (11), 6141–6147. https://doi.org/10.1128/jb.171.11.6141-6147.1989.
Goh, M.H., Körber-Irrgang, B., Hederick, L.L., Rabiner, R.A., Wisplinghoff, H., Chen, A.F., Lozano-Calderon, S.A., 2025. Effect of novel antimicrobial blue light-emitting optical fiber on vancomycin-resistant Enterococcus faecium and carbapenemase-producing Klebsiella pneumoniae. J. Bone Jt. Infect. 10 (6), 561–570. https://doi.org/10.5194/jbji-10-561-2025.
Gomez, G.F., Huang, R., MacPherson, M., Ferreira Zandona, A.G., Gregory, R.L., 2016. Photo inactivation of Streptococcus mutans biofilm by violet-blue light. Curr. Microbiol. 73, 426–433. https://doi.org/10.1007/s00284-016-1075-z.
Gomez-Simmonds, A., Annavajhala, M.K., McConville, T.H., Dietz, D.E., Shoucri, S.M., Laracy, J.C., Uhlemann, A.C., 2021. Carbapenemase-producing Enterobacterales causing secondary infections during the COVID-19 crisis at a New York City hospital. J. Antimicrob. Chemother. 76 (2), 380–384. https://doi.org/10.1093/jac/dkaa466.
Gonçalves, A.S., Fernandes, J.R., Saavedra, M.J., Guimarães, N.M., Pereira, C., Simões, M., Borges, A., 2025. New insights on antibacterial mode of action of blue-light photoactivated berberine and curcumin-antibiotic combinations against *Staphylococcus aureus*. Photo Photodyn. Ther. 52, 104514. https://doi.org/10.1016/j.pdpdt.2025.104514.
Grinholc, M., Rodziewicz, A., Forys, K., Rapacka-Zdonczyk, A., Kawiak, A., Domachowska, A., Bielawski, K.P., 2015. Fine-tuning recA expression in Staphylococcus aureus for antimicrobial photoinactivation: importance of photo-induced DNA damage in the photoinactivation mechanism. Appl. Microbiol. Biotechnol. 99, 9161–9176. https://doi.org/10.1007/s00253-015-6863-z.
Guffey, J.S., Wilborn, J., 2006. vitro bactericidal effects of 405-nm and 470-nm blue light. Photomed. Laser Ther. 24 (6), 684–688. https://doi.org/10.1089/pho.2006.24.684.
Gupta, S., MacLean, M., Anderson, J.G., MacGregor, S.J., Meek, R.M.D., Grant, M.H., 2015. Inactivation of micro-organisms isolated from infected lower limb arthroplasties using high-intensity narrow-spectrum (HINS) light. Bone & Jt. J. 97 (2), 283–288. https://doi.org/10.1302/0301-620x.97b2.35154.
Gwynne, P.J., Gallagher, M.P., 2018. Light as a broad-spectrum antimicrobial. Front. Microbiol. 9, 119. https://doi.org/10.3389/fmicb.2018.00119.
Hadi, J., Wu, S., Brightwell, G., 2020. Antimicrobial blue light versus pathogenic bacteria: mechanism, application in the food industry, hurdle technologies and potential resistance. Foods 9 (12), 1895. https://doi.org/10.3390/foods9121895.
Hadi, J., Wu, S., Soni, A., Gardner, A., Brightwell, G., 2021. Genetic factors affect the survival and behaviors of selected bacteria during antimicrobial blue light treatment. Int. J. Mol. Sci. 22 (19), 10452. https://doi.org/10.3390/ijms221910452.
Halliwell, B., Gutteridge, J.M., 2015. Free radicals in biology and medicine. Oxford University Press. https://doi.org/10.1093/acprof:oso/9780198717478.001.0001.

Hamblin, M.R., Viveiros, J., Yang, C., Ahmadi, A., Ganz, R.A., Tolkoff, M.J., 2005. Helicobacter pylori accumulates photoactive porphyrins and is killed by visible light. Antimicrob. Agents Chemother. 49 (7), 2822–2827. https://doi.org/10.1128/aac.49.7.2822-2827.2005.

Hamblin, M.R., Huang, Y.Y., Heiskanen, V., 2019. Non-mammalian hosts and photobiomodulation: do all life-forms respond to light? Photochem. Photobiol. 95 (1), 126–139. https://doi.org/10.1111/php.12951.

Hamblin, M.R., Abrahamse, H., 2018. Inorganic salts and antimicrobial photodynamic therapy: mechanistic conundrums? Molecules 23 (12), 3190. https://doi.org/10.3390/molecules23123190.

Hamblin, M.R., Abrahamse, H., 2020. Oxygen-independent antimicrobial photoinactivation: Type III photochemical mechanism? Antibiotics 9 (2), 53. https://doi.org/10.3390/antibiotics9020053.

Halliwell, B., Adhikary, A., Dingfelder, M., Dizdaroglu, M., 2021. Hydroxyl radical is a significant player in oxidative DNA damage in vivo. Chem. Soc. Rev. 50 (15), 8355–8360. https://doi.org/10.1039/d1cs00044f.

Halstead, F.D., Thwaite, J.E., Burt, R., Laws, T.R., Raguse, M., Moeller, R., Oppenheim, B. A., 2016. Antibacterial activity of blue light against nosocomial wound pathogens growing planktonically and as mature biofilms. Appl. Environ. Microbiol. 82 (13), 4006–4016. https://doi.org/10.1128/aem.00756-16.

Halstead, F.D., Hadis, M.A., Marley, N., Brock, K., Milward, M.R., Cooper, P.R., Palin, W. M., 2019. Violet-blue light arrays at 405 nanometers exert enhanced antimicrobial activity for photodisinfection of monomicrobial nosocomial biofilms. Appl. Environ. Microbiol. 85 (21), e01346-19. https://doi.org/10.1128/aem.01346-19.

Händel, N., Hoeksema, M., Freijo Mata, M., Brul, S., ter Kuile, B.H., 2016. Effects of stress, reactive oxygen species, and the SOS response on de novo acquisition of antibiotic resistance in Escherichia coli. Antimicrob. Agents Chemother. 60 (3), 1319–1327. https://doi.org/10.1128/aac.02684-15.

Heelis, P.F., 1982. The photophysical and photochemical properties of flavins (isoalloxazines). Chem. Soc. Rev. 11 (1), 15–39. https://doi.org/10.1039/CS9821100015.

Henningham, A., Döhrmann, S., Nizet, V., Cole, J.N., 2015. Mechanisms of group A Streptococcus resistance to reactive oxygen species. FEMS Microbiol. Rev. 39 (4), 488–508. https://doi.org/10.1093/femsre/fuu009.

Hessling, M., Spellerberg, B., Hoenes, K., 2017. Photoinactivation of bacteria by endogenous photosensitizers and exposure to visible light of different wavelengths–a review on existing data. Microbiol. Lett. 364 (2), fnw270. https://doi.org/10.1093/femsle/fnw270.

Hessling, M., Wenzel, U., Meurle, T., Spellerberg, B., Hönes, K., 2020. Photoinactivation results of *Enterococcus moraviensis* with blue and violet light suggest the involvement of an unconsidered photosensitizer. Biochem. Biophys. Res. Commun. 533 (4), 813–817. https://doi.org/10.1016/j.bbrc.2020.09.091.

Hoenes, K., Wenzel, U., Spellerberg, B., Hessling, M., 2020. Photoinactivation Sensitivity of Staphylococcus carnosus to Visible-light Irradiation as a Function of Wavelength. Photochem. Photobiol. 96 (1), 156–169. https://doi.org/10.1111/php.13168.

Hoenes, K., Bauer, R., Spellerberg, B., Hessling, M., 2021a. Microbial photoinactivation by visible light results in limited loss of membrane integrity. Antibiotics 10 (3), 341. https://doi.org/10.3390/antibiotics10030341.

Hoenes, K., Bauer, R., Meurle, T., Spellerberg, B., Hessling, M., 2021b. Inactivation effect of violet and blue light on ESKAPE pathogens and closely related non-pathogenic bacterial species–a promising tool against antibiotic-sensitive and antibiotic-resistant microorganisms. Front. Microbiol. 11, 612367. https://doi.org/10.3389/fmicb.2020.612367.

Hu, X., Zhang, X., Luo, S., Wu, J., Sun, X., Liu, M., Wang, X., 2021. Enhanced sensitivity of Salmonella to antimicrobial blue light caused by inactivating rfaC gene involved in lipopolysaccharide biosynthesis. Foodborne Pathog. Dis. 18 (8), 599–606. https://doi.org/10.1089/fpd.2020.2888.

Huang, R., Choe, E., Min, D.B., 2004. Kinetics for singlet oxygen formation by riboflavin photosensitization and the reaction between riboflavin and singlet oxygen. J. Food Sci. 69 (9). https://doi.org/10.1111/j.1365-2621.2004.tb09924.x.

Huang, S., Lin, S., Qin, H., Jiang, H., Liu, M., 2023. The Parameters Affecting Antimicrobial Efficiency of Antimicrobial Blue Light Therapy: *A Review and Prospect*. Biomedicines 11 (4), 1197. https://doi.org/10.3390/biomedicines11041197.

Hyun, J.E., Moon, S.K., Lee, S.Y., 2021. Antibacterial activity and mechanism of 460–470 nm light-emitting diodes against pathogenic bacteria and spoilage bacteria at different temperatures. Food Control 123, 107721. https://doi.org/10.1016/j.foodcont.2020.107721.

Imlay, J.A., 2013. The molecular mechanisms and physiological consequences of oxidative stress: lessons from a model bacterium. Nat. Rev. Microbiol. 11 (7), 443–454. https://doi.org/10.1038/nrmicro3032.

Jori, G., 1996. Tumour photosensitizers: approaches to enhance the selectivity and efficiency of photodynamic therapy. J. Photochem. Photobiol. B Biol. 36 (2), 87–93. https://doi.org/10.1016/S1011-1344(96)07352-6.

Jori, G., Fabris, C., Soncin, M., Ferro, S., Coppellotti, O., Dei, D., Roncucci, G., 2006. Photodynamic therapy in the treatment of microbial infections: basic principles and perspective applications. Lasers Surg. Med. Off. J. Am. Soc. Laser Med. Surg. 38 (5), 468–481. https://doi.org/10.1002/lsm.20361.

Jusuf, S., Dong, P.T., Hui, J., Ulloa, E.R., Liu, G.Y., Cheng, J.X., 2021. Granadaene photobleaching reduces the virulence and increases antimicrobial susceptibility of Streptococcus agalactiae. Photochem. Photobiol. 97 (4), 816–825. https://doi.org/10.1111/php.13389.

Kim, M.J., Mikš-Krajnik, M., Kumar, A., Yuk, H.G., 2016. Inactivation by 405±5 nm light emitting diode on Escherichia coli O157: H7, Salmonella Typhimurium, and Shigella sonnei under refrigerated condition might be due to the loss of membrane integrity. Food Control 59, 99–107. https://doi.org/10.1016/j.foodcont.2015.05.012.

Kim, M.J., Yuk, H.G., 2017. Antibacterial mechanism of 405-nanometer light-emitting diode against Salmonella at refrigeration temperature. Appl. Environ. Microbiol. 83 (5), e02582-16. https://doi.org/10.1128/aem.02582-16.

Kim, M.J., Bang, W.S., Yuk, H.G., 2017. 405±5 nm light emitting diode illumination causes photodynamic inactivation of Salmonella spp. on fresh-cut papaya without deterioration. Food Microbiol. 62, 124–132. https://doi.org/10.1016/j.fm.2016.10.002.

Kim, J., Park, H., Lee, J., Seo, H., Lee, S., 2018. Antimicrobial effect on Streptococcus mutans in photodynamic therapy using different light source. J. Korean Acad. Pediatr. Dent. 45 (1), 82–89. https://doi.org/10.5933/jkapd.2018.45.1.82.

Kolarova, H., Nevrelova, P., Tomankova, K., Kolar, P., Bajgar, R., Mosinger, J., 2008. Production of reactive oxygen species after photodynamic therapy by porphyrin sensitizers. Gen. Physiol. Biophys. 27 (2), 101.

Kotaki, A., Yagi, K., 1970. Fluorescence Properties of Flavins in Various Solvents. J. Biochenr 68. https://doi.org/10.1093/oxfordjournals.jbchem.a129381.

Kovacevic, A., Smith, D.R., Rahbé, E., Novelli, S., Henriot, P., Varon, E., Opatowski, L., 2024. Exploring factors shaping antibiotic resistance patterns in *Streptococcus pneumoniae* during the 2020 COVID-19 pandemic. Elife 13, e85701. https://doi.org/10.7554/elife.85701.

Kowalska, A., Gyugos, M., Szego, D., Lopez Pineda, A., Ayala, D., Xu, Y., Jabłońska, J., 2007. The thermal scanning fluorescence study on the conformational stability of glucose oxidease (GOD) from Aspergillus Niger. Zesz. Nauk. Chem. Spożywcza i Biotechnol. /Politech. Łódzka 35–48.

König, H., Fröhlich, J., 2017. Lactic acid bacteria. Biology of Microorganisms on Grapes, in Must and in Wine, 3-41. https://doi.org/10.1007/978-3-319-60021-5_134110.1007/978-3-319-60021-5_1.

Kruszewska-Naczk, B., Grinholc, M., Waleron, K., Bandow, J.E., Rapacka-Zdończyk, A., 2024. Can antimicrobial blue light contribute to resistance development? Genome-wide analysis revealed aBL-protective genes in *Escherichia coli*. Microbiol. Spectr. 12 (1), e02490-23. https://doi.org/10.1128/spectrum.02490-23.

Kumar, A., Ghate, V., Kim, M.J., Zhou, W., Khoo, G.H., Yuk, H.G., 2015. Kinetics of bacterial inactivation by 405 nm and 520 nm light emitting diodes and the role of endogenous coproporphyrin on bacterial susceptibility. J. Photochem. Photobiol. B Biol. 149, 37–44. https://doi.org/10.1016/j.jphotobiol.2015.05.005.

Kumar, A., Ghate, V., Kim, M.J., Zhou, W., Khoo, G.H., Yuk, H.G., 2016. Antibacterial efficacy of 405, 460 and 520 nm light emitting diodes on Lactobacillus plantarum, Staphylococcus aureus and Vibrio parahaemolyticus. J. Appl. Microbiol. 120 (1), 49–56. https://doi.org/10.1111/jam.12975.

Lacombe, A., Niemira, B.A., Sites, J., Boyd, G., Gurtler, J.B., Tyrell, B., Fleck, M., 2016. Reduction of bacterial pathogens and potential surrogates on the surface of almonds using high-intensity 405-nanometer light. J. Food Prot. 79 (11), 1840–1845. https://doi.org/10.4315/0362-028x.jfp-15-418.

Lang, E., Thery, T., Peltier, C., Colliau, F., Adamuz, J., Grangeteau, C., Dupont, S., Beney, L., 2022. Ultra-high irradiance (UHI) blue light: Highlighting the potential of a novel LED-based device for short antifungal treatments of food contact surfaces. Appl. Microbiol. Biotechnol. 106, 415–424. https://doi.org/10.1007/s00253-021-11718-9.

Langford, B.J., So, M., Raybardhan, S., Leung, V., Westwood, D., MacFadden, D.R., Daneman, N., 2020. Bacterial co-infection and secondary infection in patients with COVID-19: a living rapid review and meta-analysis. Clin. Microbiol. Infect. 26 (12), 1622–1629. https://doi.org/10.1016/j.cmi.2020.07.016.

Leanse, L.G., Goh, X.S., Cheng, J.X., Hooper, D.C., Dai, T., 2020. Dual-wavelength photo-killing of methicillin-resistant Staphylococcus aureus. JCI Insight 5 (11), e134343.

Leanse, L.G., Dos Anjos, C., Mushtaq, S., Dai, T., 2022. Antimicrobial blue light: A 'Magic Bullet'for the 21st century and beyond? Adv. Drug Deliv. Rev. 180, 114057. https://doi.org/10.1016/j.addr.2021.114057.

Liang, J.Y., Yuann, J.M.P., Cheng, C.W., Jian, H.L., Lin, C.C., Chen, L.Y., 2013. Blue light induced free radicals from riboflavin on *E. coli* DNA damage. J. Photochem. Photobiol. B Biol. 119, 60–64. https://doi.org/10.1016/j.jphotobiol.2012.12.007.

Liang, J.Y., Cheng, C.W., Yu, C.H., Chen, L.Y., 2015. Investigations of blue light-induced reactive oxygen species from flavin mononucleotide on inactivation of E. coli. J. Photochem. Photobiol. B Biol. 143, 82–88. https://doi.org/10.1016/j.jphotobiol.2015.01.005.

Lins de Sousa, D., Araújo Lima, R., Zanin, I.C., Klein, M.I., Janal, M.N., Duarte, S., 2015. Effect of twice-daily blue light treatment on matrix-rich biofilm development. PloS One 10 (7), e0131941. https://doi.org/10.1371/journal.pone.0131941.

Liu, G.Y., Doran, K.S., Lawrence, T., Turkson, N., Puliti, M., Tissi, L., Nizet, V., 2004. Sword and shield: Linked group B streptococcal β-hemolysin/cytolysin and carotenoid pigment function to subvert host phagocyte defense. Proc. Natl. Acad. Sci. USA 2004 101, 14491–14496. https://doi.org/10.1073/pnas.0406143101.

Liu, G.Y., Essex, A., Buchanan, J.T., Datta, V., Hoffman, H.M., Bastian, J.F., Fierer, J., Nizet, V., 2005. *Staphylococcus aureus* golden pigment impairs neutrophil killing and promotes virulence through its antioxidant activity. J. Exp. Med. 2005 202, 209–215. https://doi.org/10.1084/jem.20050846.

Luo, S., Yang, X., Wu, S., Li, Y., Wu, J., Liu, M., Hu, X., 2022. Understanding a defensive response of methicillin-resistant Staphylococcus aureus after exposure to multiple cycles of sub-lethal blue light. FEMS Microbiol. Lett. 369 (1), fnac050. https://doi.org/10.1093/femsle/fnac050.

Ma, J., Hiratsuka, T., Etoh, T., Akada, J., Fujishima, H., Shiraishi, N., Inomata, M., 2018. Anti-proliferation effect of blue light-emitting diodes against antibiotic-resistant *Helicobacter pylori*. J. Gastroenterol. Hepatol. 33 (8), 1492–1499. https://doi.org/10.1111/jgh.14066.

Maclean, M., MacGregor, S.J., Anderson, J.G., Woolsey, G.A., 2008a. The role of oxygen in the visible-light inactivation of *Staphylococcus aureus*. J. Photochem. Photobiol. B Biol. 92 (3), 180–184. https://doi.org/10.1016/j.jphotobiol.2008.06.006.

Maclean, M., MacGregor, S.J., Anderson, J.G., Woolsey, G.A., 2008b. High-intensity narrow-spectrum light inactivation and wavelength sensitivity *of Staphylococcus aureus*. FEMS Microbiol. Lett. 285 (2), 227–232. https://doi.org/10.1111/j.1574-6968.2008.01233.x.

Maclean, M., MacGregor, S.J., Anderson, J.G., Woolsey, G., 2009. Inactivation of bacterial pathogens following exposure to light from a 405-nanometer light-emitting diode array. Appl. Environ. Microbiol. 75 (7), 1932–1937. https://doi.org/10.1128/aem.01892-08.

Marshall, J.H., Wilmoth, G.J., 1981. Pigments of *Staphylococcus aureus,* a series of triterpenoid carotenoids.(1981). J. Bacteriol. 147, 900–913. https://doi.org/10.1128/jb.147.3.900-913.1981.

Maisch, T., Wagner, J., Papastamou, V., Nerl, H.J., Hiller, K.A., Szeimies, R.M., Schmalz, G., 2009. Combination of 10% EDTA, photosan, and a blue light hand-held photopolymerizer to inactivate leading oral bacteria in dentistry in vitro. J. Appl. Microbiol. 107 (5), 1569–1578. https://doi.org/10.1111/j.1365-2672.2009.04342.x.

Maisonneuve, E., Fraysse, L., Lignon, S., Capron, L., Dukan, S., 2008. Carbonylated proteins are detectable only in a degradation-resistant aggregate state in *Escherichia coli*. J. Bacteriol. 190 (20), 6609–6614. https://doi.org/10.1128/jb.00588-08.

Marchi, S., Amodeo, D., Peccetti, B., De Palma, I., Messina, G., Montomoli, E., Trombetta, C.M., 2025. The virucidal potential effects of violet-blue light on influenza D virus. Photochem. & Photobiol. Sci. 1–10. https://doi.org/10.1007/s43630-025-00708-9.

Merigo, E., Conti, S., Ciociola, T., Manfredi, M., Vescovi, P., Fornaini, C., 2019. Antimicrobial photodynamic therapy protocols on Streptococcus mutans with different combinations of wavelengths and photosensitizing dyes. Bioengineering 6 (2), 42. https://doi.org/10.3390/bioengineering6020042.

Metzger, M., Hacobian, A., Karner, L., Krausgruber, L., Grillari, J., Dungel, P., 2022. Resistance of bacteria toward 475 nm blue light exposure and the possible role of the SOS response. Life 12 (10), 1499.

Moan, J., Berg, K., 1991. The photodegradation of porphyrins in cells can be used to estimate the lifetime of singlet oxygen. Photochem. Photobiol. 53 (4), 549–553. https://doi.org/10.1111/j.1751-1097.1991.tb03669.x.

Mohamad, S.A., Milward, M.R., Kuehne, S.A., Hadis, M.A., Palin, W.M., Cooper, P.R., 2021. Potential for direct application of blue light for photo-disinfection of dentine. J. Photochem. Photobiol. B Biol. 215, 112123. https://doi.org/10.3390/life12101499.

Mohamad, S.A., Megson, I.L., Kean, A.H., 2023. Blue light photoinhibition of Streptococcus mutans: potential chromophores and mechanisms. Lasers Dent. Sci. 7 (4), 195–205. https://doi.org/10.1007/s41547-023-00204-2.

Moradi, M., Fazlyab, M., Pourhajibagher, M., Chiniforush, N., 2022. Antimicrobial action of photodynamic therapy on Enterococcus faecalis biofilm using curing light, curcumin and riboflavin. Aust. Endod. J. 48 (2), 274–282. https://doi.org/10.1111/aej.12565.

Mussi, M.A., Gaddy, J.A., Cabruja, M., Arivett, B.A., Viale, A.M., Rasia, R., Actis, L.A., 2010. The Opportunistic Human Pathogen *Acinetobacter Baumannii* Senses and Responds to Light, 2010 J. Bacteriol. 192, 6336–6345. https://doi.org/10.1128/JB.00917-10.

Müller, G.L., Tuttobene, M., Altilio, M., Martinez Amezaga, M., Nguyen, M., Cribb, P., Mussi, M.A., 2017. Light modulates metabolic pathways and other novel physiological traits in the human pathogen *Acinetobacter baumannii.* J. Bacteriol. 199 (10), 10–1128. https://doi.org/10.1128/jb.00011-17.

Negri, L.B., Korupolu, S., Farinelli, W., Jolly, A.K., Redmond, R.W., Aggarwal, S., Gelfand, J.A., 2025. Antimicrobial Blue Light Reduces Human-Wound Pathogens' Resistance to Tetracycline-Class Antibiotics in Biofilms. Cells 14 (3), 219. https://doi.org/10.3390/cells14030219.

Nikinmaa, S., Alapulli, H., Auvinen, P., Vaara, M., Rantala, J., Kankuri, E., Pätilä, T., 2020. Dual-light photodynamic therapy administered daily provides a sustained antibacterial effect on biofilm and prevents *Streptococcus mutans* adaptation. PloS One 15 (5), e0232775. https://doi.org/10.1371/journal.pone.0232775.

Nori, P., Szymczak, W., Puius, Y., Sharma, A., Cowman, K., Gialanella, P., Guo, Y., 2020. Emerging co-pathogens: New Delhi metallo-beta-lactamase producing *Enterobacterales* infections in New York City COVID-19 patients. Int. J. Antimicrob. Agents 56 (6), 106179. https://doi.org/10.1016/j.ijantimicag.2020.106179.

Ogilby, P.R., 2010. Singlet oxygen: there is indeed something new under the sun. Chem. Soc. Rev. 39 (8), 3181–3209. https://doi.org/10.1039/B926014P.

Oliveira, L.M.C., Tuchin, V.V., 2019. The optical clearing method: A new tool for Clinical Practice and Biomedical Engineering. Springer Nature. https://doi.org/10.1007/978-3-030-33055-2_3.

Orlandi, V.T., Martegani, E., Bolognese, F., 2018. Catalase A is involved in the response to photooxidative stress in *Pseudomonas aeruginosa.* Photo Photodyn. Ther. 22, 233–240. https://doi.org/10.1016/j.pdpdt.2018.04.016.

Ozdemir, G.D., Dos Anjos, C., Ozdemir, M.A., Leanse, L.G., Dai, T., 2025. Lights out for Superbugs: Is antimicrobial blue light a potential approach for future infection Control? Adv. Drug Deliv. Rev., 115654 https://doi.org/10.1016/j.addr.2025.115654.

Paschoal, M.A., Tonon, C.C., Spolidório, D.M., Bagnato, V.S., Giusti, J.S., Santos-Pinto, L., 2013. Photodynamic potential of curcumin and blue LED against *Streptococcus mutans* in a planktonic culture. Photo Photodyn. Ther. 10 (3), 313–319. https://doi.org/10.1016/j.pdpdt.2013.02.002.

Paschoal, M.A., Lin, M., Santos-Pinto, L., Duarte, S., 2015. Photodynamic antimicrobial chemotherapy on *Streptococcus mutans* using curcumin and toluidine blue activated by a novel LED device. Lasers Med. Sci. 30, 885–890. https://doi.org/10.1007/s10103-013-1492-1.

Pereira, C.A., Costa, A.C.B.P., Carreira, C.M., Junqueira, J.C., Jorge, A.O.C., 2013. Photodynamic inactivation of Streptococcus mutans and Streptococcus sanguinis biofilms in vitro. Lasers Med. Sci. 28, 859–864. https://doi.org/10.1007/s10103-012-1175-3.

Perez, S., 2020. Increase in hospital-acquired carbapenem-resistant Acinetobacter baumannii infection and colonization in an acute care hospital during a surge in COVID-19 admissions—New Jersey, February–July 2020. MMWR. Morb. Mortal. Wkly. Rep. 69. https://doi.org/10.15585/mmwr.mm6948e1.

Pieranski, M., Sitkiewicz, I., Grinholc, M., 2020. Increased photoinactivation stress tolerance of *Streptococcus agalactiae* upon consecutive sublethal phototreatments. Free Radic. Biol. Med. 160, 657–669.

Pileggi, G., Wataha, J.C., Girard, M., Grad, I., Schrenzel, J., Lange, N., Bouillaguet, S., 2013. Blue light-mediated inactivation of Enterococcus faecalis in vitro. Photo Photodyn. Ther. 10 (2), 134–140. https://doi.org/10.1016/j.pdpdt.2012.11.002.

Plattfaut, I., Demir, E., Fuchs, P.C., Schiefer, J.L., Sturmer, E.K., Bruning, A.K.E., Oplander, C., 2021. Characterization of Blue Light Treatment for Infected Wounds: Antibacterial Efficacy of 420, 455, and 480 nm Light-Emitting Diode Arrays Against Common Skin Pathogens Versus Blue Light-Induced Skin Cell Toxicity. Photo Photomed. Laser Surg. 2021 (39), 339–348. https://doi.org/10.1089/photob.2020.4932.

Plaetzer, K., Krammer, B., Berlanda, J., Berr, F., Kiesslich, T., 2009. Photophysics and photochemistry of photodynamic therapy: fundamental aspects. Lasers Med. Sci. 24 (2), 259–268. https://doi.org/10.1007/s10103-008-0539-1.

Plavskii, V.Y., Mikulich, A. v, Tretyakova, A.I., Leusenka, I.A., Plavskaya, L.G., Kazyuchits, O.A., Dobysh, I.I., Krasnenkova, T.P., 2018. Porphyrins and flavins as endogenous acceptors of optical radiation of blue spectral region determining photoinactivation of microbial cells. J. Photochem. Photobiol. B Biol. 183, 172–183. https://doi.org/10.1016/j.jphotobiol.2018.04.021.

Pourhajibagher, M., Ghafari, H.A., Bahrami, R., Bahador, A., 2024. Photoinactivation of Enterococcus faecalis Biofilm: In Vitro Antimicrobial Effect of Photoexcited Rutin-Gallium (III) Complex via Visible Blue Light. J. Endod. 50 (5), 602–611. https://doi.org/10.1016/j.joen.2024.01.007.

Prates, R.A., da Silva, E.G., Yamada, A.M., Suzuki, L.C., Paula, C.R., Ribeiro, M.S., 2008. The irradiation parameters investigation of photodynamic therapy on yeast cells. Proc. SPIE 6846 Mech. Low. Light Ther. III, 684606. https://doi.org/10.1117/12.763059.

Quiroz-Segoviano, R.I., Serratos, I.N., Rojas-González, F., Tello-Solís, S.R., Sosa-Fonseca, R., Medina-Juárez, O., García-Sánchez, M.A., 2014. On tuning the fluorescence emission of porphyrin free bases bonded to the pore walls of organo-modified silica. Molecules 19 (2), 2261–2285. https://doi.org/10.3390/molecules19022261.

Ramsey, M., Hartke, A., & Huycke, M. (2014). The Physiology and Metabolism of *Enterococci*. ⟨https://www.ncbi.nlm.nih.gov/books/NBK190432/⟩.

Ramstad, S., Le Anh-Vu, N., Johnsson, A., 2006. The temperature dependence of porphyrin production in *Propionibacterium acnes* after incubation with 5-aminolevulinic acid (ALA) and its methyl ester (m-ALA). Photochem. & Photobiol. Sci. 5 (1), 66–72. https://doi.org/10.1039/B512837D.

Rapacka-Zdonczyk, A., Wozniak, A., Pieranski, M., Woziwodzka, A., Bielawski, K.P., Grinholc, M., 2019. Development of *Staphylococcus aureus* tolerance to antimicrobial photodynamic inactivation and antimicrobial blue light upon sub-lethal treatment. Sci. Rep. 9 (1), 9423. https://doi.org/10.1038/s41598-019-45962-x.

Rapacka-Zdonczyk, A., Wozniak, A., Kruszewska, B., Waleron, K., Grinholc, M., 2021. Can gram-negative bacteria develop resistance to antimicrobial blue light treatment? Int. J. Mol. Sci. 22 (21), 11579. https://doi.org/10.3390/ijms222111579.

Rapacka-Zdonczyk, 2025. Beyond Resistance: Tolerance and Resilience of Bacteria to Photodynamic and Oxidative Stress. Int. J. Mol. Sci. 26 (18), 8908. https://doi.org/10.3390/ijms26188908.

Rapacka-Zdonczyk, 2026. Beyond Resistance: Phenotypic Plasticity in Bacterial Responses to Antibiotics, Oxidative Stress and Antimicrobial Photodynamic Inactivation. Molecules 31 (3), 567. https://doi.org/10.3390/molecules31030567.

Roh, H.J., Kim, A., Kang, G.S., Kim, D.H., 2016. Photoinactivation of major bacterial pathogens in aquaculture. Fish. Aquat. Sci. 19, 1–7. https://doi.org/10.1186/s41240-016-0029-5.

Rosa-Fraile, M., Rodríguez-Granger, J., Haidour-Benamin, A., Cuerva, J.M., Sampedro, A., 2006. Granadaene: Proposed structure of the Group B Streptococcus polyenic pigment. Appl. Environ. Microbiol 2006 (72), 6367–6370. https://doi.org/10.1128/aem.00756-06.

Ruiz-Arellano, X., Araque, M. del C., 2026. Microbial photoinactivation by blue light: advances and therapeutic perspectives in infections caused by multidrug-resistant pathogens. Int. J. Res. Med. Sci. 14 (1), 291–297. https://doi.org/10.18203/2320-6012.ijrms20254396.

Sampaio, L.S., de Annunzio, S.R., de Freitas, L.M., Dantas, L.O., De Boni, L., Donatoni, M. C., Fontana, C.R., 2020. Influence of light intensity and irradiation mode on methylene blue, chlorin-e6 and curcumin-mediated photodynamic therapy against Enterococcus faecalis. Photo Photodyn. Ther. 31, 101925. https://doi.org/10.1016/j.pdpdt.2020.101925.

Santamaría-Hernando, S., Cerna-Vargas, J.P., Martínez-García, P.M., de Francisco-de Polanco, S., Nebreda, S., Rodríguez-Palenzuela, P., Rodríguez-Herva, J.J., López-Solanilla, E., 2020. Blue-light perception by epiphytic Pseudomonas syringae drives chemoreceptor expression, enabling efficient plant infection. Mol. Plant Pathol. 21 (12), 1606–1619. https://doi.org/10.1111/mpp.13001.

Sarkar, A.R., Jana, N.R., 2025. Nanotechnology-Based Alternative Antimicrobial Materials and Surfaces: A Review. ACS Appl. Nano Mater. 9 (1), 1–27.

Seo, H.W., Dai, T., 2026. Unveiling the Microbial Bullseyes: Microbial Target of Antimicrobial Blue Light. Handbook of Antimicrobial Photoinactivation. Springer Nature Switzerland, Cham, pp. 1–21.

Schmid, J., Hoenes, K., Vatter, P., Hessling, M., 2019. Antimicrobial effect of visible light—photoinactivation of Legionella rubrilucens by irradiation at 450, 470, and 620 nm. Antibiotics 8 (4). https://doi.org/10.3390/antibiotics8040187.

Schmidt-Erfurth, U., Hasan, T., 2000. Mechanisms of action of photodynamic therapy with verteporfin for the treatment of age-related macular degeneration. Surv. Ophthalmol. 45 (3), 195–214. https://doi.org/10.1016/S0039-6257(00)00158-2.

Shany-Kdoshim, S., Polak, D., Houri-Haddad, Y., Feuerstein, O., 2019. Killing mechanism of bacteria within multi-species biofilm by blue light. J. Oral. Microbiol. 11 (1), 1628577. https://doi.org/10.1080/20002297.2019.1628577.

Shehatou, C., Logunov, S.L., Dunman, P.M., Haidaris, C.G., Klubben, W.S., 2019. Characterizing the antimicrobial properties of 405 nm light and the Corning® light-diffusing fiber delivery system. Lasers Surg. Med. 51 (10), 887–896. https://doi.org/10.1002/lsm.23132.

Shiotsu-Ogura, Y., Yoshida, A., Kan, P., Sasaki, H., Toyama, T., Izukuri, K., Yoshino, F., 2019. Antimicrobial photodynamic therapy using a plaque disclosing solution on Streptococcus mutans. Photo Photodyn. Ther. 26, 252–257. https://doi.org/10.1002/lsm.23132.

Snell, S.B., Gill, A.L., Haidaris, C.G., Foster, T.H., Baran, T.M., Gill, S.R., 2021. Staphylococcus aureus tolerance and genomic response to photodynamic inactivation. Msphere 6 (1), 10–1128. https://doi.org/10.1128/msphere.00762-20.

Sommers, C., Gunther, N.W., Sheen, S., 2017. Inactivation of Salmonella spp., pathogenic Escherichia coli, Staphylococcus spp., or Listeria monocytogenes in chicken purge or skin using a 405-nm LED array. Food Microbiol. 64, 135–138. https://doi.org/10.1016/j.fm.2016.12.011.

Song, S.H., Dick, B., Penzkofer, A., 2007. Photo-induced reduction of flavin mononucleotide in aqueous solutions. Chem. Phys. 332 (1), 55–65. https://doi.org/10.1016/j.chemphys.2006.11.023.

Squire, M.S., Townsend, H.A., Actis, L.A., 2022. The influence of blue light and the BlsA photoreceptor on the oxidative stress resistance mechanisms of Acinetobacter baumannii. Front. Cell. Infect. Microbiol. 12, 856953. https://doi.org/10.3389/fcimb.2022.856953.

St. Denis, T.G., Huang, L., Dai, T., Hamblin, M.R., 2011. Analysis of the bacterial heat shock response to photodynamic therapy-mediated oxidative stress. Photochem. Photobiol. 87 (3), 707–713. https://doi.org/10.1111/j.1751-1097.2011.00902.x.

Steinberg, D., Moreinos, D., Featherstone, J., Shemesh, M., Feuerstein, O., 2008. Genetic and physiological effects of noncoherent visible light combined with hydrogen peroxide on Streptococcus mutans in biofilm. Antimicrob. Agents Chemother. 52 (7), 2626–2631. https://doi.org/10.1128/aac.01666-07.

Tardu, M., Bulut, S., Kavakli, I.H., 2017. MerR and ChrR mediate blue light induced photo-oxidative stress response at the transcriptional level in Vibrio cholerae. Sci. Rep. 7 (1), 40817. https://doi.org/10.1038/srep40817.

Tomb, R.M., Maclean, M., Coia, J.E., MacGregor, S.J., Anderson, J.G., 2017. Assessment of the potential for resistance to antimicrobial violet-blue light in Staphylococcus aureus. Antimicrob. Resist. Infect. Control 6, 1–13. https://doi.org/10.1186/s13756-017-0261-5.

Tomb, R.M., White, T.A., Coia, J.E., Anderson, J.G., MacGregor, S.J., Maclean, M., 2018. Review of the comparative susceptibility of microbial species to photoinactivation using 380–480 nm violet-blue light. Photochem. Photobiol. 94 (3), 445–458. https://doi.org/10.1111/php.12883.

Touati, D., 2000. Iron and oxidative stress in bacteria. Arch. Biochem. Biophys. 373 (1), 1–6. https://doi.org/10.1006/abbi.1999.1518.

Tschowri, N., Busse, S., Hengge, R., 2009. The BLUF-EAL Protein YcgF Acts as a Direct Anti-Repressor in a Blue-Light Response of *Escherichia coli.*. https://doi.org/10.1101/gad.499409 Genes Dev. 2009 (23), 522–534. https://doi.org/10.1101/gad.499409.

Tschowri, N., Lindenberg, S., Hengge, R., 2012. Molecular Function and Potential Evolution of the Biofilm-Modulating Blue Light-Signalling Pathway of *Escherichia coli*. Mol. Microbiol 2012 (85), 893–906. https://doi.org/10.1111/j.1365-2958.2012.08147.x.

Tsutsumi-Arai, C., Arai, Y., Terada-Ito, C., Imamura, T., Tatehara, S., Ide, S., Satomura, K., 2022. Microbicidal effect of 405-nm blue LED light on *Candida albicans* and *Streptococcus mutans* dual-species biofilms on denture base resin. Lasers Med. Sci. 37 (2), 857–866. https://doi.org/10.1007/s10103-021-03323-z.

Turunen, S., Käpylä, E., Terzaki, K., Viitanen, J., Fotakis, C., Kellomäki, M., Farsari, M., 2011. Pico-and femtosecond laser-induced crosslinking of protein microstructures: evaluation of processability and bioactivity. Biofabrication 3 (4), 045002. https://doi.org/10.1088/1758-5082/3/4/045002.

Tuttobene, M.R., Fernández-García, L., Blasco, L., Cribb, P., Ambroa, A., Müller, G.L., Fernández-Cuenca, F., Bleriot, I., Rodríguez, R.E., Barbosa, B.G.V., Lopez-Rojas, R., Trastoy, R., López, M., Bou, G., Tomás, M., Mussi, M.A., 2019. Quorum and Light Signals Modulate Acetoin/Butanediol Catabolism in *Acinetobacter* spp. Front. Microbiol. 10, 1376. https://doi.org/10.3389/fmicb.2019.01376.

Tuttobene, M.R., Müller, G.L., Blasco, L., Arana, N., Hourcade, M., Diacovich, L., Mussi, M.A., 2021. Blue light directly modulates the quorum network in the human pathogen *Acinetobacter baumannii*. Sci. Rep. 11 (1), 13375. https://doi.org/10.1038/s41598-021-92845-1.

Valliammai, A., Selvaraj, A., Muthuramalingam, P., Priya, A., Ramesh, M., Pandian, S.K., 2021. Staphyloxanthin inhibitory potential of thymol impairs antioxidant fitness, enhances neutrophil-mediated killing and alters membrane fluidity of methicillin-resistant *Staphylococcus aureus*. Biomed. Pharm. 2021 (141), 111933. https://doi.org/10.1016/j.biopha.2021.111933.

Vanberg, C., Lutnaes, B.F., Langsrud, T., Nes, I.F., Holo, H., 2007. Propionibacterium jensenii produces the polyene pigment granadaene and has hemolytic properties similar to those of Streptococcus agalactiae. Appl. Environ. Microbiol. 73 (17), 5501–5506. https://doi.org/10.1128/aem.00545-07.

Vanbogelen, R.A., Kelley, P.M., Neidhardt, F.C., 1987. Differential induction of heat shock, SOS, and oxidation stress regulons and accumulation of nucleotides in *Escherichia coli*. J. Bacteriol. 169 (1), 26–32. https://doi.org/10.1128/jb.169.1.26-32.1987.

Vatansever, F., de Melo, W.C., Avci, P., Vecchio, D., Sadasivam, M., Gupta, A., Hamblin, M.R., 2013. Antimicrobial strategies centered around reactive oxygen species–bactericidal antibiotics, photodynamic therapy, and beyond. FEMS Microbiol. Rev. 37 (6), 955–989. https://doi.org/10.1111/1574-6976.12026.

Voronkina, I., Liptakova, A., Dyachenko, V., Derkach, S., Sklyar, N., 2024. Efficiency of photodynamic inactivation Actinomyces israelii and Prevotella melaninogenica. Bratisl. Med. J. /Bratisl. é Lek. árske Listy 125 (11). https://doi.org/10.4149/bll_2024_112.

Walker, P., Taylor, A.J., Hitchcock, A., Webb, J.P., Green, J., Weinstein, J., Kelly, D.J., 2022. Exploiting violet-blue light to kill Campylobacter jejuni: analysis of global responses, modeling of transcription factor activities, and identification of protein targets. Msystems 7 (4), e00454-22. https://doi.org/10.1128/msystems.00454-22.

Walter, A.B., Simpson, J., Jenkins, J.L., Skaar, E.P., Jansen, E.D., 2020. Optimization of optical parameters for improved photodynamic therapy of Staphylococcus aureus using endogenous coproporphyrin III. Photo Photodyn. Ther. 29, 101624. https://doi.org/10.1016/j.pdpdt.2019.101624.

Wan, X., Xu, Y., Li, Y., Liao, Q., Tao, H., Wang, H., 2022. Photodynamic inactivation of Staphylococcus aureus in the system of titanium dioxide nanoparticles sensitized by hypocrellin B and its application in food preservation. Food Res. Int. 156, 111141. https://doi.org/10.1016/j.foodres.2022.111141.

Wang, Y., Wu, X., Chen, J., Amin, R., Lu, M., Bhayana, B., Dai, T., 2016. Antimicrobial blue light inactivation of gram-negative pathogens in biofilms: in vitro and in vivo studies. J. Infect. Dis. 213 (9), 1380–1387. https://doi.org/10.1093/infdis/jiw070.

Wang, Y., Wang, Y., Wang, Y., Murray, C.K., Hamblin, M.R., Hooper, D.C., Dai, T., 2017a. Antimicrobial blue light inactivation of pathogenic microbes: State of the art. Drug Resist. Updates 33, 1–22. https://doi.org/10.1016/j.drup.2017.10.002.

Wang, Y., Ferrer-Espada, R., Baglo, Y., Yang, Q., Mylonakis, E., Nielsen, P.V., Hamblin, M.R., 2017b. Antimicrobial blue light inactivation of *Pseudomonas aeruginosa* by photo-exciting endogenous porphyrins: In vitro and in vivo studies. Lasers Surg. Med. 49 (1), 62–71. https://doi.org/10.1002/lsm.22474.

Wang, Y., Ferrer-Espada, R., Baglo, Y., Gu, Y., Dai, T., 2019. Antimicrobial blue light inactivation of Neisseria gonorrhoeae: roles of wavelength, endogenous photosensitizer, oxygen, and reactive oxygen species. Lasers Surg. Med. 51 (9), 815–823. https://doi.org/10.1002/lsm.23104.

Wang, R., Liu, Q., Gao, A., Tang, N., Zhang, Q., Zhang, A., Cui, D., 2022. Recent developments of sonodynamic therapy in antibacterial application. Nanoscale 14 (36), 12999–13017. https://doi.org/10.1039/d2nr01847k.

Wang, Y., Li, X., Chen, H., Yang, X., Guo, L., Ju, R., Dai, T., Li, G., 2024. Antimicrobial blue light inactivation of Pseudomonas aeruginosa: Unraveling the multifaceted impact of wavelength, growth stage, and medium composition. J. Photochem. Photobiol. B Biol. 259, 113023. https://doi.org/10.1093/nar/gks017.

Wei, Q., Le Minh, P.N., Dötsch, A., Hildebrand, F., Panmanee, W., Elfarash, A., Cornelis, P., 2012. Global regulation of gene expression by OxyR in an important human opportunistic pathogen. Nucleic Acids Res. 40 (10), 4320–4333. https://doi.org/10.1093/nar/gks017.

Whidbey, C., Harrell, M.I., Burnside, K., Ngo, L., Becraft, A.K., Iyer, L.M., Aravind, L., Hitti, J., Adams Waldorf, K.M., Rajagopal, L., 2013. A hemolytic pigment of Group B Streptococcus allows bacterial penetration of human placenta. J. Exp. Med. 2013 (210), 1265–1281. https://doi.org/10.1084/jem.20122753.

Wozniak, A., Grinholc, M., 2018. Combined antimicrobial activity of photodynamic inactivation and antimicrobials–state of the art. Front. Microbiol. 9, 930. https://doi.org/10.3389/fmicb.2018.00930.

Wu, J., Chu, Z., Ruan, Z., Wang, X., Dai, T., Hu, X., 2018. Changes of intracellular porphyrin, reactive oxygen species, and fatty acids profiles during inactivation of methicillin-resistant *Staphylococcus aureus* by antimicrobial blue light. Front. Physiol. 9, 1658. https://doi.org/10.3389/fphys.2018.01658.

Wu, S., Subharat, P., Brightwell, G., 2021. A new insight into the bactericidal mechanism of 405 nm blue light-emitting-diode against dairy sourced *Cronobacter sakazakii*. Foods 10 (9), 1996. https://doi.org/10.3390/foods10091996.

Wu, S., Hadi, J., Brightwell, G., 2022. Growth medium-and strain-dependent bactericidal efficacy of blue light against Shiga toxin-producing *Escherichia coli* on food-grade stainless steel and plastic. Food Microbiol. 103, 103953. https://doi.org/10.1016/j.fm.2021.103953.

Wu, J., Lu, X., Huang, M., Wu, S., Zeng, M., Liu, Z., Hu, X., 2025. The impact of sublethal antimicrobial blue light on lipidomic changes of *Escherichia coli* and *Salmonella* Typhimurium. Front. Cell. Infect. Microbiol. 15, 1612638. https://doi.org/10.3389/fcimb.2025.1612638.

Xuan, W., He, Y., Huang, L., Huang, Y.Y., Bhayana, B., Xi, L., Hamblin, M.R., 2018. Antimicrobial photodynamic inactivation mediated by tetracyclines in vitro and in vivo: photochemical mechanisms and potentiation by potassium iodide. Sci. Rep. 8 (1), 17130. https://doi.org/10.1038/s41598-018-35594-y.

Yang, P., Wang, N., Wang, C., Yao, Y., Fu, X., Yu, W., Cai, R., Yao, M., 2017. 460 nm visible light irradiation eradicates MRSA via inducing prophage activation. J. Photochem. Photobiol. B Biol. 166, 311–322. https://doi.org/10.1016/j.jphotobiol.2016.12.001.

Yang, J., Yun, S., Park, W., 2023. Blue Light Sensing BlsA-Mediated Modulation of Meropenem Resistance and Biofilm Formation in *Acinetobacter baumannii*. mSystems 8 (1), e00897-22. https://doi.org/10.1128/msystems.00897-22.

Yang, R., Xu, Y., Xu, J., Li, Y., Wan, X., Kong, R., Wang, H.L., 2024. The transcriptional changes of LrgA discriminates the responsiveness of Staphylococcus aureus towards blue light from that of photodynamic inactivation. J. Photochem. Photobiol. B Biol. 258, 112967. https://doi.org/10.1016/j.jphotobiol.2024.112967.

Yin, R., Dai, T., Avci, P., Jorge, A.E.S., de Melo, W.C., Vecchio, D., Hamblin, M.R., 2013. Light based anti-infectives: ultraviolet C irradiation, photodynamic therapy, blue light, and beyond. Curr. Opin. Pharmacol. 13 (5), 731–762. https://doi.org/10.1016/j.coph.2013.08.009.

Yoshida, A., Sasaki, H., Toyama, T., Araki, M., Fujioka, J., Tsukiyama, K., Yoshino, F., 2017. Antimicrobial effect of blue light using Porphyromonas gingivalis pigment. Sci. Rep. 7 (1), 5225. https://doi.org/10.1038/s41598-017-05706-1.

Yuan, L., Wang, Y., Zong, Y., Dong, F., Zhang, L., Wang, G., Dong, H., Wang, Y., 2023. Response of genes related to iron and porphyrin transport in Porphyromonas gingivalis to blue light. J. Photochem. Photobiol. B Biol. 241, 112670. https://doi.org/10.1016/j.jphotobiol.2023.112670.

Zhang, Y., Zhu, Y., Gupta, A., Huang, Y., Murray, C.K., Vrahas, M.S., Dai, T., 2014. Antimicrobial blue light therapy for multidrug-resistant Acinetobacter baumannii infection in a mouse burn model: implications for prophylaxis and treatment of combat-related wound infections. J. Infect. Dis. 209 (12), 1963–1971. https://doi.org/10.1093/infdis/jit842.

Zhang, L., Li, Y., Zhang, Q., Du, N., Li, X., Zhang, Q., Wang, Y., 2020. Antimicrobial activity of an implantable wireless blue light-emitting diode against root canal biofilm in vitro. Photo Photomed. Laser Surg. 38 (11), 694–702. https://doi.org/10.1089/photob.2020.4821.

## 8.2. Publication no. 2.

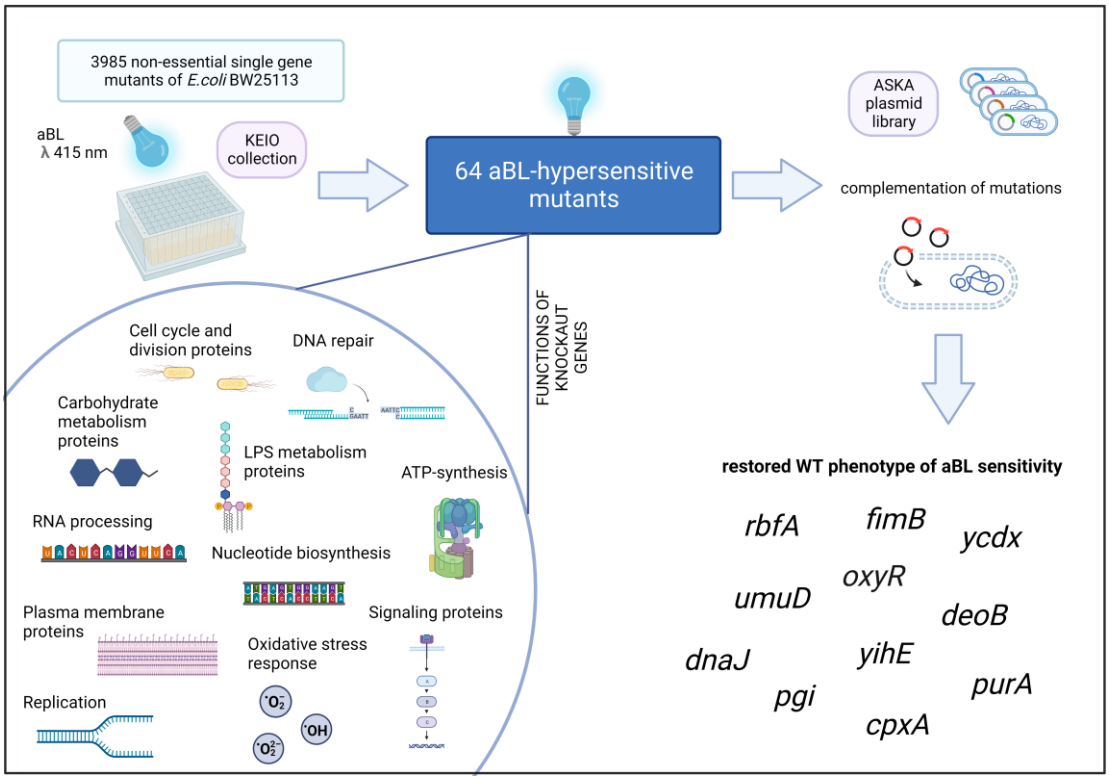


Figure 2. Graphical abstract of Publication no. 2.

AMERICAN SOCIETY FOR MICROBIOLOGY | Microbiology Spectrum

| Genetics and Molecular Biology | Research Article

# Can antimicrobial blue light contribute to resistance development? Genome-wide analysis revealed aBL-protective genes in *Escherichia coli*

**Beata Kruszewska-Naczk,[1,2] Mariusz Grinholc,[1] Krzysztof Waleron,[2] Julia Elisabeth Bandow,[3] Aleksandra Rapacka-Zdończyk[2]**

**AUTHOR AFFILIATIONS** See affiliation list on p. 18.

**ABSTRACT** Antimicrobial blue light (aBL) is a promising non-antibiotic approach to fighting multidrug-resistant bacteria. However, the complete mechanism of aBL action is not fully understood yet. This study contributes to a better understanding that the response to aBL depends on many factors and that it is hardly possible to identify a predominant mechanism underlying microbial sensitivity to photoinactivation. The results of this study provide insights into genetic changes that may lead to bacterial survival at higher aBL doses, giving rise to aBL-resistant strains. To our best knowledge, this is the first study concerning genome-wide mutant testing of aBL. We managed to identify 64 single-gene mutants that lacked certain protective genes expressing aBL-increased sensitivity.

**IMPORTANCE** Increasing antibiotic resistance and the lack of new antibiotic-like compounds to combat bacterial resistance are significant problems of modern medicine. The development of new alternative therapeutic strategies is extremely important. Antimicrobial blue light (aBL) is an innovative approach to combat multidrug-resistant microorganisms. aBL has a multitarget mode of action; however, the full mechanism of aBL antibacterial action requires further investigation. In addition, the potential risk of resistance development to this treatment should be considered.

**KEYWORDS** antimicrobial blue light, *Escherichia coli*, genome-wide analysis, hypersensitive mutants, resistance

According to data from the World Health Organization (1), an estimated 600 million cases of foodborne diseases and 420,000 deaths related to pathogens occur worldwide each year. Food products, especially minimally processed foods such as raw seafood, fresh vegetables, fruits, and raw juices, as well as food processing environments, are vulnerable to diarrheal disease pathogens. Consumer awareness of the harmfulness of preservatives and pesticides, as well as the potential loss of foods' nutritional and organoleptic values, increases the need for the development of sterilization technology based on non-thermal approaches (2).

*Escherichia coli* (*E. coli*) is an intensively studied bacterial species widely present in the environment. Usually considered a harmless commensal bacterium, pathogenic strains are capable of causing diseases in humans and animals (3). An example of such pathogenic strains is the verotoxigenic foodborne pathogen *E. coli* O157:H7, which causes hemorrhagic colitis, hemolytic uremic syndrome, or even death (4). Multiple studies worldwide document increasing antibiotic resistance and associated healthcare threats (5–10). *E. coli* O157:H7 is the third leading cause of life-threatening foodborne illnesses among pathogens, next to *Salmonella* and *Listeria monocytogenes* (11). In the USA alone, the *E. coli* O157:H7 serotype causes 73,000 illnesses annually (12). The

**Editor** Minsu Kim, Emory University, Atlanta, Georgia, USA

Address correspondence to Aleksandra Rapacka-Zdończyk, a.rapacka-zdonczyk@gumed.edu.pl.

The authors declare no conflict of interest.

See the funding table on p. 18.

**Received** 19 June 2023
**Accepted** 24 October 2023
**Published** 8 December 2023

lack of new antibiotic-like compounds to combat bacterial resistance is a significant concern of modern medicine. According to *The Review on Antimicrobial Resistance*, it is estimated that by 2050, if new solutions do not slow down the rise in the drug resistance of pathogens, 10 million lives a year will be at risk due to multidrug-resistant infections. Without new effective antimicrobials, key medical procedures could become too dangerous to perform (13). Thus, the development of new alternative therapeutic strategies for treating multidrug-resistant infections is extremely crucial.

Antimicrobial blue light (aBL), an innovative light-based non-antibiotic and non-thermal approach to fighting multidrug-resistant microbes, has attracted increasing attention lately. It is believed to have a multitarget mode of action caused by the rapid reaction of reactive oxygen species (ROS) with a wide range of cellular macromolecules such as proteins, lipids, and nucleic acids (DNA and RNA), which results in cell death (14, 15). According to Hyun and Lee, aBL has antimicrobial potential against foodborne pathogens, is "eco-friendly," and is a cheap and safe alternative to thermal approaches and ultraviolet (UV) radiation (16). Nevertheless, the complete mechanism of the antibacterial action of aBL is not fully understood yet and needs further analysis (17, 18). Moreover, the potential risk of resistance development should also be considered. In previous reports, our team has shown that the development of tolerance to aBL is possible for both gram-positive (19, 20) and gram-negative (21) bacteria. Nevertheless, no aBL resistance has been demonstrated so far.

The main aim of this study was to identify genes and proteins that are crucial for the bacterial response to aBL in *E. coli*. The resource for genome-wide testing of mutational effects was the Keio knockout collection, a set of precisely defined, single-gene deletions of non-essential genes in the strain background of *E. coli* BW25113 (22). The entire *E. coli* Keio collection was screened to distinguish single-gene mutants that express the aBL-hypersensitive phenotype.

## MATERIALS AND METHODS

The experimental workflow is presented in Fig. 1.

### Strains and culture conditions

Analyses were performed using a collection of *E. coli* BW25113 single-gene knockout mutants [the Keio collection, 3,985 strains (22)] and a complete set of ORF clones of *E. coli* (ASKA plasmid library) kindly provided by the National BioResource Project and the National Institute of Genetics [Shizuoka, Japan (23)].

All the strains were cultured in Luria–Bertani (LB) broth (BTL, Łódź, Poland) or LB agar medium (A&A, Gdansk, Poland) at 37°C under aerobic conditions in an orbital incubator (Innova 40, Brunswick, Germany) at 150 rpm. Knockout mutants were maintained in the presence of 15 µg/mL of kanamycin, whereas strains harboring plasmids were treated in the presence of 150 µg/mL chloramphenicol. The strains were stored in 96-deep well plates filled with LB, and 15% glycerol medium was administered to them for storage at −80°C. Before the cells were used, they were freshly stamped into new microtiter plates filled with the LB medium and incubated overnight (16–20 h) in an orbital incubator at 150 rpm.

### Chemicals

Kanamycin sulfate was purchased from Gibco (Paisley, UK), and chloramphenicol, from Sigma-Aldrich (Darmstadt, Germany). Stock solutions, at concentrations of 15 or 150 mg/mL, respectively, were prepared in $ddH_2O$ and stored at −20°C. Isopropyl β-d-1-thiogalactopyranoside (IPTG) (100 mg/mL; Blirt, Gdansk, Poland) stock solution was prepared and stored at −20°C.

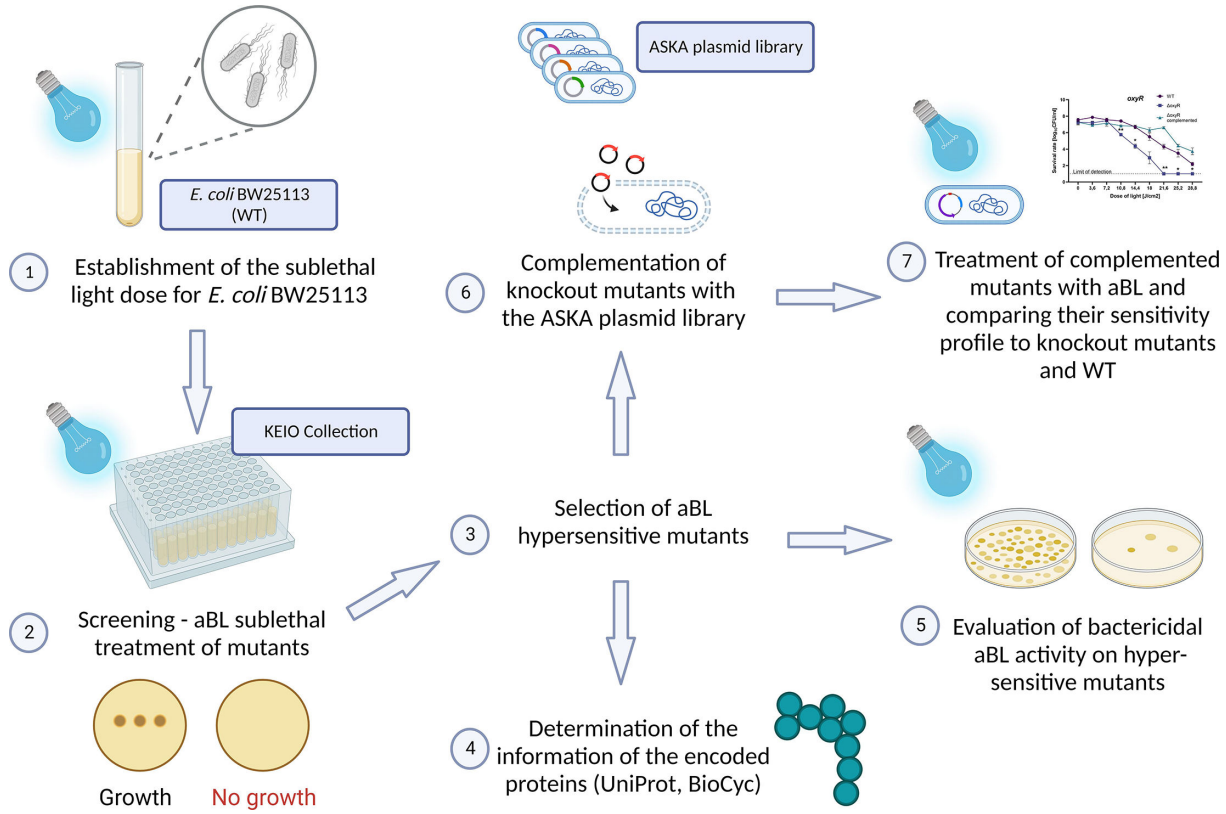


**FIG 1** Experimental workflow.

## Light source

Irradiation was performed with an LED light source that emitted blue light (λmax 415 nm, irradiance 25 mW/cm$^2$; Cezos, Gdynia, Poland). The light source allows 96 samples to be exposed to irradiation simultaneously. The LED light source was constructed to reach a homogeneous light distribution, and it is equipped with an optical lens to allow the equal distribution of light to ensure that equal doses of light are able to reach each sample. The emission spectra of light sources were measured using a Digikrom CM110 spectrograph (CVI Laser Corporation, USA) equipped with a ST-6V CCD camera (SBIG, USA). Irradiance was measured for each illumination spot (referring to each of the 96 wells) to evidence that the light distribution is homogenous and the differences between light densities do not exceed 10% (except for a few fields, which were taken into account when performing the experiments). To increase power homogeneity, the 96-well plates were placed in different orientations relative to the light source. The picture of the LED light source and the map of irradiance distribution over the illuminated area were presented in Fig. S1.

## aBL sensitivity of the *E. coli* parental strain BW25113

To quantify the aBL sensitivity of the *E. coli* BW25113 parental strain, microbial overnight cultures were adjusted to an optical density of 0.5 McFarland (McF; 5 × 10$^7$ CFU/mL). Next, aliquots of 100 µL per well were transferred to 96-well microtiter plates and irradiated with different light doses (0–64.8 J/cm$^2$). After their illumination, 10 µL aliquots of each sample were serially diluted 10 times in phosphate-buffered saline (PBS, Sigma-Aldrich, Germany) to generate dilutions of $10^{-1}$–$10^{-4}$, which were streaked horizontally on plates. The plates were incubated at 37°C for 16–20 h, after which colonies were counted to estimate the survival rate, expressed in $\log_{10}$ CFU/mL. Each experiment was performed thrice. The minimal duration of the killing of 99% of the

cells ($MDK_{99}$, defined further as the sublethal dose) of irradiation was estimated for application in a screening of the Keio collection.

### Screening of the Keio collection

The main focus of this experiment was to identify *E. coli* single-gene mutants, which are especially sensitive to aBL treatment. Overnight cultures of knockout mutants prepared in microtiter plates were diluted 10 times in PBS. From each well that contained mutant cultures, 2 µL was dropped onto an LB agar plate supplemented with kanamycin. After 1-h incubation at 37°C, the spots were subjected to aBL at the light dose assigned as sublethal for the parental *E. coli* BW25113 strain. Dark controls (without irradiation) were also prepared. Afterward, the plates were incubated at 37°C overnight. The experiment was performed in three biologically independent repetitions. For each mutant, the number of experiments in which no cells were observed after overnight incubation (post-irradiation) was summed up to give a score. Mutants with a score of 2 or 3 were classified as aBL-sensitive, as Krewing et al. (24) described for other stressors.

### aBL sensitivity of the selected mutants

This analysis was performed to obtain quantified profiles of the aBL sensitivity of mutants and to compare them to the parental strain profile. Microbial overnight cultures were adjusted to an optical density of 0.5 McF ($5 \times 10^7$ CFU/mL), and aliquots of 100 µL per well were transferred to 96-well microtiter plates and irradiated with different light doses (0–43.2 J/cm$^2$). After the illumination, 10 µL aliquots of each sample were serially diluted 10 times in PBS to generate dilutions of $10^{-1}$–$10^{-4}$, which were streaked horizontally on LB agar plates. The plates were incubated at 37°C for 16–20 h, and then, colonies were counted to estimate the survival rates. Each experiment was performed thrice for each mutant.

### Complementation

The experiment was conducted to check if the complementation of the deleted genes would restore the wild-type (WT) phenotype of aBL sensitivity to hypersensitive mutants. The selected mutants of the Keio collection were transformed with the plasmid pCA24N of the ASKA collection, which harbors the respective gene under the control of an IPTG-inducible promoter for complementation of the knockout and with the selective gene of chloramphenicol resistance (22). Plasmids of interest were isolated with the EndoFree Plasmid Maxi Kit (Syngen, Wrocław, Poland). Next, complementation was performed with a standard protocol using $CaCl_2$ (Sigma-Aldrich, Germany). An overnight culture of a strain of interest was diluted at the ratio of 1:100 in a fresh LB medium with kanamycin. Then, the strains were incubated at 37°C in an orbital incubator (Innova 40, Brunswick, Germany) at 150 rpm to reach an optical density of 0.4–0.6. The bacterial suspension was centrifuged and suspended in a 50 mM $CaCl_2$ cold solution in half volume of the primary culture and incubated on ice for 0.5 h. Next, the suspensions were centrifuged and suspended in 1 mL of the $CaCl_2$ solution and incubated for 1 h. After this, 200 µL of the suspensions was transferred into new tubes, and approximately 200 ng of isolated plasmid DNA was added. No DNA was added to the control probe. Next, the probes were incubated for 1 h, transferred to 43°C for 3 min, and then immediately placed on ice for 3 min. Next, 1 mL of the LB medium was added, and the probes were incubated in the orbital rotator for 1 h at 37°C. After that, the probes were streaked on LB agar plates with kanamycin (growth control) or chloramphenicol to verify proper transformation. Additionally, the presence or absence of a gene of interest was verified by PCR reaction using specified primers dedicated to the ASKA collection (oligonucleotides were synthesized by Oligo, Warsaw, Poland). The complemented and verified strains were used in the next experiments.

## Evaluation of the optimized experimental conditions adequate for proper analysis of the *E. coli* BW25113 Δ*oxyR* deletion mutant and the complemented strain response to aBL

The experimental conditions were optimized with the use of one representative of the *E. coli* mutants (i.e., *E. coli* BW25113 Δ*oxyR* and its complemented derivative).

### *Evaluation of the IPTG concentration*

Overnight cultures of the complemented Δ*oxyR* strain were diluted at the volume-to-volume (vol/vol) ratio of 1:100 in the fresh LB medium supplemented with specified antibiotics. The IPTG solution was added to the cultures to obtain total concentrations of 2, 1, and 0.5 µM. After 2 h of incubation (37°C, 150 rpm), the cultures were adjusted to 0.5 McF and treated with a range of light doses: 0–36 J/cm$^2$. After the irradiation, aliquots were plated to determine CFU/mL, as described in previous experiments.

### *Evaluation of the IPTG induction time for the complemented mutant and choice of the bacterial growth phase for the deletion mutant*

Two overnight cultures of the complemented Δ*oxyR* strain with specific antibiotics were prepared. IPTG was administered to the first culture at the start of the culture to obtain 1 µM of IPTG. Then, the samples were incubated at 37°C with shaking (at 150 rpm) for 16 h. The second overnight culture was diluted after 16 h of incubation (37°C, 150 rpm) at the vol/vol ratio of 1:100 in the fresh LB medium supplemented with specified antibiotics and 1 µM IPTG. After 2 h of incubation (37°C, 150 rpm), the cultures were diluted to 0.5 McF and then treated with 0–28.8 J/cm$^2$ of light doses. After the irradiation, the aliquots were plated to determine the CFU/mL, as described in previous experiments. The culture time selection for knockout mutants was set up with the same experimental workflow but without the addition of IPTG. Each experiment was performed three times for each strain.

### *Evaluation of the impact of different IPTG concentrations on bacterial growth*

The growth curve of complemented strains in a range of different IPTG concentrations was determined. Overnight cultures of the strain were diluted at the vol/vol ratio of 1:20 and supplemented with IPTG to obtain the final concentrations of 0–1,000 µM. The growth was monitored for 6 h in an EnVision Multilabel Plate Reader (PerkinElmer, USA). The $OD_{600}$ value was measured every 15 min with incubation at 37°C with shaking (150 rpm). All the experiments were performed in three biological repetitions.

## aBL sensitivity of the knockout and complemented mutants

This experiment was designed to compare the aBL sensitivity profiles of the wild-type and knockout mutants and the complemented strains. Overnight cultures of the selected mutants were diluted at the vol/vol ratio of 1:100 in the fresh LB medium supplemented with specified antibiotics. The IPTG solution was added to the complemented mutant culture to obtain a total concentration of 1 µM. Then, the samples were incubated for 2 h at 37°C and 150 rpm. Next, the cultures were adjusted to a 0.5-McF optical density, and 100 µL aliquots were placed in 96-well plates. The previously prepared IPTG stock was added to the complemented mutant solutions to reach a 1 µM concentration. Then, the probes were irradiated with 0–28.8 J/cm$^2$ doses of light. After the illumination, aliquots of each sample were serially diluted, streaked, and cultured as described previously. All the analyses were also performed for the parental strain of *E. coli*. All the experiments were performed thrice for each strain.

## Bioinformatical and statistical analysis

All the statistical analyses and figures were created using GraphPad Prism version 9.0 (GraphPad Software, Inc., CA, USA). The statistical differences between the groups were

calculated using two-way analysis of variance (ANOVA) with $P < 0.05$ and Tukey's multiple comparison tests. Functional analysis of hypersensitive genes was performed using the BioCyc database and the Omics Dashboard. Protein–protein functional interaction networks were analyzed using the STRING database with a medium score of confidence of 0.4. The analysis was performed using the data from the curated databases that were experimentally determined (25). The graphic figures were prepared with the use of BioRender.com (accessed on 13 November 2022).

## RESULTS

### Determination of the aBL sensitivity of the *E. coli* BW25113

The first step was to determine the irradiation conditions that were sublethal ($MDK_{99}$) for the wild-type *E. coli* BW25113 strain but could be lethal ($\geq MDK_{99.9}$) for aBL-sensitive mutants. The conditions that resulted in a 2 $log_{10}$ reduction in treated parental strains for the Keio collection screening were determined as 43.2 J/cm$^2$ (Fig. 2).

### Establishment of aBL-hypersensitive mutants

All the single-gene deletion mutants were treated with aBL at the light dose assigned as sublethal for the parental strain (43.2 J/cm$^2$) in three biological repetitions. Screening analysis enabled the detection of 64 knockout mutants with increased sensitivity to aBL, which are listed in Table 1. The genes and their functions are compared in Table S1 (Supplement Materials) and Fig. 3. Some of the genes could be assigned different functional categories.

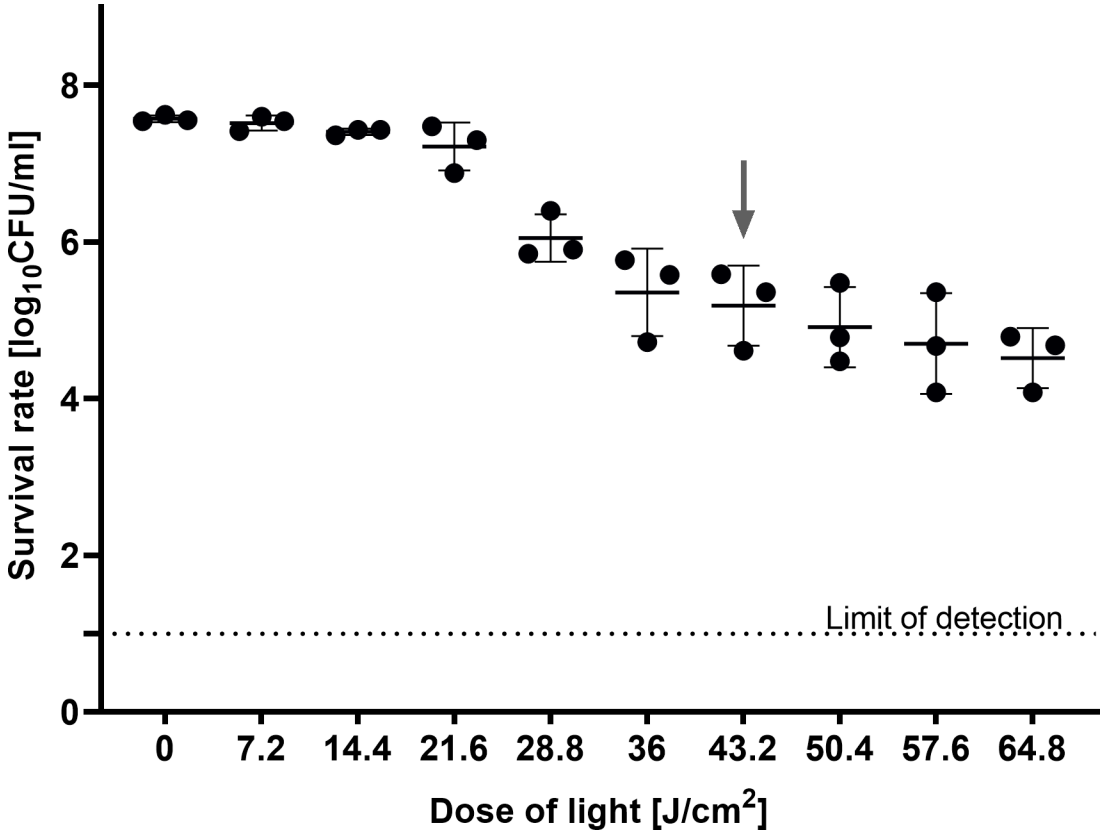


**FIG 2** aBL sensitivity of the *E. coli* BW25113. The detection limit was 10 CFU/mL. The arrow indicates the sublethal treatment chosen for the screening of the Keio collection. Overnight cultures of the BW25113 strain were diluted to 0.5 McF and irradiated with 0–64.8 J/cm$^2$ light doses. The CFU/mL was estimated with serial dilutions of 10 µL aliquots of the irradiated samples and plated on LB agar. The plots present the reduction of $log_{10}$ units of CFU/mL. The experiment was performed in a biological triplicate.

**TABLE 1** List of 64 *E. coli* BW25113 single-gene mutants identified as "aBL-hypersensitive" (no growth after the aBL dose of 43.2 J/cm$^2$ in at least two of three biological repetitions)[a]

| Lp. | Gene name | Synonyms | Description | Number of points |
|---|---|---|---|---|
| **1.** | *atpA* | *papA // uncA* | ATP synthase subunit alpha | 2 |
| **2.** | *atpB* | *papD // uncB* | ATP synthase subunit a | 3 |
| **3.** | *atpC* | *papG // uncC* | ATP synthase epsilon chain | 2 |
| **4.** | *atpD* | *papB // uncD* | ATP synthase subunit beta | 3 |
| **5.** | *atpE* | *papH // uncE* | ATP synthase subunit c | 3 |
| **6.** | *atpF* | *papF // uncF* | ATP synthase subunit b | 3 |
| **7.** | *atpG* | *papC // uncG* | ATP synthase gamma chain | 2 |
| **8.** | *atpH* | *papE // uncH* | ATP synthase subunit delta | 3 |
| **9.** | *cpxA* | *rssE // ecfB // eup // ssd // ecf* | Sensor histidine kinase CpxA | 2 |
| **10.** | *cydD* | *htrD* | ATP-binding/permease protein CydD | 2 |
| **11.** | *dacA* | *Pfv* | D-Alanyl-D-alanine carboxypeptidase DacA | 2 |
| **12.** | *deoB* | *tlr // drm // thyR* | Phosphopentomutase | 2 |
| **13.** | *dnaJ* | *groP // grpC* | Chaperone protein DnaJ | 2 |
| **14.** | *dnaK* | *groPF // groPC // seg // grpF // grpC // groPAB* | Chaperone protein DnaK | 3 |
| **15.** | *ecnB* | *yjeU* | Entericidin B | 2 |
| **16.** | *fabH* | | 3-Oxoacyl-[acyl-carrier-protein] synthase 3 | 2 |
| **17.** | *fimB* | *PiI* | Type 1 fimbriae regulatory protein FimB | 2 |
| **18.** | *gmhB* | *yaeD* | D-Glycero-beta-D-manno-heptose-1,7-bisphosphate 7-phosphatase | 2 |
| **19.** | *gntK* | | Thermoresistant gluconokinase | 2 |
| **20.** | *hldD* | *yqiF // rfaE // gmhC // waaE* | ADP-L-glycero-D-manno-heptose-6-epimerase | 2 |
| **21.** | *holD* | | DNA polymerase III subunit psi | 2 |
| **22.** | *metR* | | HTH-type transcriptional regulator MetR | 3 |
| **23.** | *narL* | *frdR // narR* | Nitrate/nitrite response regulator protein NarL | 2 |
| **24.** | *nuoN* | | NADH-quinone oxidoreductase subunit N | 2 |
| **25.** | *oxyR* | *momR // mor* | Hydrogen peroxide-inducible genes activator | 3 |
| **26.** | *pfkA* | | ATP-dependent 6-phosphofructokinase isozyme 1 | 2 |
| **27.** | *pgi* | | Glucose-6-phosphate isomerase | 2 |
| **28.** | *pgm* | *gpmA //blu* | 2,3-Bisphosphoglycerate-dependent phosphoglycerate mutase | 3 |
| **29.** | *phoQ* | | Sensor protein PhoQ | 2 |
| **30.** | *ppc* | *asp // glu* | Coenzyme A biosynthesis bifunctional protein CoaBC | 2 |
| **31.** | *priA* | *srgA* | Primosomal protein N′ | 3 |
| **32.** | *purA* | *adeK* | Adenylosuccinate synthetase | 3 |
| **33.** | *pyrE* | | Orotate phosphoribosyltransferase | 2 |
| **34.** | *rbfA* | *sdr-43 // yhbB* | 30S ribosome-binding factor | 2 |
| **35.** | *rfaC* | *rfa-2 // waaC // yibC* | Lipopolysaccharide heptosyltransferase 1 | 3 |
| **36.** | *rfaE* | *hldE // yqiF // gmhC // waaE* | Bifunctional protein HldE | 2 |
| **37.** | *rfaG* | *waaG* | Lipopolysaccharide core biosynthesis protein RfaG | 2 |
| **38.** | *rnt* | | Ribonuclease T | 3 |
| **39.** | *rpe* | *dod // yhfD* | Ribulose-phosphate 3-epimerase | 2 |
| **40.** | *sstT* | *ygjU* | Serine/threonine transporter SstT | 2 |
| **41.** | *surA rfaD* | *waaD // hldD // htrM // nbsB* | Chaperone SurA | 3 |
| **42.** | *thyA* | | Thymidylate synthase | 3 |
| **43.** | *tolA* | *cim // excC // lky // tol-2* | Tol-Pal system protein TolA | 2 |
| **44.** | *tpiA* | *Tpi* | Triosephosphate isomerase | 2 |
| **45.** | *truA* | *asuC // hisT // leuK* | tRNA pseudouridine synthase A | 3 |
| **46.** | *ubiC* | | Chorismate pyruvate-lyase | 2 |
| **47.** | *umuD* | | Protein UmuD | 2 |
| **48.** | *ybaP* | | TraB family protein YbaP | 2 |
| **49.** | *yccM* | | Putative electron transport protein YccM | 2 |
| **50.** | *ydcE* | *pptA* | Tautomerase PptA | 2 |

(*Continued on next page*)

**TABLE 1** List of 64 *E. coli* BW25113 single-gene mutants identified as "aBL-hypersensitive" (no growth after the aBL dose of 43.2 J/cm$^2$ in at least two of three biological repetitions)[a] (*Continued*)

| Lp. | Gene name | Synonyms | Description | Number of points |
|---|---|---|---|---|
| **51.** | *ydcx* | *ortT* | Orphan toxin OrtT | 2 |
| **52.** | *ydeU* | *orfT // ydeK // ydeU // b1509 // b1510 // ECK1502* | AIDA-I family autotransporter YneO | 2 |
| **53.** | *yegS* | | Lipid kinase YegS | 2 |
| **54.** | *yfbB* | *menH* | 2-Succinyl-6-hydroxy-2,4-cyclohexadiene-1-carboxylate synthase | 2 |
| **55.** | *yfeH* | | Putative symporter YfeH | 2 |
| **56.** | *yfgL* | *bamB* | Outer membrane protein assembly factor BamB | 2 |
| **57.** | *ygfZ* | *yzzW* | tRNA-modifying protein YgfZ | 2 |
| **58.** | *yheM* | *tusC* | Protein TusC | 2 |
| **59.** | *yhhH* | | PF15631 family protein YhhH | 2 |
| **60.** | *yigL* | | Pyridoxal phosphate phosphatase YigL | 2 |
| **61.** | *yihE* | *orfA // srkA* | Stress response kinase A | 2 |
| **62.** | *yjeK* | *epmB* | L-Lysine 2,3-aminomutase | 2 |
| **63.** | *yncA* | *mnaT* | L-Amino acid N-acyltransferase MnaT | 2 |
| **64.** | *ypjD* | | Inner membrane protein YpjD | 2 |

[a]The number of points indicates the number of biological repetitions in which no growth was observed.

## Determination of bactericidal aBL activity against mutants with increased sensitivity

To check differences in the aBL sensitivity of the hypersensitive mutants, the bactericidal aBL activity was evaluated against all the identified mutants with increased sensitivity. The survival rate of each mutant was determined and compared with the wild-type BW25113 strain survival rate after aBL treatment. Most of the strains expressed higher sensitivity to aBL than to the BW25113 strain, with a few exceptions [i.e., Δ*narL*, Δ*priA*, Δ*ubiC*, and Δ*yfgL* (revealing parental-like response to aBL) and Δ*nuoN*, Δ*ppc*, Δ*purA*, Δ*rpe*, and Δ*sst* (expressing lower aBL sensitivity compared to the parental strain; Fig. 4)]. Lower doses of irradiation were presented in Fig. S2. Selected single-gene deletion mutants were demonstrated as significantly more susceptible to aBL in the exponential growth phase (2 h) than in the stationary growth phase (16 h) (Fig. 5D; Fig. S3).

## Determination of the appropriate IPTG concentration for the complementation experiments

Complementation was performed with ASKA plasmids (NIG, Shizuoka, Japan) for 12 selected mutant strains (i.e., Δ*rbfA*, Δ*oxyR*, Δ*dnaK*, Δ*dnaJ*, Δ*purA*, Δ*fimB*, Δ*yihE*, Δ*ydcX*, Δ*umuD,* Δ*pgi,* Δ*cpxA*, and Δ*deoB*). These knockout mutants were chosen as they lack genes for which involvement in aBL response in *E. coli* could be rationalized (i.e., DNA repair, oxidative stress response, protein stress, or others). Complementation was verified using PCR gene detection.

Next, the optimal IPTG concentration was chosen for gene expression in the complemented *oxyR* deletion strain (with IPTG-inducible promoter). The impact of different IPTG concentrations on the complemented strain was verified (Fig. 5A; Fig. S4). The results showed that the range of IPTG lowest concentrations does not significantly affect the growth of the complemented strains, as well as in the case of the WT strain, WT harboring the empty vector (pCA24N) and one selected mutant (Δ*oxyR*). The highest IPTG concentrations like 100 and 1,000 µM affect the growth of *cpxA, umuD,* and *yihE* single-gene mutants in comparison to the growth without IPTG.

In the next step, based on the *oxyR* results, three IPTG concentrations were chosen: 0.5, 1, and 2 µM, and the aBL sensitivity of the 12 selected mutants was investigated. The bacterial cultures supplemented with 1 and 2 µM of IPTG responded to the aBL treatment in a manner similar to that of 21.6 J/cm$^2$ of light, while higher irradiation doses caused significantly lower sensitivity of the complemented strain induced with 2 µM of IPTG. The complemented strain, induced with 0.5 µM of IPTG, was significantly more

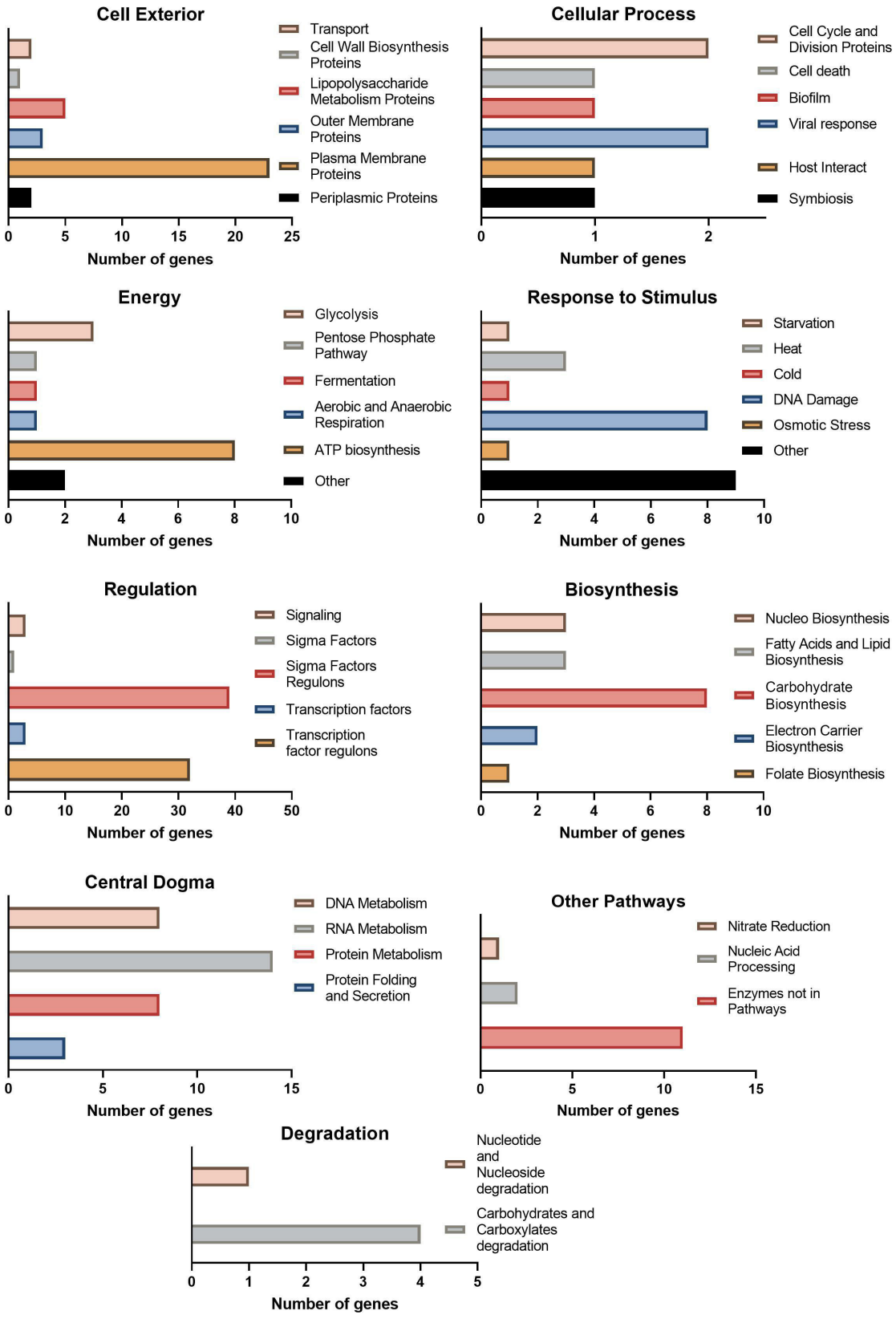


**FIG 3** Functional analysis of genes important for surviving aBL with the BioCyc Database.

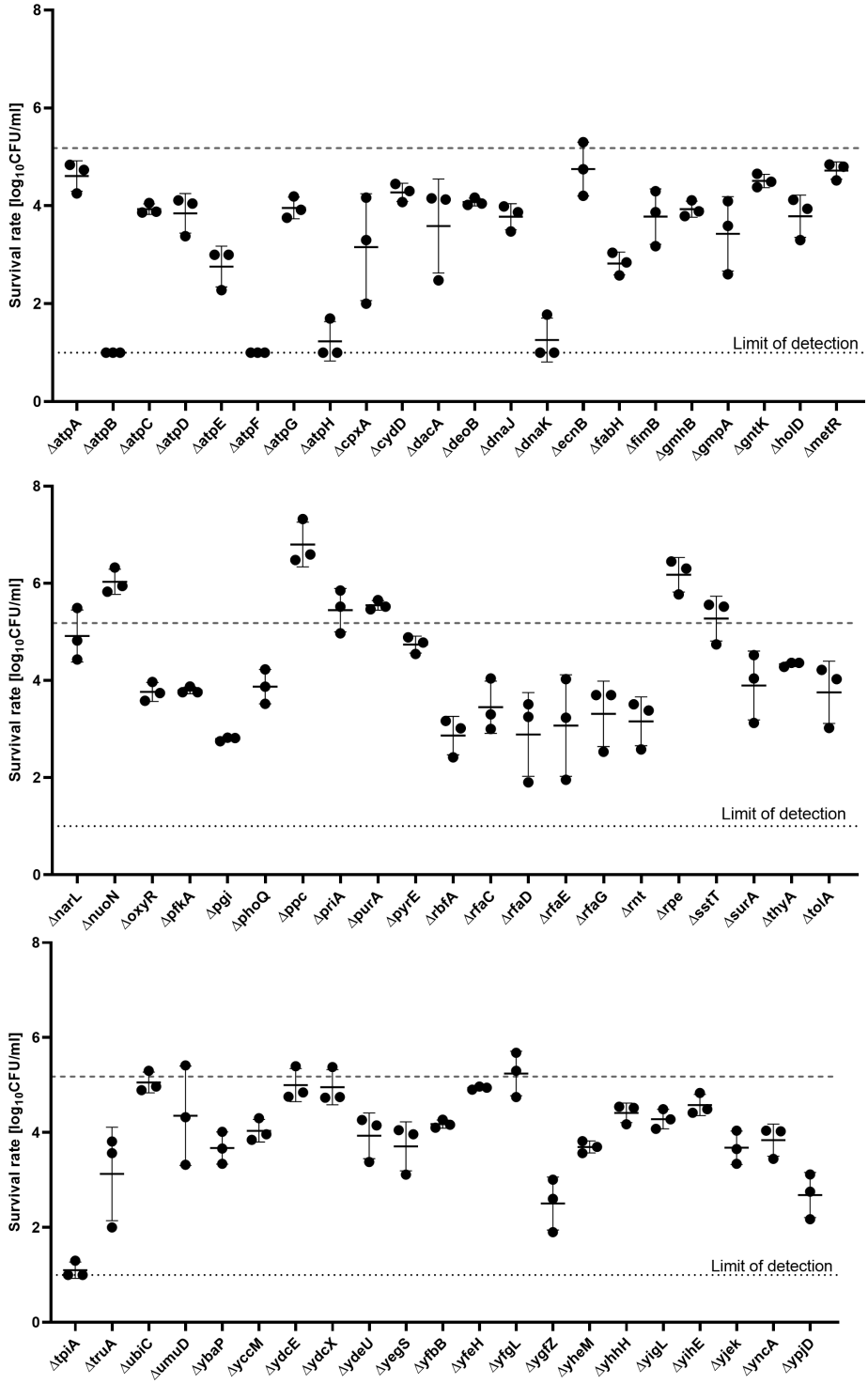


**FIG 4** Comparison of the survival rates of the single-gene mutants irradiated with 43.2 J/cm$^2$ of aBL and the BW25113 strain (indicated with dashed lines). The detection limit was 10 CFU/mL. Overnight cultures of the wild-type and mutant strains were diluted to 0.5 McF in the medium and then irradiated with 43.2 J/cm$^2$ of aBL. The CFU/mL was estimated with serial dilutions of 10 µL aliquots of the irradiated samples and plated on LB agar. The plots present the reduction of $\log_{10}$ units of the CFU/mL. The experiment was performed in three biological repetitions. The value is the mean of the three separate experiments, with the bars as the ±SD of the mean.

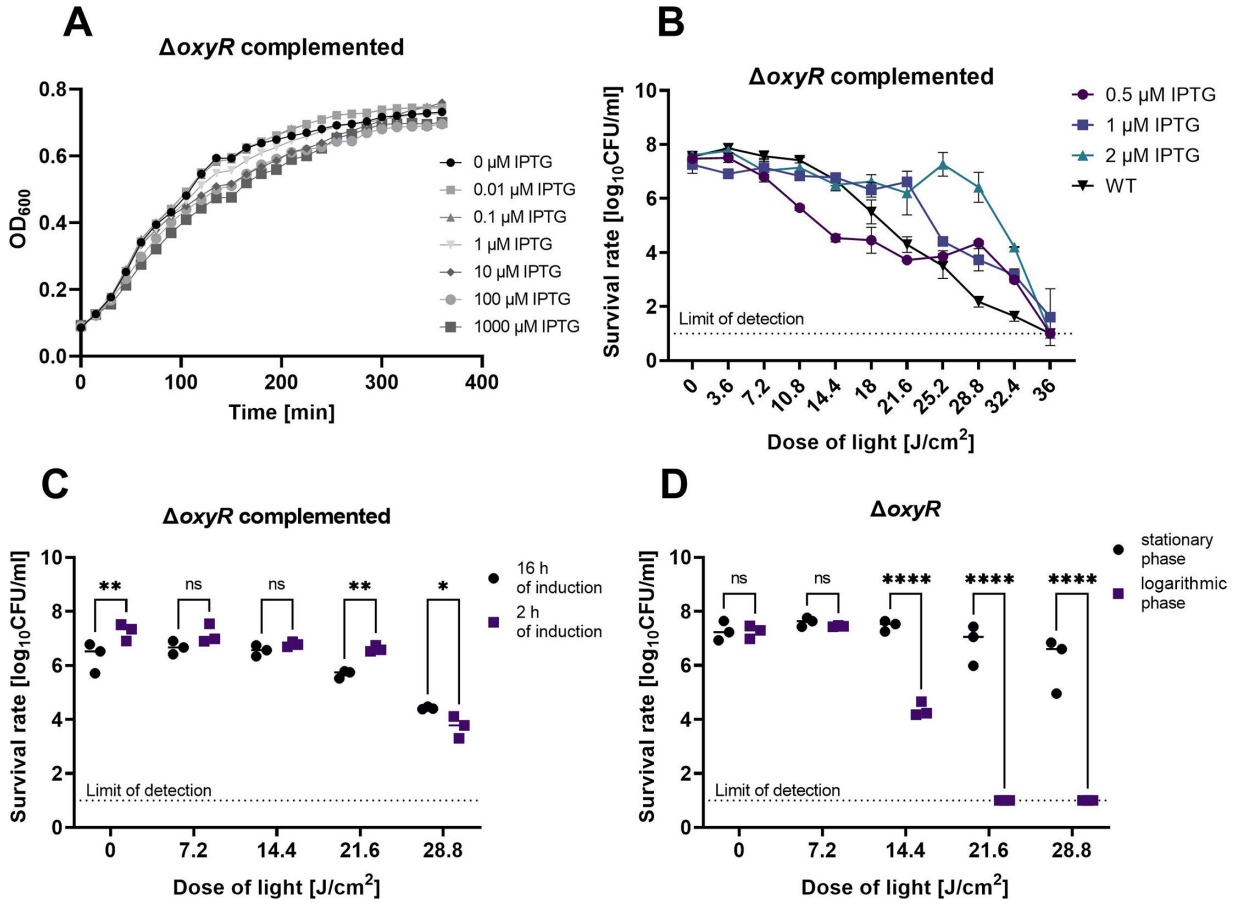


**FIG 5** Evaluation of the *E. coli* BW25113 Δ*oxyR* deletion mutant and the complemented strain response to aBL. (A) Growth curve of the complemented Δ*oxyR* strain cultured with different IPTG concentrations. Overnight cultures of the strain were diluted at the vol/vol ratio of 1:20 and supplemented with IPTG to obtain the final concentrations of 0–1,000 µM. The growth was monitored for 6 h. The $OD_{600}$ was measured every 15 min. (B) Comparison of the complemented Δ*oxyR* strain response to aBL depending on the IPTG concentration. Overnight cultures of the complemented strain were diluted at the vol/vol ratio of 1:100 in the fresh LB medium supplemented with specified antibiotics. The IPTG solution was added to cultures to obtain total concentrations of 2, 1, and 0.5 µM. After 2 h of incubation (37°C, 150 rpm), the cultures were diluted to 0.5 McF and treated with 0–36 J/cm$^2$ of light doses. (C) Comparison of the complemented Δ*oxyR* strain depending on the growth phase and the induction time. The 16 and 2 h cultures were induced with 1 µM IPTG and treated with 0–28.8 J/cm$^2$ light doses. (D) Comparison of the aBL sensitivity profiles of the Δ*oxyR* mutant depending on the growth phase. Overnight cultures (16 h, stationary phase) and log-phase cultures (2 h, exponential phase) were irradiated with 0–28.8 J/cm$^2$ light doses. All the experiments were performed in three biological repetitions. The detection limit was 10 CFU/mL. The value is the mean of the three separate experiments, and the bars give the ±SD of the mean. Significance at the respective *P* values is marked with asterisks (ns $P > 0.05$; *$P < 0.05$; **$P < 0.01$; ***$P < 0.001$; ****$P \leq 0.0001$).

sensitive to aBL than the parental strain (Fig. 5B); thus, 1 µM of IPTG was chosen as the highest concentration that does not affect bacterial growth and results in an aBL response most similar to that of the WT strain.

Next, the aBL sensitivity of the complemented strain (induced with 1 µM IPTG) at different times of induction and growth phases was analyzed. The aBL susceptibility of the complemented strain with induced gene expression depended more strongly on the IPTG level than on the growth phase (Fig. 5C). Different phenomena occurred during native gene expression. The Δ*oxyR* aBL sensitivity depended on the growth phase. Logarithmic cultures are more sensitive to aBL than stationary cultures (Fig. 5D). In the next step, cultures in the exponential growth phase were chosen to show differences in aBL response in the phase of growth where bacterial metabolism is the most active.

### Restoration of the aBL sensitivity to at least wild-type level via complementation of the deleted genes

The aBL responses of the selected single-gene mutants, the wild-type strain, and the complemented strains were compared. First, in most cases, the complementation of the mutation restored the wild-type phenotype or made the complemented strain even more tolerant to aBL treatment (Fig. 6). The most significant differences in the aBL sensitivity of the single-gene deletion mutants and the wild-type strains were noticed for *oxyR*, *ydcX*, *yihE*, *rbfA*, *fimB*, *umuD*, and *deoB*. Though all of the 12 tested strains exhibited the phenotype with increased sensitivity to aBL through screening, the strains that lacked *purA*, *dnaK*, *cpxA*, *dnaJ*, or *pgi* responded similarly to aBL as the parental strain during further quantitative analysis. In the case of the mutants that lacked *purA*, *cpxA*, *dnaJ*, or *pgi*, the complementation of the deleted genes made the strains significantly less sensitive to aBL treatment than the uncomplemented mutant. In the case of mutants lacking the *fimB* gene, complementation only partially restored the sensitivity of WT. Since the aBL response of the mutant that lacked *dnaK* was comparable to the aBL response of its complemented mutants, it can be assumed that IPTG concentrations were insufficient or expression failed for other reasons. Thus, in the case of *dnaK*, the analysis was also performed with 2-µM IPTG. Indeed, the increased IPTG concentration resulted in decreased aBL sensitivity of the complemented Δ*dnaK* mutant, indicating that this gene might also be involved in protection against aBL as overproduction gives full protection against the tested aBL doses.

## DISCUSSION

The efficiency of aBL is considered the result of its multitarget mode of action. Nevertheless, it must be admitted that the entire mechanism of aBL action is not yet completely understood. The most widely accepted hypothesis concerning aBL treatment indicates that the key role in aBL bactericidal activity is played by the endogenous photoreactive compounds that naturally occur in bacterial cells (i.e., coproporphyrin, uroporphyrin, and protoporphyrin). These endogenous photosensitizing compounds absorb the Sored-band light of appropriate wavelengths between 405 and 420 nm, which leads to their excitation and finally to the production of reactive oxygen species, which include singlet oxygen, hydroxyl radicals, peroxides, and superoxides (26). ROS, a toxic factor, plays a crucial role in exerting the cytotoxic effects of aBL on multiple cellular structures via protein oxidation, enzyme inactivation, DNA damage, and alterations in the lipid profiles and transmembrane potential (ion leakage), which results in microbial cell death (27–29).

It should be mentioned that resistance to aBL has not been described yet. Due to the multitarget mode of action of aBL, it is considered a low-risk treatment to develop bacterial resistance (30). Indeed, in our previous studies, we included data that were very supportive of this hypothesis by providing proof that even using an adequate and approved experimental resistance assessment methodology did not result in microbial resistance development to aBL treatment, though multiple aBL exposures might lead to the development of aBL-tolerant phenotypes (19, 21). Also, Luo et al. (31) revealed that after multiple sublethal aBL exposures, bacterial adaptation and changed aBL susceptibility occurred in *Staphylococcus aureus* (31). It is well known that gram-negative bacteria, represented by *E. coli*, are capable of adapting to many chemicals and physical and environmental stressors [i.e., antibiotics (32), organic solvents (33, 34), heavy metals (35, 36), acids (37, 38), UV radiation (39), and ionizing radiation (40)]. Moreover, it was also noticed that this adaptation process involved another unfavorable phenomenon, such as cross-tolerance or cross-protection. Ramteke (41) demonstrated that 90% of 448 coliform isolates showed resistance to one or more antibiotics but demonstrated tolerance to multiple metals (41). Rowe and Kirk (42) investigated the phenomenon of cross-protection in *E. coli* O157:H7 and reported increased salt or heat tolerance when the bacteria were prestressed with acid, which indicated that this could affect food processing (42).

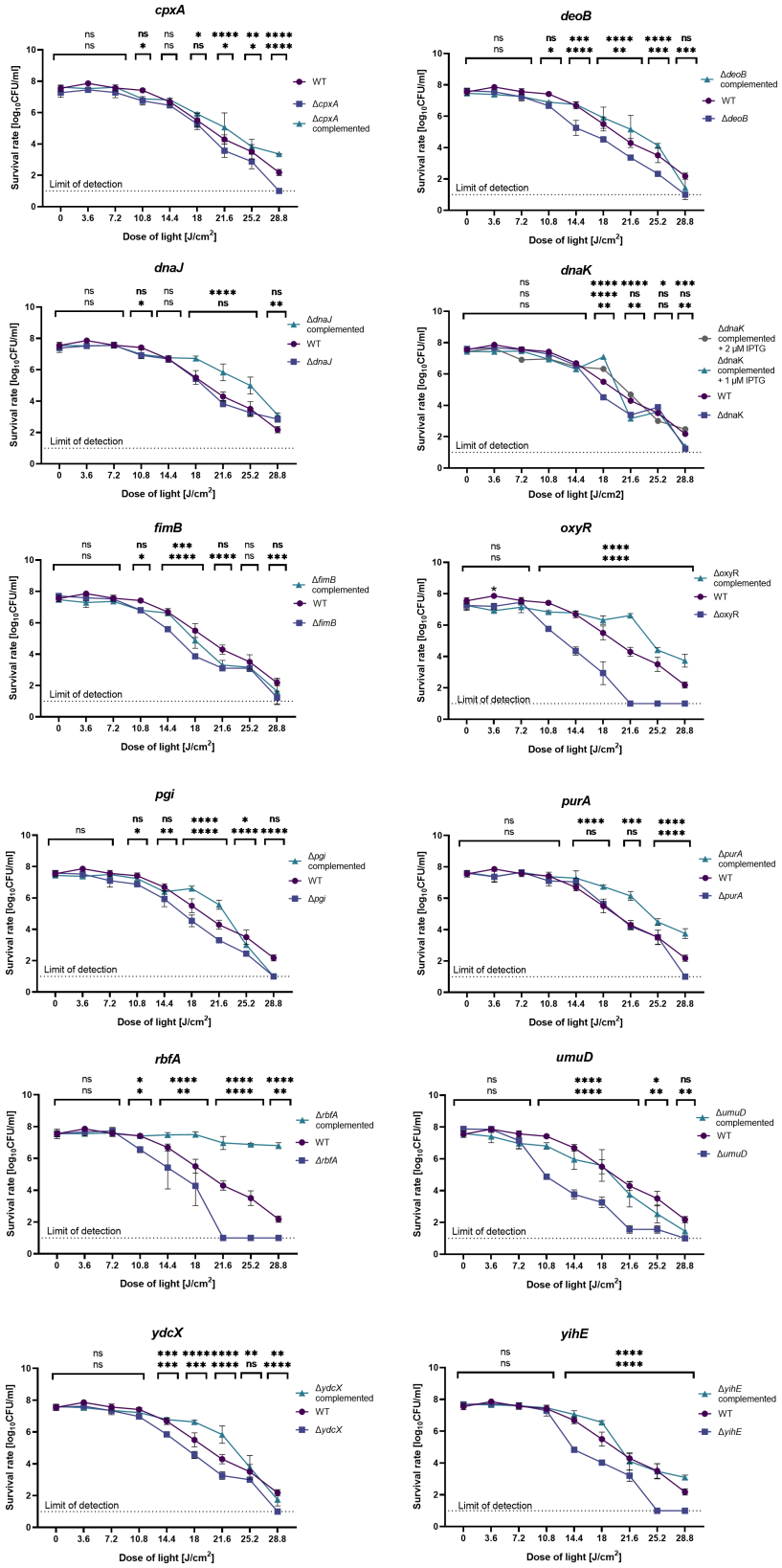


**FIG 6** Response of the *E. coli* BW25113 (WT), single-gene deletion mutants, and complemented mutant strains to aBL. Overnight cultures of all the strains were diluted at the vol/vol ratio of 1:100 in the fresh LB medium supplemented with appropriate antibiotics. The IPTG solution was added to the complemented

(Continued on next page)

**FIG 6** (Continued)

strain cultures to obtain a total concentration of 1 µM. After 2 h of incubation (37°C, 150 rpm), the cultures were diluted to 0.5 McF and treated with 0–28.8 J/cm$^2$ aBL doses. The experiment was performed thrice. The detection limit was 10 CFU/mL. The value is the mean of the three experiments; bars represent the ±SD of the mean. The significance at the respective *P*-values is marked with asterisks (ns $P > 0.05$; *$P < 0.05$; **$P < 0.01$; ***$P < 0.001$). The statistical significance was tested with the deletion strain as the reference. In all the cases (except for that of the *dnaK* mutant), the upper row of asterisks refers to the comparison of the deletion mutant and the complemented strain, and the lower row of asterisks refers to the comparison of the WT and the deletion mutant strain. In the case of the *dnaK* mutant, the upmost row of asterisks refers to the comparison of the deletion mutant and the complemented strain induced with 2 µM of IPTG, and the second row from the top refers to the comparison of the deletion mutant and the complemented strain induced with 1-µM IPTG.

For this reason, it is of high importance to analyze the possible development of microbial tolerance and/or resistance to any new and alternative antimicrobial approach (i.e., visible light-based therapies).

In this study, we performed screening analysis using the Keio knockout collection. This collection is an extensively studied and adequate genetically based tool for determining the effects of single-gene deletions under different stress conditions and performing genome-wide analysis (22). It has already been used for research, including on biofilm formation (43), swarming (44), growth in human blood (45), antibiotic hypersensitivity (46, 47), antibiotic resistance (48), non-thermal atmospheric pressure plasma hypersensitivity (24), hydroxyurea sensitivity (49), control of bacterial conjugation of antibiotic resistance (50), cysteine tolerance (51), colicin cytotoxicity (52), oxidizing agent resistance (53), copper stress (54), tolerance to chelants (55), susceptibility to microcin PDI (56), and glycogen metabolism (57). For instance, Mohiuddin et al. (58) determined genes critical for bacterial persistence and identified 55 genes of ofloxacin persistence and 50 genes related to ampicillin resistance (58). Krewing et al. (24) found 87 mutants that exhibited increased plasma sensitivity (24). Chen et al. (53) performed genome-wide analysis to identify genes involved in oxidizing agent resistance and identified 114 candidate genes related to HOCl resistance and 217 genes associated with resistance to $H_2O_2$. Of all the identified genes, 63 (in the case of HOCl) and 105 (in the case of $H_2O_2$) have not yet been associated with oxidative stress response (53). Those results proved that genome-wide analysis enables the exploration of unknown mechanisms of bacterial response to various factors and supplies novel data for the development of new therapeutic approaches. Referring to Nakayashiki and Mori (49), the genome-wide screening may reveal the emergence of unexpected clones, indicating that scientists do not yet understand all aspects of gene functions or interactions between genes in bacterial intracellular networks (49).

In this study, we screened almost 4,000 single-gene mutants and demonstrated 64 aBL-protective genes that could potentially be involved in the development of tolerance or resistance of *E. coli*, for example, due to genetic alterations that would lead to their overexpression. The performed analysis revealed that these genes contribute to a wide range of biological processes, mainly biosynthesis, metabolism, regulation, stress response, DNA repair, and others. The STRING database analysis revealed interactions and functional associations between the proteins encoded by the identified genes (Fig. 7).

During the screening, we identified 64 knockout mutants with extended sensitivity to aBL. After further analysis, the majority of the mutants exhibited hypersensitivity, some of them (e.g., *ΔpyrE* and *ΔyfeH*) exhibited a moderate increase in sensitivity, and only a few of them showed similar sensitivity to the WT strain (e.g., *ΔubiC* and *ΔyfgL*). However, we chose to include all mutants identified by screening in the further analysis, as the lack of growth in at least two out of three replicates was not due to growth defects, which was supported by appropriate controls and what is consistent with the observations of the authors of the Keio collection, that most of the mutants did not show any distinct

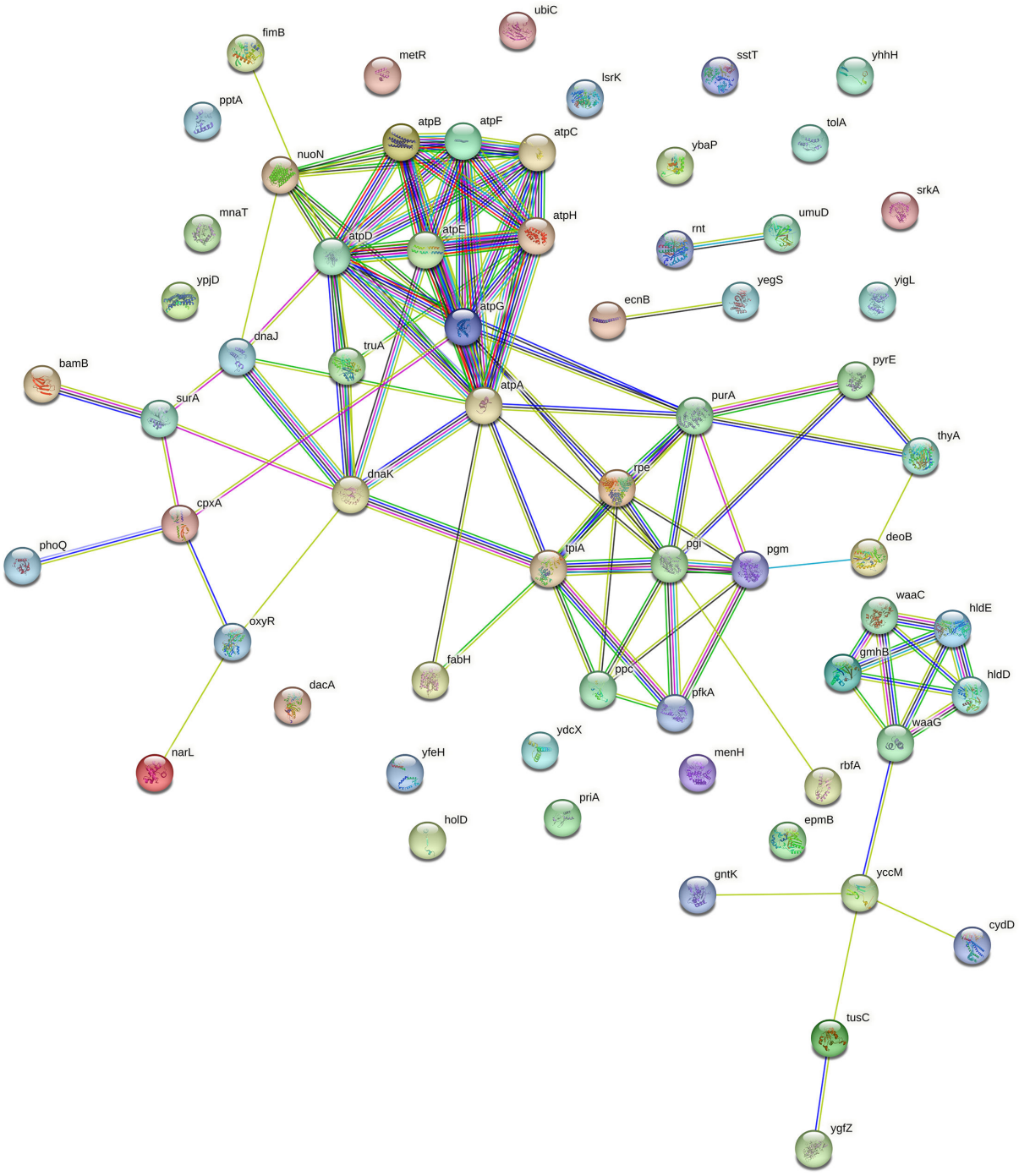


**FIG 7** Protein–protein functional interaction networks. Protein–protein functional interaction networks of the proteins encoded by 64 aBL-protective genes. The analysis was performed with the STRING database with a medium confidence score of 0.4. The colors of the lines denote the following: light blue, interactions known from curated databases; pink, interactions experimentally determined; bright green, predicted reaction (gene neighborhood); red, gene fusions; dark blue, gene co-occurrence; green, textmining; black, co-expression; and blue, protein homology.

growth defects in rich media (22). The discrepancies may also result from the difference in the density of the bacteria used in the qualitative (screening) and quantitative (profiles of the aBL sensitivity) tests.

Due to the performed analysis, we were able to identify several genes, which, if lacking, may lead to aBL increased sensitivity and can be engaged in the cellular response to this treatment. One of them may be *oxyR*. OxyR protein, termed an "oxidative

stress regulator," is responsible for the protection of bacterial cells against the toxicity caused by ROS. Furthermore, multiple studies revealed that the key role of *oxyR* is to regulate the expression of numerous genes involved in the microbial response to oxidative stress (59, 60). Though the existence of this direct link of *oxyR* to stress response has been established, no report has indicated the direct impact of *oxyR* on *E. coli* sensitivity to aBL. This study demonstrated that cells that lack the *oxyR* product are more susceptible to aBL treatment, and on the other hand, the complementation of Δ*oxyR* deletion restored the wild-type phenotype and increased strain tolerance to aBL. The results of this study supported the hypothesis that aBL generates ROS, which plays a crucial role in aBL toxicity against microbial cells (17). *oxyR* regulates the expression of numerous genes (i.e., *metR,* the deletion of which was also demonstrated to result in aBL hypersensitivity). However, the expression level of *oxyR* in the complemented strain can be much higher than that in the WT, as OxyR serves as both a transcriptional activator and a repressor of *oxyR* transcription (61).

According to the functional analysis of hypersensitive genes performed using the BioCyc database and the Omics Dashboard, 12.5% of all the identified genes (eight genes; i.e., *umuD*, *rnt*, *rbfA*, *priA*, *oxyR*, *purA*, *fimB*, and *deoB*) were involved in the cellular response to DNA damage. This might have been expected, as the bacteria increased the adaptation potential of the genes by modulating the rate of mutation (62). In addition, the aBL exerts mutagenic potential and could trigger a repair response. McGinty and Fowler observed base-pair substitution (transversions at both G:C and A:T sites) and frameshift mutations in *E. coli* induced with blue light irradiation (450 nm) (63). One of the genes investigated in this study, *umuD*, encodes UmuD, which is a part of the *E. coli* umuD'2C complex (PolV SOS), an error-prone DNA polymerase responsible for UV protection and the main factor that leads to SOS mutagenesis. It enables DNA replication across DNA lesions (64). Interestingly, in our previous studies, we observed no development of adaptation to aBL in an *umuD*-deficient mutant of *E. coli* BW25113 when it was subjected to multiple sublethal aBL treatments ((in comparison to the parental strain) (21). Next, RNase T, the product of the *rnt*, was identified as involved not only in tRNA processing but also in single-stranded DNA degradation, which may suggest its role in DNA repair. Viswanathan et al. (65) revealed that RNase T may serve as a high-copy suppressor of UV sensitivity in DNA exonucleases-deficient *E. coli* mutants (65). Another gene, whose deficiency resulted in the highest aBL sensitivity, is *rbfA*. This gene encodes the 30S ribosome binding factor responsible for ribosomal maturation and/or the initiation of translation and is suggested to be a cold-shock protein. Jones and Inouye (66) showed that the absence of *rbfA* triggers the cold - shock response; whereas in the case of RbfA overproduction, it resulted in increased total protein synthesis and faster growth adaptation to the lower temperature (66). Moreover, Rooney et al. (67) highlighted the role of RbfA in DNA damage response during their investigation of DNA repair after the alkylation process (67).

The next identified gene (*priA*) encodes a polypeptide PriA, which is required for immediate restarting of DNA synthesis after UV irradiation (68). It has also been demonstrated, in the case of *Bacillus subtilis*, that PriA is a crucial factor for microbial survival after severe DNA damage induced by numerous antibiotics (69) and is an essential factor for the survival and persistence of *Helicobacter pylori* in mouse stomach mucosa (70). Another gene detected in this study was *purA*, which encodes adenylosuccinate synthetase that is responsible for catalyzing *de novo* synthesis of AMP. Sun et al. demonstrated that the DNA damage induced by acidic conditions was significantly higher in *purA*-deficient mutants than in wild-type *E. coli*. These results clearly indicate that microbial survival in extreme environmental conditions involves metabolic processes that require ATP, i.e., an ATP-dependent DNA repair system (71). This is in line with our results, indicating that deficiency in one of the seven genes involved in ATP processing pathways (i.e., *atpA*, *atpB*, *atpC*, *atpE*, *atpF*, *atpG*, and *atpH*) results in aBL hypersensitivity. All the mentioned genes encode ATP synthase (F0F1 synthase) complex subunits required for ATP biosynthesis.

The analysis performed with the use of BioCyc database and the Omics Dashboard indicated that almost half (48%) of hypersensitive gene products are localized at a cell exterior where plasma membrane proteins (36% of all genes), lipopolysaccharide metabolism proteins (7.8%), and outer membrane proteins (4.7%) can be partly found. It may support the generally accepted thesis that bacterial envelopes serve as primary targets of blue light treatment, and these microbial structures are a crucial part of a bacterial first line of defense against the damaging effects of aBL (18, 72, 73).

An example of an inner membrane protein encoded by one of the identified genes was the orphan toxin gene (*ortT*). OrtT is a protein toxin activated under conditions that induce a stringent response. OrtT reduces cell growth and metabolism during nutritional or antimicrobially caused stress (e.g., trimethoprim and sulfamethoxazole), leads to cell membrane damage, and reduces the intracellular ATP level (74). Next, *ecnB*, which is a part of an antidote/toxin system (entericidin), plays a role in starvation adaptation by supporting further cell growth at the expense of dying subpopulations and is involved in programmed bacterial cell death (75). Segura et al. (76) revealed that *ecnB* could be one of the factors involved in the persistence of a Shiga toxin-producing *E. coli* O157:H7 strain in bovine intestine content (76). Another gene that encodes inner membrane protein is *tolA*. TolA interacts with the *E. coli* porins (e.g., OmpF) and is essential for the functionality and stability of the *E. coli* outer membrane (77). *E. coli tolA* contains a highly variable tandem repeat region (78, 79), the size of which was demonstrated to contribute to the fitness of *E. coli* under specific stress conditions, influencing its tolerance (79). Our previous study also supported the assumption of the significant role of *tolA* in aBL response, as the *tolA*-deficient *E. coli* BW25113 mutant was significantly more sensitive to aBL than the wild-type strain and did not develop a significant aBL tolerance, unlike the wild-type strain (21).

Finally, in this study, two heat shock proteins (DnaJ and DnaK) were also demonstrated to play an aBL-protective role. This corresponds with another study by Kim et al. (80) concerning oxidative stress, reporting that DnaK/DnaJ chaperone protects *Salmonella* against the cytotoxic effects resulting from ROS activity (protection against protein carbonylation) (80).

One of the key point of our study was to determine the proper irradiation conditions that were sublethal ($MDK_{99}$) for the wild-type *E. coli* BW25113 strain but could be lethal ($\geq MDK_{99.9}$) for aBL-sensitive mutants. The dose–exposure time relationship in the context of phototherapy is an important issue. We have knowledge from the previous studies of our research group (81) that the irradiation power influences mortality dynamics. We have observed that the greater the irradiation power, the greater the bacterial mortality. The mortality curves reach the detection limit at various irradiation time when the irradiation power is changed, and we can conclude that the detection limit is reached faster when irradiation power is higher (and the time of exposure is shorter). Moreover, we are convinced that the exposure time of irradiation could influence the gene expression and has impact on activating protective and repair mechanisms in the bacterial cell. For example, the biological half-life of SOS repair is 20–30 min (according to the decay of error-prone repair activity) (82). Taking into account the above and the time needed for one generation of bacteria, the exposure time (defined as "sublethal dose," at the maximum power of the light source) of 30 min (used for screening, i.e., qualitative analysis, where the inoculum was higher) or 20 min (used for quantitative analysis, where the inoculum was lower) seemed optimal.

Foodborne diseases are mainly associated with ingesting contaminated water and food. Gram-negative bacteria are predominant in food-processing environments (2). Antimicrobial resistance is a challenge that is not restricted to clinics but also the food industry and wastewater. Wastewater, along with wastewater treatment plants, is not only reservoirs but also "hotspots" for horizontal gene transfer (83). Antimicrobial blue light is a promising strategy for decontaminating food products (84–86) and surfaces (84, 87, 88). aBL is still seen as demonstrating an advantage over antibiotic treatment, which involves low-risk resistance development, due to its multitarget mode of action. Indeed,

the development of resistance to aBL has never been observed. However, reports on aBL tolerance cannot be unequivocally ruled out; over time, the phenomenon of adaptation to aBL will be observed. We managed to indicate 64 aBL-protective genes that could be the potential candidates for the development of tolerance or resistance of *E. coli* to this visible light treatment. This study can contribute to a better understanding of bacterial response to aBL and makes this treatment an attractive alternative bactericidal approach not only in clinical use but also in environmental application.

## ACKNOWLEDGMENTS

The authors thank the National BioResource Project (NBRP, NIG, Japan) for contributing to our work by providing us with *E. coli* BW25113 mutants from the Keio collection and ASKA library. The graphic figures were prepared with the use of BioRender.com (accessed on 13 November 2022).

This work was supported by the National Science Centre under grant no. 2020/36/C/NZ7/00061 (A.R.-Z.).

Conceptualization was performed by A.R.-Z, M.G., and K.W.; data curation was performed by B.K.-N.; formal analysis was performed by B.K.-N.; funding acquisition was performed by A.R.-Z.; investigation was performed by B.K.-N.; methodology was performed by A.R.-Z., B.K.-N., M.G., and J.E.B.; project administration was performed by A.R.-Z.; resources were secured by A.R.-Z. and M.G.; software was secured by B.K.-N.; supervision was performed by A.R.-Z. and M.G.; validation was performed by B.K.-N. and A.R.Z.; visualization was performed by B.K.-N.; roles/writing (original draft) was performed by A.R-Z. and B.K.-N.; writing (review and editing) was performed by M.G., J.E.B., and K.W.

## AUTHOR AFFILIATIONS

[1]Laboratory of Photobiology and Molecular Diagnostics, Intercollegiate Faculty of Biotechnology, University of Gdansk and Medical University of Gdansk, Gdansk, Poland
[2]Department of Pharmaceutical Microbiology, Faculty of Pharmacy, Medical University of Gdansk, Gdansk, Poland
[3]Applied Microbiology, Faculty of Biology and Biotechnology, Ruhr University Bochum, Universitätsstraße, Bochum, Germany

## AUTHOR ORCIDs

Julia Elisabeth Bandow http://orcid.org/0000-0003-4100-8829
Aleksandra Rapacka-Zdończyk http://orcid.org/0000-0002-7611-0359

## FUNDING



| Funder | Grant(s) | Author(s) |
|---|---|---|
| Narodowe Centrum Nauki (NCN) | 2020/36/C/NZ7/00061 | Aleksandra Rapacka-Zdończyk |



## AUTHOR CONTRIBUTIONS

Beata Kruszewska-Naczk, Data curation, Formal analysis, Investigation, Methodology, Software, Validation, Visualization, Writing – original draft | Mariusz Grinholc, Conceptualization, Methodology, Resources, Supervision, Writing – review and editing | Krzysztof Waleron, Conceptualization, Writing – review and editing | Julia Elisabeth Bandow, Methodology, Writing – review and editing | Aleksandra Rapacka-Zdończyk, Conceptualization, Funding acquisition, Methodology, Resources, Validation, Writing – original draft

## ADDITIONAL FILES

The following material is available online.

## Supplemental Material

**Supplemental material (Spectrum02490-23-S0001.docx).** Supplemental figures and table.

**Graphical abstract (Spectrum02490-23-S0002.tif).** Graphical abstract.

## REFERENCES


1. World health organization. 2015. World health organization. WHO estimates of the global burden of Foodborne diseases: Foodborne diseases in the WHO regions (no.WHO/FOS/15.5). World Health Organization.
2. Hadi J, Wu S, Brightwell G. 2020. Antimicrobial blue light versus pathogenic bacteria: mechanism, application in the food industry, hurdle technologies and potential resistance. Foods 9:1895. https://doi.org/10.3390/foods9121895
3. van Elsas JD, Semenov AV, Costa R, Trevors JT. 2011. Survival of *Escherichia coli* in the environment: fundamental and public health aspects. ISME J 5:173–183. https://doi.org/10.1038/ismej.2010.80
4. Perna NT, Plunkett G, Burland V, Mau B, Glasner JD, Rose DJ, Mayhew GF, Evans PS, Gregor J, Kirkpatrick HA, et al. 2001. Genome sequence of enterohaemorrhagic *Escherichia coli* O157: H7. Nature 409:529–533. https://doi.org/10.1038/35054089
5. Zhang S, Zhu X, Wu Q, Zhang J, Xu X, Li H. 2015. Prevalence and characterization of *Escherichia coli* O157 and O157: H7 in retail fresh raw meat in South China. Ann Microbiol 65:1993–1999. https://doi.org/10.1007/s13213-015-1037-x
6. Ahmed AM, Shimamoto T. 2015. Molecular analysis of multidrug resistance in Shiga toxin-producing *Escherichia coli* O157: H7 isolated from meat and dairy products. International Journal of Food Microbiology 193:68–73. https://doi.org/10.1016/j.ijfoodmicro.2014.10.014
7. Joseph Fuh N. 2018. Prevalence and antibiotic resistance of *Escherichia coli* O157: H7 serotype from chicken droppings produced by free-ranged and poultry birds in cross river, Nigeria. AJBLS 6:51. https://doi.org/10.11648/j.ajbls.20180603.13
8. Abreham S, Teklu A, Cox E, Sisay Tessema T. 2019. *Escherichia coli* O157: H7: distribution, molecular characterization, antimicrobial resistance patterns and source of contamination of sheep and goat carcasses at an export abattoir, Mojdo, Ethiopia. BMC Microbiol. 19:215. https://doi.org/10.1186/s12866-019-1590-8
9. Obaidat MM. 2020. Prevalence and antimicrobial resistance of listeria monocytogenes, salmonella enterica and *Escherichia coli* O157: H7 in imported beef cattle in Jordan. Comp Immunol Microbiol Infect Dis 70:101447. https://doi.org/10.1016/j.cimid.2020.101447
10. Onmaz NE, Yildirim Y, Karadal F, Hizlisoy H, Al S, Gungor C, Disli HB, Barel M, Dishan A, Akai Tegin RA, Simsek E. 2020. *Escherichia coli* O157 in fish: prevalence, antimicrobial resistance, biofilm formation capacity, and molecular characterization. LWT 133:109940. https://doi.org/10.1016/j.lwt.2020.109940
11. Paswan R, Park YW. 2020. Survivability of salmonella and *Escherichia coli* O157: H7 pathogens and food safety concerns on commercial powder milk products. Dairy 1:189–201. https://doi.org/10.3390/dairy1030014
12. Rivas L, Mellor GE, Gobius K, Fegan N. 2015. Introduction to pathogenic *Escherichia coli*. Detection and Typing Strategies for Pathogenic Escherichia coli:1–38. https://doi.org/10.1007/978-1-4939-2346-5
13. O'Neill J. 2016. Tackling drug-resistant infections globally: final report and recommendations. The review on antimicrobial resistance chaired by Jim O'Neill. Wellcome Trust and HM Government, London.
14. Glaeser J, Nuss AM, Berghoff BA, Klug G. 2011. Singlet oxygen stress in microorganisms, p 141–173. In In advances in microbial physiology
15. Maisch T. 2015. Resistance in antimicrobial photodynamic inactivation of bacteria. Photochem Photobiol Sci 14:1518–1526. https://doi.org/10.1039/c5pp00037h
16. Hyun JE, Lee SY. 2020. Blue light-emitting diodes as eco-friendly non-thermal technology in food preservation. Trends in Food Science & Technology 105:284–295. https://doi.org/10.1016/j.tifs.2020.09.008
17. Wang Y, Harrington OD, Wang Y, Murray CK, Hamblin MR, Dai T. 2017. In vivo investigation of antimicrobial blue light therapy for multidrug-resistant *Acinetobacter baumannii* burn infections using bioluminescence imaging. J Vis Exp 122:54997. https://doi.org/10.3791/54997
18. Wu J, Chu Z, Ruan Z, Wang X, Dai T, Hu X. 2018. Changes of intracellular porphyrin, reactive oxygen species, and fatty acids profiles during inactivation of methicillin-resistant *Staphylococcus aureus* by antimicrobial blue light. Front Physiol 9:1658. https://doi.org/10.3389/fphys.2018.01658
19. Rapacka-Zdonczyk A, Wozniak A, Pieranski M, Woziwodzka A, Bielawski KP, Grinholc M. 2019. Development of *Staphylococcus aureus* tolerance to antimicrobial photodynamic inactivation and antimicrobial blue light upon sub-lethal treatment. Sci Rep 9:9423. https://doi.org/10.1038/s41598-019-45962-x
20. Pieranski M, Sitkiewicz I, Grinholc M. 2020. Increased Photoinactivation stress tolerance of *Streptococcus agalactiae* upon consecutive sublethal phototreatments. Free Radic Biol Med 160:657–669. https://doi.org/10.1016/j.freeradbiomed.2020.09.003
21. Rapacka-Zdonczyk A, Wozniak A, Kruszewska B, Waleron K, Grinholc M. 2021. Can gram-negative bacteria develop resistance to antimicrobial blue light treatment IJMS 22:11579. https://doi.org/10.3390/-ijms222111579
22. Baba T, Ara T, Hasegawa M, Takai Y, Okumura Y, Baba M, Datsenko KA, Tomita M, Wanner BL, Mori H. 2006. Construction of *Escherichia coli* k - 12 in - frame, single - gene knockout mutants: the keio collection. Mol Syst Biol 2:2006–2008. https://doi.org/10.1038/msb4100050
23. Kitagawa M, Ara T, Arifuzzaman M, Ioka-Nakamichi T, Inamoto E, Toyonaga H, Mori H. 2005. Complete set of ORF clones of *Escherichia coli* ASKA library (A complete set of E. coli K12 ORF Archive): unique resources for biological research. DNA Research 12:291–299. https://doi.org/10.1093/dnares/dsi012
24. Krewing M, Jarzina F, Dirks T, Schubert B, Benedikt J, Lackmann JW, Bandow JE. 2019. Plasma-sensitive *Escherichia coli* mutants reveal plasma resistance mechanisms . J R Soc Interface 16:20180846. https://doi.org/10.1098/rsif.2018.0846
25. Szklarczyk D, Morris JH, Cook H, Kuhn M, Wyder S, Simonovic M, Santos A, Doncheva NT, Roth A, Bork P, Jensen LJ, von Mering C. 2017. The STRING database in 2017: quality-controlled protein-protein association networks, made broadly accessible. Nucleic Acids Res 45:D362–D368. https://doi.org/10.1093/nar/gkw937
26. Amin RM, Bhayana B, Hamblin MR, Dai T. 2016. Antimicrobial blue light inactivation of *Pseudomonas aeruginosa* by photoexcitation of endogenous porphyrins: In vitro and in vivo studies. Lasers Surg Med 48:562–568. https://doi.org/10.1002/lsm.22474
27. Alves E, Faustino MA, Neves MG, Cunha A, Tome J, Almeida A. 2014. An insight on bacterial cellular targets of photodynamic inactivation. Future Med Chem 6:141–164. https://doi.org/10.4155/fmc.13.211
28. Cieplik F, Späth A, Leibl C, Gollmer A, Regensburger J, Tabenski L, Hiller K-A, Maisch T, Schmalz G. 2014. Blue light kills aggregatibacter actinomycetemcomitans due to its endogenous photosensitizers. Clin Oral Investig 18:1763–1769. https://doi.org/10.1007/s00784-013-1151-8
29. Dai T. 2017. The antimicrobial effect of blue light: what are behind Virulence 8:649–652. https://doi.org/10.1080/21505594.2016.1276691
30. Zhu H, Kochevar IE, Behlau I, Zhao J, Wang F, Wang Y, Sun X, Hamblin MR, Dai T. 2017. Antimicrobial blue light therapy for infectious keratitis: ex vivo and in vivo studies. Invest Ophthalmol Vis Sci 58:586–593. https://doi.org/10.1167/iovs.16-20272
31. Luo S, Yang X, Wu S, Li Y, Wu J, Liu M, Liu Z, Yu K, Wang X, Dai T, Huang X, Hu X. 2022. Understanding a defensive response of methicillin-resistant *Staphylococcus aureus* after exposure to multiple cycles of sub-lethal blue light. FEMS Microbiol Lett 369:fnac050. https://doi.org/10.1093/femsle/fnac050
32. Oliveira J, Reygaert WC. 2022. Gram negative bacteria. StatPearls [Internet]. Treasure 567 Island (FL): StatPearls Publishing. Available from: https://www.ncbi.nlm.nih.gov/books/NBK538213/

33. Aono R, Kobayashi H. 1997. Cell surface properties of organic solvent-tolerant mutants of *Escherichia coli* K12. Appl Environ Microbiol 63:3637–3642. https://doi.org/10.1128/aem.63.9.3637-3642.1997
34. Li XZ, Zhang L, Poole K. 1998. Role of the multidrug efflux systems of *Pseudomonas aeruginosa* in organic solvent tolerance. J Bacteriol 180:2987–2991. https://doi.org/10.1128/JB.180.11.2987-2991.1998
35. Nakajima H, Kobayashi K, Kobayashi M, Asako H, Aono R. 1995. Overexpression of the robA gene increases organic solvent tolerance and multiple antibiotic and heavy metal ion resistance in *Escherichia coli*. Appl Environ Microbiol 61:2302–2307. https://doi.org/10.1128/aem.61.6.2302-2307.1995
36. Nguyen CC, Hugie CN, Kile ML, Navab-Daneshmand T. 2019. Association between heavy metals and antibiotic-resistant human pathogens in environmental reservoirs: A review. Frontiers of Environmental Science & Engineering 13:1–17. https://doi.org/10.1007/s11783-019-1129-0
37. Arnold CN, McElhanon J, Lee A, Leonhart R, Siegele DA. 2001. Global analysis of *Escherichia coli* gene expression during the acetate-induced acid tolerance response. J Bacteriol 183:2178–2186. https://doi.org/10.1128/JB.183.7.2178-2186.2001
38. Benjamin MM, Datta AR. 1995. Acid tolerance of enterohemorrhagic *Escherichia coli*. Appl Environ Microbiol 61:1669–1672. https://doi.org/10.1128/aem.61.4.1669-1672.1995
39. Witkin EM. 1947. Genetics of resistance to radiation in *Escherichia coli*. Genetics 32:221–248. https://doi.org/10.1093/genetics/32.3.221
40. Harris DR, Pollock SV, Wood EA, Goiffon RJ, Klingele AJ, Cabot EL, Schackwitz W, Martin J, Eggington J, Durfee TJ, Middle CM, Norton JE, Popelars MC, Li H, Klugman SA, Hamilton LL, Bane LB, Pennacchio LA, Albert TJ, Perna NT, Cox MM, Battista JR. 2009. Directed evolution of ionizing radiation resistance in *Escherichia coli* . J Bacteriol 191:5240–5252. https://doi.org/10.1128/JB.00502-09
41. Ramteke PW. 1997. Plasmid mediated Co-transfer of antibiotic resistance and heavy metal tolerance in Coliforms. Indian J. Microbiol 37:177–182. https://doi.org/10.5897/AJMR12.1563
42. Rowe MT, Kirk R. 1999. Investigation into the phenomenon of cross-protection in *Escherichia coli* O157: H7. Food Microbiology 16:157–164. https://doi.org/10.1006/fmic.1998.0229
43. Niba ETE, Naka Y, Nagase M, Mori H, Kitakawa M. 2007. A genome-wide approach to identify the genes involved in biofilm formation in *Escherichia coli*. DNA Res 14:237–246. https://doi.org/10.1093/dnares/dsm024
44. Inoue T, Shingaki R, Hirose S, Waki K, Mori H, Fukui K. 2007. Genome-wide screening of genes required for swarming motility in *Escherichia coli* K12. J Bacteriol 189:950–957. https://doi.org/10.1128/JB.01294-06
45. Samant S, Lee H, Ghassemi M, Chen J, Cook JL, Mankin AS, Neyfakh AA. 2008. Nucleotide biosynthesis is critical for growth of bacteria in human blood. PLoS Pathog. 4:e37. https://doi.org/10.1371/journal.ppat.0040037
46. Liu A, Tran L, Becket E, Lee K, Chinn L, Park E, Tran K, Miller JH. 2010. Antibiotic sensitivity profiles determined with an *Escherichia coli* gene knockout collection: generating an antibiotic bar code. Antimicrob Agents Chemother 54:1393–1403. https://doi.org/10.1128/AAC.00906-09
47. Tamae C, Liu A, Kim K, Sitz D, Hong J, Becket E, Bui A, Solaimani P, Tran KP, Yang H, Miller JH. 2008. Determination of antibiotic hypersensitivity among 4,000 single-gene-knockout mutants of *Escherichia coli*. J Bacteriol 190:5981–5988. https://doi.org/10.1128/JB.01982-07
48. Malekian N, Agrawal AA, Berendonk TU, Al-Fatlawi A, Schroeder M. 2022. A genome-wide scan of wastewater *E. coli* for genes under positive selection: focusing on mechanisms of antibiotic resistance. Sci Rep 12:8037. https://doi.org/10.1038/s41598-022-11432-0
49. Nakayashiki T, Mori H. 2013. Genome-wide screening with Hydroxyurea reveals a link between nonessential ribosomal proteins and reactive oxygen species production. J Bacteriol 195:1226–1235. https://doi.org/10.1128/JB.02145-12
50. Alalam H, Graf FE, Palm M, Abadikhah M, Zackrisson M, Boström J, Fransson A, Hadjineophytou C, Persson L, Stenberg S, Mattsson M, Ghiaci P, Sunnerhagen P, Warringer J, Farewell A. 2020. A high-throughput method for screening for genes controlling bacterial conjugation of antibiotic resistance. mSystems 5:e01226-20. https://doi.org/10.1128/mSystems.01226-20
51. Wiriyathanawudhiwong N, Ohtsu I, Li ZD, Mori H, Takagi H. 2009. The outer membrane TolC is involved in cysteine tolerance and overproduction in *Escherichia coli*. Appl Microbiol Biotechnol 81:903–913. https://doi.org/10.1007/s00253-008-1686-9
52. Sharma O, Datsenko KA, Ess SC, Zhalnina MV, Wanner BL, Cramer WA. 2009. Genome-wide screens: novel mechanisms in colicin import and cytotoxicity. Mol Microbiol 73:571–585. https://doi.org/10.1111/j.1365-2958.2009.06788.x
53. Chen H, Wilson J, Ercanbrack C, Smith H, Gan Q, Fan C. 2021. Genome-wide screening of oxidizing agent resistance genes in *Escherichia Coli*. Antioxidants (Basel) 10:861. https://doi.org/10.3390/antiox10060861
54. Casanova-Hampton K, Carey A, Kassam S, Garner A, Donati GL, Thangamani S, Subashchandrabose S. 2021. A genome-wide screen reveals the involvement of enterobactin-mediated iron acquisition in *Escherichia coli* survival during copper stress. Metallomics 13:mfab052. https://doi.org/10.1093/mtomcs/mfab052
55. Paterson JR, Beecroft MS, Mulla RS, Osman D, Reeder NL, Caserta JA, Young TR, Pettigrew CA, Davies GE, Williams JAG, Sharples GJ. 2022. Insights into the antibacterial mechanism of action of chelating agents by selective deprivation of iron, manganese, and zinc. Appl Environ Microbiol 88:e0164121. https://doi.org/10.1128/AEM.01641-21
56. Zhao Z, Eberhart LJ, Orfe LH, Lu SY, Besser TE, Call DR. 2015. Genome-wide screening identifies six genes that are associated with susceptibility to *Escherichia coli* microcin PDI. Appl Environ Microbiol 81:6953–6963. https://doi.org/10.1128/AEM.01704-15
57. Eydallin G, Montero M, Almagro G, Sesma MT, Viale AM, Muñoz FJ, Rahimpour M, Baroja-Fernández E, Pozueta-Romero J. 2010. Genome-wide screening of genes whose enhanced expression affects glycogen accumulation in *Escherichia coli*. DNA Res. 17:61–71. https://doi.org/10.1093/dnares/dsp028
58. Mohiuddin SG, Massahi A, Orman MA. 2022. High-throughput screening of a promoter library reveals new persister mechanisms in *Escherichia coli*. Microbiol Spectr 10:e0225321. https://doi.org/10.1128/spectrum.02253-21
59. Mongkolsuk S, Helmann JD. 2002. Regulation of inducible peroxide stress responses. Mol Microbiol 45:9–15. https://doi.org/10.1046/j.1365-2958.2002.03015.x
60. Zheng M, Wang X, Doan B, Lewis KA, Schneider TD, Storz G. 2001. Computation-directed identification of OxyR DNA binding sites in *Escherichia coli*. J Bacteriol 183:4571–4579. https://doi.org/10.1128/JB.183.15.4571-4579.2001
61. Tao K, Makino K, Yonei S, Nakata A, Shinagawa H. 1991. Purification and characterization of the *Escherichia coli* OxyR protein, the positive regulator for a hydrogen peroxide-inducible regulon. J Biochem 109:262–266.
62. Tenaillon O, Denamur E, Matic I. 2004. Evolutionary significance of stress-induced mutagenesis in bacteria. Trends Microbiol 12:264–270. https://doi.org/10.1016/j.tim.2004.04.002
63. McGinty LD, Fowler RG. 1982. Visible light mutagenesis in *Escherichia coli*. Mutat Res 95:171–181. https://doi.org/10.1016/0027--5107(82)90255-x
64. Tang M, Pham P, Shen X, Taylor JS, O'Donnell M, Woodgate R, Goodman MF. 2000. Roles of *E. coli* DNA polymerases IV and V in lesion-targeted and untargeted SOS mutagenesis. Nature 404:1014–1018. https://doi.org/10.1038/35010020
65. Viswanathan M, Lanjuin A, Lovett ST. 1999. Identification of RNase T as a high-copy suppressor of the UV sensitivity associated with single-strand DNA exonuclease deficiency in *Escherichia coli*. Genetics 151:929–934. https://doi.org/10.1093/genetics/151.3.929
66. Jones PG, Inouye M. 1996. RbfA, a 30s ribosomal binding factor, is a cold - shock protein whose absence triggers the cold - shock response. Mol Microbiol 21:1207–1218. https://doi.org/10.1111/j.1365-2958.1996.tb02582.x
67. Rooney JP, George AD, Patil A, Begley U, Bessette E, Zappala MR, Huang X, Conklin DS, Cunningham RP, Begley TJ. 2009. Systems based mapping demonstrates that recovery from alkylation damage requires DNA repair, RNA processing, and translation associated networks. Genomics 93:42–51. https://doi.org/10.1016/j.ygeno.2008.09.001
68. Rangarajan S, Woodgate R, Goodman MF. 2002. Replication restart in UV - irradiated *Escherichia coli* involving pols II, III, V, PriA, RecA and RecFOR proteins. Mol Microbiol 43:617–628. https://doi.org/10.1046/j.1365-2958.2002.02747.x

69. Matthews LA, Simmons LA. 2022. The *Bacillus subtilis* PriA winged helix domain is critical for surviving DNA damage. J Bacteriol 204:e0053921. https://doi.org/10.1128/JB.00539-21
70. Singh A, Blaskovic D, Joo J, Yang Z, Jackson SH, Coleman WG, Yan M. 2016. Investigating the role of helicobacter Pylori PriA protein. Helicobacter 21:295–304. https://doi.org/10.1111/hel.12283
71. Sun Y, Fukamachi T, Saito H, Kobayashi H. 2011. ATP requirement for acidic resistance in *Escherichia coli*. J Bacteriol 193:3072–3077. https://doi.org/10.1128/JB.00091-11
72. Bhavya ML, Umesh Hebbar H. 2019. Efficacy of blue LED in microbial inactivation: effect of photosensitization and process parameters. Int J Food Microbiol 290:296–304. https://doi.org/10.1016/j.ijfoodmicro.2018.10.021
73. Kim M-J, Mikš-Krajnik M, Kumar A, Yuk H-G. 2016. Inactivation by 405 ± 5 nM light-emitting diode on *Escherichia coli* O157: H7, salmonella typhimurium, and Shigella sonnei under refrigerated condition might be due to the loss of membrane integrity. Food Control 59:99–107. https://doi.org/10.1016/j.foodcont.2015.05.012
74. Islam S, Benedik MJ, Wood TK. 2015. Orphan toxin OrtT (YdcX) of *Escherichia coli* reduces growth during the stringent response. Toxins (Basel) 7:299–321. https://doi.org/10.3390/toxins7020299
75. Bishop RE, Leskiw BK, Hodges RS, Kay CM, Weiner JH. 1998. The entericidin locus of *Escherichia coli* and its implications for programmed bacterial cell death. J Mol Biol 280:583–596. https://doi.org/10.1006/jmbi.1998.1894
76. Segura A, Auffret P, Bibbal D, Bertoni M, Durand A, Jubelin G, Kérourédan M, Brugère H, Bertin Y, Forano E. 2018. Factors involved in the persistence of a Shiga toxin-producing *Escherichia coli* O157: H7 strain in bovine feces and gastro-intestinal content. Front Microbiol 9:375. https://doi.org/10.3389/fmicb.2018.00375
77. Derouiche R, Gavioli M, Bénédetti H, Prilipov A, Lazdunski C, Lloubès R. 1996. Tola central domain interacts with Escherichia coli Porins. EMBO J 15:6408–6415. https://doi.org/10.1002/j.1460-2075.1996.tb01032.x
78. Zhou K, Vanoirbeek K, Aertsen A, Michiels CW. 2012. Variability of the tandem repeat region of the *Escherichia coli* tolA gene. Res Microbiol 163:316–322. https://doi.org/10.1016/j.resmic.2012.05.003
79. Zhou K, Michiels CW, Aertsen A. 2012. Variation of Intragenic Tandem repeat tract of tolA modulates *Escherichia coli* stress tolerance. PLoS ONE 7:e47766. https://doi.org/10.1371/journal.pone.0047766
80. Kim J-S, Liu L, Vázquez-Torres A. 2021. The DnaK/DnaJ chaperone system enables RNA polymerase-DksA complex formation in salmonella experiencing oxidative stress. mBio 12:e03443-20. https://doi.org/10.1128/mBio.03443-20
81. Brasel M, Pieranski M, Grinholc M. 2020. An extended logistic model of Photodynamic inactivation for various levels of Irradiance using the example of *Streptococcus agalactiae*. Sci Rep 10:14168. https://doi.org/10.1038/s41598-020-71033-7
82. Peters J, Jagger J. 1981. Inducible repair of near-UV radiation lethal damage in *E. coli*. Nature 289:194–195. https://doi.org/10.1038/289194a0
83. Karkman A, Do TT, Walsh F, Virta MPJ. 2018. Antibiotic-resistance genes in waste water. Trends Microbiol. 26:220–228. https://doi.org/10.1016/j.tim.2017.09.005
84. Gunther NW, Phillips JG, Sommers C. 2016. The effects of 405-nM visible light on the survival of campylobacter on chicken skin and stainless steel. Foodborne Pathog Dis 13:245–250. https://doi.org/10.1089/fpd.2015.2084
85. Li X, Kim MJ, Bang WS, Yuk HG. 2018. Anti-biofilm effect of 405-nM leds against listeria monocytogenes in simulated ready-to-eat fresh salmon storage conditions. Food Control 84:513–521. https://doi.org/10.1016/j.foodcont.2017.09.006
86. Sommers C, Gunther NW, Sheen S. 2017. Inactivation of salmonella spp., pathogenic *Escherichia coli*, *Staphylococcus* spp., or listeria monocytogenes in chicken purge or skin using a 405-nM LED array. Food Microbiol 64:135–138. https://doi.org/10.1016/j.fm.2016.12.011
87. Hyun JE, Lee SY. 2020. Antibacterial effect and mechanisms of action of 460–470 nM light-emitting diode against listeria monocytogenes and pseudomonas fluorescens on the surface of packaged sliced cheese. Food Microbiol 86:103314. https://doi.org/10.1016/j.fm.2019.103314
88. McKenzie K, Maclean M, Timoshkin IV, Endarko E, MacGregor SJ, Anderson JG. 2013. Photoinactivation of bacteria attached to glass and acrylic surfaces by 405 nM light: potential application for biofilm decontamination. Photochem Photobiol 89:927–935. https://doi.org/10.1111/php.12077

## 8.2.1. Supplementary Materials

Supplementary Table. 1. Hyperensitive genes and their functions

| | | Function | | Name of gene |
|---|---|---|---|---|
| Biosynthesis | Nucleotide and Nucleoside biosynthesis | Purine biosynthesis | | *purA* |
| | | Pyrimidine biosynthesis | | *thyA* |
| | | | | *pyrE* |
| | Fatty acids and lipid biosynthesis | Fatty Acid Biosynthesis Initiation | | *fabH* |
| | | Lipid A- core biosynthesis | | *waaC* |
| | | | | *waaG* |
| | Cofactor, Carrier, Vitamin synthesis | Electron Carrier Biosynthesis | | *menH* |
| | | | | *ubiC* |
| | | Folate Biosynthesis | | *thyA* |
| | Carbohydrate synthesis | Gluconeogenesis | | *tpiA* |
| | | | | *pgi* |
| | | Glycan Biosynthesis | | *pgm* |
| | | | | *waaC* |
| | | | | *waaG* |
| | | Glycogen and Starch Biosynthesis | | *pgm* |
| | | Sugar nucleotde Biosynthesis | ADP-sugar biosynthesis | *gmhB* |
| | | | | *hldE* |
| | | | | *rfaD* |
| | | | dTSP-sugar biosynthesis | *pgm* |
| | | | GDP-sugar biosynthesis | *pgi* |
| | | | UDP-sugar biosynthesis | *pgm* |
| | | | | *pgi* |
| | Other | 4-hydroxybenzoate | | *ubiC* |
| Degradation | Nucleotide and Nucleoside degradation | Purines and pyrimidines | | *deoB* |

| | | | |
|---|---|---|---|
| | Carbohydrates and Carboxylates degradation | Carbohydrates | *pgm*<br>*deoB*<br>*yigL* |
| | | Carboxylates degradation | *gntK* |
| **Energy** | | Glycolisis | *pfkA*<br>*tpiA*<br>*pgi* |
| | | Pentose Phosphate Pathway (PPP) | *rpe* |
| | | Aerobic and anaerobic respiration | *nuoN* |
| | | ATP biosynthesis | *atpG*<br>*atpF*<br>*atpA*<br>*atpH*<br>*atpC*<br>*atpE*<br>*atpB*<br>*atpD* |
| | Other | sedoheptulose bisphosphate bypass | *pfkA* |
| | DNA Metabolism | Replication | *dnaK*<br>*dnaJ*<br>*rnt*<br>*priA*<br>*holD* |
| | | Recombination | *priA*<br>*fimB* |
| | | Repair | *umuD*<br>*rnt*<br>*priA* |
| | | Integration | *fimB* |
| | RNA Metabolism | RNA Processing | *rnt*<br>*rbfA* |
| | | tRNA Processing | *rnt* |

| | | | |
|---|---|---|---|
| | | | *truA* |
| | | | *ygfZ* |
| | | | *tusC* |
| | | Regulation of RNA Methabolic Process | *dnaK* |
| | | | *dnaJ* |
| | | | *umuD* |
| | | | *narL* |
| | | | *metR* |
| | | | *oxyR* |
| | | Other Proteins involved in RNA Metabolism | *priA* |
| | Protein Metabolism | Proteolysis | *dacA* |
| | | | *umuD* |
| | | Regulation | *thyA* |
| | | Other Proteins involved in Protein Metabolism | *phoQ* |
| | | | *epmB* |
| | | | *cpxA* |
| | | Protein Folding | *surA* |
| | | | *dnaJ* |
| | | | *dnaK* |
| **Cellular Processes** | | Cell Cycle and Division Proteins | *dacA* |
| | | | *tolA* |
| | | Proteins involved in cell death | *ortT* |
| | | Proteins involved in Biofilm formation | *cpxA* |
| | | Proteins Involved in response to virus | *tolA* |
| | | | *dnaJ* |
| | | Proteins Involved in interaction with Host and Symbiosis | *tolA* |
| **Cell Exterior** | Transport | Transporters of Amino Acids and their Derivatives | *cydD* |
| | | | *sstT* |
| | | Cell Wall Biogenesis/Organization Proteins | *dacA* |
| | | Lipopolysaccharide Metabolism Proteins | *gmhB* |
| | | | *waaG* |
| | | | *waaC* |
| | | | *rfaD* |

| | | | |
|---|---|---|---|
| | | | *hldE* |
| | | Outer Membrane Proteins | *yneO* |
| | | | *bamB* |
| | | | *ecnB* |
| | | Plasma Membrane Proteins | *dnaK dacA tolA cydD yccM* |
| | | | *phoQ ortT yneO nuoN yfeH* |
| | | | *ypjD sstT yhhH waaC atpC atpG* |
| | | | *atpA atpH atpF atpE atpB cpxA* |
| | | | *ecnB* |
| | | Periplasmic Proteins | *surA* |
| | | | *dacA* |
| **Response to stimulus** | | Proteins Involved in Response to Starvation | *phoQ* |
| | | Proteins Involved in Response to Heat | *dnaK* |
| | | | *dnaJ* |
| | | Proteins Involved in Response to Cold | *rbfA* |
| | | Proteins Involved in Response to DNA Damage | *umuD rnt rbfA priA oxyR purA* |
| | | | *fimB deoB* |
| | | Proteins Involved in Response to osmotic Stress | *phoQ* |
| | | Other Proteins involved in Stimulus Response | *tolA* |
| | | | *holD* |
| | | | *ecnB* |
| | | | *pgi* |
| | | | *cpxA* |
| | | | *srkA* |
| | | | *narL* |
| | | | *yigL* |
| **Regulation** | Signaling | CpxAR Two-Component Signal Transduction System | *cpxA* |
| | | NarQ Two-Component Signal Transduction System, nitrate dependent | *narL* |
| | | NarX Two-Component Signal Transduction System, nitrate dependent | *narL* |

| | | |
|---|---|---|
| | PhoQP Two-Component Signal Transduction System, magnesium-dependent | *phoQ* |
| Sigma Factors Regulons | Regulon of RNA polymerase sigma factor RpoD | *cydD fabH umuD narL rnt nuoN thyA rbfA rpe gntK rfaD waaC waaG atpC atpG atpA atpH atpF atpE atpB srkA cpxA pfkA tpiA oxyR pgi, ubiC purA fimB deoB* |
| | Regulon of RNA polymerase sigma factor RpoH | *dnaK*<br>*dnaJ*<br>*phoQ*<br>*waaC*<br>*rfaD* |
| | Regulon of RNA polymerase sigma factor RpoE | *surA*<br>*phoQ*<br>*bamB*<br>*rfaD*<br>*waaC* |
| | Regulon of RNA polymerase sigma factor RpoS | *cpxA*<br>*ecnB*<br>*pgi*<br>*pfkA*<br>*tpiA*<br>*oxyR* |
| | Transcription factors | *oxyR*<br>*metR*<br>*narL* |
| Transcription factor regulons | Regulon of DNA-binding transcriptional dual regulator OxyR | *metR*<br>*oxyR* |
| | Regulon of DNA-binding transcriptional dual regulator H-NS | *fimB* |
| | Regulon of DNA-binding transcriptional dual repressor DeoR | *deoB* |

| | | |
|---|---|---|
| | Regulon of DNA-binding transcriptional dual regulator Nac | *yccM*<br>*ortT*<br>*waaG*<br>*yigL*<br>*metR*<br>*ppc*<br>*ecnB* |
| | Regulon of DNA-binding transcriptional dual regulator NagC, BasR | *fimB* |
| | Regulon of DNA-binding transcriptional dual regulator SoxS | *pgi* |
| | Regulon of DNA-binding transcriptional dual regulator PhoB, PhoP | *phoQ* |
| | Regulon of DNA-binding transcriptional activator ZraR | *rfaD* |
| | Regulon of DNA-binding transcriptional dual regulator ArcA | *cydD*<br>*nuoN*<br>*sstT*<br>*ubiC* |
| | Regulon of DNA-binding transcriptional repressor LexA | *umuD* |
| | Regulon of DNA-binding transcriptional activator GadE | *purA* |
| | Regulon of NanR | *fimB* |
| | Regulon of DNA-binding transcriptional dual regulator HU | *pgm* |
| | Regulon of DNA-binding transcriptional dual regulator OmpR | *sstT*<br>*ecnB* |
| | Regulon of DNA-binding transcriptional repressor CytR | *deoB* |
| | Regulon of DNA-binding transcriptional dual regulator FNR | *cydD*<br>*narL*<br>*ortT* |

| | | | |
|---|---|---|---|
| | | | *nuoN* |
| | | | *ubiC* |
| | | Regulon of DNA-binding transcriptional dual regulator CpxR | *srkA* |
| | | | *cpxA* |
| | | Regulon of MetJ-S-adenosylmethionine | *metR* |
| | | Regulon of DNA-binding transcriptional dual regulator ArcA, NarL | *cydD* |
| | | | *nuoN* |
| | | | *narL* |
| | | | *ubiC* |
| **Other Pathways** | | Nitrate Reduction | *nuoN* |
| | | Nucleic Acid Processing | *rnt* |
| | | | *tusC* |
| | | Enzymes not in Pathways | *dnaK* |
| | | | *dnaJ* |
| | | | *surA* |
| | | | *umuD* |
| | | | *mnaT* |
| | | | *pptA* |
| | | | *yegS* |
| | | | *truA* |
| | | | *srkA* |
| | | | *epmB* |
| | **Genes not present in any subsystem** | | *ybaP* |

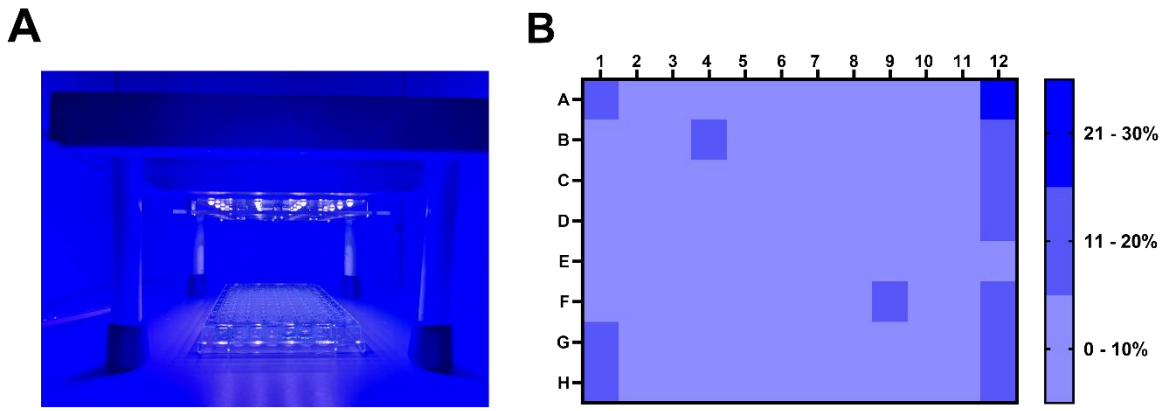


**Supplementary Figure 1. The LED light source used in research.** A. The picture of the LED light source used in the research. B. The map of irradiance distribution over the illuminated area. Percentage indicate deviations from the mean power for all irradiation areas. The LED light source was constructed to reach a homogeneous light distribution. The differences between light densities do not exceed 10% (except for a few fields, which were considered when performing the experiments). The 96-well plates from different biological replicates were placed in different orientations relative to the light source to increase power homogeneity.

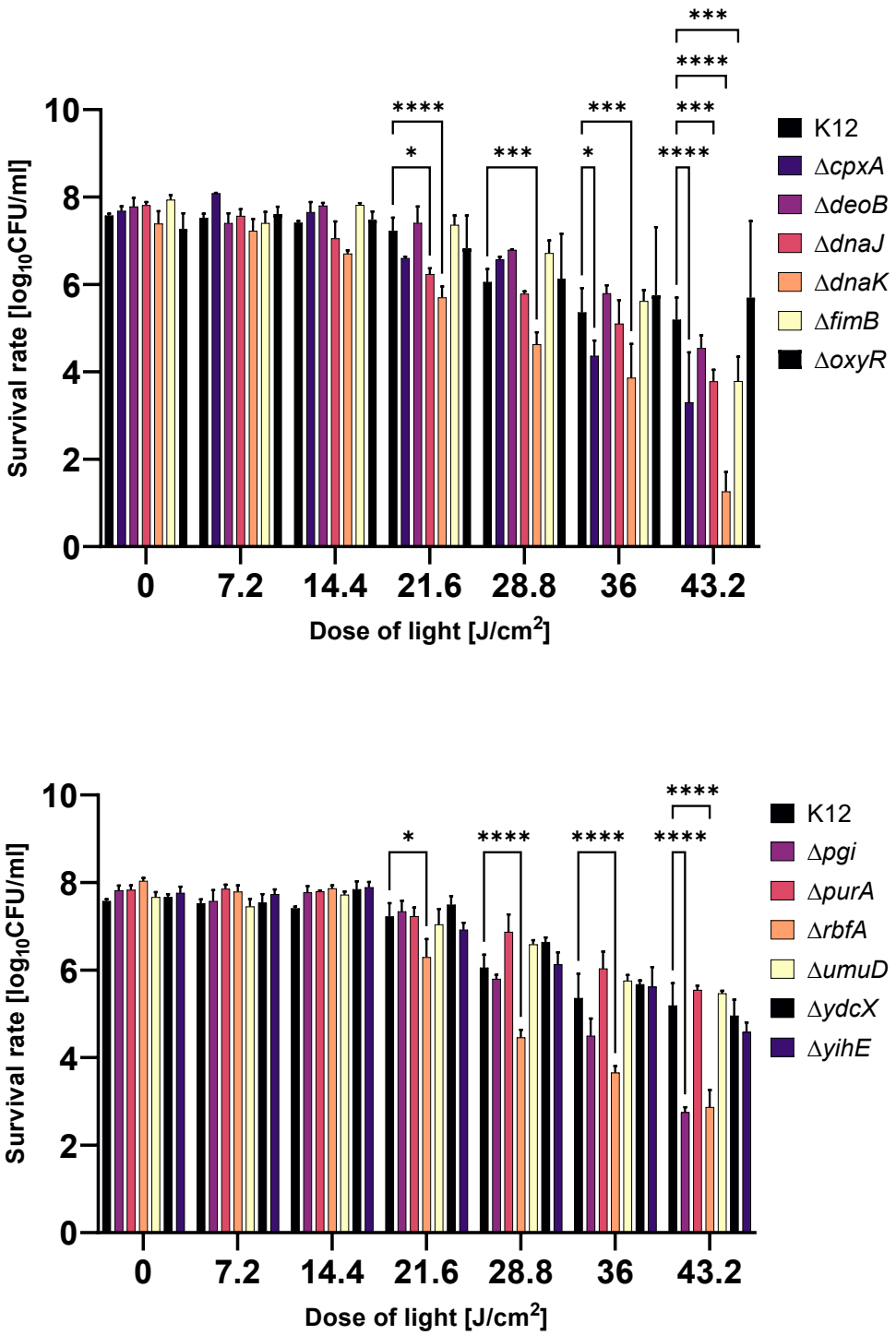


**Supplementary Figure. 2 Survival rate of single gene mutants irradiated with 0-43.2 J/cm² in comparison to WT (BW25113) survival rate.** The detection limit was 10 CFU/ml. Overnight cultures of wild and mutant strains were diluted to 0.5 McF in medium and then irradiated with 43.2 J/cm². Colony-forming units (CFU/mL) were estimated with serial dilutions of 10 µL aliquots of irradiated samples and plated on LB agar. Plots present the reduction of $\log_{10}$ units of CFU/ml. The experiment was performed in three biological repetitions. The value is a mean of three separate experiments with bars as ± SD of the mean.

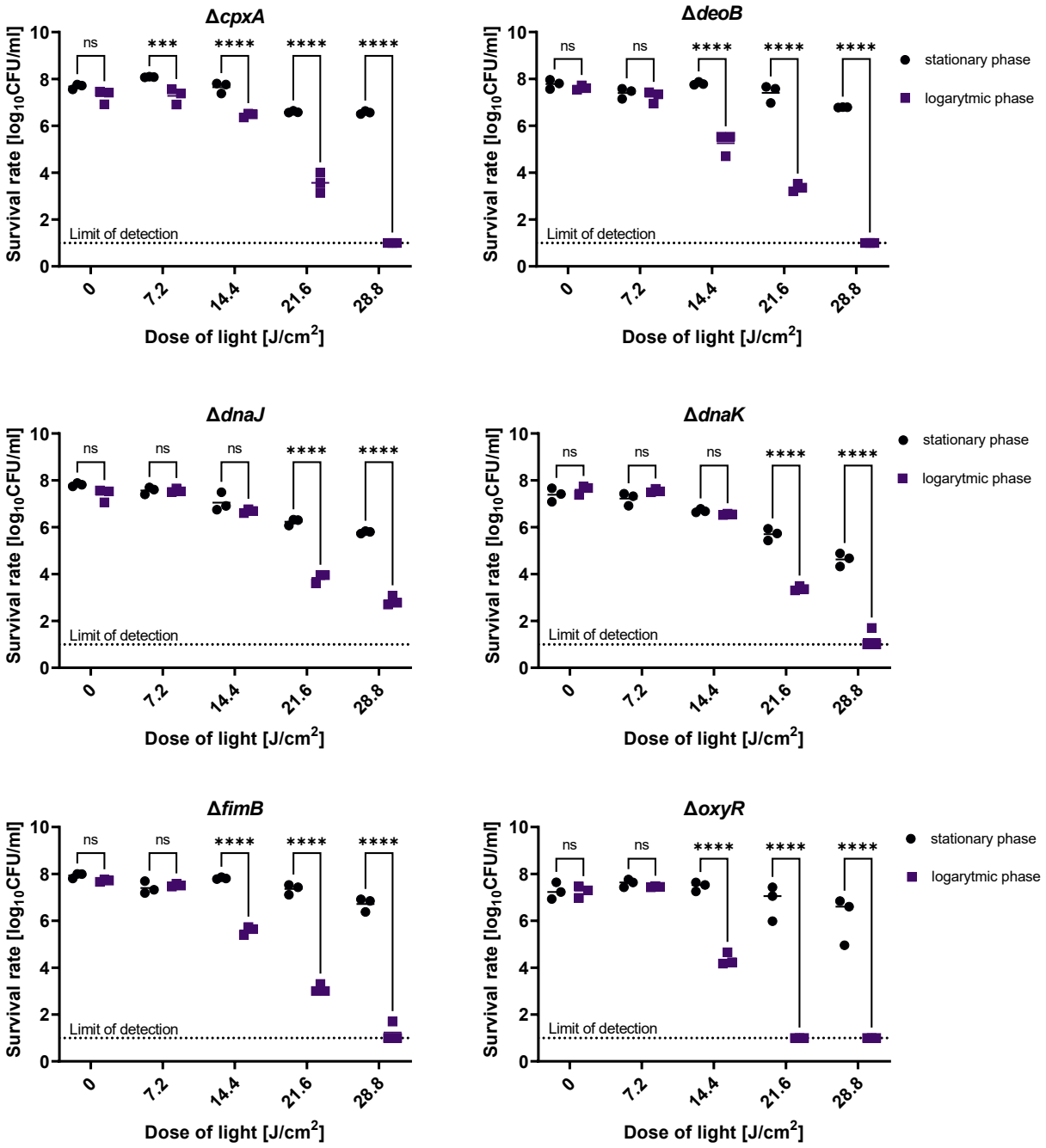
ΔcpxA
ΔdeoB
ΔdnaJ
ΔdnaK
ΔfimB
ΔoxyR
Survival rate [log10CFU/ml]
Dose of light [J/cm2]
Limit of detection
ns
***
****
stationary phase
logarytmic phase
0
7.2
14.4
21.6
28.8

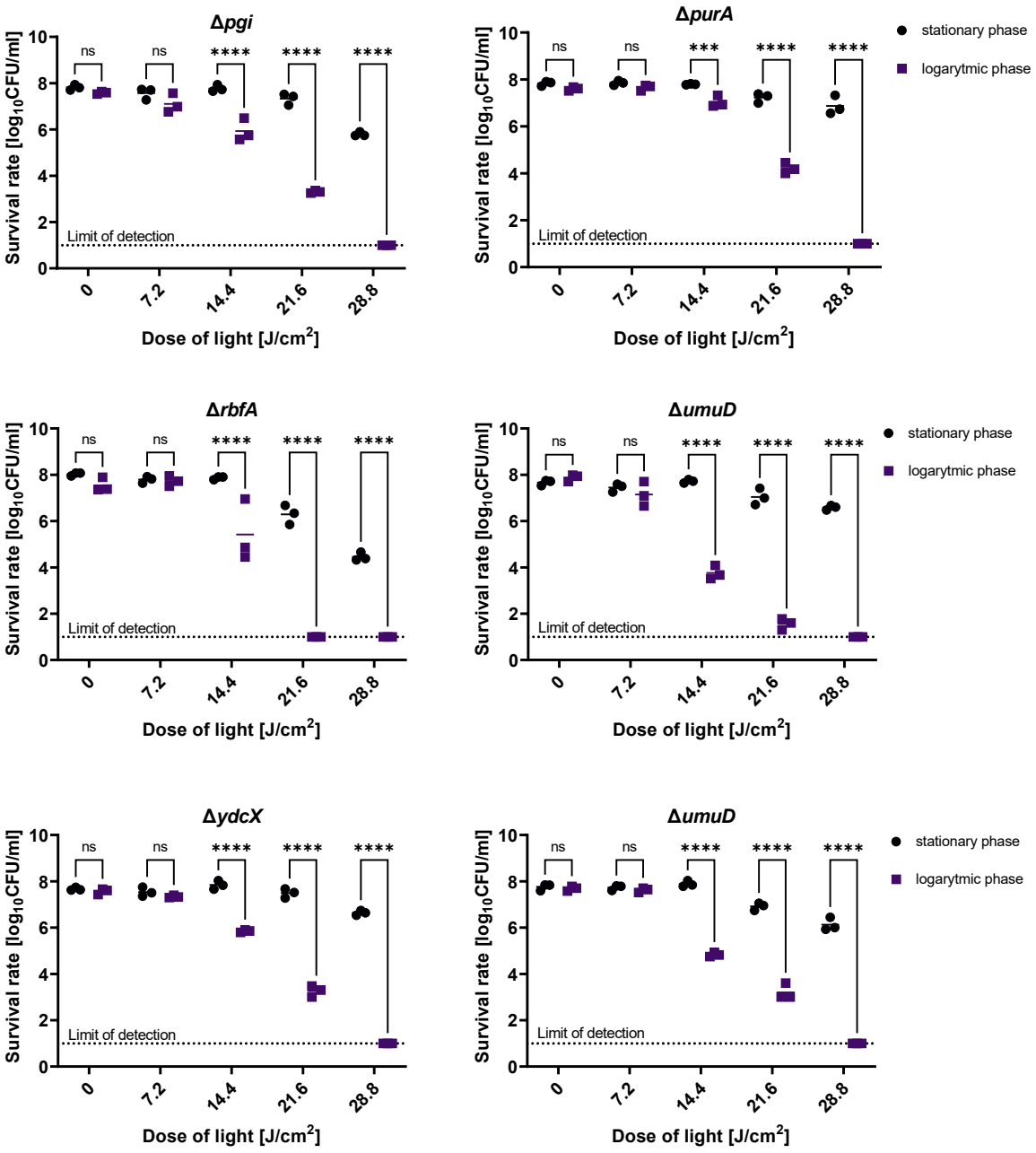


**Supplementary Figure. 3. Comparison of the aBL sensitivity profiles of the selected single gene mutants depending on the growth phase.** Overnight cultures (16 h, stationary phase) and logarithmic phase cultures (2 h, exponential phase) were irradiated with 0–28.8 J/cm$^2$ light doses. All the experiments were performed in three biological repetitions. The detection limit was 10 CFU/ml. Significance at the respective p values is marked with asterisks [ns $p > 0.05$; ****$p \leq 0.0001$]

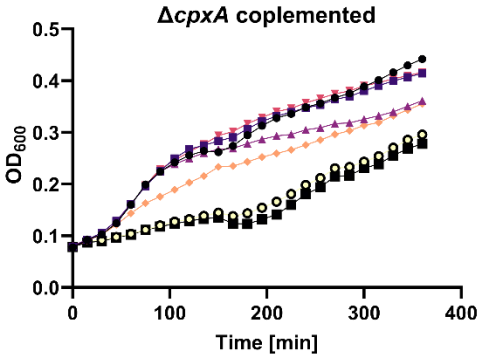
ΔcpxA coplemented
OD600
Time [min]

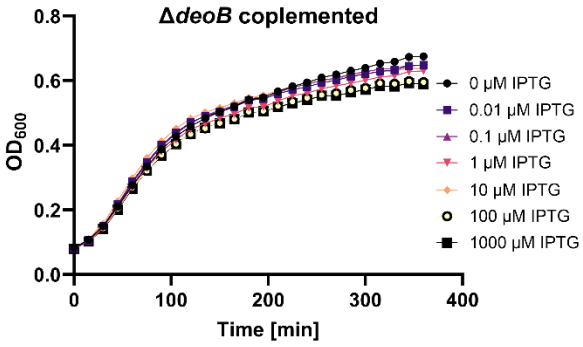
ΔdeoB coplemented
OD600
Time [min]
0 µM IPTG
0.01 µM IPTG
0.1 µM IPTG
1 µM IPTG
10 µM IPTG
100 µM IPTG
1000 µM IPTG

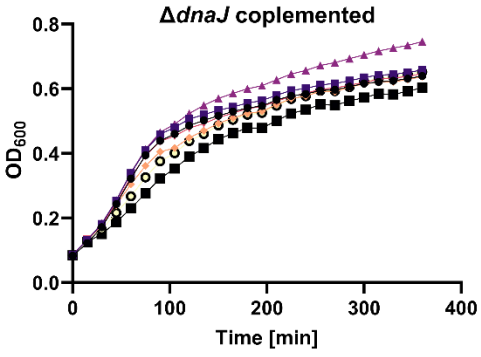
ΔdnaJ coplemented
OD600
Time [min]

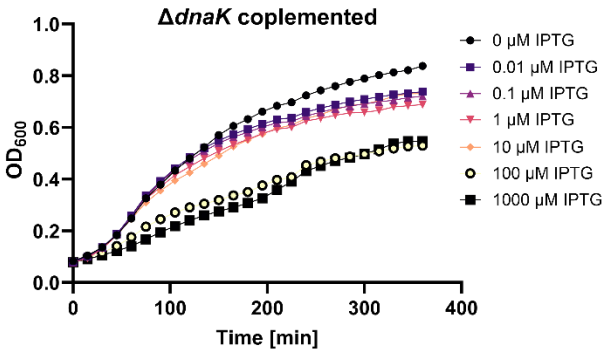
ΔdnaK coplemented
OD600
Time [min]
0 µM IPTG
0.01 µM IPTG
0.1 µM IPTG
1 µM IPTG
10 µM IPTG
100 µM IPTG
1000 µM IPTG

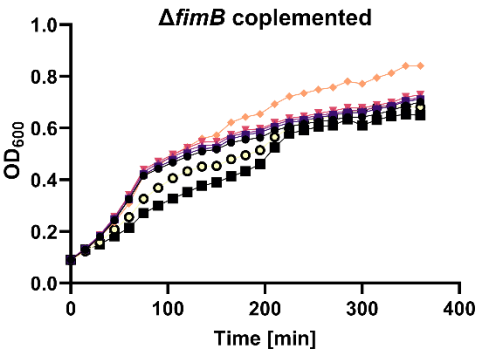
ΔfimB coplemented
OD600
Time [min]

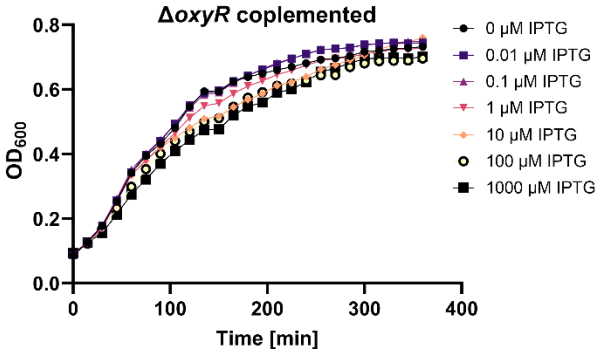
ΔoxyR coplemented
OD600
Time [min]
0 µM IPTG
0.01 µM IPTG
0.1 µM IPTG
1 µM IPTG
10 µM IPTG
100 µM IPTG
1000 µM IPTG

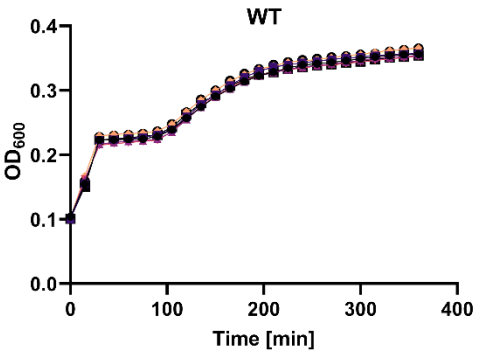
WT
OD600
Time [min]

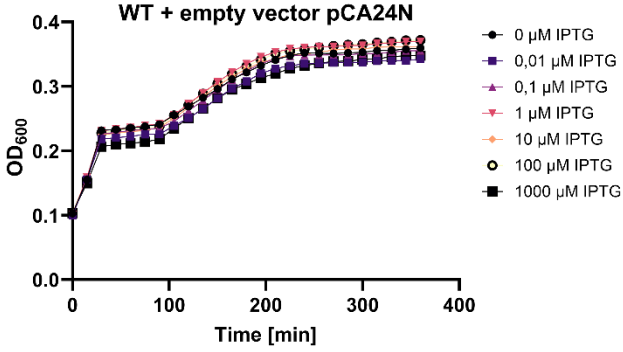
WT + empty vector pCA24N
OD600
Time [min]
0 µM IPTG
0,01 µM IPTG
0,1 µM IPTG
1 µM IPTG
10 µM IPTG
100 µM IPTG
1000 µM IPTG

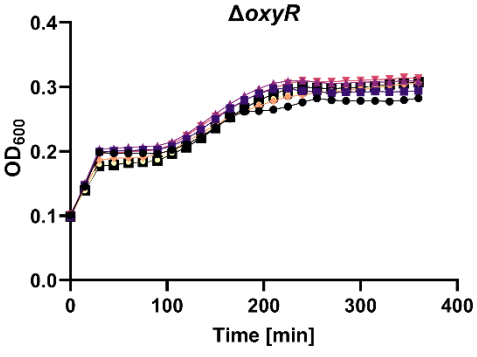
ΔoxyR
OD600
Time [min]

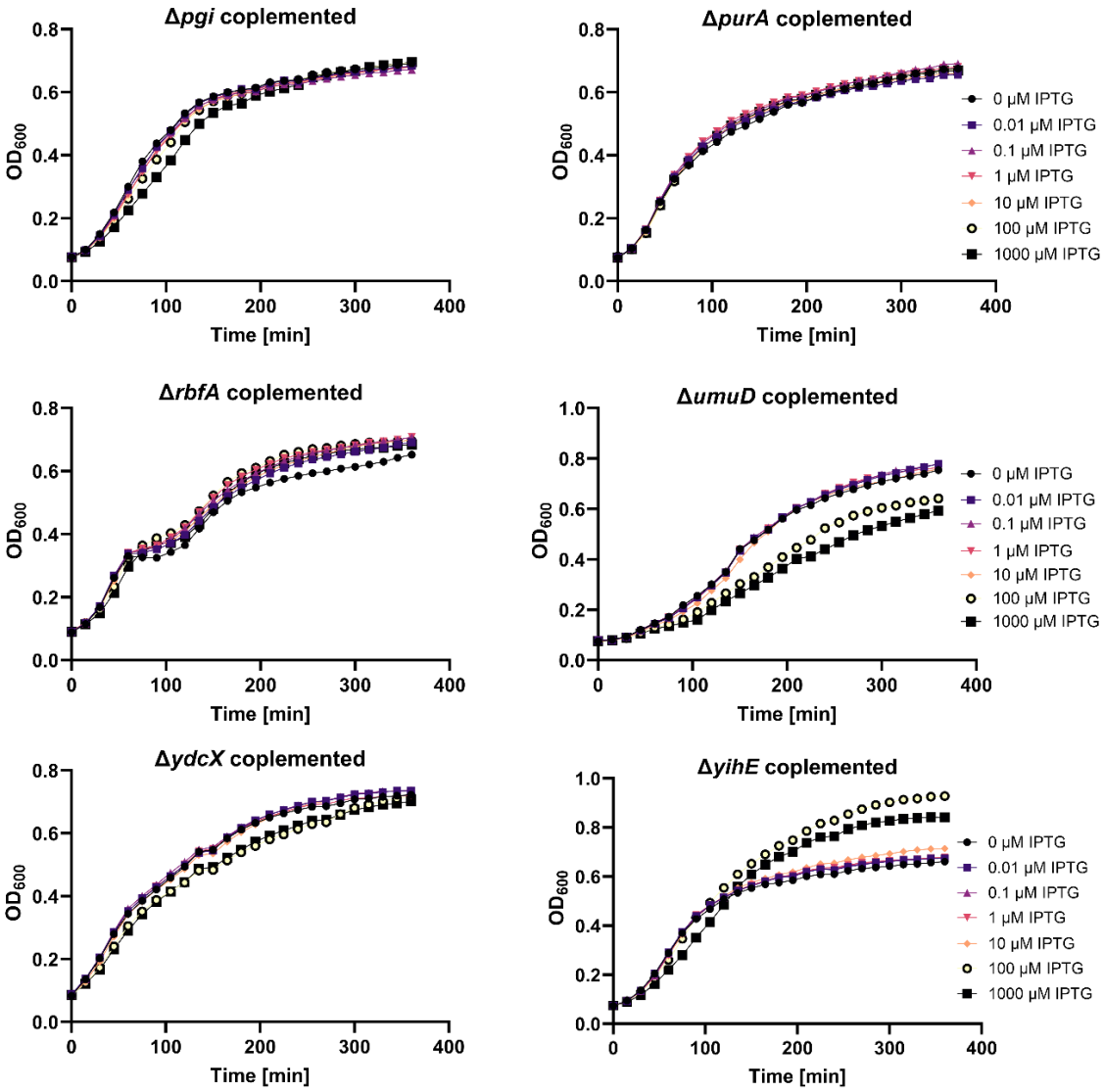


**Supplementary Figure. 4. Growth curve of the complemented strains, WT, WT harbouring the empty vector pCA24N and Δ*oxyR* mutant cultured with different IPTG concentrations.** Overnight cultures of the strain were diluted at the v/v ratio of 1:20 and supplemented with IPTG to obtain the final concentrations of 0–1000 μM. The growth was monitored for 6 h. The $OD_{600}$ was measured every 15 min. All the experiments were performed in three biological repetitions.

## 8.3. Publication no. 3.

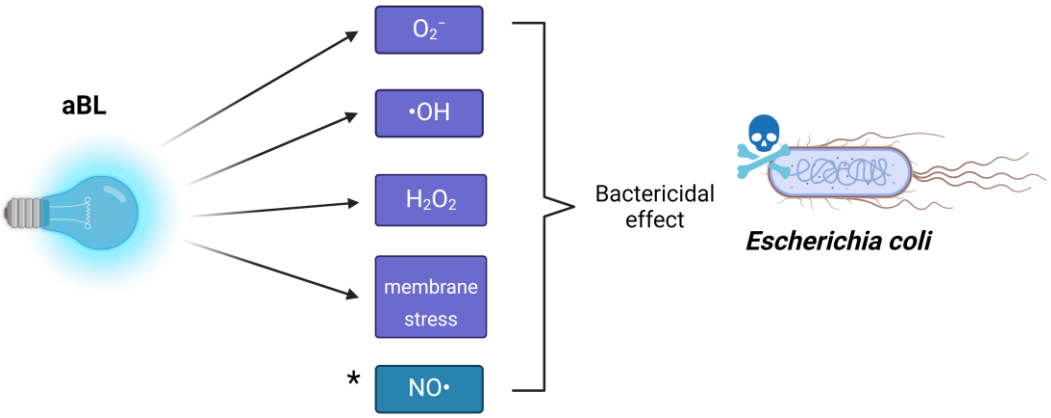


Figure 3. Graphical abstract of Publication no. 3.

*antioxidants*

MDPI

*Article*

# Mimicking the Effects of Antimicrobial Blue Light: Exploring Single Stressors and Their Impact on Microbial Growth

**Beata Kruszewska-Naczk [1], Mariusz Grinholc [1] and Aleksandra Rapacka-Zdonczyk [1,2,*]**

[1] Laboratory of Photobiology and Molecular Diagnostics, Intercollegiate Faculty of Biotechnology, University of Gdansk and Medical University of Gdansk, Abrahama 58, 80-307 Gdansk, Poland; beata.kruszewska@phdstud.ug.edu.pl (B.K.-N.); mariusz.grinholc@biotech.ug.edu.pl (M.G.)

[2] Department of Pharmaceutical Microbiology, The Faculty of Pharmacy, Medical University of Gdansk, Hallera 107, 80-416 Gdansk, Poland

* Correspondence: aleksandra.rapacka-zdonczyk@ug.edu.pl

**Abstract:** Antimicrobial blue light (aBL) has become a promising non-invasive method that uses visible light, typically within the 405–470 nm wavelength range, to efficiently inactivate a wide variety of pathogens. However, the mechanism of antimicrobial blue light (aBL) has not been fully understood. In this study, our research group investigated the sensitivity of *Escherichia coli* BW25113 single-gene deletion mutants to individual stressors generated by aBL. Sixty-four aBL-sensitive mutants were tested under conditions mimicking the stress generated by irradiation with aBL, with their growth defects compared to the wild-type strain. Results revealed no positive correlation between aBL and single stressors, indicating that aBL's effectiveness is due to the simultaneous generation of multiple stressors. This multifactorial effect suggests that aBL targets microbial cells more precisely than single stressors such as hydrogen peroxide. No single gene knockout conferred specific resistance, highlighting aBL's potential as an antimicrobial strategy.

**Keywords:** antimicrobial blue light (aBL); *Escherichia coli*; hydrogen peroxide; hydroxyl radicals; Keio collection; oxidative stress; superoxide anion; single stressors



**Citation:** Kruszewska-Naczk, B.; Grinholc, M.; Rapacka-Zdonczyk, A. Mimicking the Effects of Antimicrobial Blue Light: Exploring Single Stressors and Their Impact on Microbial Growth. *Antioxidants* **2024**, *13*, 1583. https://doi.org/10.3390/antiox13121583

Academic Editor: Michel Havaux

Received: 30 October 2024
Revised: 3 December 2024
Accepted: 20 December 2024
Published: 23 December 2024



## 1. Introduction

Antibiotic resistance is one of the most serious and frequent threats that the modern community has to face. According to the WHO Bacterial Priority Pathogens List (2024 update), critical pathogens, due to limited treatment options and high mortality rates, are carbapenem-resistant *Acinetobacter baumannii* (CRAB) and Enterobacterales (CRE), and also third-generation cephalosporin-resistant Enterobacterales (3GCRE). Since the previous report in 2017, no new, effective antibiotic treatment has been developed to combat infections caused by these pathogens, prompting the search for innovative strategies to fight bacterial infections [1]. One of the most promising strategies is the use of antibacterial blue light (aBL), which has been repeatedly proven to be effective in fighting antibiotic-resistant pathogens [2,3]. aBL treatment has emerged as a promising non-invasive approach that utilizes visible light, typically in the 405–470 nm range, to effectively inactivate a broad spectrum of pathogens. Unlike traditional antibiotics, aBL offers a selective mechanism that minimizes host tissue damage while targeting microbial cells. The efficacy of aBL is due to its ability to generate reactive oxygen species (ROS) within bacterial cells, due to the excitation of photosensitizing endogenous chromophores, such as flavins and porphyrins [4,5]. Upon the absorption of photon, these molecules generate singlet oxygen ($^1O_2$), hydrogen peroxide ($H_2O_2$), superoxide anions ($O_2^{\bullet-}$), and hydroxyl radicals (•OH), which cause oxidative stress, leading to cell damage and death [5–7]. This mechanism of action is effective against both Gram-negative and Gram-positive bacteria, including antibiotic-resistant strains, making aBL an attractive alternative to conventional antimicrobials [8,9]. This study aimed to check the sensitivity of single-gene deletion mutants of *Escherichia coli* (*E. coli*)

BW25113 [10,11] to single stressors generated by aBL to elucidate the aBL protective role of each aBL-hypersensitive gene, which may contribute to explaining the aBL mode of action. Sixty-four-aBL sensitive mutants were tested in conditions mimicking single species stress generated by aBL. Mutants' hypersensitivity against individual stressors connected with aBL was tested measuring the growth defect compared to the wild-type strain, following a methodology analogous to that used in studies of nonthermal plasma [12].

## 2. Materials and Methods

### 2.1. Bacterial Strains

The analysis utilized a set of 64 *E. coli* BW25113 single-gene knockout mutants, (known as the Keio collection, consisting of 3985 strains as described by Baba et al., 2006 [10]) which were previously identified as aBL hypersensitive [11]. The list of aBL hypersensitive mutants used in this study includes the following: *atpA*, *atpB*, *atpC*, *atpD*, *atpE*, *atpF*, *atpG*, *atpH*, *cpxA*, *cydD*, *dacA*, *deoB*, *dnaJ*, *dnaK*, *ecnB*, *fabH*, *fimB*, *gmhB*, *gntK*, *hldD*, *holD*, *metR*, *narL*, *nuoN*, *oxyR*, *pfkA*, *pgi*, *pgm*, *phoQ*, *ppc*, *priA*, *purA*, *pyrE*, *rbfA*, *rfaC*, *rfaE*, *rfaG*, *rnt*, *rpe*, *sstT*, *surA*, *thyA*, *tolA*, *tpiA*, *truA*, *ubiC*, *umuD*, *ybaP*, *yccM*, *ydcE*, *ydcX*, *ydeU*, *yegS*, *yfbB*, *yfeH*, *yfgL*, *ygfZ*, *yheM*, *yhhH*, *yigL*, *yihE*, *yjeK*, *yncA*, and *ypjD*. All of them were described in detail in our previous research [11]. The wild-type strain *E. coli* BW25113 was used as a control. Table S4 lists the aBL-hypersensitive mutants with a description of the protein encoded by the deleted gene.

Single-gene mutants were cultured in LB medium (Carl Roth, Karlsruhe, Germany) containing 15 µM of kanamycin (Gibco, Zawroty, Poland). The wild-type strain was cultured in the same medium without antibiotics. Overnight cultures were prepared in an orbital incubator (Innova 40, Brunswick, Germany) at 37 °C, 150 rpm for 16–20 h.

### 2.2. Reagents

Paraquat and $K_3PO_4$ were purchased from Sigma Aldrich (Darmstadt, Germany), Triton X—Serva Electrophoresis (Heidelberg, Germany), $H_2O_2$—Pol-Aura (Zawroty, Poland), $CuCl_2$—Thermofisher Scientific (Waltham, MA USA), Sodium Nitroprusside, and HCl—CHEMPUR (Piekary Śląskie, Poland).

### 2.3. Determining aBL Sensitivity

Overnight cultures of mutants were diluted to obtain 0.5 McF. A total volume of aliquots which was transferred to 96-microliter plates was 100 µL. The samples were irradiated with 43.2 J/cm$^2$ of LED blue light (λmax 415 nm, irradiance 25 mW/cm$^2$) (Cezos, Gdynia, Poland) according to previously described studies [11]. Then, 10 µL of aliquots was collected and streaked horizontally onto LB-agar plates (A&A, Gdansk, Poland) to assess growth reductions. Plates were incubated at 37 °C overnight, and surviving colonies were counted. Experiments were performed in triplicate.

### 2.4. Screening Against Defined Stressors

The workflow is presented in Figure 1.

Overnight cultures of single-gene mutants of *E. coli* BW25113 [10] incubated at 37 °C by 16–20 h under aerobic conditions in an orbital incubator (Innova 40, Brunswick, Germany) were 100-fold diluted in LB in 96-well plates, and stressors were added. A medium containing the stressor at the appropriate concentration, determined as the dose, reduced the growth of the WT strain by 30–40%. A similar range of growth reduction was previously used in a study conducted by Krewing et al. (2019) [12] examining single plasma stressors. Concentrations of stressors are listed in Table 1. Reagents to investigate Fenton reaction products were prepared in a sterile LB medium buffered with $K_3PO_4$, pH = 6. After sterilization, $CuCl_2$ and $H_2O_2$ were freshly added before experiments.

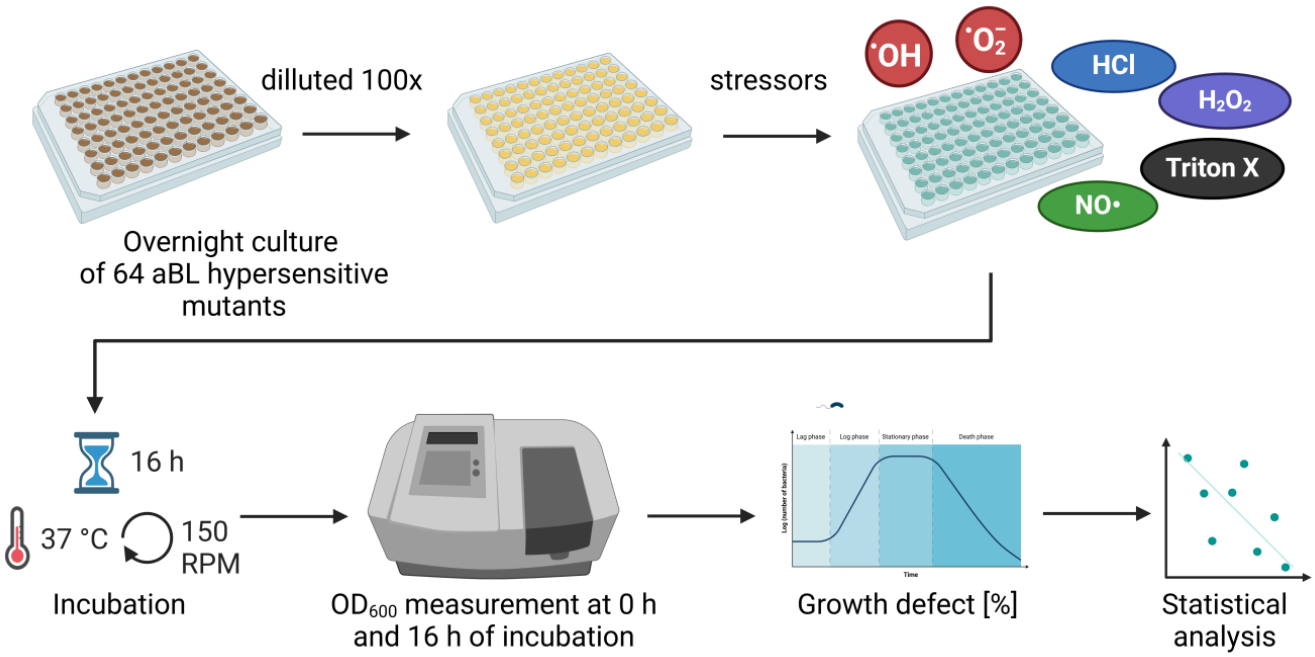


**Figure 1.** The experimental workflow.

**Table 1.** Concentrations of stressors used in this study.

| Stressor | Substance | Concentration |
|---|---|---|
| NO• | Sodium nitroprusside | 0.5 mM |
| $O_2^-$ | Paraquat | 1 mM |
| Membrane stress | TritonX | 0.125% |
| Acid stress | HCl | 7 mM |
| | $H_2O_2$ | 1 mM |
| •OH | $CuCl_2$, $H_2O_2$ | 2.5 mM $CuCl_2$ + 1.5 mM $H_2O_2$ |

The $OD_{600}$ value of bacteria with stressors and controls without stressors were measured in an EnVision Multilabel Plate Reader (PerkinElmer, Waltham, MA, USA) at 0 h and after 16 h of incubation at 37 °C with shaking (150 rpm). All the experiments were performed in five biological replicates.

$\Delta OD_{600}$ values ($OD_{600}$ 16 h − $OD_{600}$ 0 h) were determined, and the sensitivity of each mutant was calculated according to the formula:

$$\textbf{grown defect [\%]} = 100 - 100 \times \Delta OD_{WT} \times \Delta OD^{-1}{}_{WT,\,stressed} \times (\Delta OD_{\,mutant} \times \Delta OD - 1_{\,mutant,\,stressed})^{-1}$$

The greater the growth defect value, the higher the sensitivity of the single-gene mutant to particular stress conditions. Strains with a growth defect of 20% or higher were termed 'sensitive' towards that stressor.

### *2.5. Statistical Analysis*

The mean and standard deviation are used to describe continuous variables. For all statistical tests, a significance level of $\alpha = 0.05$ was assumed. Due to the distribution of variables deviating from the normal distribution, the Spearman correlation coefficient with its statistical significance was calculated to investigate the correlation between aBL and stressors.

To calculate the probability that a mutant sensitive to a given stressor is also sensitive to another stressor, the formula for conditional probability was used:

$$P(A|B) = \frac{P(A \cap B)}{P(B)}$$

Explanation of the formula: P(A | B)—the probability that mutants A and B are simultaneously sensitive to a given stressor (in both cases, the average of 5 measurements is >20 or < −20). P(B)—the probability that the mutant is sensitive to stressor B.

Cluster analysis was performed to group mutants into groups with a similar stressor sensitivity profile. The analysis began by reducing the dimension of the data by using a Principal Component Analysis (PCA) performed on scaled data.

For the proper cluster analysis, the k-means++ method with cosine distances was used. The number of clusters was selected based on the WSS (Within-Cluster Sum of Squares) index and the Silhouette statistics. The Mann–Whitney U test was used to characterize the clusters to check the differences between stressors in different clusters. Due to multiple comparisons, the *p*-value was adjusted by the FDR (False Discovery Rate).

Protein–protein functional interaction networks and gene co-expression within clusters were analyzed using the STRING database. The analysis was performed using the data from the curated databases that were experimentally determined.

## 3. Results

### *3.1. Growth Defects of aBL Hypersensitive Mutants Exposed to a Single Stressor*

Single-gene mutants' growth was affected by stressors in various ways, depending on the kind of stressor used. Table 2 presents growth defect values calculated according to the formula described in the Material and Methods Section, taking into account the growth of mutants without stressors and comparing it to the wild-type growth defect.

**Table 2.** Growth defects [%] of aBL hypersensitive mutants exposed to single stressors compared with aBL sensitivity [$\log_{10}$ CFU/mL]. Calculations are performed for 5 biological replicates. Values with growth defects higher than 20% are bolded.

| | | Stressors | | | | | |
|---|---|---|---|---|---|---|---|
| **Mutant** | **aBL Sensitivity** | **$H_2O_2$** | **$O_2^-$** | **NO•** | **Acidic pH** | **Membrane Stress** | **•OH** |
| *atpA* | 4.61 | −134.65 (±37.8) | −2.2 (±10.43) | 12.35 (±18.21) | −90.3 (±37.87) | −1.78 (±8.48) | **95.48 (±3.28)** |
| *atpB* | 1.00 | −13.9 (±149.98) | −4.03 (±45.42) | −6.06 (±41.91) | −75.59 (±26.4) | 18.49 (±9.59) | **95.89 (±3.28)** |
| *atpC* | 3.93 | −168.96 (±36.7) | **59.31 (±20.35)** | **51 (±29.07)** | −26.43 (±19.82) | **43.94 (±8.45)** | **51.06 (±47.38)** |
| *atpD* | 3.85 | −227.06 (±51.25) | 6.47 (±13.64) | 7.63 (±34.86) | −84.74 (±25.35) | −2.32 (±26.9) | −52.43 (±24.94) |
| *atpE* | 2.76 | 2.02 (±125.97) | **32.85 (±40.98)** | 8.39 (±36.26) | −55.05 (±31.93) | **31.19 (±27.72)** | **95.97 (±1.91)** |
| *atpF* | 1.00 | 91.81 (±3.33) | −30.66 (±30.57) | **40.24 (±23.59)** | −54.69 (±38.16) | **30.21 (±13.47)** | **95.89 (±3.79)** |
| *atpG* | 3.96 | −51.25 (±155.4) | **69.61 (±23.38)** | **46.51 (±20.24)** | −65.69 (±47.99) | −9.68 (±31.25) | **96.68 (±2.02)** |
| *atpH* | 1.23 | −0.02 (±129.74) | −18.11 (±31.97) | −2.82 (±36.1) | −80.81 (±40.86) | **25.36 (±12.23)** | **95.8 (±5.45)** |
| *cpxA* | 3.16 | −102.12 (±108.26) | **34.43 (±18.78)** | 16.84 (±29.9) | −81.65 (±16) | 12.67 (±12.29) | **97.31 (±2.04)** |
| *cydD* | 4.28 | −218.89 (±16.31) | **52.31 (±20.19)** | **87.11 (±8.58)** | −95.42 (±24.8) | −3.58 (±8.36) | **77.15 (±45.4)** |
| *dacA* | 3.59 | −128.05 (±50.37) | **80.23 (±6.83)** | **63.23 (±8.5)** | −52.23 (±8.09) | 11.04 (±19.48) | **71.53 (±47.16)** |
| *deoB* | 4.08 | −172.58 (±43.14) | **29.26 (±27.82)** | **42.02 (±16.05)** | −29.15 (±38.28) | 2.88 (±27.49) | −124 (±11.84) |
| *dnaJ* | 3.78 | −36.93 (±133.44) | **29.25 (±32.98)** | −5.97 (±29.17) | −82.4 (±38.27) | −0.61 (±12.8) | **98.58 (±1.38)** |
| *dnaK* | 1.26 | −189 (±25.15) | 19.47 (±25.12) | 5.93 (±26.75) | −87.37 (±30.17) | 0.75 (±28.14) | −122.76 (±10.51) |
| *ecnB* | 4.75 | −207.51 (±26.82) | 4.05 (±11.31) | **25.26 (±20.25)** | −86.37 (±25.34) | 16.66 (±3.25) | **23.94 (±114.4)** |
| *fabH* | 2.82 | −30.08 (±142.87) | 19.4 (±23.52) | 3.76 (±25.18) | −88.74 (±38.58) | −9.42 (±32.18) | **46.18 (±68.28)** |
| *fimB* | 3.78 | −166.25 (±68.29) | 17.69 (±33.13) | 9.32 (±29.85) | −141.79 (±44.04) | −65.31 (±53.56) | **97.3 (±2.45)** |
| *gmhB* | 3.93 | −148.78 (±36.83) | **33.44 (±55.38)** | **55.39 (±16.57)** | −77.78 (±43.53) | **60.66 (±6.07)** | **97.42 (±2.21)** |
| *gntK* | 4.51 | −143.54 (±61.26) | 16.33 (±22.69) | 11.45 (±30.13) | −77.17 (±39.44) | −43.69 (±4.8) | **29.19 (±98.23)** |
| *holD* | 3.79 | −190.55 (±69.39) | **28.85 (±9.87)** | **40.55 (±42.29)** | −30.97 (±18.8) | 13.3 (±22.79) | **76.81 (±44.43)** |
| *metR* | 4.72 | −119.01 (±73.02) | 10.25 (±40.14) | **48.18 (±9.14)** | −45.78 (±44.83) | −4.28 (±27.65) | −88.81 (±48.94) |
| *narL* | 4.91 | −163.49 (±47.2) | **23.64 (±27.57)** | **62.32 (±14.41)** | −46.47 (±28.79) | 6.47 (±26.48) | −115.65 (±22.38) |
| *nuoN* | 6.03 | −118.98 (±30.6) | **55.65 (±15.03)** | **41.32 (±15.03)** | −52.15 (±11.24) | 4.87 (±14.32) | **20.86 (±104.77)** |
| *oxyR* | 5.69 | −164.37 (±75.84) | **62.53 (±15.66)** | **36.03 (±32.12)** | −45.03 (±34.09) | **27.51 (±23.22)** | 2.42 (±61.69) |
| *pfkA* | 3.80 | −134.27 (±48.88) | **40.11 (±30.89)** | **57.22 (±8.21)** | −46.31 (±42.02) | 12.18 (±21.63) | −75 (±57.62) |
| *pgi* | 2.79 | −113.64 (±45.57) | **37.64 (±16.31)** | **52.77 (±8.07)** | −41.07 (±10.14) | 4.1 (±21.54) | **48.78 (±108.45)** |
| *pgm* | 3.43 | −140.32 (±84.01) | **38.95 (±15.56)** | **35.61 (±16.85)** | −59.53 (±36.21) | 17.47 (±22.74) | **46.1 (±73.31)** |
| *phoQ* | 3.87 | −84.48 (±139.55) | **66.91 (±46.06)** | **48.66 (±12.1)** | −58.83 (±38.61) | −5.88 (±27.88) | **54.54 (±95.91)** |
| *ppc* | 6.80 | −154.47 (±169.15) | **44.06 (±25.28)** | **35.24 (±8.34)** | −90.37 (±45.68) | −39.37 (±37.86) | −210.34 (±77.81) |
| *priA* | 5.45 | −53.04 (±84.24) | 7.59 (±60.1) | **36.27 (±6.14)** | −77.97 (±37.42) | −6.38 (±6.64) | **100.09 (±1.12)** |
| *purA* | 5.54 | −128.16 (±132.92) | −0.56 (±16.97) | −15.44 (±31.35) | −80.22 (±24.5) | −12.57 (±37.88) | **24.72 (±102.15)** |
| *pyrE* | 4.74 | −309.35 (±19.3) | 2.3 (±32.84) | −27.4 (±37.32) | −76.66 (±107.67) | −75.19 (±47.46) | −7.77 (±151.65) |

**Table 2.** *Cont.*

| | | Stressors | | | | | |
|---|---|---|---|---|---|---|---|
| **Mutant** | **aBL Sensitivity** | **$H_2O_2$** | **$O_2^-$** | **NO•** | **Acidic pH** | **Membrane Stress** | **•OH** |
| *rbfA* | 2.86 | **21.01 (±166.8)** | 8.06 (±10.56) | **33.65 (±12.02)** | −82.54 (±58.02) | −15.16 (±34.11) | **97.41 (±2.85)** |
| *rfaC* | 3.45 | **97.14 (±1.12)** | 15.54 (±14.47) | 5.71 (±29.65) | −56.98 (±4.34) | 7.27 (±23.69) | −87.13 (±9.31) |
| *rfaD* | 2.89 | −67.18 (±93.64) | **31.37 (±13.92)** | **48.52 (±10.63)** | −37.98 (±29.32) | **49.3 (±10.15)** | **57.13 (±91.19)** |
| *rfaE* | 3.07 | −128.04 (±21.89) | 14.07 (±8.66) | **35.87 (±12.35)** | −72.34 (±50.57) | **25.47 (±17.14)** | **76.47 (±46.67)** |
| *rfaG* | 3.31 | −44.48 (±131.42) | **23.03 (±9.84)** | **36.55 (±16.5)** | −59.04 (±27.59) | −10.47 (±21.51) | **48.36 (±73.29)** |
| *rnt* | 3.16 | −149.17 (±62.64) | **40.77 (±20.82)** | **24.6 (±24.89)** | −56.45 (±93.29) | 16.47 (±2.83) | −101.47 (±14.6) |
| *rpe* | 6.17 | −219.05 (±39.01) | **58.63 (±12.95)** | **50.89 (±11.9)** | −41.58 (±59.99) | −8.78 (±26.48) | −77.51 (±25.54) |
| *sstT* | 5.27 | −210.03 (±204.21) | −24.06 (±20.82) | **26.66 (±17.35)** | −138.41 (±60.75) | −49.4 (±38.47) | −123.18 (±68.15) |
| *surA* | 3.89 | −65.17 (±154.66) | −20.62 (±33.54) | **32.45 (±24.58)** | −138.14 (±59.38) | 13.71 (±38.37) | **94.49 (±4.25)** |
| *thyA* | 4.33 | −136.19 (±42.18) | **60.58 (±30.63)** | **81.64 (±8.19)** | −29.87 (±27.49) | 1.01 (±33.81) | **47.66 (±62.09)** |
| *tolA* | 3.75 | −205.09 (±40.21) | **28.77 (±17.16)** | **28.96 (±36.67)** | −8.43 (±96.09) | 8.6 (±20.65) | **65.12 (±45.69)** |
| *tpiA* | 3.00 | −73.66 (±103.76) | **81.33 (±10.03)** | **64.24 (±10.77)** | −66.96 (±24.71) | −1.32 (±2.73) | **79.21 (±44.3)** |
| *truA* | 3.13 | −78.67 (±60.31) | **74.54 (±17.93)** | **33.11 (±16.65)** | −63.16 (±25.4) | 2.47 (±4.11) | **97.34 (±0.83)** |
| *ubiC* | 5.05 | −68.31 (±161.13) | **43.08 (±23.62)** | **20.37 (±25.65)** | −70.02 (±14.93) | −22.36 (±24.72) | **97.74 (±2.09)** |
| *umuD* | 4.35 | −21.3 (±68.99) | 72.87 (±16.18) | 50.65 (±10.61) | −3.18 (±27.29) | −26.02 (±26.69) | 66.74 (±69.81) |
| *ybaP* | 3.67 | −55.11 (±138.78) | **30.34 (±29.77)** | **24.66 (±9.9)** | −89.11 (±37.37) | −13.5 (±5.31) | **97.1 (±2.44)** |
| *yccM* | 4.04 | **62.93 (±70.19)** | **80 (±2.26)** | **31.49 (±14.63)** | −117.78 (±43.5) | −32.86 (±31.47) | **97.05 (±4.61)** |
| *ydcE* | 5.00 | −281.61 (±123.85) | **27 (±34.7)** | 3.93 (±36.09) | −99.98 (±50.99) | −48.81 (±35.15) | −66.91 (±160.6) |
| *ydcX* | 4.95 | −217.59 (±32.43) | −4.93 (±12.79) | −11.21 (±34.76) | −32.58 (±88.8) | −31.43 (±35.46) | −6.77 (±105.28) |
| *ydeU* | 3.93 | −156.77 (±78.48) | −10.67 (±21.77) | 7.5 (±20.75) | −99.88 (±51.27) | −41.07 (±37.79) | **77.3 (±43.22)** |
| *yegS* | 3.71 | **62.76 (±71.68)** | **45.29 (±24.26)** | **32.98 (±18.99)** | −112.6 (±89.9) | −15.79 (±28.14) | **77.42 (±43.28)** |
| *yfbB* | 4.18 | **70.57 (±52.43)** | 0.41 (±20.9) | 41.36 (±13.22) | −133.11 (±60.68) | −22.42 (±34.34) | **97.64 (±1.29)** |
| *yfeH* | 4.94 | −230.42 (±72.37) | −7.21 (±7.94) | −18.13 (±40.46) | −100.87 (±39.21) | −22.6 (±33.19) | **65.5 (±68.98)** |
| *yfgL* | 5.24 | −29.96 (±115.43) | **20.86 (±29.65)** | **35.42 (±13.97)** | −57.53 (±13.77) | −10.85 (±10.49) | **46.19 (±116.29)** |
| *ygfZ* | 2.50 | **21.51 (±164.65)** | −86.41 (±51) | −40.88 (±39.91) | −259.54 (±72.84) | −199.89 (±92.33) | −531.32 (±89.95) |
| *yheM* | 3.00 | −154.13 (±79.36) | 13.39 (±31.54) | **34.44 (±24.65)** | −92.84 (±48.09) | −3.96 (±31.28) | −41.73 (±141.74) |
| *yhhH* | 4.41 | −83.13 (±128.4) | **56.35 (±28.8)** | **33.97 (±19.35)** | −48.01 (±34.47) | **22.42 (±8.68)** | −117.43 (±18.78) |
| *yigL* | 4.28 | −165.97 (±138.93) | −1.23 (±57.34) | **27.78 (±10.29)** | −167.66 (±80.66) | −53.8 (±37.53) | **48.89 (±109.08)** |
| *yihE* | 4.58 | −21.93 (±113.08) | **75.01 (±12.93)** | **44.39 (±13.07)** | −38.37 (±58.47) | 8.52 (±3.91) | **44.24 (±109.43)** |
| *yjeK* | 3.68 | −48.06 (±133.73) | **26.68 (±37.56)** | **37.88 (±23.77)** | −81.49 (±23.54) | −3.65 (±36.66) | −130.9 (±19.59) |
| *yncA* | 3.84 | −146.47 (±72.89) | −28.03 (±33.87) | **23.27 (±16.8)** | −103.51 (±50.94) | −54.74 (±38.3) | **26.3 (±98.73)** |
| *ypjD* | 2.68 | −4.02 (±132.26) | 7.18 (±32.02) | **30.29 (±13.93)** | −87.37 (±39.37) | −43.1 (±29.95) | **23.16 (±118.13)** |

The mean and standard deviation for each stressor are provided in Table S1 in the Supplementary Materials.

### *3.2. Correlation Between aBL and Stressors*

Table 3 shows the ρ-Spearman correlation coefficient (due to the data distribution being different from the normal distribution) along with the result of the test verifying its significance. This coefficient was calculated between aBL and each stressor. Based on the results, the following can be summarized:

- There is a negative, statistically significant correlation between aBL and $H_2O_2$ ($\rho = -0.45$, $p < 0.001$).
- There is a negative, statistically significant correlation between aBL and membrane stress ($\rho = -0.31$, $p < 0.05$).

**Table 3.** The ρ-Spearman correlation coefficient between aBL and stressors. Statistically significant results for $\alpha = 0.05$ are bolded. * the *p*-value is less than **0.05** ($p < 0.05$), *** the *p*-value is less than **0.001** ($p < 0.001$).

| aBL | Single Stressors | Spearman's ρ | *p*-Value | *p*-Value Significance |
|---|---|---|---|---|
| aBL sensitivity | $H_2O_2$ | −0.450 | 0.0002 | *** |
| | Membrane stress | −0.310 | 0.0132 | * |
| | •OH | −0.230 | 0.0698 | |
| | NO• | 0.099 | 0.4380 | |
| | $O_2^-$ | 0.093 | 0.4630 | |
| | Acidic pH | 0.060 | 0.6380 | |

Correlograms are used to illustrate the correlation between aBL sensitivity and various stressors, including $H_2O_2$, $O_2^-$, NO•, acidic pH, membrane stress, and •OH. This visualization helps to assess how aBL sensitivity correlates with the growth defect of selected mutants induced by each stressor, if this is a positive or negative type of correlation. Such representations can facilitate the search for patterns and relationships, highlighting the interplay between the antimicrobial effects of aBL and single stressors. These insights are helpful in understanding the multifactorial effects of aBL and the potential mechanisms underlying microbial susceptibility under different stress conditions.

For other stressors, no significant correlation was observed.

Figure 2 presents correlation test results between aBL and stressors in the form of correlograms.

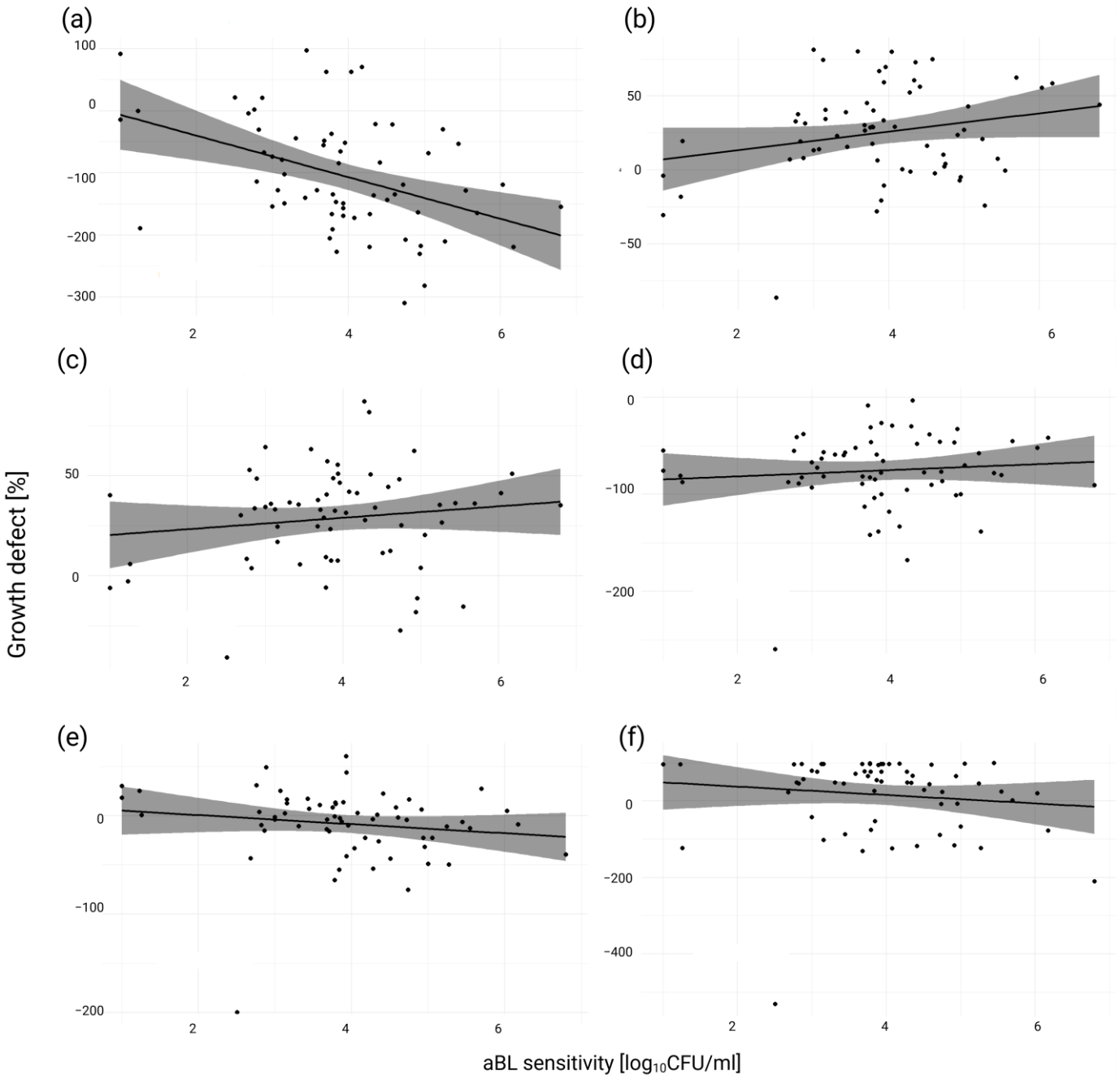


**Figure 2.** Correlograms illustrate the correlation between aBL and stressors: (**a**) $H_2O_2$, (**b**) $O_2^-$, (**c**) NO•, (**d**) Acidic pH, (**e**) membrane stress, and (**f**) •OH. The X-axis represents aBL sensitivity values [$\log_{10}$ CFU/mL], while the Y-axis growth defect [%] for each stressor.

### *3.3. Evaluation of the Probability That a Mutant That Is Sensitive to One Stressor Is Sensitive to Another Stressor*

In the next step, the conditional probability was calculated to check how the probability is distributed such that the mutant will be sensitive to stressor A, provided that it is also sensitive to stressor B. Results are presented in Table 4.

**Table 4.** The probability of sensitivity to stressor A subject to sensitivity to stressor B. The number of mutants sensitive to both selected stress factors is given in brackets.

| Stressor A | Stressor B | | | | | |
|---|---|---|---|---|---|---|
| | $H_2O_2$ | $O_2^-$ | NO• | Acidic pH | Membrane Stress | •OH |
| $H_2O_2$ | x | 0.98 (40) | 0.98 (46) | 0.94 (58) | 0.88 (23) | 0.93 (57) |
| $O_2^-$ | 0.67 (40) | x | 0.79 (37) | 0.63 (39) | 0.58 (15) | 0.66 (40) |
| NO• | 0.77 (46) | 0.9 (37) | x | 0.73 (45) | 0.69 (18) | 0.74 (45) |
| Acidic pH | 0.97 (58) | 0.95 (39) | 0.96 (45) | x | 0.96 (25) | 0.97 (59) |
| Membrane stress | 0.38 (23) | 0.37 (15) | 0.38 (18) | 0.4 (25) | x | 0.38 (23) |
| •OH | 0.95 (57) | 0.98 (40) | 0.96 (45) | 0.95 (59) | 0.88 (23) | x |

Based on the data obtained, the following can be observed:

- Mutants sensitive to $H_2O_2$ are also sensitive to acidic pH and •OH with more than 90% probability and to $O_2^-$ and NO• with more than 60% probability.
- Mutants sensitive to $O_2^-$ are also sensitive to $H_2O_2$, NO•, acidic pH, and •OH with more than 90% probability.
- NO• sensitive mutants are also sensitive to $H_2O_2$, acidic pH, and •OH with more than 90% probability and to $O_2^-$ with more than 75% probability.
- Mutants sensitive to acidic pH are sensitive to $H_2O_2$ and •OH with more than 90% probability, and to $O_2^-$ and NO• with more than 60% probability.
- Mutants sensitive to membrane stress are also sensitive to $H_2O_2$ with a probability of 0.88, to acidic pH and •OH with a probability greater than 80%, and to $O_2^-$ and NO• with a probability of more than 50%.
- Mutants sensitive to •OH are also sensitive to $H_2O_2$ and acidic pH with more than 90% probability and to $O_2^-$ and NO• with more than 65% probability.

Detailed analysis is presented in Supplementary Materials (Tables S2 and S3; Figures S1 and S2).

### *3.4. Cluster Analysis*

To group mutants into groups with a similar stressor sensitivity profile, cluster analysis was performed. Because the data table has six different columns, there was a need to reduce the data dimension before the actual analysis, i.e., create two such variables that will represent the six source columns. To achieve this, a Principal Component Analysis (PCA) was performed.

Before the PCA procedure began, the data were scaled so that their mean and standard deviation were 0 and 1, respectively. Because this analysis is very sensitive to outliers, the mutant *ygfZ* was removed from the analysis, whose values were significantly different from the rest. The data have also been centered around 0 to remove constants from the data that add nothing to the knowledge of data variation.

To select the number of dimensions, a landfill chart was made based on which such a selection can be made. This graph is shown in Figure 3.

In Figure 3, two dimensions (components) "explain" 60.6% of the variability.

Table 5 shows the factor loadings and the coefficient of determination (factor loading squared) for each component. Factor loads measure the correlation between a given component and a source variable, i.e., they represent the influence of individual variables on a given principal component. In the results of our analysis, factor loadings measure the variability of six stressors and show how strongly each stressor is connected with the given component. Factors loadings for particular stressors whose values are closer to 0 are more weakly correlated with the given components than values close to 1 and −1. The coefficient of determination $R^2$ shows the percentage of the variability of a given component that is explained by a given input variable.

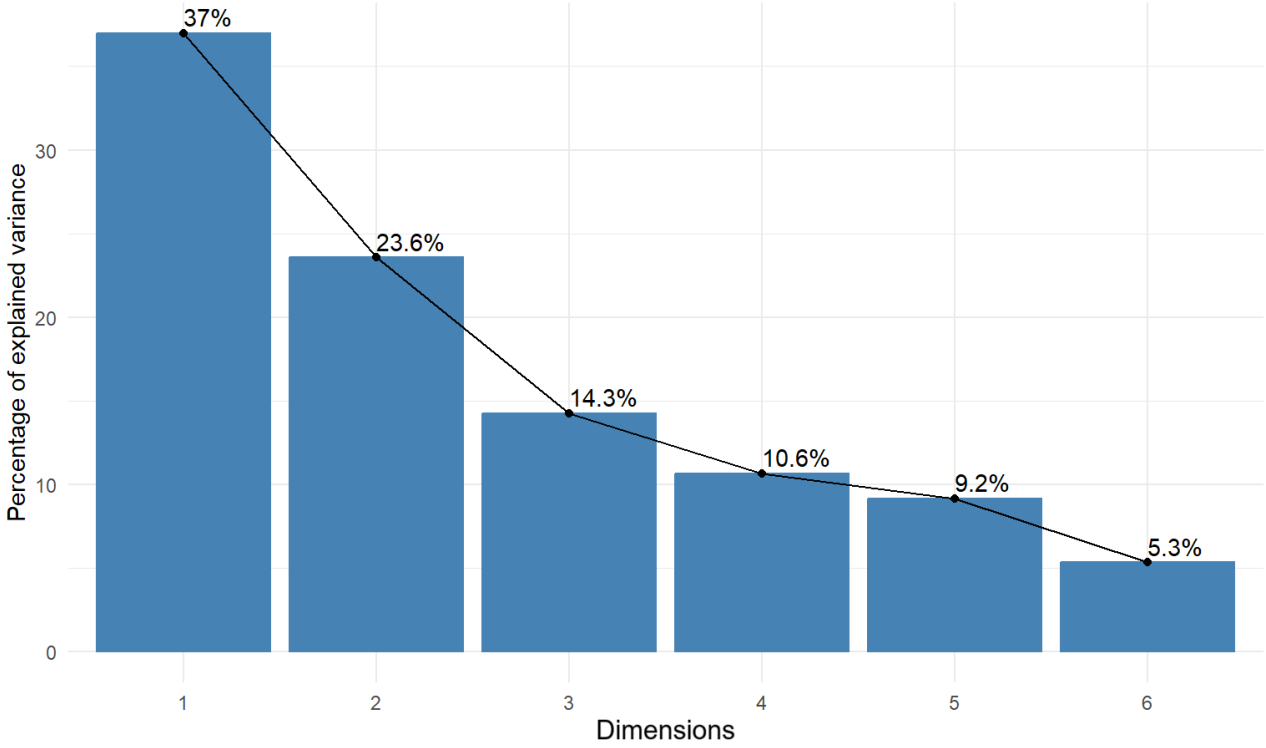


**Figure 3.** Scree plot. The X-axis shows the number of dimensions, while the Y-axis shows the percentage of variance explained by each dimension. The scree point is observed where variance starts to level off after the second dimension.

**Table 5.** Principal Component Analysis (PCA) analysis results. PC1 and PC2 represent the individual principal components independent from each other and capture the data's maximum variance. $R^2$ is the coefficient of determination.

| | PC1 | | PC2 | |
|---|---|---|---|---|
| **Stressor** | **Factor Loading** | **$R^2$** | **Factor Loading** | **$R^2$** |
| $H_2O_2$ | 0.15 | 0.02 | 0.66 | 0.44 |
| $O_2^-$ | 0.51 | 0.26 | −0.11 | 0.01 |
| NO• | 0.50 | 0.25 | −0.06 | 0.00 |
| Acidic pH | 0.50 | 0.25 | −0.23 | 0.05 |
| Membrane stress | 0.47 | 0.22 | 0.15 | 0.02 |
| •OH | 0.05 | 0.00 | 0.69 | 0.48 |

For further analysis, the first two components were considered, the first of which explains 37% of the variability of the output variables, and the second 23.6%, so, together, they explain more than 60% of the variability of the output data. All factor loadings for PC1 are positive, which means that, as PC1 increases, the stressor values will also increase. In the case of PC2, this will be the case for $H_2O_2$. For membrane stress and •OH, the opposite situation is true, i.e., as PC2 increases, the stressor values will decrease.

In the next step, cosine distances were calculated for the data from both main components, necessary for further analysis.

The first of such analyses is the creation of a distance map, in which each pair of mutants is assigned a color according to their previously calculated distance. In this way, it is possible to initially draw attention to potential groups of similar mutants. Because a given map is symmetrical along the diagonal, one of them is paid attention to when interpreting. The cosine distance heatmap is presented in Figure 4.

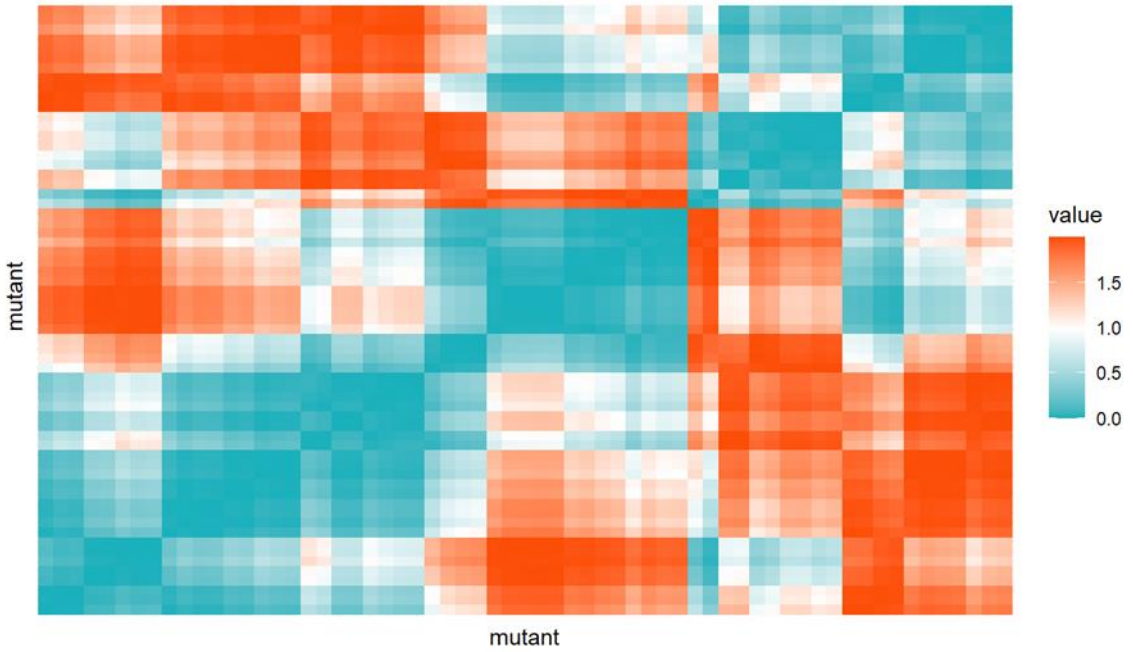


**Figure 4.** Cosine distances heatmap: On the X-axis, mutants are listed from left to right in order: *tolA*, *pfkA*, *yhhH*, *narL*, *rpe*, *metR*, *deoB*, *rnt*, *oxyR*, *nuoN*, *cydD*, *holD*, *atpC*, *thyA*, *dacA*, *pgi*, *pgm*, *atpG*, *truA*, *phoQ*, *umuD*, *gmhB*, *rfaD*, *tpiA*, *yihE*, *rfaE*, *rfaG*, *atpE*, *yfgL*, *ybaP*, *atpB*, *atpH*, *dnaJ*, *yfbB*, *priA*, *rbfA*, *ubiC*, *yegS*, *atpF*, *rfaC*, *cpxA*, *yccM*, *ppc*, *yjeK*, *pyrE*, *sstT*, *dnaK*, *yheM*, *ecnB*, *ydcX*, *atpD*, *ydcE*, *atpA*, ypjD, *fabH*, *surA*, *purA*, *fimB*, *ydeU*, *yigL*, *gntK*, *yfeH*, *yncA*. The Y-axis mutants are presented in the opposite order than on the X-axis.

In the next step, the clustering method was selected. The k-means++ method was chosen, so the appropriate number of clusters must be selected in advance. One method is to select the number of clusters based on the WSS (Within-Cluster Sum of Squares) ratio (Figure 5).

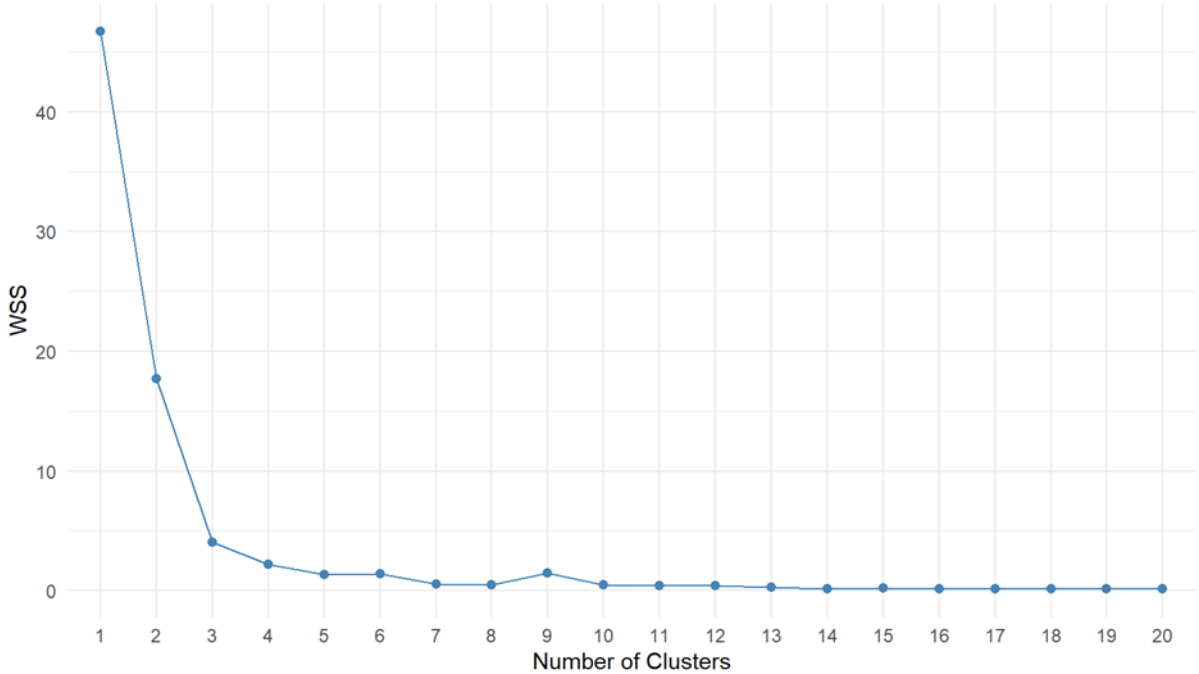


**Figure 5.** The WSS plot for determining the number of clusters. WSS—Within-Cluster Sum of Squares. The number of 3 clusters was chosen as the optimal value.

The optimal number of clusters is the one at which the WSS value does not increase significantly after increasing the number of clusters. In this case, looking at Figure 5, we conjectured that the optimal number of clusters is equal to three. To verify this, another measure—the Silhouette statistic—was used, which measures how well each of the observations fits into the cluster assigned to it. A value close to one means that the observation is placed very close to the center of the cluster, and a statistic close to zero means that the observation lies on the border of two clusters. Negative values indicate that the value is potentially matched to the wrong cluster.

The silhouette plot (Figure 6) confirmed that the optimal number of clusters is equal to three. Based on the above, the division of the data into three clusters was chosen. Figure 7 shows the final division of data into three clusters using the k-means++ algorithm.

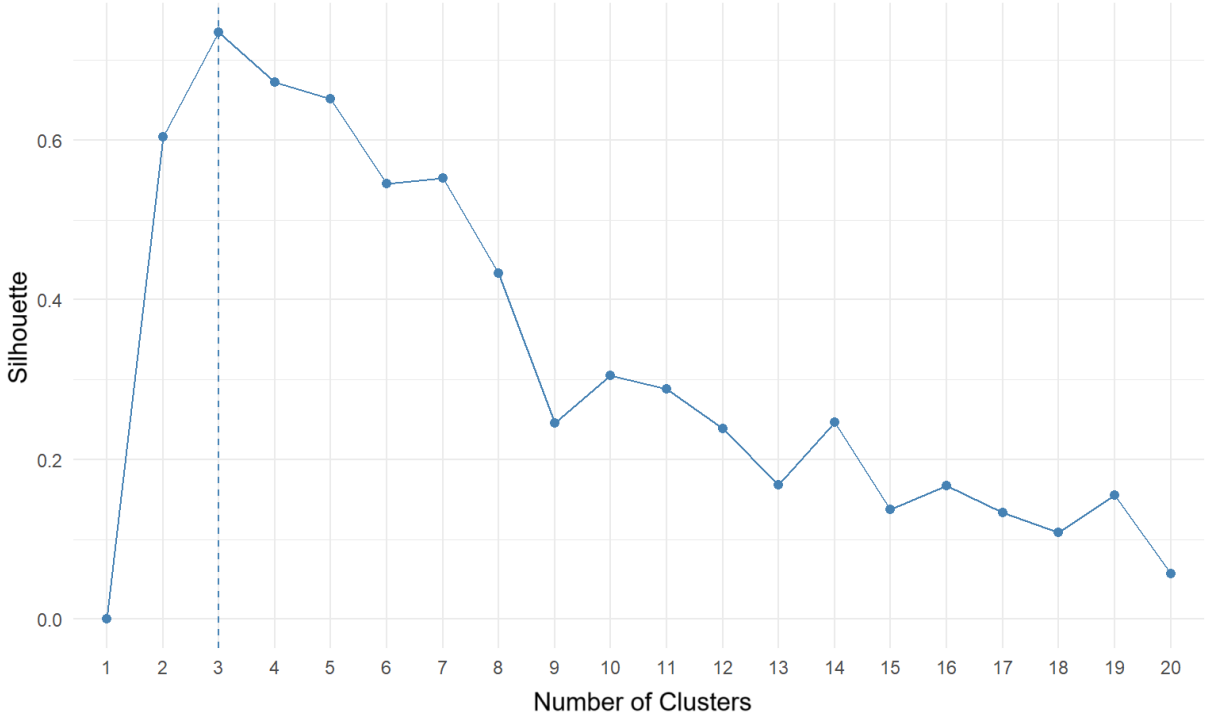


**Figure 6.** Silhouette plot for determining the number of clusters. The Y-axis shows the silhouette score for each cluster shown on the X-axis.

Based on the statistical analysis, mutants were grouped into three clusters, and their characteristics are presented below. Figure 8 shows the silhouette stat values for each point (mutant). The horizontal red line is at the height of the average value of the statistic for the entire set.

The value for the mutant *yjeK* is below 0. Such a value can be interpreted as a potentially incorrectly assigned value, but it is worth remembering that this criterion refers to the distance of a given point from the center of the cluster (marked with a slightly larger point than the others).

The list of mutants assigned to one of three clusters is summarized in Table 6. The genes assigned to cluster 1 are involved in the key cellular processes such as energy metabolism and core cellular processes (*atpC*, *atpG*, *nuoN*, *pfkA*, *pgi*, *pgm*, *rpe*, *tpiA*, *deoB*), oxidative stress response and adaptation (*oxyR*), regulation and adaptation (*phoQ*, *metR*), membrane integrity and structure (*tolA*, *rfaD*), DNA replication and repair (*thyA*, *umuD*), and translation (*truA*, *rnt*). The genes assigned to cluster 2 are involved in processes such as energy generation (*atpA*, *atpB*, *atpE*, *atpF*, *atpH*), stress response and environmental adaptation (*cpxA*, *dnaJ*), and fatty acid biosynthesis (*fabH)*. Cluster 3 comprises genes

involved in stress response (*dnaK*, *ecnB*), metabolism (*gntK*, *ppc*, *purA*, *sstT)*, and DNA repair and genome stability (*ydcE*, *ydcX*, and *pyrE*) under conditions of stress or damage.

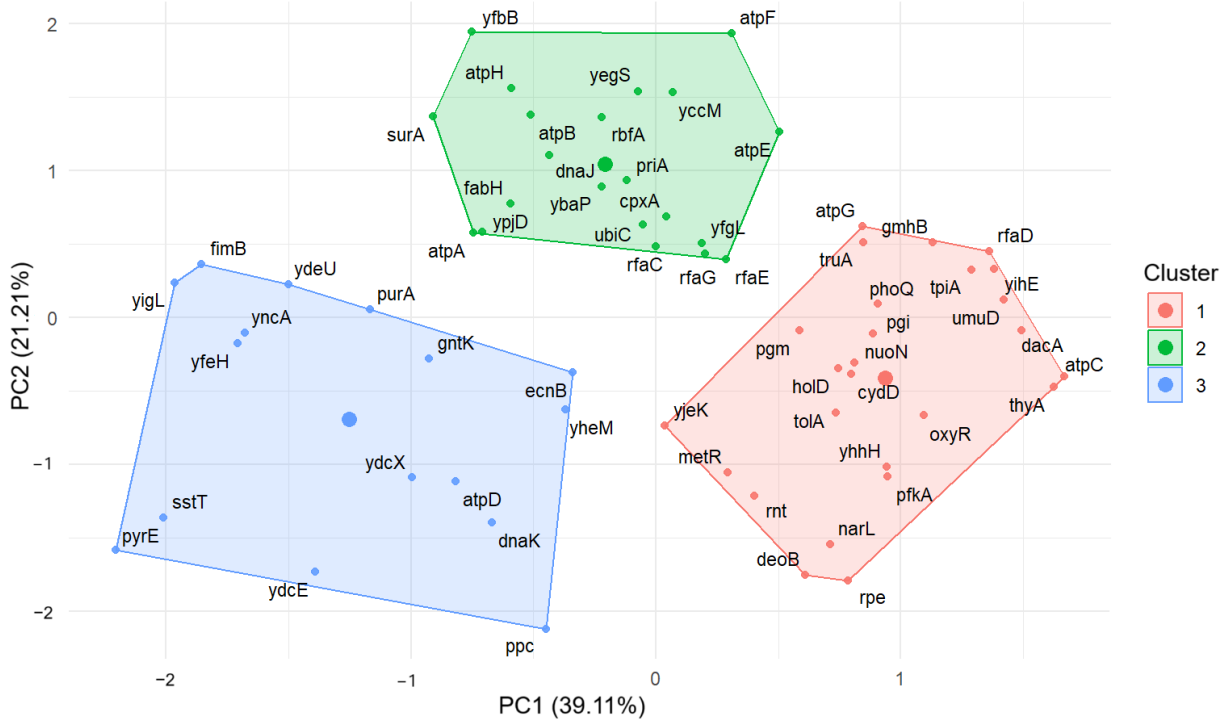


**Figure 7.** Results of k-means++ algorithm for both principal components (PC1—X-axis and PC2—Y-axis) summarizing clustering analysis. Bolded dots in the center of each cluster represent their centroids placed at the longest distance from other clusters.

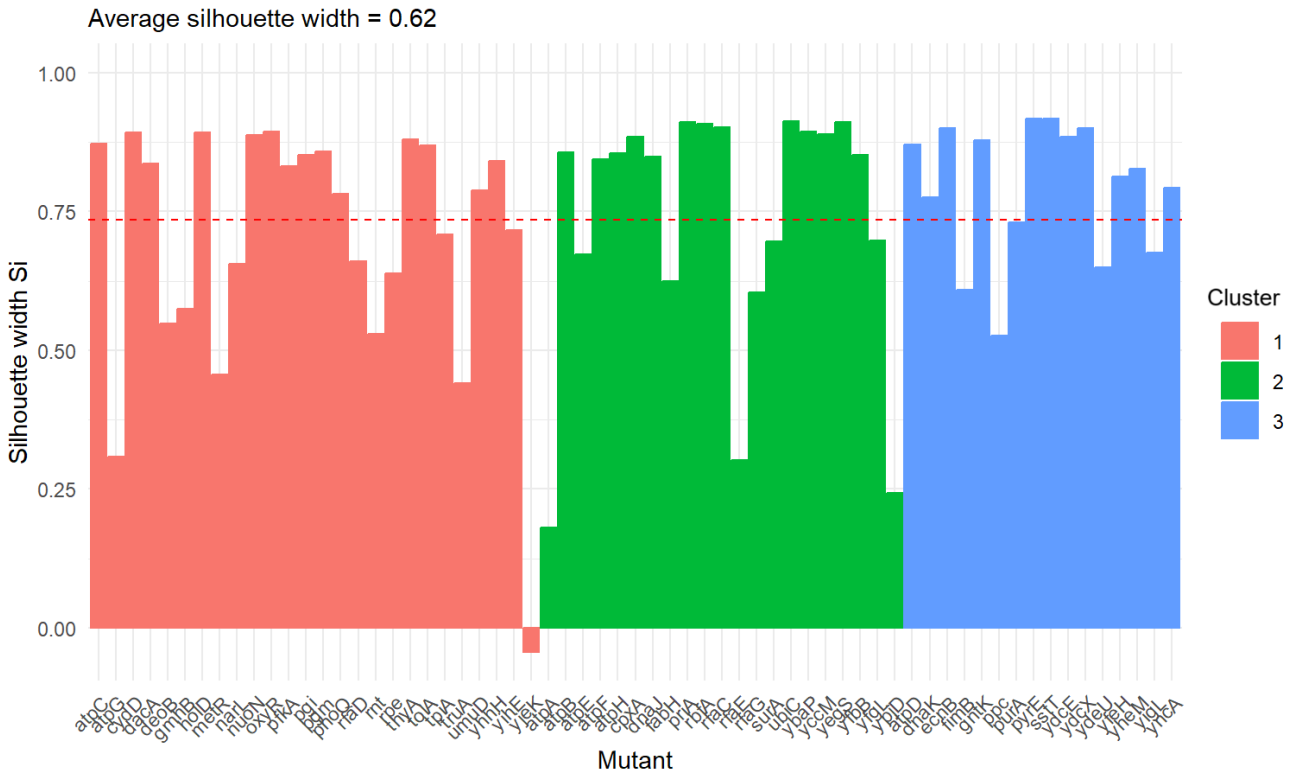


**Figure 8.** Cluster silhouette plot representing the silhouette width for each mutant in every cluster. The red line indicates the average value for the entire set.

Table 7 provides information about the median and interquartile range of growth defects for each cluster and each stressor. Univariate tests were also performed comparing these medians between each pair of clusters. To perform this, the Mann–Whitney U test was performed, which checks the statistical significance between the two medians (the median comparison test was chosen due to the lack of normality of the data distribution). As multiple comparisons were made, a *p*-value adjustment (FDR) was applied.

Data from Table 7 are also presented in Figure 9 and Figures S3 and S4 in Supplementary Materials.

The analysis results demonstrated several key findings:

- When exposed to an acidic pH, the median growth defect for all mutants across the clusters was less than 0. However, the first cluster exhibited the highest median growth defect at −46.39 [−59.36; −38.08], which was statistically significantly higher than that of the other clusters. The medians of the second and third clusters did not differ significantly from each other, with values of −81.65 [−89.11; −70.02] for cluster 2 and −91.61 [−101.53; −83.61] for cluster 3.
- In the presence of $H_2O_2$, the median growth defect remained less than 0 in all clusters, with statistically significant differences observed between each pair of clusters. The second cluster showed the largest growth defect, at −177.62 [−219.96; −154.38], while the first cluster exhibited the smallest defect at −29.96 [−55.11; −21.01].
- When exposed to membrane stress, the median growth defect for the first cluster was positive (5.67 [−3.02, 15.68]), but it was not statistically significantly different from the second cluster, which had a median of −6.38 [−15.16, 13.71]. The third cluster, however, showed a statistically significantly smaller median defect (−40.22 [−50.5; −10.42]) compared to the other two clusters.
- Upon exposure to nitric oxide (NO•), the median growth defect for all clusters was greater than 0, with significant differences between each pair of clusters. The first cluster exhibited the largest growth defect (48.35 [38.55; 54.74]), whereas the second cluster had the smallest (30.29 [8.39; 35.42]).
- In response to $O_2-$, the median growth defect was greater than 0 for all clusters. The first cluster showed the largest and most statistically significantly different median (53.98 [31.89; 65.82]), while the medians for the second and third clusters were not significantly different from each other.
- Lastly, when mutants were exposed to hydroxyl radicals (•OH), the median growth defect was again greater than 0 across all clusters. The second cluster exhibited the largest median defect (95.89 [76.47; 97.31]), which was statistically significantly different from the other two clusters, whose medians were not significantly different from each other.

**Table 6.** The list of deleted genes in single-gene mutants of *E. coli* assigned to individual clusters.

| Cluster 1 | Cluster 2 | Cluster 3 |
|---|---|---|
| *atpC* | *atpA* | *atpD* |
| *atpG* | *atpB* | *dnaK* |
| *cydD* | *atpE* | *ecnB* |
| *dacA* | *atpF* | *fimB* |
| *deoB* | *atpH* | *gntK* |
| *gmhB* | *cpxA* | *ppc* |
| *holD* | *dnaJ* | *purA* |
| *metR* | *fabH* | *pyrE* |
| *narL* | *priA* | *sstT* |
| *nuoN* | *rbfA* | *ydcE* |
| *oxyR* | *rfaC* | *ydcX* |
| *pfkA* | *rfaE* | *ydeU* |
| *pgi* | *rfaG* | *yfeH* |
| *pgm* | *surA* | *yheM* |

**Table 6.** *Cont.*

| Cluster 1 | Cluster 2 | Cluster 3 |
|---|---|---|
| *phoQ* | *ubiC* | *yigL* |
| *rfaD* | *ybaP* | *yncA* |
| *rnt* | *yccM* | |
| *rpe* | *yegS* | |
| *thyA* | *yfbB* | |
| *tolA* | *yfgL* | |
| *tpiA* | *ypjD* | |
| *truA* | | |
| *umuD* | | |
| *yhhH* | | |
| *yihE* | | |
| *yjeK* | | |

**Table 7.** Median and interquartile range and the result of one-dimensional tests comparing these medians between each pair of clusters. [1] U Mann–Whitney Test with FDR correction. * the *p*-value is less than **0.05** ($p < 0.05$), ** the *p*-value is less than **0.01** ($p < 0.01$), *** the *p*-value is less than **0.001** ($p < 0.001$), **** the *p*-value is less than **0.0001** ($p < 0.0001$), ns not statistically significant.

| | Group 1 | | Group 2 | | | |
|---|---|---|---|---|---|---|
| **Stressor** | **Cluster** | **Median (IQR)** | **Cluster** | **Median (IQR)** | ***p*-Value[1]** | ***p*-Value Significance [1]** |
| $H_2O_2$ | 1 | −131.16 (−164.15, −79.79) | 2 | −29.96 (−55.11, 21.01) | 0.0000 | **** |
| | 1 | −131.16 (−164.15, −79.79) | 3 | −177.62 (−219.96, −154.38) | 0.0006 | *** |
| | 2 | −29.96 (−55.11, 21.01) | 3 | −177.62 (−219.96, −154.38) | 0.0000 | **** |
| Membrane stress | 1 | 5.67 (−3.02, 15.68) | 2 | −6.38 (−15.16, 13.71) | 0.0740 | ns |
| | 1 | 5.67 (−3.02, 15.68) | 3 | −40.22 (−50.5, −10.42) | 0.0000 | **** |
| | 2 | −6.38 (−15.16, 13.71) | 3 | −40.22 (−50.5, −10.42) | 0.0020 | ** |
| NO• | 1 | 48.35 (38.55, 54.74) | 2 | 30.29 (8.39, 35.42) | 0.0000 | **** |
| | 1 | 48.35 (38.55, 54.74) | 3 | 8.47 (0.15, 25.61) | 0.0000 | **** |
| | 2 | 30.29 (8.39, 35.42) | 3 | 8.47 (0.15, 25.61) | 0.0370 | * |
| $O_2^-$ | 1 | 53.98 (31.89, 65.82) | 2 | 15.54 (0.41, 30.34) | 0.0000 | **** |
| | 1 | 53.98 (31.89, 65.82) | 3 | 3.18 (−5.5, 16.67) | 0.0000 | **** |
| | 2 | 15.54 (0.41, 30.34) | 3 | 3.18 (−5.5, 16.67) | 0.1080 | ns |
| •OH | 1 | 48.22 (−76.88, 70.33) | 2 | 95.89 (76.47, 97.31) | 0.0006 | *** |
| | 1 | 48.22 (−76.88, 70.33) | 3 | 8.59 (−56.05, 34.11) | 0.2420 | ns |
| | 2 | 95.89 (76.47, 97.31) | 3 | 8.59 (−56.05, 34.11) | 0.0002 | *** |
| Acidic pH | 1 | −46.39 (−59.36, −38.08) | 2 | −81.65 (−89.11, −70.02) | 0.0000 | **** |
| | 1 | −46.39 (−59.36, −38.08) | 3 | −91.61 (−101.53, −83.61) | 0.0000 | **** |
| | 2 | −81.65 (−89.11, −70.02) | 3 | −91.61 (−101.53, −83.61) | 0.0630 | ns |

Protein–protein functional interaction networks and gene co-expression analysis performed with the STRING database (https://string-db.org, accessed on 28 October 2024) revealed that many genes within one cluster are related in some way (e.g., protein–protein interactions, gene neighborhood, gene fusions, gene co-occurrence, co-expression, protein homology). The data obtained from the STRING database are presented in Figure 10.

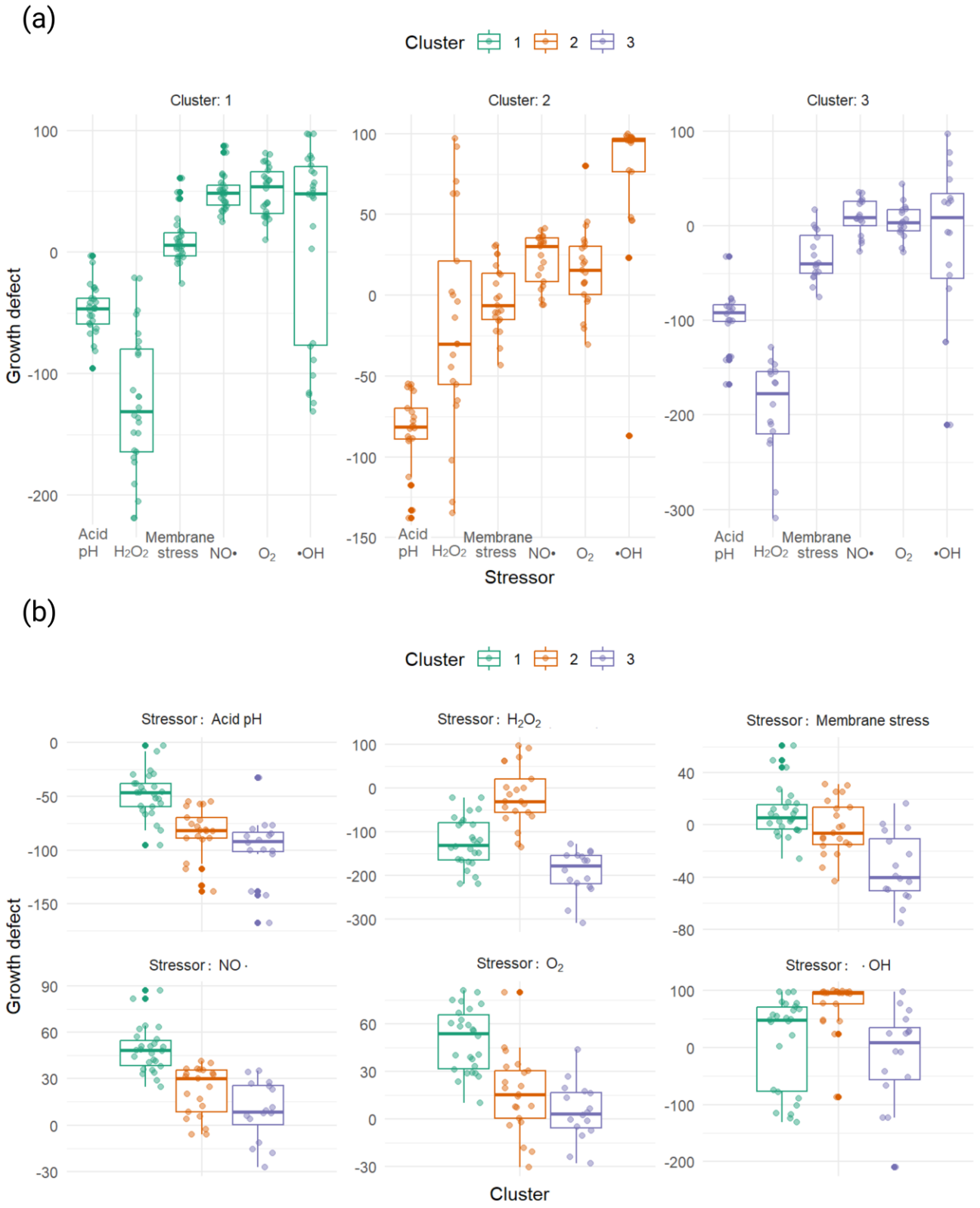


**Figure 9.** Growth defects of mutants by clusters: (**a**) characterization of growth defect profiles for 3 clusters; and (**b**) characterization of cluster profiles for each stressor.

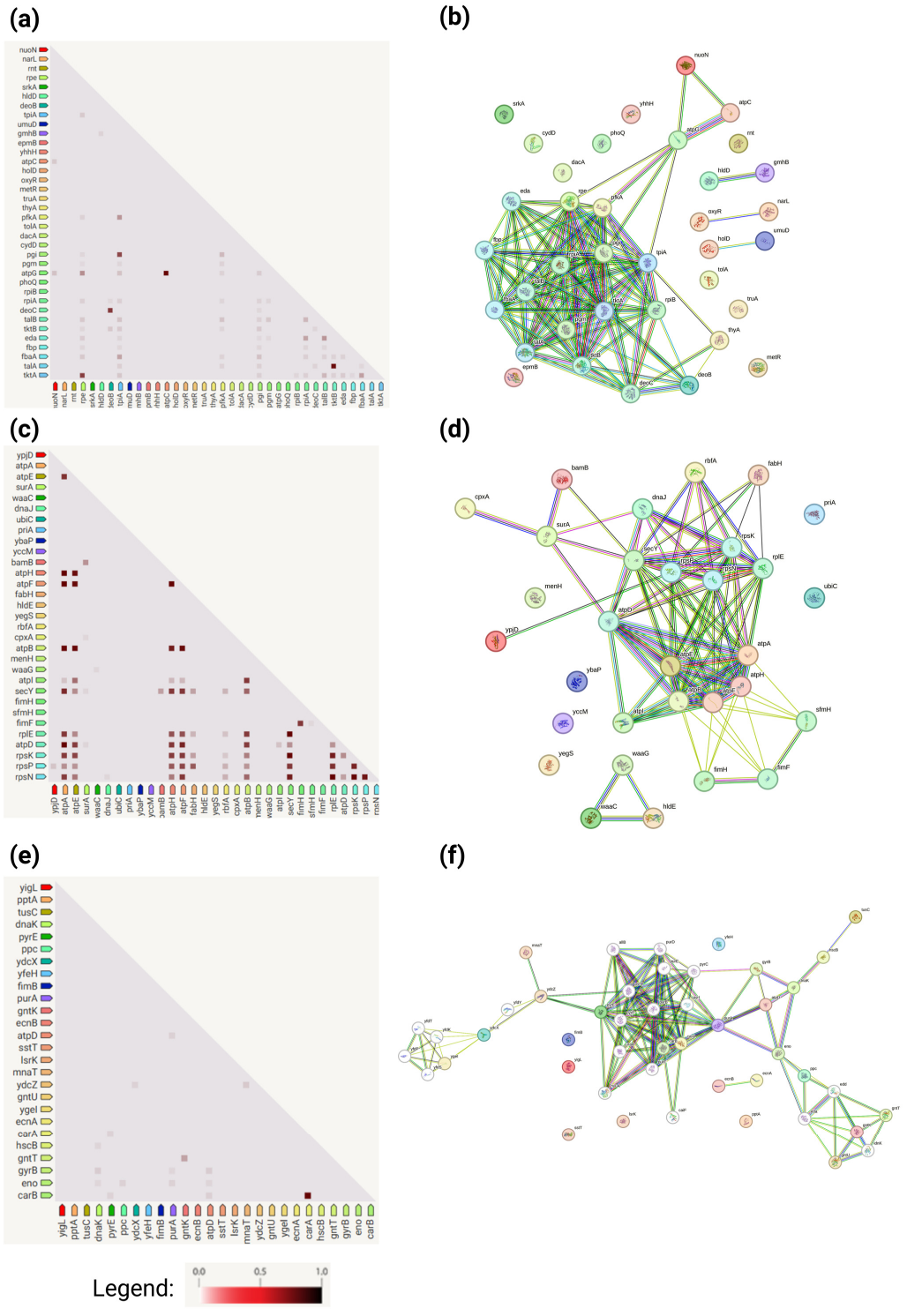


**Figure 10.** Protein–protein functional interaction networks and gene co-expression. Protein–protein functional interaction networks of the proteins are divided into 3 clusters: (**a**) Gene co-expression within cluster 1; (**b**) protein–protein functional interaction networks within cluster 1; (**c**) gene co-expression within cluster 2; (**d**) protein–protein functional interaction networks within cluster 2; (**e**) gene co-expression within cluster 3; (**f**) protein–protein functional interaction networks within cluster 3. The analysis was performed with the STRING database (https://string-db.org). The colors of the lines denote the following: light blue, interactions known from curated databases; pink, interactions experimentally determined; bright green, predicted reaction (gene neighborhood); red, gene fusions; dark blue, gene co-occurrence; green, textmining; black, co-expression; and blue, protein homology.

## 4. Discussion

Bacterial populations exhibit a remarkable ability to adapt to extreme environmental fluctuations. In some cases, adaptation to one stressful condition confers a fitness advantage when cells encounter a second stressor, a phenomenon referred to as cross-stress protection [13]. aBL has a multi-target mode of action, which is a key factor contributing to its efficacy against a wide range of microorganisms [8]. Unlike traditional antibiotics that often target one specific metabolic pathway or cellular component, aBL is based on generating ROS that simultaneously affect multiple cellular targets [7,14]. These ROS, including singlet oxygen ($^1O_2$) [7,15], superoxide anions ($O_2-$) [5], hydroxyl radicals (•OH) [7], and hydrogen peroxide ($H_2O_2$) [5,6], are produced within the microbial cells during exposure to aBL and cause widespread oxidative damage [7]. This study aimed to assess the sensitivity of single-gene deletion mutants of *E. coli* BW25113 to individual stressors generated by aBL to elucidate the protective role of each gene associated with aBL hypersensitivity. A total of 64 aBL-sensitive mutants that had been identified in our previous study [11] were tested under conditions that simulated the specific, single stress factors produced by aBL. The hypersensitivity of the mutants to individual aBL-related stressors was evaluated by measuring their growth defects, in comparison to the wild-type strain. By isolating and assessing the effects of single stressors, we aimed to dissect the complex interplay between these reactive molecules and better understand their individual roles in microbial inactivation. Studying single stressors, such as $H_2O_2$, with selected mutants provides a clearer picture of how bacteria respond to targeted oxidative stress. This study also clarifies that the combination of stressors generated by aBL is often more effective than any single factor alone. Furthermore, understanding how different mutants respond differently to individual stressors compared to aBL as a whole may reveal vulnerabilities in microbial defense mechanisms that could be exploited in the clinical settings in the future.

Hydrogen peroxide is a widely used antimicrobial agent that generates ROS directly upon application [16–18]. When $H_2O_2$ comes in contact with microbial cells, it can be broken down into hydroxyl radicals and other ROS via Fenton reactions or catalase activity [19]. These ROS attack cellular structures, including DNA [20]. While both aBL and $H_2O_2$ generate ROS, aBL relies on the internal activation of chromophores within the microorganisms [21], whereas $H_2O_2$ is an external oxidative agent that can penetrate and damage cells on contact. aBL has the advantage of being non-toxic to mammalian tissues [22], avoiding the issues of toxicity associated with $H_2O_2$ [23].

The superoxide anion ($O_2-$) is highly reactive and toxic to microbial cells. Once generated, it can initiate a cascade of oxidative reactions that damage essential cellular components, such as lipid peroxidation, DNA and protein damage, and the disruption of cellular enzymes [24,25]. It can also lead to secondary ROS production: $O_2-$ can be converted into other ROS, such as $H_2O_2$ and •OH, through enzymatic or non-enzymatic dismutation reactions. For instance, superoxide dismutase (SOD) in microbial cells can convert $O_2-$ into $H_2O_2$ [26,27].

The highly reactive hydroxyl radicals (•OH) can be generated through the Fenton reaction, where hydrogen peroxide ($H_2O_2$) reacts with transition metals like iron ($Fe^{2+}$). This process converts $H_2O_2$ into hydroxyl radicals [28]:

$$H_2O_2 + Fe^{2+} \rightarrow Fe^{3+} + \bullet OH + OH-.$$

Hydroxyl radicals (•OH) are one of the most destructive forms of ROS that cause extensive damage to essential microbial cellular components [29]. Because hydroxyl radicals react almost immediately with any biological molecule they encounter, their antimicrobial effect is rapid and highly destructive [25]. The non-specific nature of •OH means that it can attack a wide variety of targets within microbial cells, making it a critical player in the cell-killing process. It is assumed that these radicals (along with singlet oxygen) have a broad spectrum of antimicrobial activity of aBL [7,30].

Nitric oxide (NO•) is a type of reactive nitrogen species (RNS) known for its antimicrobial properties. NO• production is often associated with immune responses in mammalian cells [31]. It is not typically produced as a primary reactive species during aBL irradiation; however, combining aBL with nitric oxide donors could provide a synergistic antimicrobial effect [32,33]. The combination of NO• and ROS from aBL could enhance oxidative and nitrosative stress in microbes. Moreover, Liebmann et al. (2010) showed that blue light up to a wavelength of 453 nm is capable of releasing nitric oxide from nitrosated proteins and that NO• can initiate cell differentiation in human skin [34].

The pH of the environment can play a significant role in the effectiveness of aBL, especially if the environment is acidic [35]. Acidic pH could promote the accumulation of intracellular ROS [36]. In clinical applications, understanding the pH of the infection site can increase the treatment effectiveness [37–39]. For example, infections associated with the elevated alkaline milieu, such as chronic wounds [40], may require adjustments of aBL protocols to maximize efficiency.

In our study, we also mimicked the membrane stress, because aBL induces significant membrane stress, due to lipid peroxidation, which disrupts the bacterial cell membrane, increasing permeability and compromising cellular integrity [4].

Similar studies have been conducted in the context of plasma by Krewing et al. (2019). The researchers exposed mutant strains of E. coli to stressors mimicking plasma species, such as $H_2O_2$, $O_2-$ and NO•, to analyze growth defects in the single-gene mutants. The results revealed that $H_2O_2$, $O_2-$, and NO• showed the highest severity scores, suggesting that the absence of the protective genes makes the cells particularly vulnerable to plasma exposure [12].

This research presents that (excluding singlet oxygen, which was not studied here) the most significant single stressor in the bacterial response to aBL could be •OH and $O_2$ because the highest number of aBL-hypersensitive mutants (45) treated with these stressors has a defect of growth greater than 20% compared to the wild-type strain (Table 7). The next stressors that affected mutant growth the most were NO• (36), membrane stress (9), and $H_2O_2$ (7). No mutant's growth was affected by acidic pH, which may indicate that acidic pH, when applied as a single stressor, does not significantly affect the growth of E. coli mutants; however, it is known that acidic pH plays a role in the bacterial response to aBL [35]. While acidic pH alone is not enough to cause growth inhibition, it could sensitize the bacteria to oxidative stress from ROS induced during aBL exposure.

The observed discrepancies in sensitivity between stressor A and stressor B (and vice versa) (Table 4) may be caused by both the substitution of data into the conditional probability formula and also by the different biological effects induced by different stressors.

Mathematically, the formula $P(A \mid B) = P(A \cap B)/P(B)$ inherently depends on the distribution of sensitive mutants in the data set. For example, if the mutants sensitive to stressor B constitute a smaller subset, the probability P(B) in the denominator decreases the overall conditional probability. Conversely, if a larger number of mutants are sensitive to stressor A, this increases the numerator ($P(A \cap B)$), leading to higher probabilities in one direction compared to the other. Biologically, differences in the reactivity and mechanisms of action of the stressors also play a significant role. For example, $H_2O_2$ and $O_2^-$ differ in their redox potential and target specificity within the cell, which may lead to varying degrees of overlap in sensitivity between mutants. Moreover, these two ROS forms activate different oxidative stress response pathways in bacteria cells [41]. Mutants that are sensitive to $H_2O_2$ may exhibit cross-sensitivity to $O_2^-$, but the inverse may not hold true due to differences in their cellular pathways and stress responses.

Mutants sensitive to four stressors were as follows: *atpC*, *gmhB*, *rfaD*, and *yccM*. *atpC* encodes a subunit of the ATP synthase complex. ATP synthase plays a crucial role in cellular energy metabolism, particularly when energy production is challenged. For instance, a rapid increase in ATP could be observed after DNA damage [42]. It is probable that, when cells face oxidative stress, they require efficient ATP production to activate stress-response mechanisms and repair oxidative damage. Defects in ATP synthase function can impair

the ability of *E. coli* to cope with oxidative stress. *gmhB* and *rfaD* are genes involved in the lipopolysaccharide (LPS) biosynthesis pathway. Mutations in LPS biosynthesis genes could increase membrane permeability, making cells more vulnerable to environmental stresses (such as oxidative stress). A study conducted by Seregina et al. (2022) revealed that the inactivation of *gmhB* and *rfaD* led to dramatic changes in the redox status of cells [43]. Disruptions in LPS assembly, like those caused by *gmhB* and *rfaD* mutations, can lead to heightened sensitivity to ROS and other stressors. Mutants unaffected by any stressors were *atpD* and *ydcX* probably because they respond only to the combination of stressors, or the growth defect can be caused by other aBL-generated stressors (for example, singlet oxygen not tested in this study).

Because no positive correlation between aBL and single stressors was found, we can conclude that the bactericidal role of aBL is a sum of the combination of stressors, not an effect of the single one. aBL produces a variety of ROS ($^1O_2$, $O_2-$, •OH, $H_2O_2$) [7,44]. These ROS act together to cause oxidative stress and damage to microbial cells [45–47]. By treating bacterial cells with $H_2O_2$ or other single stressors alone, we could not observe additive or synergistic effects of these other ROS: the different types of ROS generated by aBL can interact with each other. For instance, superoxide anion ($O_2-$) and $H_2O_2$ are relatively non-toxic per se but, via the Fenton reaction, they lead to hydroxyl radical (•OH) production, which is much more reactive and damaging [19,46,48]. By using only $H_2O_2$, perhaps not enough (if any) of the other important ROS were generated, which may explain the lack of positive correlation. What is no less important, during aBL, ROS are generated within the microbial cells, often near sensitive cellular components like the membranes, organelles, nucleic acids, or enzymes [19,47,49]. In contrast, adding $H_2O_2$ externally might not replicate this localized effect. $H_2O_2$ itself in an aqueous solution does not oxidatively modify DNA, lipids, or proteins in the absence of catalysts for radical formation [50,51]. $H_2O_2$ diffuses freely, and its action is more generalized, leading to less specific damage [52] compared to ROS released during aBL.

A selection of the optimal concentration of $H_2O_2$ was also complicated during this study. Too low a concentration may not cause significant oxidative damage, while too high a concentration could trigger bacterial defense mechanisms (e.g., catalase or peroxidase activity), reducing its impact [52]. Probably, aBL generates smaller, controlled amounts of $H_2O_2$ along with other ROS, potentially allowing for more sustained damage without triggering strong defense responses. aBL might overwhelm microbial defenses by generating ROS in bursts during irradiation, whereas $H_2O_2$ application as a single stressor might allow bacteria more time to respond and detoxify the environment [53–55]. When exposed to $H_2O_2$ alone, bacterial cells may upregulate protective enzymes more effectively compared to exposure to aBL. As a result, cells may be better armed to cope with $H_2O_2$ as a single stressor than with the mixed ROS profile generated by aBL. Moreover, $H_2O_2$ is less reactive compared to other ROS: $H_2O_2$ is relatively more stable than other ROS like singlet oxygen or hydroxyl radicals [19,46]. Therefore, when used as a single stressor, its impact might be weaker or slower. Singlet oxygen ($^1O_2$) and hydroxyl radicals (•OH) are much more reactive and can cause more immediate and severe damage to microbial components [56,57], which $H_2O_2$ alone probably cannot mimic.

Based on the results, the division of the data into three clusters was chosen. The key functional and biological significance across the clusters was summarized in the table below (Table 8).

Cluster 1 focuses on central metabolism and oxidative stress, integrating glycolysis, LPS biosynthesis, ROS protection, and nitrogen metabolism. It is also connected with significantly higher sensitivity to $O_2^-$ and NO• of this cluster in comparison to cluster 2 and 3.

Cluster 2 is strongly tied to energy generation needed for the activity of detoxification enzymes, membrane integrity, and adaptation to environmental stress. Mutants in this cluster are significantly more sensitive to $H_2O_2$ and •OH stressors in comparison to mutants from other clusters.

**Table 8.** Key functional and biological significance across the clusters.

| Cluster | Gene(s) | Function | Associated Pathway | Biological Significance |
|---|---|---|---|---|
| 1 | *atpC*, *atpG*, *nuoN* | ATP synthesis via oxidative phosphorylation | Energy metabolism | Key for ATP production and cellular energy homeostasis. |
| | *pfkA*, *pgi*, *pgm*, *rpe*, *tpiA* | Glycolysis, pentose phosphate pathway | Carbohydrate metabolism | Critical for energy production and biosynthetic precursors. |
| | *oxyR*, *narL*, *cydD* | Oxidative stress response | ROS detoxification, nitrogen metabolism | Protects cells under oxidative or nitrogen stress. |
| | *phoQ*, *metR* | Cellular adaptation, stress response | Phosphate and methionine regulation | Adaptation to nutrient limitations and environmental stress. |
| 2 | *tolA*, *rfaD* | Membrane integrity, LPS synthesis | Membrane structure and protection | Essential for outer membrane stability and function. |
| | *atpA*, *atpB*, *atpE*, *atpF*, *atpH* | F1Fo ATP synthase complex | Energy metabolism | Core to ATP generation and proton gradient maintenance. |
| | *cpxA* | Sensor for membrane stress | Two-component regulatory system | Activates stress response to misfolded membrane proteins. |
| | *dnaJ* | Molecular chaperone | Heat shock response | Repairs misfolded proteins and supports thermal adaptation. |
| | *fabH* | Fatty acid biosynthesis | Lipid metabolism | Initiates synthesis of membrane lipids, vital for adaptation. |
| 3 | *dnaK*, *fimB* | Protein folding, repair, adhesion regulation | Heat shock response, fimbriae assembly | Facilitates adaptation to stress and host interactions. |
| | *atpD*, *gntK*, *ppc* | Energy metabolism and intermediary pathways | Glycolysis, TCA cycle | Supports energy generation and carbon flux management. |
| | *purA*, *pyrE* | Nucleotide biosynthesis | Purine and pyrimidine metabolism | Provides precursors for DNA, RNA synthesis under stress. |
| | *yheM*, *yigL*, *ydeU* | Hypothetical | Unknown | Likely involved in environmental stress response and adaptation. |

Meanwhile, cluster 3 emphasizes protein quality control, intermediary metabolism, and cellular nucleotide synthesis. These general functions do not play a crucial role in the tested bacterial stress response, as evidenced by the minimal growth defects observed in this cluster compared to others. Moreover, some cross-cluster functional integration may be observed: energy metabolism and stress response genes (*atp*, *dnaK*, *cpxA*) span clusters, indicating their centrality to bacterial survival. Furthermore, stress response regulators (*oxyR*, *cpxA*, *dnaJ*) link different metabolic pathways that may play a role in the coordinated adaptation process. Functional interaction networks and gene co-expression analysis performed with the STRING database present connections between genes and their collaboration in the particular stress response [58]. This also confirms that this process is multigene-regulated.

## 5. Conclusions

Because no positive correlation between aBL and single stressors was found, we can conclude that the effectiveness of aBL depends on the variety of stressors that are generated simultaneously during irradiation. When aBL is applied, the production of ROS occurs naturally within microbial cells. It probably makes the process highly targeted. This could distinguish aBL from single chemical stressors like hydrogen peroxide, which introduces ROS from an external source. The presented results indicate that aBL is multifactorial, and the bactericidal role of aBL is a sum of the combination of stressors, not an effect of the singular one. Moreover, no specific genes were detected, the knockout of which determines the development of a definite resistance to stressors. This suggests that aBL may be a promising strategy in the fight against pathogens.

**Supplementary Materials:** The following supporting information can be downloaded at https://www.mdpi.com/article/10.3390/antiox13121583/s1.

**Author Contributions:** Conceptualization was performed by A.R.-Z. and B.K.-N.; data curation was performed by B.K.-N.; formal analysis was performed by B.K.-N.; funding acquisition was performed by A.R.-Z.; investigation was performed by B.K.-N.; methodology was performed by A.R.-Z., B.K.-N.; project administration was performed by A.R.-Z.; resources were secured by A.R.-Z.; software was secured by B.K.-N.; supervision was performed by A.R.-Z. and M.G.; validation was performed by B.K.-N. and A.R.-Z.; visualization was performed by B.K.-N.; writing (original draft) was performed by A.R-Z. and B.K.-N.; writing (review and editing) was performed by M.G. All authors have read and agreed to the published version of the manuscript.

**Funding:** This work was supported by the National Science Centre under Grant No. 2020/36/C/NZ7/00061 (A.R.-Z.) and UG-Grants Start 4 No. 533-BGB0-GS52-24 (B.K.-N.).

**Institutional Review Board Statement:** Not applicable.

**Data Availability Statement:** The raw data supporting the conclusions of this article will be made available by the authors upon request.

**Acknowledgments:** The authors would like to thank Anna Koelmer, M.A., a specialist biostatistician from the Centre of Biostatistics and Bioinformatics Analysis, Medical University of Gdansk, Poland, for the mathematical analysis of the results. The authors thank the National BioResource Project (NBRP, NIG, Japan) for contributing to our work by providing us with *E. coli* BW25113 mutants from the Keio collection. The graphics were prepared with the use of BioRender.com (accessed on 17 October 2024).

**Conflicts of Interest:** The authors declare no conflicts of interest.

## References

1. World Health Organization. *WHO Bacterial Priority Pathogens List*; World Health Organization: Geneva, Switzerland, 2024; pp. 12–13.
2. Hoenes, K.; Bauer, R.; Meurle, T.; Spellerberg, B.; Hessling, M. Inactivation effect of violet and blue light on ESKAPE pathogens and closely related non-pathogenic bacterial species–a promising tool against antibiotic-sensitive and antibiotic-resistant microorganisms. *Front. Microbiol.* **2021**, *11*, 612367. [CrossRef] [PubMed]
3. Dos Anjos, C.; Wang, Y.; Truong-Bolduc, Q.C.; Bolduc, P.K.; Liu, M.; Hooper, D.C.; Anderson, R.R.; Dai, T.; Leanse, L.G. Blue Light Compromises Bacterial β-Lactamases Activity to Overcome β-Lactam Resistance. *Lasers Surg. Med.* **2024**, *56*, 673–681. [CrossRef] [PubMed]
4. Wu, J.; Chu, Z.; Ruan, Z.; Wang, X.; Dai, T.; Hu, X. Changes of intracellular porphyrin, reactive oxygen species, and fatty acids profiles during inactivation of methicillin-resistant *Staphylococcus aureus* by antimicrobial blue light. *Front. Physiol.* **2018**, *9*, 1658. [CrossRef] [PubMed]
5. Wang, Y.; Ferrer-Espada, R.; Baglo, Y.; Gu, Y.; Dai, T. Antimicrobial blue light inactivation of Neisseria gonorrhoeae: Roles of wavelength, endogenous photosensitizer, oxygen, and reactive oxygen species. *Lasers Surg. Med.* **2019**, *51*, 815–823. [CrossRef] [PubMed]
6. Rapacka-Zdonczyk, A.; Wozniak, A.; Pieranski, M.; Woziwodzka, A.; Bielawski, K.P.; Grinholc, M. Development of Staphylococcus aureus tolerance to antimicrobial photodynamic inactivation and antimicrobial blue light upon sub-lethal treatment. *Sci. Rep.* **2019**, *9*, 9423. [CrossRef]
7. Dos Anjos, C.; Leanse, L.G.; Ribeiro, M.S.; Sellera, F.P.; Dropa, M.; Arana-Chavez, V.E.; Lincopan, N.; Baptista, M.S.; Pogliani, F.C.; Dai, T.; et al. New insights into the bacterial targets of antimicrobial blue light. *Microbiol. Spectr.* **2023**, *11*, e02833-22. [CrossRef]
8. Ferrer-Espada, R.; Wang, Y.; Goh, X.S.; Dai, T. Antimicrobial blue light inactivation of microbial isolates in biofilms. *Lasers Surg. Med.* **2020**, *52*, 472–478. [CrossRef]
9. Wang, Y.; Li, X.; Chen, H.; Yang, X.; Guo, L.; Ju, R.; Dai, T.; Li, G. Antimicrobial blue light inactivation of Pseudomonas aeruginosa: Unraveling the multifaceted impact of wavelength, growth stage, and medium composition. *J. Photochem. Photobiol. B Biol.* **2024**, *259*, 113023. [CrossRef]
10. Baba, T.; Ara, T.; Hasegawa, M.; Takai, Y.; Okumura, Y.; Baba, M.; Datsenko, K.A.; Tomita, M.; Wanner, B.L.; Mori, H. Construction of *Escherichia coli* K-12 in-frame, single-gene knockout mutants: The Keio collection. *Mol. Syst. Biol.* **2006**, *2*, 2006-0008. [CrossRef] [PubMed]
11. Kruszewska-Naczk, B.; Grinholc, M.; Waleron, K.; Bandow, J.E.; Rapacka-Zdończyk, A. Can antimicrobial blue light contribute to resistance development? Genome-wide analysis revealed aBL-protective genes in *Escherichia coli*. *Microbiol. Spectr.* **2024**, *12*, e02490-23. [CrossRef]
12. Krewing, M.; Jarzina, F.; Dirks, T.; Schubert, B.; Benedikt, J.; Lackmann, J.W.; Bandow, J.E. Plasma-sensitive *Escherichia coli* mutants reveal plasma resistance mechanisms. *J. R. Soc. Interface* **2019**, *16*, 20180846. [CrossRef]

13. Dragosits, M.; Mozhayskiy, V.; Quinones-Soto, S.; Park, J.; Tagkopoulos, I. Evolutionary potential, cross-stress behavior and the genetic basis of acquired stress resistance in *Escherichia coli*. *Mol. Syst. Biol.* **2013**, *9*, 643. [CrossRef]
14. Lubart, R.; Lipovski, A.; Nitzan, Y.; Friedmann, H. A possible mechanism for the bactericidal effect of visible light. *Laser Ther.* **2011**, *20*, 17–22. [CrossRef]
15. Yoshida, A.; Sasaki, H.; Toyama, T.; Araki, M.; Fujioka, J.; Tsukiyama, K.; Hamada, N.; Yoshino, F. Antimicrobial effect of blue light using Porphyromonas gingivalis pigment. *Sci. Rep.* **2017**, *7*, 5225. [CrossRef]
16. Marshall, M.V.; Cancro, L.P.; Fischman, S.L. Hydrogen peroxide: A review of its use in dentistry. *J. Periodontol.* **1995**, *66*, 786–796. [CrossRef] [PubMed]
17. Finnegan, M.; Linley, E.; Denyer, S.P.; McDonnell, G.; Simons, C.; Maillard, J.Y. Mode of action of hydrogen peroxide and other oxidizing agents: Differences between liquid and gas forms. *J. Antimicrob. Chemother.* **2010**, *65*, 2108–2115. [CrossRef]
18. Medina-Cordoba, L.K.; Valencia-Mosquera, L.L.; Tarazona-diaz, G.P.; Arias-Palacios, J.D.C. Evaluation of the efficacy of a hydrogen peroxide disinfectant. *Int. J. Pharm. Pharm. Sci.* **2018**, *10*, 104. [CrossRef]
19. Kruk, I. Biological Damages Caused by Reactive Oxygen Species. In *Environmental Toxicology and Chemistry of Oxygen Species*; Springer: Berlin/Heidelberg, Germany, 1998; pp. 89–138.
20. Imlay, J.A. Oxidative stress. *EcoSal Plus* **2009**, *3*, 10–1128. [CrossRef]
21. Wang, Y.; Wu, X.; Chen, J.; Amin, R.; Lu, M.; Bhayana, B.; Zhao, J.; Murray, C.K.; Hamblin, M.R.; Hooper, D.C.; et al. Antimicrobial blue light inactivation of gram-negative pathogens in biofilms: In vitro and in vivo studies. *J. Infect. Dis.* **2016**, *213*, 1380–1387. [CrossRef]
22. Yin, R.; Dai, T.; Avci, P.; Jorge, A.E.S.; De Melo, W.C.; Vecchio, D.; Huang, Y.Y.; Gupta, A.; Hamblin, M.R. Light based anti-infectives: Ultraviolet C irradiation, photodynamic therapy, blue light, and beyond. *Curr. Opin. Pharmacol.* **2013**, *13*, 731–762. [CrossRef] [PubMed]
23. Gülden, M.; Jess, A.; Kammann, J.; Maser, E.; Seibert, H. Cytotoxic potency of $H_2O_2$ in cell cultures: Impact of cell concentration and exposure time. *Free. Radic. Biol. Med.* **2010**, *49*, 1298–1305. [CrossRef] [PubMed]
24. Valko, M.; Leibfritz, D.; Moncol, J.; Cronin, M.T.; Mazur, M.; Telser, J. Free radicals and antioxidants in normal physiological functions and human disease. *Int. J. Biochem. Cell Biol.* **2007**, *39*, 44–84. [CrossRef] [PubMed]
25. Edge, R.; Truscott, T.G. The reactive oxygen species singlet oxygen, hydroxy radicals, and the superoxide radical anion—Examples of their roles in biology and medicine. *Oxygen* **2021**, *1*, 77–95. [CrossRef]
26. Wang, Y.; Branicky, R.; Noë, A.; Hekimi, S. Superoxide dismutases: Dual roles in controlling ROS damage and regulating ROS signaling. *J. Cell Biol.* **2018**, *217*, 1915–1928. [CrossRef]
27. Andrés, C.M.C.; Pérez de la Lastra, J.M.; Andrés Juan, C.; Plou, F.J.; Pérez-Lebeña, E. Superoxide anion chemistry—Its role at the core of the innate immunity. *Int. J. Mol. Sci.* **2023**, *24*, 1841. [CrossRef]
28. Halliwell, B. Reactive species and antioxidants. Redox biology is a fundamental theme of aerobic life. *Plant Physiol.* **2006**, *141*, 312–322. [CrossRef]
29. Gligorovski, S.; Strekowski, R.; Barbati, S.; Vione, D. Environmental implications of hydroxyl radicals (•OH). *Chem. Rev.* **2015**, *115*, 13051–13092. [CrossRef] [PubMed]
30. Leanse, L.G.; Anjos, C.D.; Kaler, K.R.; Hui, J.; Boyd, J.M.; Hooper, D.C.; Anderson, R.R.; Dai, T. Blue light potentiates antibiotics in bacteria via parallel pathways of hydroxyl radical production and enhanced antibiotic uptake. *Adv. Sci.* **2023**, *10*, 2303731. [CrossRef] [PubMed]
31. Wink, D.A.; Hines, H.B.; Cheng, R.Y.; Switzer, C.H.; Flores-Santana, W.; Vitek, M.P.; Ridnour, L.A.; Colton, C.A. Nitric oxide and redox mechanisms in the immune response. *J. Leukoc. Biol.* **2011**, *89*, 873–891. [CrossRef] [PubMed]
32. Poh, W.H.; Rice, S.A. Recent developments in nitric oxide donors and delivery for antimicrobial and anti-biofilm applications. *Molecules* **2022**, *27*, 674. [CrossRef] [PubMed]
33. Sorbo, L.D.; Michaelsen, V.S.; Ali, A.; Wang, A.; Ribeiro, R.V.; Cypel, M. High doses of inhaled nitric oxide as an innovative antimicrobial strategy for lung infections. *Biomedicines* **2022**, *10*, 1525. [CrossRef]
34. Liebmann, J.; Born, M.; Kolb-Bachofen, V. Blue-light irradiation regulates proliferation and differentiation in human skin cells. *J. Investig. Dermatol.* **2010**, *130*, 259–269. [CrossRef] [PubMed]
35. McKenzie, K.; Maclean, M.; Timoshkin, I.V.; MacGregor, S.J.; Anderson, J.G. Enhanced inactivation of *Escherichia coli* and *Listeria monocytogenes* by exposure to 405 nm light under sub-lethal temperature, salt and acid stress conditions. *Int. J. Food Microbiol.* **2014**, *170*, 91–98. [CrossRef] [PubMed]
36. Coulson, G.B.; Johnson, B.K.; Zheng, H.; Colvin, C.J.; Fillinger, R.J.; Haiderer, E.R.; Hammer, N.D.; Abramovitch, R.B. Targeting Mycobacterium tuberculosis sensitivity to thiol stress at acidic pH kills the bacterium and potentiates antibiotics. *Cell Chem. Biol.* **2017**, *24*, 993–1004. [CrossRef] [PubMed]
37. Schneider, L.A.; Korber, A.; Grabbe, S.; Dissemond, J. Influence of pH on wound-healing: A new perspective for wound-therapy? *Arch. Dermatol. Res.* **2007**, *298*, 413–420. [CrossRef]
38. Percival, S.L.; McCarty, S.; Hunt, J.A.; Woods, E.J. The effects of pH on wound healing, biofilms, and antimicrobial efficacy. *Wound Repair Regen.* **2014**, *22*, 174–186. [CrossRef]
39. Sim, P.; Strudwick, X.L.; Song, Y.; Cowin, A.J.; Garg, S. Influence of acidic pH on wound healing in vivo: A novel perspective for wound treatment. *Int. J. Mol. Sci.* **2022**, *23*, 13655. [CrossRef]

40. Wallace, L.A.; Gwynne, L.; Jenkins, T. Challenges and opportunities of pH in chronic wounds. *Ther. Deliv.* **2019**, *10*, 719–735. [CrossRef] [PubMed]
41. Krumova, K.; Cosa, G. Overview of reactive oxygen species. In *Singlet Oxygen: Applications in Biosciences and Nanosciences*; Comprehensive Series in Photochemical & Photobiological Sciences; Royal Society of Chemistry: London, UK, 2016. [CrossRef]
42. Dahan-Grobgeld, E.; Livneh, Z.; Maretzek, A.F.; Polak-Charcon, S.; Eichenbaum, Z.; Degani, H. Reversible induction of ATP synthesis by DNA damage and repair in *Escherichia coli*: In vivo NMR studies. *J. Biol. Chem.* **1998**, *273*, 30232–30238. [CrossRef] [PubMed]
43. Seregina, T.A.; Petrushanko, I.Y.; Shakulov, R.S.; Zaripov, P.I.; Makarov, A.A.; Mitkevich, V.A.; Mironov, A.S. The inactivation of LPS biosynthesis genes in *E. coli* cells leads to oxidative stress. *Cells* **2022**, *11*, 2667. [CrossRef]
44. Hamblin, M.R.; Abrahamse, H. Can light-based approaches overcome antimicrobial resistance? *Drug Dev. Res.* **2019**, *80*, 48–67. [CrossRef]
45. Storz, G.; Imlayt, J.A. Oxidative stress. *Curr. Opin. Microbiol.* **1999**, *2*, 188–194. [CrossRef]
46. Cabiscol Catalā, E.; Tamarit Sumalla, J.; Ros Salvador, J. Oxidative stress in bacteria and protein damage by reactive oxygen species. *Internatl. Microbiol.* **2000**, *3*, 3–8.
47. Imlay, J.A. The molecular mechanisms and physiological consequences of oxidative stress: Lessons from a model bacterium. *Nat. Rev. Microbiol.* **2013**, *11*, 443–454. [CrossRef] [PubMed]
48. Bienert, G.P.; Schjoerring, J.K.; Jahn, T.P. Membrane transport of hydrogen peroxide. *Biochim. Et Biophys. Acta (BBA)-Biomembr.* **2006**, *1758*, 994–1003. [CrossRef] [PubMed]
49. Liang, J.Y.; Cheng, C.W.; Yu, C.H.; Chen, L.Y. Investigations of blue light-induced reactive oxygen species from flavin mononucleotide on inactivation of *E. coli*. *J. Photochem. Photobiol. B Biol.* **2015**, *143*, 82–88. [CrossRef] [PubMed]
50. Juven, B.J.; Pierson, M.D. Antibacterial effects of hydrogen peroxide and methods for its detection and quantitation. *J. Food Prot.* **1996**, *59*, 1233–1241. [CrossRef]
51. Möller, M.N.; Cuevasanta, E.; Orrico, F.; Lopez, A.C.; Thomson, L.; Denicola, A. Diffusion and transport of reactive species across cell membranes. In *Bioactive Lipids in Health and Disease*; Springer: Berlin/Heidelberg, Germany, 2019; pp. 3–19.
52. Sen, A.; Imlay, J.A. How microbes defend themselves from incoming hydrogen peroxide. *Front. Immunol.* **2021**, *12*, 667343. [CrossRef]
53. Imlay, J.A. Cellular defenses against superoxide and hydrogen peroxide. *Annu. Rev. Biochem.* **2008**, *77*, 755–776. [CrossRef] [PubMed]
54. Nóbrega, C.S.; Pauleta, S.R. Reduction of hydrogen peroxide in gram-negative bacteria–bacterial peroxidases. *Adv. Microb. Physiol.* **2019**, *74*, 415–464. [PubMed]
55. Mishra, S.; Imlay, J. Why do bacteria use so many enzymes to scavenge hydrogen peroxide? *Arch. Biochem. Biophys.* **2012**, *525*, 145–160. [CrossRef] [PubMed]
56. Girotti, A. Photosensitized lipid peroxidation in biological membranes. *Photodyn. Ther. Neoplast. Dis.* **1990**, *1*, 229–245.
57. Glaeser, J.; Nuss, A.M.; Berghoff, B.A.; Klug, G. Singlet oxygen stress in microorganisms. *Adv. Microb. Physiol.* **2011**, *58*, 141–173. [PubMed]
58. Szklarczyk, D.; Morris, J.H.; Cook, H.; Kuhn, M.; Wyder, S.; Simonovic, M.; Santos, A.; Doncheva, N.T.; Roth, A.; Bork, P.; et al. The STRING database in 2017: Quality-controlled protein-protein association networks, made broadly accessible. *Nucleic Acids Res.* **2017**, *45*, D362–D368. [CrossRef] [PubMed]

## 8.3.1. Supplementary Materials

**Supplementary Materials:** *Mimicking the effects of antimicrobial blue light: exploring single stressors and their impact on microbial growth* by Beata Kruszewska-Naczk, Mariusz Grinholc and Aleksandra Rapacka-Zdonczyk

**Table S1**. The mean and standard deviation for each stressor.

| **Characteristic** | **N = 64**[1] |
|---|---|
| aBL sensitivity | 3.91 (1.17) |
| $H_2O_2$ | -104 (91) |
| $O_2^-$ | 25 (32) |
| NO• | 29 (25) |
| Acid pH | -76 (40) |
| Membrane stress | -8 (36) |
| •OH | 17 (105) |

[1]Mean (SD)

**Table S2.** The number of mutants (n) for which the growth defect was higher than 20% and the mean growth defect for each stressor.

| Stressor | n | Mean growth defect |
|---|---|---|
| $H_2O_2$ | 7 | 61.1 |
| Membrane stress | 9 | 35.12 |
| •OH | 45 | 41.58 |
| NO• | 36 | 47.1 |
| $O_2^-$ | 45 | 70.35 |
| Acid pH | 0 | - |

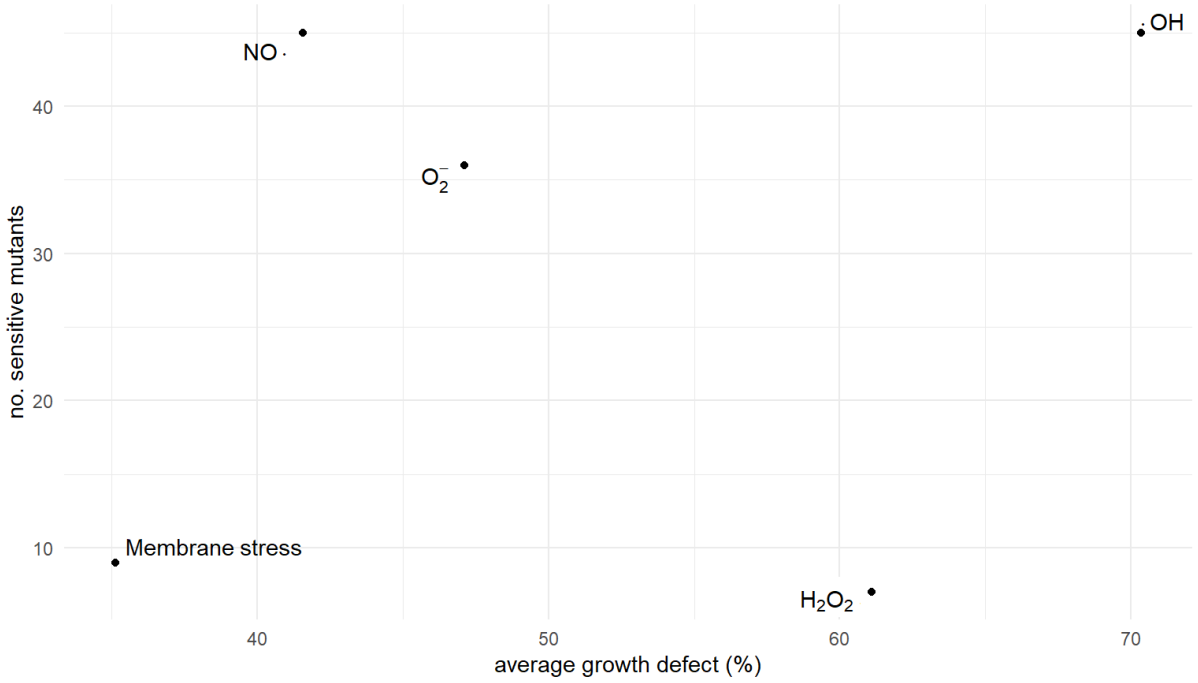


**Figure S1.** The count of knockout mutants displaying a growth defect, surpassing 20% against the mean growth deficiency of these strains.

**Table S3.** The number of mutants (n) for which the growth defect was smaller than -20% and the mean growth defect for each stressor.

| Stressor | n | Mean growth defect |
|---|---|---|
| $H_2O_2$ | 53 | -133.16 |
| Membrane stress | 17 | -51.30 |
| •OH | 2 | -34.14 |
| NO• | 5 | -37.96 |
| $O_2^-$ | 16 | -129.16 |
| Acid pH | 62 | -77.75 |

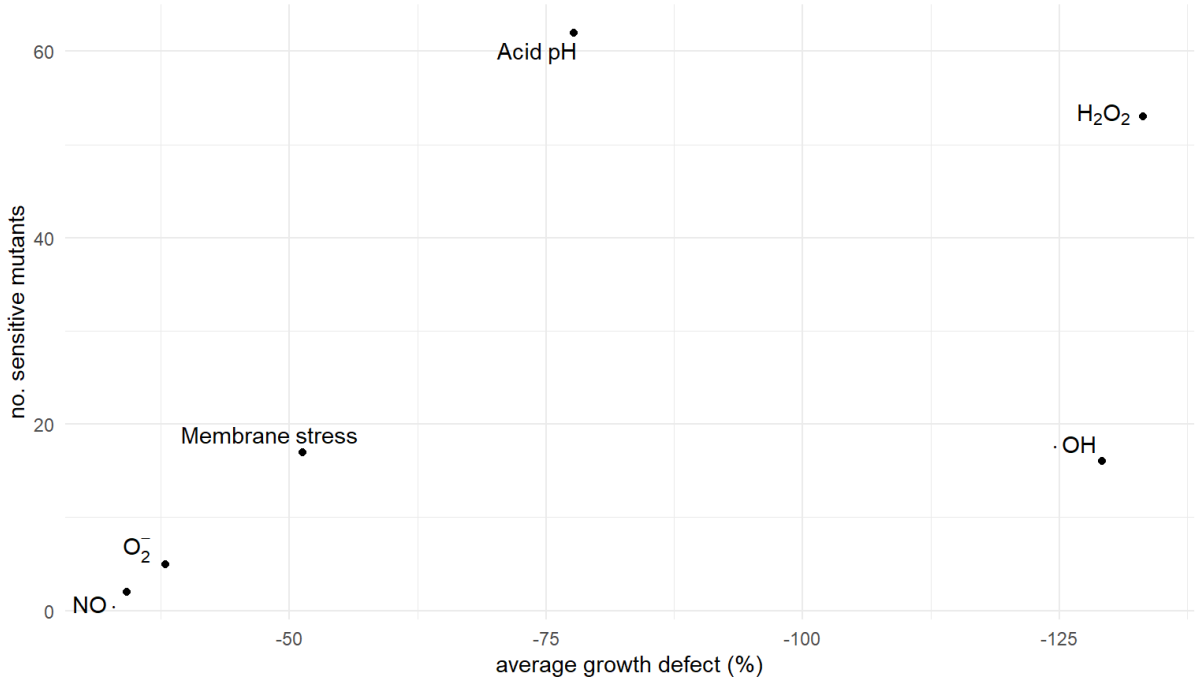


**Figure S2.** The count of knockout mutants displaying a growth defect smaller than -20% against the mean growth deficiency of these strains.

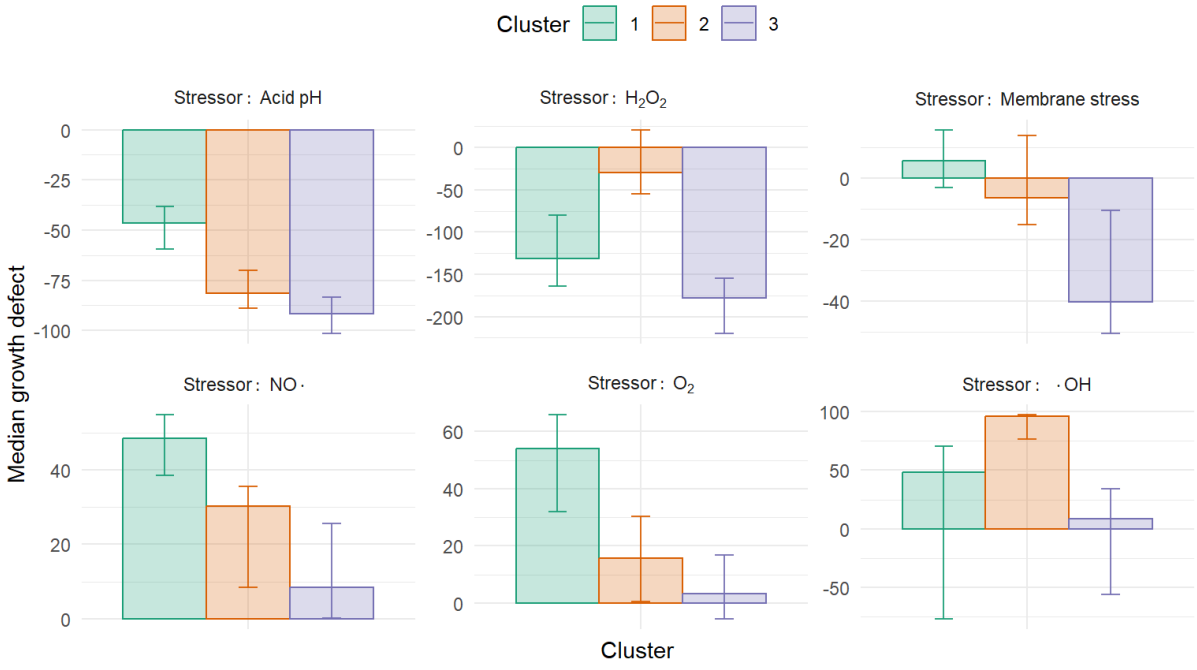


**Figure S3.** Median growth defect for clusters. A characterization of growth defect profiles for 3 clusters. The bars represents median values, while the error bars denote the Interquartile Range (IQS).

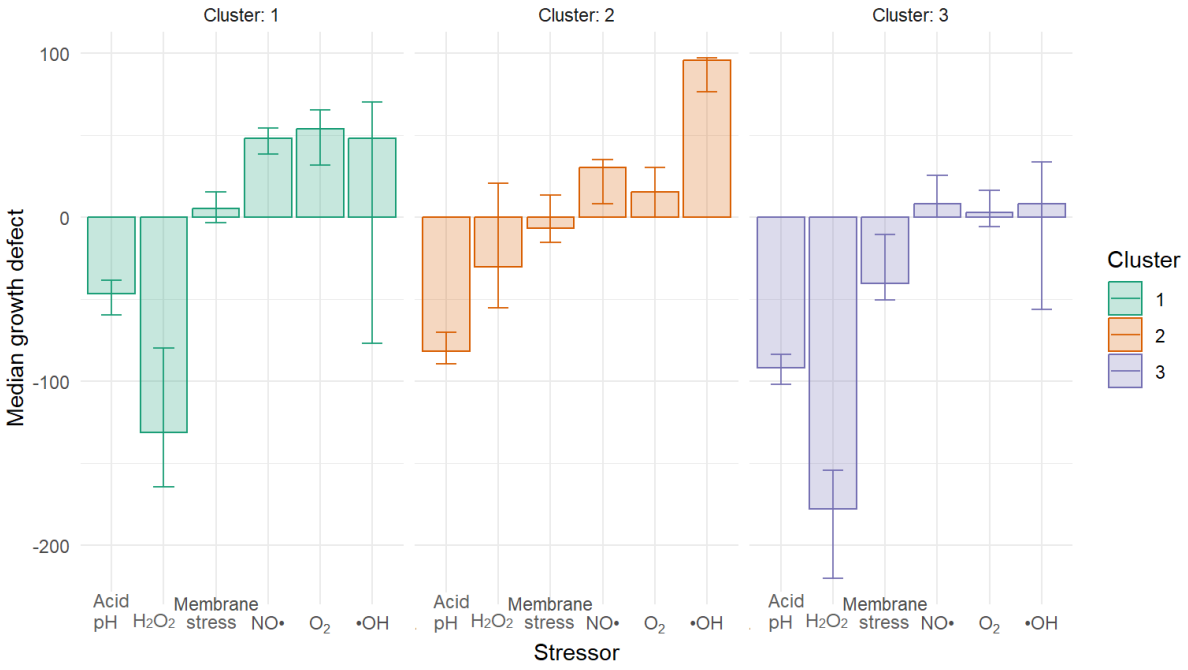


**Figure S4. Median growth defect for clusters.** A characterization of cluster profiles for each stressor. The bars represents median values, while the error bars denote the Interquartile Range (IQS).

**Table S4. List of aBL hypersensitive mutants with a description of the protein encoded by the deleted gene.**

| Lp. | Gene name | Synonyms | Description |
|---|---|---|---|
| 1. | *atpA* | *papA // uncA* | ATP synthase subunit alpha |
| 2. | *atpB* | *papD // uncB* | ATP synthase subunit a |
| 3. | *atpC* | *papG // uncC* | ATP synthase epsilon chain |
| 4. | *atpD* | *papB // uncD* | ATP synthase subunit beta |
| 5. | *atpE* | *papH // uncE* | ATP synthase subunit c |
| 6. | *atpF* | *papF // uncF* | ATP synthase subunit b |
| 7. | *atpG* | *papC // uncG* | ATP synthase gamma chain |
| 8. | *atpH* | *papE // uncH* | ATP synthase subunit delta |
| 9. | *cpxA* | *rssE // ecfB // eup // ssd // ecf* | Sensor histidine kinase CpxA |
| 10. | *cydD* | *htrD* | ATP-binding/permease protein CydD |
| 11. | *dacA* | *pfv* | D-alanyl-D-alanine carboxypeptidase DacA |
| 12. | *deoB* | *tlr // drm // thyR* | Phosphopentomutase |
| 13. | *dnaJ* | *groP // grpC* | Chaperone protein DnaJ |
| 14. | *dnaK* | *groPF // groPC // seg //* | Chaperone protein DnaK |

| | | | |
|---|---|---|---|
| | | *grpF // grpC // groPAB* | |
| 15. | *ecnB* | *yjeU* | Entericidin B |
| 16. | *fabH* | | 3-oxoacyl-[acyl-carrier-protein] synthase 3 |
| 17. | *fimB* | *pil* | Type 1 fimbriae regulatory protein FimB |
| 18. | *gmhB* | *yaeD* | D-glycero-beta-D-manno-heptose-1,7-bisphosphate 7-phosphatase |
| 19. | *gntK* | | Thermoresistant gluconokinase |
| 20. | *hldD* | *yqiF // rfaE // gmhC // waaE* | ADP-L-glycero-D-manno-heptose-6-epimerase |
| 21. | *holD* | | DNA polymerase III subunit psi |
| 22. | *metR* | | HTH-type transcriptional regulator MetR |
| 23. | *narL* | *frdR // narR* | Nitrate/nitrite response regulator protein NarL |
| 24. | *nuoN* | | NADH-quinone oxidoreductase subunit N |
| 25. | *oxyR* | *momR // mor* | Hydrogen peroxide-inducible genes activator |
| 26. | *pfkA* | | ATP-dependent 6-phosphofructokinase isozyme 1 |
| 27. | *pgi* | | Glucose-6-phosphate isomerase |
| 28. | *pgm* | *gpmA //blu* | 2,3-bisphosphoglycerate-dependent phosphoglycerate mutase |
| 29. | *phoQ* | | Sensor protein PhoQ |
| 30. | *ppc* | *asp // glu* | Coenzyme A biosynthesis bifunctional protein CoaBC |
| 31. | *priA* | *srgA* | Primosomal protein N' |
| 32. | *purA* | *adeK* | Adenylosuccinate synthetase |
| 33. | *pyrE* | | Orotate phosphoribosyltransferase |
| 34. | *rbfA* | *sdr-43 // yhbB* | 30S ribosome-binding factor |
| 35. | *rfaC* | *rfa-2 // waaC // yibC* | Lipopolysaccharide heptosyltransferase 1 |
| 36. | *rfaE* | *hldE // yqiF // gmhC // waaE* | Bifunctional protein HldE |
| 37. | *rfaG* | *waaG* | Lipopolysaccharide core biosynthesis protein RfaG |
| 38. | *rnt* | | Ribonuclease T |
| 39. | *rpe* | *dod // yhfD* | Ribulose-phosphate 3-epimerase |
| 40. | *sstT* | *ygjU* | Serine/threonine transporter SstT |
| 41. | *surA rfaD* | *waaD // hldD // htrM // nbsB* | Chaperone SurA |

| | | | |
|---|---|---|---|
| 42. | *thyA* | | Thymidylate synthase |
| 43. | *tolA* | *cim // excC // lky // tol-2* | Tol-Pal system protein TolA |
| 44. | *tpiA* | *tpi* | Triosephosphate isomerase |
| 45. | *truA* | *asuC // hisT // leuK* | tRNA pseudouridine synthase A |
| 46. | *ubiC* | | Chorismate pyruvate-lyase |
| 47. | *umuD* | | Protein UmuD |
| 48. | *ybaP* | | TraB family protein YbaP |
| 49. | *yccM* | | Putative electron transport protein YccM |
| 50. | *ydcE* | *pptA* | Tautomerase PptA |
| 51. | *ydcx* | *ortT* | Orphan toxin OrtT |
| 52. | *ydeU* | *orfT // ydeK // ydeU // b1509 // b1510 // ECK1502* | AIDA-I family autotransporter YneO |
| 53. | *yegS* | | Lipid kinase YegS |
| 54. | *yfbB* | *menH* | 2-succinyl-6-hydroxy-2,4-cyclohexadiene-1-carboxylate synthase |
| 55. | *yfeH* | | Putative symporter YfeH |
| 56. | *yfgL* | *bamB* | Outer membrane protein assembly factor BamB |
| 57. | *ygfZ* | *yzzW* | tRNA-modifying protein YgfZ |
| 58. | *yheM* | *tus*C | Protein TusC |
| 59. | *yhhH* | | PF15631 family protein YhhH |
| 60. | *yigL* | | Pyridoxal phosphate phosphatase YigL |
| 61. | *yihE* | *orfA // srkA* | Stress response kinase A |
| 62. | *yjeK* | *epmB* | L-lysine 2,3-aminomutase |
| 63. | *yncA* | *mnaT* | L-amino acid N-acyltransferase MnaT |
| 64. | *ypjD* | | Inner membrane protein YpjD |

## 8.4. Publication no. 4.

frontiers | Frontiers in Molecular Biosciences

TYPE Original Research
PUBLISHED 06 January 2025
DOI 10.3389/fmolb.2024.1467726



OPEN ACCESS

EDITED BY
Andrey Turchinovich,
German Cancer Research Center (DKFZ), Germany

REVIEWED BY
Yubin Ma,
Ocean University of China, China
Julia Veryaskina,
Institute of Molecular and Cellular Biology (RAS), Russia

*CORRESPONDENCE
Aleksandra Rapacka-Zdonczyk,
aleksandra.rapacka-zdonczyk@ug.edu.pl

RECEIVED 20 July 2024
ACCEPTED 10 December 2024
PUBLISHED 06 January 2025

CITATION
Kruszewska-Naczk B, Grinholc M and Rapacka-Zdonczyk A (2025) Identification and validation of reference genes for quantitative gene expression analysis under 409 and 415 nm antimicrobial blue light treatment. *Front. Mol. Biosci.* 11:1467726. doi: 10.3389/fmolb.2024.1467726



# Identification and validation of reference genes for quantitative gene expression analysis under 409 and 415 nm antimicrobial blue light treatment

Beata Kruszewska-Naczk, Mariusz Grinholc and Aleksandra Rapacka-Zdonczyk*

Laboratory of Photobiology and Molecular Diagnostics, Intercollegiate Faculty of Biotechnology, University of Gdansk and Medical University of Gdansk, Gdańsk, Poland

**Introduction:** Reverse transcription quantitative real-time polymerase chain reaction Q7 (RT-qPCR) is a commonly used tool for gene expression quantification. Because the qPCR method depends on several variables that can influence the analysis process, stably expressed genes should be selected for relative gene expression studies. To date, there is insufficient information on the selection of appropriate reference genes for antimicrobial photodynamic inactivation (aPDI) and antimicrobial blue light (aBL) treatment. Therefore, the purpose of the present study was to determine the most stable reference gene under treatment with aBL under sublethal conditions and to evaluate differences in the expression of the selected gene after aBL treatment in comparison to the nontreated control.

**Methods:** Selection of stable reference genes was performed using 4 programs: BestKeeper, geNorm, NormFinder and RefFinder under 409 and 415 nm aBL treatment.

**Results:** The results revealed that the gene encoding the integration host factor β subunit (ihfB) in *Escherichia coli* was the most stably expressed gene after both 409 and 415 nm aBL treatment. Three programs, RefFinder, geNorm, and NormFinder, indicated that this gene had the most stable expression in comparison to the other reference gene candidates. The next best candidates were cysG, uidA, and gyrA. NormFinder revealed ihfB as the single gene and cysG - gyrA as the combination of reference genes with the best stability.

**Discussion:** Universal reference genes are characterized by stable expression that remains consistent across various stress conditions. Consequently, it is essential to evaluate reference genes for each specific stress factor under investigation. In the case of aBL at different wavelengths, we identified genes that maintain stable expression following irradiation.

KEYWORDS

**antimicrobial blue light, BestKeeper, *Escherichia coli*, geNorm, reference gene, RT-qPCR, NormFinder, RefFinder**

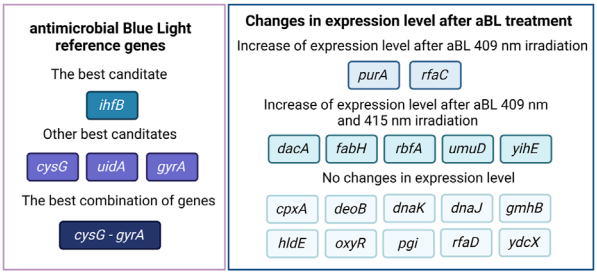


GRAPHICAL ABSTRACT

# Introduction

The increase in antibiotic resistance has been extensively reported (Hawkey, 2008; Robinson et al., 2016; Woc-Colburn and Francisco, 2020). The increasing resistance to antimicrobial agents and the lack of new molecules to combat bacterial resistance are serious problems and pose extremely dangerous health threats that modern medicine must address. The most important factor leading to multidrug resistance is the misuse and overuse of antibiotics (English and Gaur, 2010). Bacteria have continually evolved a repertoire of mechanisms to evade the effects of antibiotics (Enwemeka, 2013). Currently, approximately 700,000 people die every year due to infections caused by drug-resistant pathogens (O'Neill, 2016). To address this life-threatening public health problem, new antimicrobial strategies are being intensively sought. Among the most promising strategies are the application of antimicrobial photodynamic inactivation (aPDI) and antimicrobial blue light (aBL), which are the subjects of many basic and clinical studies. The main mechanism of action of aBL is based on reactive oxygen species generation under a specific light wavelength (in the range of 400–470 nm), which leads to bacterial eradication (Wang et al., 2017). To date, no development of bacterial resistance to aBL has been reported, suggesting that aBL is a very promising antimicrobial approach.

The photodynamic research community consists of various academic groups affiliated with two associations, the International Photodynamic Association (IPA) and the European Society of Photobiology (ESP), that are working to introduce aPDI and aBL in the clinic. Photodynamic research groups have made significant scientific progress, and their research on photodynamic inactivation has been published in desirable scientific journals, such as The Lancet (Wainwright et al., 2017), Science (Lu et al., 2021), and journals of the Nature Publishing Group (Wang et al., 2021). All of the findings indicate that aBL is a promising therapeutic alternative and may become a significant complementary treatment option to fight multidrug-resistant microbial infections. Despite the many advantages of aBL, this strategy is not frequently implemented in standard treatment procedures, possibly because the mechanism of action of aBL is not fully understood. The lack of a detailed understanding of the mechanism of action of aBL at the genetic level is a limitation and has hindered the widespread implementation of this effective method of bacterial eradication.

Transcriptomic research is one of the main branches of experimental research on the principle underlying the effect of aBL. Due to its high specificity, sensitivity and reproducibility, reverse transcription quantitative real-time polymerase chain reaction (RT-qPCR) is a "gold standard" for gene expression quantification. However, the qPCR method depends on several variables that can affect the analysis process, such as the quantity and integrity of the extracted RNA, the sample amount and the designed primers. To overcome these variabilities, it is important to perform relative normalization, wherein the expression levels of target genes are normalized relative to the expression of a reference gene (selected as a stably expressed gene, most often a housekeeping gene). Therefore, the selection of an appropriate reference gene is crucial for relative gene expression studies (Guenin et al., 2009; Gomes et al., 2018). The use of different reference genes can produce surprisingly different gene expression results.

To date, there is little information on the selection of appropriate reference genes for the PDI and aBL process. To our knowledge, there are no published data on *Escherichia coli* gene stability after aBL treatment, and our research group has shown a great need to develop this as a basic method for gene expression research and to identify reference genes for the correct analysis and interpretation of the obtained results from aBL treatment. For this reason, the present study aimed to (1) determine the most stable reference gene under treatment with aBL under sublethal conditions, (2) evaluate differences in the expression of the selected gene after aBL treatment in comparison to that in untreated cells, and (3) compare differences in gene expression for two wavelengths of blue light, namely, 409 and 415 nm. In this study, 10 genes were selected as reference gene candidates (*arcA, cysG, gyrA, hcaT, idnT, ihfB, rpoA, rssA, uidA* and *uxuR*), encoding proteins involved in essential cellular processes. Additionally, 11 genes (*cpxA, deoB, dnaK, dnaJ, oxyR, pgi, purA, rbfA, umuD, ydcX,* and *yihE*), whose deletion resulted in hypersensitivity to aBL in single-gene Keio mutants, were chosen based on prior findings (Kruszewska-Naczk et al., 2024). Furthermore, 6 genes (*rfaC, rfaD, dacA, fabH, gmhB,* and *hldE*) potentially associated with resistance mechanisms were selected, and their expression was analyzed in wild-type bacteria.

# Materials and methods

## Bacterial strain and culture conditions

In this study, the *E. coli* BW25113 strain (*E. coli* Keio Knockout Parent Strain (Baba et al., 2006)) was investigated and cultured in

Luria–Bertani (LB) broth (BTL, Łódź, Poland) or LB agar medium (A&A, Gdansk, Poland). Overnight cultures were prepared under aerobic conditions in an orbital incubator (Innova 40, Brunswick, Germany) at 150 rpm and cultured for 16–20 h at 37°C.

## Reagents

Primers were designed with the NCBI Pick Primers tool and ordered from the Institute of Biochemistry and Biophysics Polish Academy of Sciences (IBB PAN, Oligo.pl, Warsaw, Poland). The genes *arcA, cysG, gyrA, hcaT, idnT, ihfB, rpoA, rssA, uidA,* and *uxuR* were selected as reference gene candidates encoding proteins involved in basic cellular processes based on a literature search. The following genes were investigated for changes in expression levels under the influence of aBL: *cpxA, dacA, deoB, dnaK, dnaJ, fabH, gmhB, hldE, oxyR, pgi, purA, rbfA, rfaC (waaC), rfaD, umuD, ydcX (ortT),* and *yihE (srkA),* reported as aBL-hypersensitive genes in (Kruszewska-Naczk et al., 2024). All primer sequences are listed in Supplementary Table S1 in Supplementary Material, while the genes and their functions are listed in Table 1. Information about proteins encoded by genes was obtained from http://www.ecocyc.org.

## Light sources

Two LED devices were used in the research. One had a $\lambda_{max}$ of 415 nm and irradiance of 25 mW/cm$^2$ (Cezos, Gdynia, Poland) (Kruszewska-Naczk et al., 2024), and the other had a $\lambda_{max}$ of 409 nm and irradiance of 5.2 mW/cm$^2$ (Cezos, Gdynia, Poland).

## aBL treatment and RNA isolation

An overnight culture of the *E. coli* BW25113 strain was diluted 1:100 and incubated at 37°C and 150 RPM for 2 h to obtain an $OD_{600}$ = 0.5. Next, 600 µL of the overnight culture was transferred to 24-well plates and irradiated for 30 min to reduce the bacterial load by ~0.5 $\log_{10}$ CFU/mL. The dose of irradiation was chosen to achieve a similar reduction in the bacterial load and an equal duration of exposure to light. Thirty minutes of irradiation corresponds to 43.2 J/cm$^2$ for the 415 nm LED and 9.36 J/cm$^2$ for the 409 nm LED. Simultaneously, the control sample was incubated in the dark. Then, the samples were incubated for 40 min at 37°C in an orbital incubator (Innova 40, Brunswick, Germany) at 150 rpm. One set of controls used for reference gene selection was directly subjected to the next steps without resting. Next, 10 µL of each sample was diluted, streaked onto an LB agar plate, and incubated at 37°C for 16–20 h to count the surviving colonies. The results are shown in Figure 1. Five hundred microliters of the irradiated samples or nonirradiated controls were diluted in RNA protection reagent and incubated for 10 min, followed by centrifugation for 10 min at 5,000 × g. Bacterial pellets were frozen at −80°C. The experiments were performed in triplicate. RNA from bacterial pellets was isolated using the Syngen Blood/Cell RNA Mini Kit (Syngen, Poland). Genomic DNA contamination was removed using the TURBO DNA-free™ Kit (Thermo Fisher Scientific Baltics UAB, Lithuania). The quality of the isolated RNA was assessed by measuring its concentration and the 260/280 and 260/230 ratios using a NanoDrop spectrophotometer (Thermo Scientific, United States). A QuantiTect Reverse Transcription Kit (Qiagen, Germany) was used to transcribe RNA to cDNA. For each sample, 500 ng of RNA was collected to obtain the same amount of cDNA.

## qPCR-based gene expression analysis

Gene expression analysis was performed using a LightCycler 480 II (Roche Life Science, Germany). The optimal concentration of primers was selected based on qPCR Cp values. The optimal concentration for each pair of primers was 0.3 µM. The reaction mixture contained the following components: 5 µL of Fast SG qPCR Master Mix (EURx, Poland), 0.3 µM each primer pair (IBB Oligo.pl, Warsaw, Poland), nuclease-free water (EURx, Poland) and 1 µL of 25-fold diluted cDNA. To control contamination with genomic DNA, RNA was added to the reaction mixture instead of cDNA. In another reagent purity control, water was added instead of cDNA. The program consisted of the following steps: initial denaturation at 95°C for 5 min; 45 cycles of denaturation at 95°C for 15 s, annealing at 60°C for 15 s and elongation at 72°C for 15 s; final elongation at 72°C for 3 min; and melting curve generation at 65°C–95°C. To evaluate the specific amplification and possible dimer formation ability of the primers, melting curve analysis was performed. For the control samples not treated with aBL, standard curves were prepared for each primer (0 min of delay for reference gene candidates and 40 min of rest for investigated genes), and the reaction efficiency was calculated. For standard curves, five dilutions of cDNA (1:5, 1:25, 1:125, 1:625, 1:3125) prepared from the nonirradiated control were used. The following parameters were assessed and are listed in Supplementary Table S2 in Supplementary Material: efficiency and slope. The experiments were performed in four technical repetitions. As a reference gene *ihfB* was chosen. The PCR efficiencies for the investigated and reference genes were not equal, so the Pfaffl gene expression analysis model was implemented according to the following equation:

$$R = \frac{\left(E_{target\,gene}\right)^{\Delta Cp\,target\,gene\,(control-sample)}}{\left(E_{reference\,gene}\right)^{\Delta Cp\,reference\,gene\,(control-sample)}}$$

where R is the gene expression ratio, $E_{target}$ is the reaction efficiency for the investigated gene, $E_{reference\ gene}$ is the reaction efficiency for the reference gene, ΔCp is the difference between the Cp values for the control and irradiated samples for the investigated gene, and ΔCp is the difference between the Cp values for the control sample and the irradiated reference gene sample (Pfaffl, 2001). The calibrator control was a nonirradiated sample, which was normalized to 1. All R values were $\log_2$ transformed and plotted as a fold change in expression level, where a value of 0 represents the expression level of the control. The R value was calculated for 3 independent biological replicates with standard deviation.

## Statistical analysis and graphs

The calculations were performed in Excel, while the figures and statistical analysis were performed with GraphPad

10.3389/fmolb.2024.1467726

TABLE 1 List of reference and investigated genes and their functions.

| Reference genes | | | |
|---|---|---|---|
| Number | Gene | Encoded protein | Function |
| 1 | *arcA* | DNA-binding transcriptional dual regulator ArcA | regulation of DNA-templated transcription |
| 2 | *cysG* | siroheme synthase | response to osmotic stress, porphyrin-containing compound biosynthetic process |
| 3 | *gyrA* | DNA gyrase subunit A | DNA topological change |
| 4 | *hcaT* | putative 3-phenylpropionate transporter | lactose transport |
| 5 | *idnT* | L-idonate/5-ketogluconate/gluconate transporter | carbohydrate transport |
| 6 | *ihfB* | integration host factor subunit β | regulation of translation, DNA recombination, DNA-templated transcription |
| 7 | *rpoA* | RNA polymerase subunit α | DNA-templated transcription, response to heat, cellular response to cell envelope stress |
| 8 | *rssA* | putative patatin-like phospholipase RssA | lipid metabolic process |
| 9 | *uidA* | β-D-glucuronidase | glucuronoside catabolic process |
| 10 | *uxuR* | DNA-binding transcriptional repressor UxuR | DNA-templated transcription |
| **Investigated genes** | | | |
| Number | Gene | Encoded protein | Function |
| 1 | *cpxA* | sensor histidine kinase CpxA | response to radiation, cellular response to cell envelope stress, cell adhesion involved in biofilm formation, protein autophosphorylation |
| 2 | *dacA* | D-alanyl-D-alanine carboxypeptidase DacA | peptidoglycan metabolic process, regulation of cell shape, proteolysis |
| 3 | *deoB* | phosphopentomutase | DNA damage response |
| 4 | *dnaK* | chaperone protein DnaK | response to heat, cellular response to unfolded protein, DNA replication |
| 5 | *dnaJ* | chaperone protein DnaJ | DNA replication, protein folding and unfolding, response to heat |
| 6 | *fabH* | 3-oxoacyl- [acyl carrier protein] synthase 3 | fatty acid metabolic process |
| 7 | *gmhB* | D-glycero-β-D-manno-heptose-1,7-bisphosphate 7-phosphatase | lipopolysaccharide core region biosynthetic process |
| 8 | *hldE* | fused heptose 7-phosphate kinase/heptose 1-phosphate adenyltransferase | lipopolysaccharide core region biosynthetic process |
| 9 | *oxyR* | DNA-binding transcriptional dual regulator OxyR | DNA damage response, response to oxidative stress |
| 10 | *pgi* | glucose-6-phosphate isomerase | glycolytic process, cellular response to oxidative stress, gluconeogenesis |
| 11 | *purA* | adenylosuccinate synthetase | purine nucleotide biosynthetic process, DNA damage response |
| 12 | *rbfA* | 30S ribosome binding factor | DNA damage response, ribosome biogenesis |
| 13 | *rfaC (waaC)* | ADP-heptose: LPS heptosyltransferase 1 | lipopolysaccharide core region biosynthetic process |
| 14 | *rfaD* | ADP-L-glycero-D-mannoheptose 6-epimerase | lipopolysaccharide core region biosynthetic process |
| 15 | *umuD* | DNA polymerase V protein UmuD | DNA damage response, SOS response |
| 16 | *ydcX (ortT)* | orphan toxin OrtT | autolysis |
| 17 | *yihE (srkA)* | stress response kinase A | response to stress, phosphorylation |

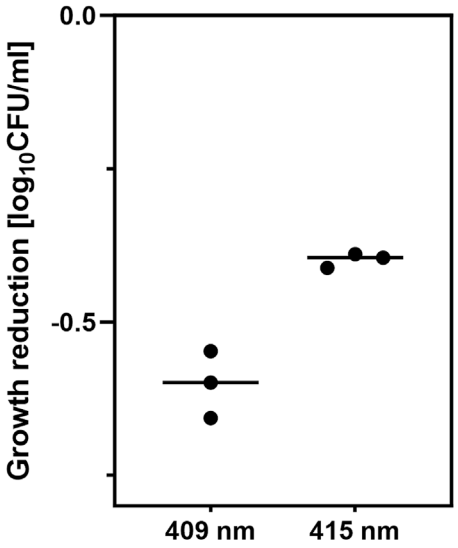


FIGURE 1
Growth reduction by aBL caused by 30 min of irradiation with two LED sources, 409 nm and 415 nm. The irradiation time was equal for both light sources. The experiments were performed in triplicate.

Prism version 9.0 (GraphPad Software, Inc., CA, United States). The significant differences between the groups were calculated using two-way analysis of variance (ANOVA) with $P < 0.05$ and Dunnett multiple comparison tests. The figures were prepared with BioRender.com (accessed on 27 May 2024).

## Selection of stable reference genes

This step was performed using 4 programs: geNorm (Vandesompele et al., 2002), BestKeeper (Pfaffl et al., 2004), NormFinder (Andersen et al., 2004), and RefFinder (Xie et al., 2012; Xie et al., 2023) with the comparative delta-Ct method (Silver et al., 2006). The obtained Cp values were used for the analysis performed with ReFinder and BestKeeper. For the analysis with geNorm and NormFinder, the Cp values were normalized according to the Cp of the control samples and the reaction efficiency for each primer pair. Four conditions for WT strain treatment were implemented in three biological and four technical repetitions: 0 and 40 min of resting without aBL treatment (control) and 40 min of resting after aBL 409 nm and aBL 415 nm treatment.

# Results

The results of the ReFinder reference gene analysis are presented in Table 2, the BestKeeper analysis in Table 3, and the geNorm and NormFinder analyses in Table 4. In Figure 2 distribution of reference gene data for threshold cycles was presented. The threshold cycle values for the most stable reference gene candidates were close to 20 for the best candidates (Figure 2).

## *ihfB* is the gene with the most stable expression after aBL treatment

The *ihfB* gene encoding the integration host factor β subunit was confirmed to be the best reference gene candidate for aBL treatment at both 409 and 415 nm. Three programs, RefFinder, geNorm, and NormFinder, indicated that this gene had the most stable expression in comparison to the other reference candidates. The next best candidates were *cysG, uidA* and *gyrA* with parameters similar to *ihfB* (Table 2). NormFinder revealed *ihfB* as the single gene and *cysG-gyrA* as the combination of reference genes with the greatest stability. The results from geNorm and NormFinder with data normalized according to the reaction efficiency and gene expression in the control were not comparable to the results of the algorithms used in RefFinder. However, in the final ranking, both approaches revealed the same genes as the best and worst candidates. ReFinder and BestKeeper were used to analyze the Cp values without normalization. BestKeeper was used to determine the reaction efficiency for analysis. According to the BestKeeper criteria, the standard deviation of Cp should be less than 1, the standard deviation of the regulation coefficient should be less than 2, and the correlation coefficient should be close to 1 for *arcA, cysG, idnT,* and *uidA,* with the best values observed for *cysG* (Table 3). According to geNorm and its automated settings, the most stable genes with M values less than 1.5 were arcA, *cysG, gyrA, hcaT, idnT, ihfB*, and uidA, while *ihfB* had the lowest value. M values above 1.5 was suggested as indicating the least stable candidates. NormFinder analysis revealed that only the *ihfB* gene met all the program criteria (Table 4). According to the comprehensive ranking and the delta Ct results calculated by RefFinder, *ihfB* was also the best candidate (Figure 3; Table 2).

## There were no statistically significant differences in gene expression between the aBL 409 and 415 nm treatments for most of the investigated genes

The expression levels of aBL-hypersensitive genes after aBL treatment at both wavelengths were statistically similar. A difference was noted only for the *oxyR* expression level. After aBL 409 nm irradiation, *oxyR* expression was significantly greater than that after aBL 415 nm treatment (Figures 4A, B).

## The expression of *dacA, fabH, rbfA, umuD, and yihE* increased after aBL treatment for both wavelengths of blue light

The patterns of gene expression changes after aBL irradiation at both wavelengths were similar. The expression levels of five of the seventeen genes, *dacA, fabH, rbfA, umuD,* and *yihE*, were significantly greater than those in the control. The expression levels of *purA* and *rfaC* increased only after treatment with aBL 409 nm. The greatest differences were noted for *fabH, purA, rbfA, umuD* and *yihE*. The remaining genes investigated, *cpxA, deoB, dnaJ, dnaK, gmhB, hldE, oxyR, pgi, rfaD, and ydcX,* were not expressed at significantly higher levels (Figures 4C, D).

TABLE 2 ReFinder analysis results.

| Gene | Comprehensive ranking (Geomean ranking values) | Delta Ct method (average of standard deviation) | Bestkeeper Cp (standard deviation) | NormFinder (stability value) | geNorm (stability value) |
|---|---|---|---|---|---|
| *arcA* | 4.56 | 1.56 | 0.78 | 1.001 | 1.235 |
| *cysG* | 2.45 | 1.4 | 0.667 | 0.708 | 1.098 |
| *gyrA* | 4.86 | 1.48 | 1.19 | 0.847 | 1.182 |
| *hcaT* | 8 | 1.72 | 1.49 | 1.345 | 1.348 |
| *idnT* | 3.16 | 1.49 | 1 | 0.954 | 0.793 |
| *ihfB* | 1.57 | 1.31 | 1.14 | 0.625 | 0.793 |
| *rpoA* | 9 | 1.89 | 1.51 | 1.579 | 1.435 |
| *rssA* | 7.65 | 1.68 | 1.67 | 1.23 | 1.287 |
| *uidA* | 2.45 | 1.4 | 0.83 | 0.692 | 0.969 |
| *uxuR* | 8.41 | 2.45 | 1.06 | 2.257 | 1.639 |

TABLE 3 BestKeeper analysis results. Bold values meet the criteria set by the program.

| | *arcA* | *cysG* | *gyrA* | *hcaT* | *idnT* | *ihfB* | *rpoA* | *rssA* | *uidA* | *uxuR* |
|---|---|---|---|---|---|---|---|---|---|---|
| n | 12 | 12 | 12 | 12 | 12 | 12 | 12 | 12 | 12 | 12 |
| geo Mean [CP] | 21.19 | 21.51 | 22.65 | 24.90 | 26.68 | 19.29 | 17.07 | 21.68 | 24.17 | 22.47 |
| ar Mean [CP] | 21.21 | 21.53 | 22.70 | 24.96 | 26.71 | 19.34 | 17.15 | 21.75 | 24.19 | 22.51 |
| min [CP] | 19.57 | 19.89 | 20.50 | 22.28 | 24.63 | 17.66 | 14.47 | 19.58 | 22.61 | 19.81 |
| max [CP] | 22.62 | 23.26 | 24.87 | 27.99 | 28.77 | 21.93 | 20.00 | 24.07 | 26.78 | 24.82 |
| std dev [±CP] | **0.80** | **0.69** | 1.28 | 1.57 | **0.95** | 1.14 | 1.39 | 1.59 | **0.80** | 1.03 |
| CV [% CP] | 3.77 | 3.21 | 5.65 | 6.28 | 3.55 | 5.89 | 8.10 | 7.31 | 3.30 | 4.57 |
| min [x-fold] | −3.04 | −2.93 | −3.78 | −5.28 | −4.30 | −3.09 | −5.78 | −4.00 | −3.23 | −5.77 |
| max [x-fold] | 2.67 | 3.19 | 3.94 | 7.13 | 4.40 | 6.24 | 7.20 | 4.84 | 7.13 | 4.75 |
| std dev [±x-fold] | **1.73** | **1.60** | 2.41 | 2.93 | **1.91** | 2.18 | 2.59 | 2.97 | **1.73** | 2.02 |
| coeff. of corr. [r] | 0.526 | **0.723** | 0.82 | 0.712 | 0.746 | **0.955** | 0.665 | **0.878** | 0.673 | −0.506 |
| p value | 0.078 | 0.008 | 0.001 | 0.009 | 0.005 | 0.001 | 0.018 | 0.001 | 0.016 | 0.092 |

## Discussion

Ogonowska et al. (2020) reported that there is no information about the selection of suitable reference genes under aPDI. In the study, the authors provided a list of candidate reference genes stably expressed under aPDI mediated with two different photosensitizers. First, they selected *gmk* and *ftsZ* for rose bengal-mediated aPDI with the use of green light and *ftsZ, proC*, and *fabD* for new methylene blue-mediated aPDI with the use of red light. Next, the research group used the selected stable reference gene candidates for measuring the expression levels of the *Staphylococcus aureus* enterotoxin b gene (*seb*) under two photodynamic treatment conditions (Ogonowska and Nakonieczna, 2020).

Because there are no published data on *E. coli* genes that are stable under aBL treatment, the present study aimed to identify a stable reference gene after aBL treatment at two light wavelengths, 409 and 415 nm, to investigate the role of the gene in antimicrobial mechanisms. To our knowledge, no such candidate stable gene

10.3389/fmolb.2024.1467726

TABLE 4 Results of the geNorm and NormFinder reference gene analyses. Bold values meet the criteria set by the program.

| Gene | geNorm - M value | NormFinder - stability value |
|---|---|---|
| *arcA* | **1.446** | 0.232 |
| *cysG* | **1,312** | 0.211 |
| *gyrA* | **1.410** | 0.190 |
| *hcaT* | 1.648 | 0.232 |
| *idnT* | **1.403** | 0.252 |
| *ihfB* | **1.258** | **0.158** |
| *rpoA* | 1.755 | 0.200 |
| *rssA* | 1.506 | 0.262 |
| *uidA* | **1.421** | 0.216 |
| *uxuR* | 2.333 | 0.310 |
| *cysG-gyrA* | - | 0.127 |

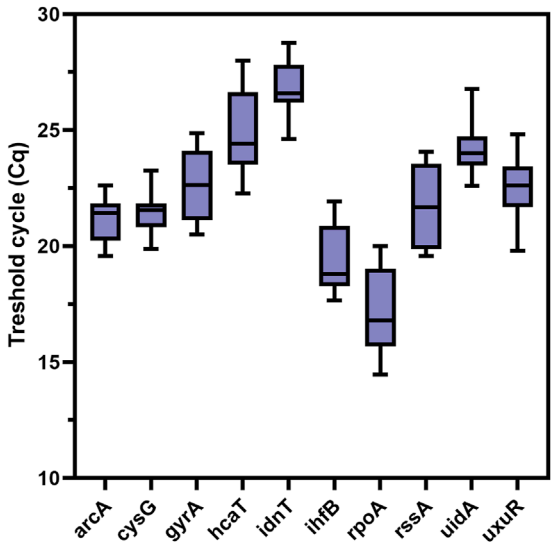


FIGURE 2
Distribution of reference gene data for threshold cycles.

has been reported to date. We found several studies evaluating stable genes whose expression does not vary under various stress conditions in *E. coli* and investigated whether these genes are also stable under blue light stress, which has a multitarget mode of action. Peng et al. (2014) evaluated the genes *hcaT* (encoding a uroporphyrin III C-methyltransferase), *cysG* (encoding a 3-phenylpropionic transporter) and *rssA* (encoding a 16S ribosomal RNA) as reference gene candidates whose expression is stable under salt and organic acid stress. RNA was isolated from bacteria in the stationary phase of growth, and the results were analyzed using the BestKeeper tool. The most stable gene was *rssA, and* the least stable gene was *cysG* (Peng et al., 2014). In our study, the stability tendency after aBL treatment was the opposite, where *cysG* was a better candidate reference gene than *rssA* and *hcaT*. In another study, Zhou et al. (2011) identified novel reference genes for testing gene transcription in recombinant protein-producing *E. coli.* Two bioinformatics tools were used: geNorm and NormFinder. The researchers tested the expression of twenty genes at 28°C and 37°C under different induction conditions. The analysis revealed three genes as the most reliable: *cysG, hcaT* and *idnT* (encoding the L-idonate/5-ketogluconate/gluconate transporter). Moreover, the *rssA* and *ihfB* genes (encoding the integration host factor subunit β) were unstable under different growth temperatures and induction conditions. The following results also do not correspond to our studies on aBL (Zhou et al., 2011). Studies by Teixeira et al. (2016) investigated stable gene expression after laser irradiation (660 and 808 nm) at different fluences. Gene expression of *E. coli genes* in the exponential growth phase was studied. The BestKeeper, geNorm and NormFinder programs were used for stability analysis. When comparing the cycle-threshold values, no significant difference was noted in the expression of the reference genes for the irradiated sample and controls. However, Excel-based tools did not demonstrate the stability of *arcA, gyrA,* or *rpoA* expression after red and infrared laser treatment. The authors suggested that the investigated conditions modulated the mRNA levels of the tested reference genes (Teixeira et al., 2016). Our analysis revealed that *arcA, gyrA, and rpoA* are also not the best reference gene candidates for aBL treatment. In another study conducted by Walker et al. (2017), three genes, namely, *ybbW* (encoding allantoin transporter), *uidA* (encoding β-D-glucuronidase) and *clpB* (encoding chaperone protein ClpB), were considered targets for detecting *E. coli* contamination in water. In the tested isolates, *ybbW* was detected by qPCR, while other investigated genes were not detected in any of the tested isolates (Walker et al., 2022).

In our previous studies, we screened for aBL sensitivity among *E. coli* mutants lacking nonessential genes. Among them, we identified 64 aBL-hypersensitive genes important in the bacterial response to blue light (Kruszewska-Naczk et al., 2024). In this study, 17 of the 64 aBL-hypersensitive genes were selected for gene expression analysis (*cpxA, deoB, dnaK, dnaJ, oxyR, pgi, purA, rbfA, umuD, ydcX,* and *yihE*, whose deletion resulted in hypersensitivity to aBL in single-gene Keio mutants and 6 additional genes (*rfaC, rfaD, dacA, fabH, gmhB,* and *hldE* that could potentially contribute to the development of resistance). Previous studies utilized mutants complemented with the deleted genes (11 complementation mutants with restored gene function). Complementation not only restored wild-type sensitivity to aBL but, in some cases, rendered mutants less sensitive to aBL than the wild-type strain (Kruszewska-Naczk et al., 2024).

These included genes from several categories depending on the function of the encoded protein: response to DNA damage, oxidative stress response, lipopolysaccharide production, fatty acid metabolic process, response to cell envelope stress, autolysis, radiation, heat, and SOS response. Four investigated genes were involved in the biosynthesis of the lipopolysaccharide core region (*gmhB, hldE, rfaC, and rfaD*), and only one of them, *rfaC,* was significantly highly expressed. Not all investigated genes responsible for the response to DNA damage were characterized by significantly increased expression. The expression levels of *purA, rbfA* and *umuD* were

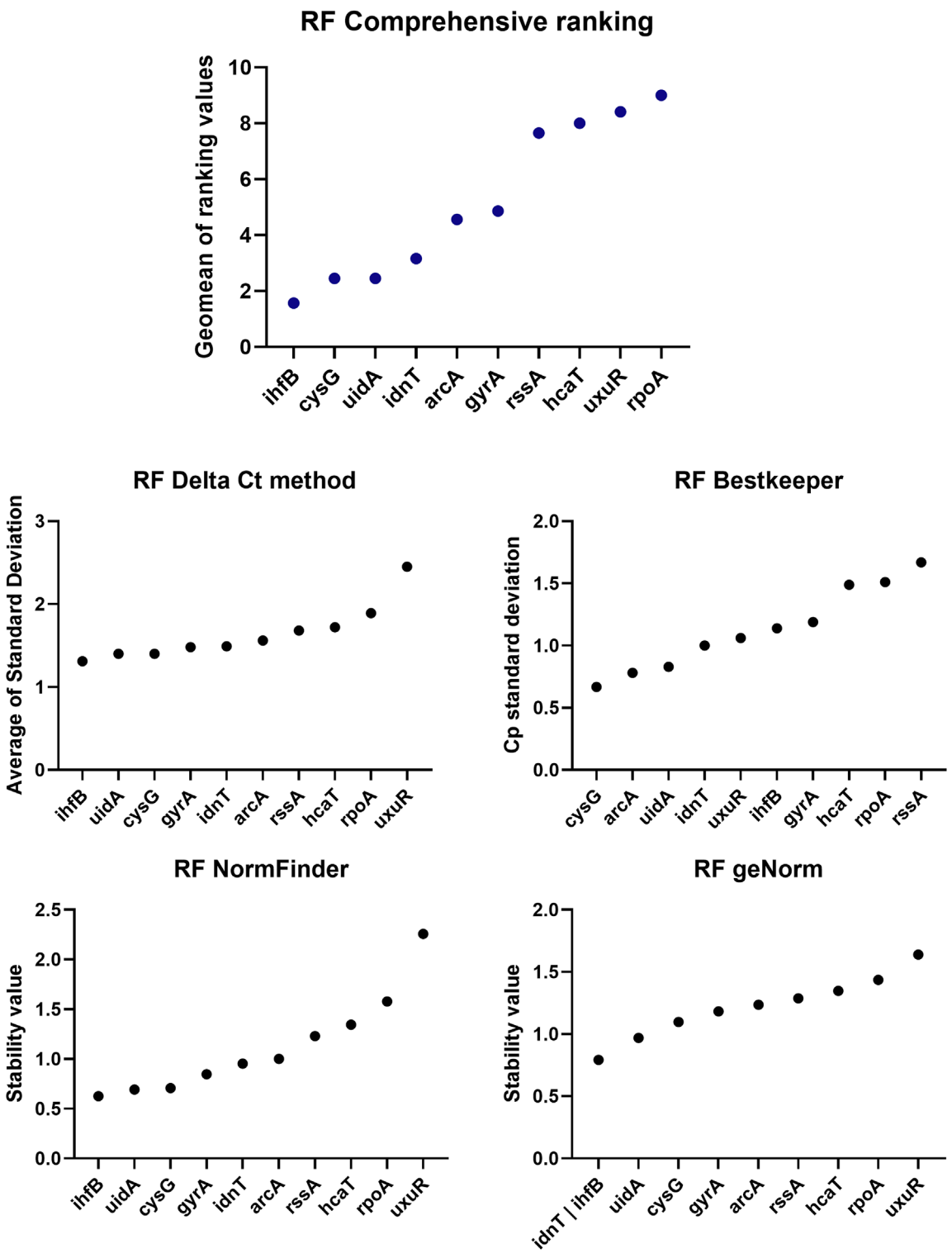


FIGURE 3
ReFinder (RF) analysis results. The comprehensive ranking consolidates all results into a single plot, utilizing the methodologies implemented in the ReFinder program.

greater than those of *deoB* and *oxyR*. This may suggest that not all repair systems are engaged in cell protection against aBL at sublethal doses of irradiation. The expression pattern may differ under higher light doses, as bacteria employ more strategies to survive light stress.

Stress generation can be observed through the expression of *yihE*, which encodes stress response kinase A (SrkA). This kinase exhibits autophosphorylation activity at serine and threonine residues (Zheng et al., 2007). SrkA is also regulated by the CpxR

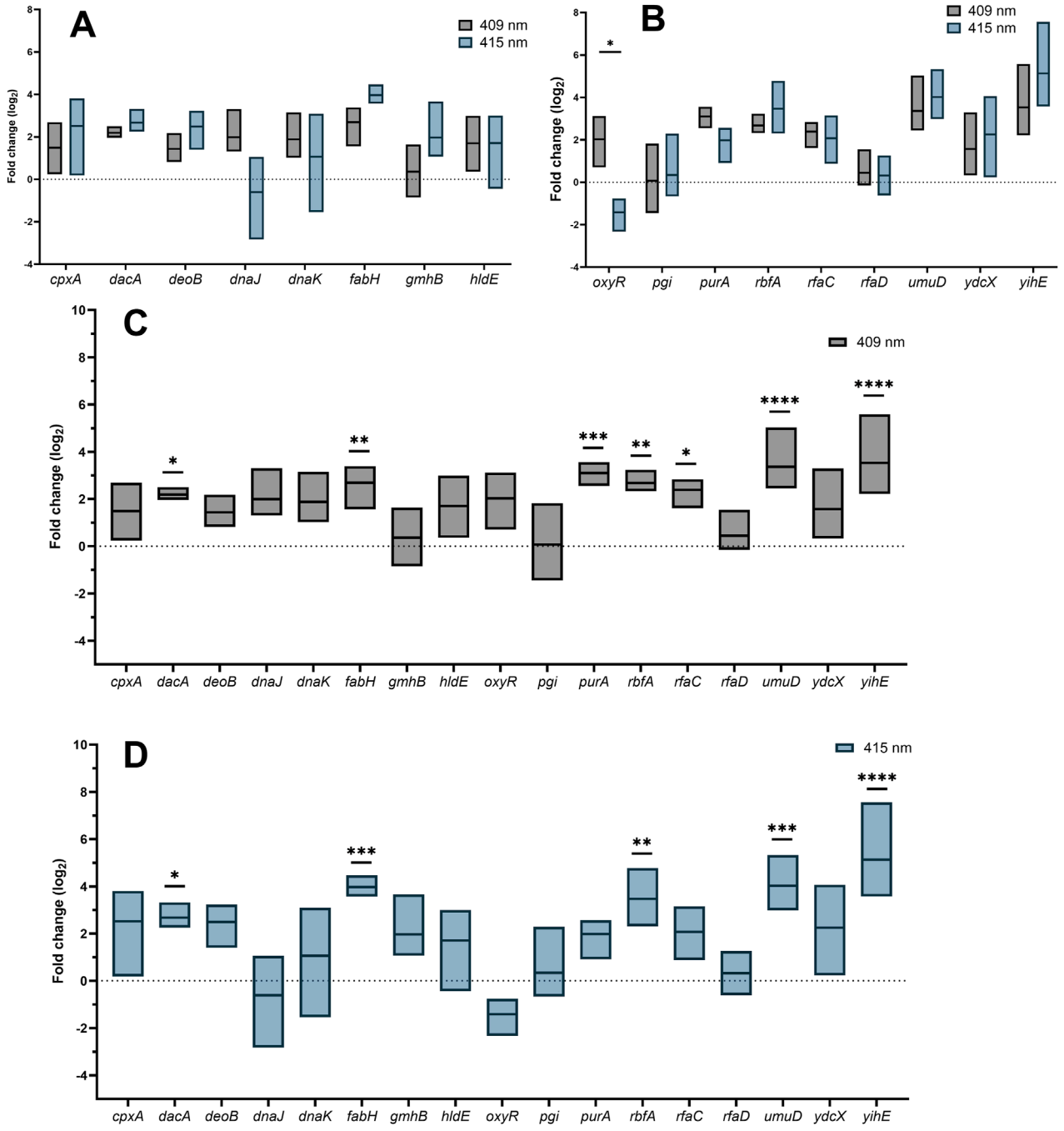


FIGURE 4
**(A, B)** Comparison of gene expression between *E. coli* treated with 409 nm and 415 nm aBL. Fold change in the expression of investigated genes after treatment with 409 nm **(C)** and 415 nm **(D)** aBL. P values indicating statistical significance are indicated with asterisks (ns $P > 0.05$;*$P < 0.05$;**$P < 0.01$;***$P < 0.001$;****$P \leq 0.0001$).

system, which is a part of the cellular response to many types of environmental stresses that lead to bacterial adaptation (Zhao et al., 2022). Additionally, *fabH* was expressed at significantly higher levels. This gene plays a significant role in the process of fatty acid biosynthesis. This is one of the targets of novel antimicrobial agents, including carbazole derivatives, dioxygenated amide derivatives, and Platencin (Chen et al., 2024; Chang et al., 2024; Wang et al., 2007).

Our previous study results (Kruszewska-Naczk et al., 2024) suggested that cell protection against aBL is an active process, which means that it has an energy cost for bacterial cells. During aBL irradiation, bacteria can actively produce ATP and use the energy reservoir fatty acids, which leads to the activation of genes that synthesize the depleted fatty acids (Olukoshi and Packter, 1994).

Fatty acids can also act as signal molecules that may be involved in the activation of cellar protective pathways. Moreover, fatty acids are a component of bacterial membranes. Chu et al. (2019) revealed that aBL causes damage to fatty acids via oxidation. Changes in cellular fatty acid profiles were also confirmed, along with a

decrease in the amount of unsaturated fatty acids (Chu et al., 2019). Wu et al. (2018) demonstrated changes in membrane permeability after aBL treatment. Research conducted by dos Anjos et al. (2023) indicated changes in bacterial shape after aBL treatment, suggesting membrane damage.

Another highly expressed gene was *umuD*, which is involved in the bacterial SOS response. The UmuD′2C protein complex is an error-prone DNA polymerase, and RecA interacts with the DNA polymerase III holoenzyme, which repairs DNA damage. UmuD′2C has been reported to act as a DNA damage checkpoint system and regulate the appropriate timing and level of DNA synthesis in bacteria under DNA damage stress (Frank et al., 1993; Sutton et al., 1999). This may also confirm that aBL causes DNA damage and activation of repair systems. For instance, dos Anjos et al. (2023) observed DNA degradation upon aBL treatment.

*dacA* was another highly expressed gene after aBL irradiation. DacA, i.e., penicillin-binding protein 5 (PBP5), is involved in the synthesis of peptidoglycan and is also responsible for cell shape (Nelson and Young, 2000). Additionally, deletion of this gene sensitizes bacteria to penicillin (Sarkar et al., 2010). The results presented by Choi et al. (2023) indicated that DacA plays a crucial role in growth under salt stress and a secondary role in bacterial growth under alkaline stress conditions. *dacA* may play a significant role in bacterial protection against aBL because aBL causes cell wall deformations that can be repaired by DacA (Zhang et al., 2016).

Contrary to the findings of Walker et al. (2022), we did not observe increased expression of *dnaK*, which is involved in the heat stress response. Previous studies reported the upregulation of the *dnaK* gene in *Campylobacter jejuni* treated with aBL at 405 nm (Walker et al., 2017).

An equal irradiation time for both wavelengths was used to compare changes in gene expression so that bacteria had the same amount of time to activate the expression of protective genes. The survival efficiency of bacteria after exposure was also similar. However, the light sources differed in terms of irradiance. The irradiance of the 409 nm LED was 5.2 mW/cm$^2$, while that of the 415 nm LED was 25 mW/cm$^2$. Compared with those of the control, significantly greater levels of gene expression were detected for the light source with a wavelength of 409 nm and lower irradiance. The difference in the gene expression pattern between the two wavelengths may be due to a shift in the absorption peak of endogenous porphyrins, which results in the activation of additional cell protection mechanisms, resulting in the expression of more genes at 409 nm aBL (Figures 4A-D). Notably, statistical comparison of expression levels between the two light sources revealed differences only for *oxyR* (Figures 4A-D). The expression level of this gene was greater for 409 nm aBL than for 415 nm aBL. The OxyR regulon controls the expression of genes involved in the oxidative stress response (Tartaglia et al., 1989). One hypothesis to explain why the expression level of *oxyR* may be greater for 409 nm aBL is that it likely generates more ROS than 415 nm aBL. However, this should be checked using a special detection probe.

In summary, there are no universal reference genes whose expression does not vary and is applicable under every stress condition. Therefore, there is a need to evaluate reference genes for every tested stressor. For aBL at different wavelengths, we found universal genes with stable expression after irradiation.

## Data availability statement

The data presented in the study are deposited in the Zenodo repository: https://zenodo.org/records/14506916.

## Author contributions

BK-N: Conceptualization, Data curation, Formal Analysis, Funding acquisition, Investigation, Methodology, Project administration, Software, Validation, Visualization, Writing–original draft. MG: Supervision, Writing–review and editing. AR-Z: Funding acquisition, Methodology, Resources, Supervision, Validation, Writing–original draft.

## Funding

The author(s) declare that financial support was received for the research, authorship, and/or publication of this article. This work was supported by UGrants-start 533-BGB0-GS52-24 (B.K-N) and National Science Centre under grant no. 2022/47/D/NZ7/01795 (A.R-Z).

## Acknowledgments

The authors thank the National BioResource Project (NBRP, NIG, Japan) for contributing to our work by providing the *E. coli* BW25113 strain (*E. coli* Keio knockout parent strain mutants from the Keio collection). The figures were prepared with the use of BioRender.com (accessed on 27 May 2024).

## Conflict of interest

The authors declare that the research was conducted in the absence of any commercial or financial relationships that could be construed as a potential conflict of interest.

## Publisher's note



## Supplementary material

The Supplementary Material for this article can be found online at: https://www.frontiersin.org/articles/10.3389/fmolb.2024.1467726/full#supplementary-material

# References


Andersen, C. L., Jensen, J. L., and Ørntoft, T. F. (2004). Normalization of real-time quantitative reverse transcription-PCR data: a model-based variance estimation approach to identify genes suited for normalization, applied to bladder and colon cancer data sets. *Cancer Res.* 64 (15), 5245–5250. doi:10.1158/0008-5472.CAN-04-0496

Baba, T., Ara, T., Hasegawa, M., Takai, Y., Okumura, Y., Baba, M., et al. (2006). Construction of Escherichia coli K-12 in-frame, single-gene knockout mutants: the Keio collection. *Mol. Syst. Biol.* 2 (1), 2006.0008–0008. doi:10.1038/msb4100050

Chang, H., Ji, R., Zhu, Z., Wang, Y., Yan, S., He, D., et al. (2024). Target identification, and optimization of dioxygenated amide derivatives as potent antibacterial agents with FabH inhibitory activity. *Eur. J. Med. Chem.* 265, 116064. doi:10.1016/j.ejmech.2023.116064

Chen, C. H., Liu, C. S., Guo, X. M., Tong, J. P., Huang, J., Shi, T. T., et al. (2024). Design, synthesis, and biological evaluation of carbazole derivatives as potent antibacterial agents targeting membrane function via FabH Inhibition. *J. Mol. Struct.* 1306, 137891. doi:10.1016/j.molstruc.2024.137891

Choi, U., Park, S. H., Lee, H. B., Son, J. E., and Lee, C. R. (2023). Coordinated and distinct roles of peptidoglycan carboxypeptidases DacC and DacA in cell growth and shape maintenance under stress conditions. *Microbiol. Spectr.* 11 (3), e00014-e00023. doi:10.1128/spectrum.00014-23

Chu, Z., Hu, X., Wang, X., Wu, J., Dai, T., and Wang, X. (2019). Inactivation of Cronobacter sakazakii by blue light illumination and the resulting oxidative damage to fatty acids. *Can. J. Microbiol.* 65 (12), 922–929. doi:10.1139/cjm-2019-0054

dos Anjos, C., Leanse, L. G., Ribeiro, M. S., Sellera, F. P., Dropa, M., Arana-Chavez, V. E., et al. (2023). New insights into the bacterial targets of antimicrobial blue light. *Microbiol. Spectr.* 11 (2), 028333-e2922. doi:10.1128/spectrum.02833-22

English, B. K., and Gaur, A. H. (2010) "The use and abuse of antibiotics and the development of antibiotic resistance," in *Hot topics in infection and immunity in children*. Editors A. Finn, N. Curtis, and A. Pollard (New York, NY: Springer). VI, 73–82.

Enwemeka, C. S. (2013). Antimicrobial blue light: an emerging alternative to antibiotics. *Photomed. Laser Surg.* 31, 509–511. doi:10.1089/pho.2013.9871

Frank, E. G., Hauser, J., Levine, A. S., and Woodgate, R. (1993). Targeting of the UmuD, UmuD', and MucA'mutagenesis proteins to DNA by RecA protein. *Proc. Natl. Acad. Sci.* 90 (17), 8169–8173. doi:10.1073/pnas.90.17.8169

Gomes, A. É. I., Stuchi, L. P., Siqueira, N. M. G., Henrique, J. B., Vicentini, R., Ribeiro, M. L., et al. (2018). Selection and validation of reference genes for gene expression studies in *Klebsiella pneumoniae* using Reverse Transcription Quantitative real-time PCR. *Sci. Rep.* 8 (1), 9001. doi:10.1038/s41598-018-27420-2

Guenin, S., Mauriat, M., Pelloux, J., Van Wuytswinkel, O., Bellini, C., and Gutierrez, L. (2009). Normalization of qRT-PCR data: the necessity of adopting a systematic, experimental conditions-specific, validation of references. *J. Exp. Bot.* 60 (2), 487–493. doi:10.1093/jxb/ern305

Hawkey, P. M. (2008). The growing burden of antimicrobial resistance. *J. Antimicrob. Chemother.* 62 (Suppl. l_1), i1–i9. doi:10.1093/jac/dkn241

Kruszewska-Naczk, B., Grinholc, M., Waleron, K., Bandow, J. E., and Rapacka-Zdończyk, A. (2024). Can antimicrobial blue light contribute to resistance development? Genome-wide analysis revealed aBL-protective genes in *Escherichia coli*. *Microbiol. Spectr.* 12 (1), e0249023–23. doi:10.1128/spectrum.02490-23

Lu, M., Wang, S., Wang, T., Hu, S., Bhayana, B., Ishii, M., et al. (2021). Bacteria-specific phototoxic reactions triggered by blue light and phytochemical carvacrol. *Sci. Transl. Med.* 13 (575), eaba3571. doi:10.1126/scitranslmed.aba3571

Nelson, D. E., and Young, K. D. (2000). Penicillin binding protein 5 affects cell diameter, contour, and morphology of *Escherichia coli*. *J. Bacteriol.* 182 (6), 1714–1721. doi:10.1128/JB.182.6.1714-1721.2000

Ogonowska, P., and Nakonieczna, J. (2020). Validation of stable reference genes in *Staphylococcus aureus* to study gene expression under photodynamic treatment: a case study of SEB virulence factor analysis. *Sci. Rep.* 10 (1), 16354. doi:10.1038/s41598-020-73409-1

Olukoshi, E. R., and Packter, N. M. (1994). Importance of stored triacylglycerols in Streptomyces: possible carbon source for antibiotics. *Microbiology* 140 (4), 931–943. doi:10.1099/00221287-140-4-931

O'Neill, J. (2016). *Tackling drug-resistant infections globally: final report andRecommendations–the review on antimicrobial resistance chaired by jim O'neill*. London: Wellcome Trust and HM Government.

Peng, S., Stephan, R., Hummerjohann, J., and Tasara, T. (2014). Evaluation of three reference genes of *Escherichia coli* for mRNA expression level normalization in view of salt and organic acid stress exposure in food. *FEMS Microbiol. Lett.* 355 (1), 78–82. doi:10.1111/1574-6968.12447

Pfaffl, M. W. (2001). A new mathematical model for relative quantification in real-time RT-PCR. *Nucleic Acids Res.* 29 (9), 45e–45e. doi:10.1093/nar/29.9.e45

Pfaffl, M. W., Tichopad, A., Prgomet, C., and Neuvians, T. P. (2004). Determination of stable housekeeping genes, differentially regulated target genes and sample integrity: BestKeeper–Excel-based tool using pair-wise correlations. *Biotechnol. Lett.* 26, 509–515. doi:10.1023/b:bile.0000019559.84305.47

Robinson, T. P., Bu, D. P., Carrique-Mas, J., Fèvre, E. M., Gilbert, M., Grace, D., et al. (2016). Antibiotic resistance is the quintessential One Health issue. *Trans. R. Soc. Trop. Med. Hyg.* 110 (7), 377–380. doi:10.1093/trstmh/trw048

Sarkar, S. K., Chowdhury, C., and Ghosh, A. S. (2010). Deletion of penicillin-binding protein 5 (PBP5) sensitises *Escherichia coli* cells to beta-lactam agents. *Int. J. Antimicrob. agents* 35 (3), 244–249. doi:10.1016/j.ijantimicag.2009.11.004

Silver, N., Best, S., Jiang, J., and Thein, S. L. (2006). Selection of housekeeping genes for gene expression studies in human reticulocytes using real-time PCR. *BMC Mol. Biol.* 7, 33–39. doi:10.1186/1471-2199-7-33

Sutton, M. D., Opperman, T., and Walker, G. C. (1999). The *Escherichia coli* SOS mutagenesis proteins UmuD and UmuD' interact physically with the replicative DNA polymerase. *Proc. Natl. Acad. Sci. U. S. A.* 96 (22), 12373–12378. doi:10.1073/pnas.96.22.12373

Tartaglia, L. A., Storz, G., and Ames, B. N. (1989). Identification and molecular analysis of oxyR-regulated promoters important for the bacterial adaptation to oxidative stress. *J. Mol. Biol.* 210 (4), 709–719. doi:10.1016/0022-2836(89)90104-6

Teixeira, A. F., Machado, Y. L. R. C., Fonseca, A. S., and Mencalha, A. L. (2016). Low-level lasers and mRNA levels of reference genes used in *Escherichia coli*. *Laser Phys. Lett.* 13 (11), 115602. doi:10.1088/1612-2011/13/11/115602

Vandesompele, J., De Preter, K., Pattyn, F., Poppe, B., Van Roy, N., De Paepe, A., et al. (2002). Accurate normalization of real-time quantitative RT-PCR data by geometric averaging of multiple internal control genes. *Genome Biol.* 3, RESEARCH0034–12. doi:10.1186/gb-2002-3-7-research0034

Wainwright, M., Maisch, T., Nonell, S., Plaetzer, K., Almeida, A., Tegos, G. P., et al. (2017). Photoantimicrobials—are we afraid of the light? *Lancet Infect. Dis.* 17 (2), e49–e55. doi:10.1016/S1473-3099(16)30268-7

Walker, D. I., McQuillan, J., Taiwo, M., Parks, R., Stenton, C. A., Morgan, H., et al. (2017). A highly specific *Escherichia coli* qPCR and its comparison with existing methods for environmental waters. *Water Res.* 126, 101–110. doi:10.1016/j.watres.2017.08.032

Walker, P., Taylor, A. J., Hitchcock, A., Webb, J. P., Green, J., Weinstein, J., et al. (2022). Exploiting violet-blue light to kill Campylobacter jejuni: analysis of global responses, modeling of transcription factor activities, and identification of protein targets. *Msystems* 7 (4), e0045422–22. doi:10.1128/msystems.00454-22

Wang, J., Kodali, S., Lee, S. H., Galgoci, A., Painter, R., Dorso, K., et al. (2007). Discovery of platencin, a dual FabF and FabH inhibitor with *in vivo* antibiotic properties. *Proc. Natl. Acad. Sci.* 104 (18), 7612–7616. doi:10.1073/pnas.0700746104

Wang, Y., Li, J., Zhou, Z., Zhou, R., Sun, Q., and Wu, P. (2021). Halo-fluorescein for photodynamic bacteria inactivation in extremely acidic conditions. *Nat. Commun.* 12 (1), 526. doi:10.1038/s41467-020-20869-8

Wang, Y., Wang, Y., Wang, Y., Murray, C. K., Hamblin, M. R., Hooper, D. C., et al. (2017). Antimicrobial blue light inactivation of pathogenic microbes: state of the art. *Drug Resist. Updat.* 33, 1–22. doi:10.1016/j.drup.2017.10.002

Woc-Colburn, L., and Francisco, D. M. A. (2020). "Multidrug resistance bacterial infection," in *Highly infectious diseases in critical care* (Cham: Springer), 139–146.

Wu, J., Chu, Z., Ruan, Z., Wang, X., Dai, T., and Hu, X. (2018). Changes of intracellular porphyrin, reactive oxygen species, and fatty acids profiles during inactivation of methicillin-resistant *Staphylococcus aureus* by antimicrobial blue light. *Front. Physiology* 9, 1658. doi:10.3389/fphys.2018.01658

Xie, F., Wang, J., and Zhang, B. (2023). RefFinder: a web-based tool for comprehensively analyzing and identifying reference genes. *Funct. & Integr. Genomics* 23 (2), 125. doi:10.1007/s10142-023-01055-7

Xie, F., Xiao, P., Chen, D., Xu, L., and Zhang, B. (2012). miRDeepFinder: a miRNA analysis tool for deep sequencing of plant small RNAs. *Plant Mol. Biol.* 80, 75–84. doi:10.1007/s11103-012-9885-2

Zhang, Y., Zhu, Y., Chen, J., Wang, Y., Sherwood, M. E., Murray, C. K., et al. (2016). Antimicrobial blue light inactivation of Candida albicans: *in vitro* and *in vivo* studies. *Virulence* 7 (5), 536–545. doi:10.1080/21505594.2016.1155015

Zhao, Z., Xu, Y., Jiang, B., Qi, Q., Tang, Y. J., Xian, M., et al. (2022). Systematic identification of CpxRA-regulated genes and their roles in *Escherichia coli* stress response. *Msystems* 7 (5), e00419-e00422. doi:10.1128/msystems.00419-22

Zheng, J., He, C., Singh, V. K., Martin, N. L., and Jia, Z. (2007). Crystal structure of a novel prokaryotic Ser/Thr kinase and its implication in the Cpx stress response pathway. *Mol. Microbiol.* 63 (5), 1360–1371. doi:10.1111/j.1365-2958.2007.05611.x

Zhou, K., Zhou, L., Lim, Q. E., Zou, R., Stephanopoulos, G., and Too, H. P. (2011). Novel reference genes for quantifying transcriptional responses of *Escherichia coli* to protein overexpression by quantitative PCR. *BMC Mol. Biol.* 12, 18–19. doi:10.1186/1471-2199-12-18

## 8.4.1. Supplementary Materials

Table S1. List of primers used in the study.

| Reference genes | | | |
|---|---|---|---|
| Number | Gene | Forward primer | Reverse primer |
| 1. | *arcA* | AACGGCTGTTGATGTCCAGT | GCAACCTACTGTCCCGTACC |
| 2. | *cysG* | TTGTCGGCGGTGGTGATGTC | ATGCGGTGAACTGTGGAATAAACG |
| 3. | *gyrA* | ACGCGACTTGGTTGGGTATT | GTCTCTCTGATCGTGCCTCG |
| 4. | *hcaT* | GCTGCTCGGCTTTCTCATCC | CCAACCACGCTGACCAACC |
| 5. | *idnT* | CTGTTTAGCGAAGAGGAGATGC | ACAAACGGCGGCGATAGC |
| 6. | *ihfB* | CACCCAGCAATCGCACATTC | GTCGAGGCCATATGCTCCAG |
| 7. | *rpoA* | ACGACGAATCGCCTCTTCAG | CGTGTAGAACAGCGTACCGA |
| 8. | *rssA* | GATGGATCTCTCCTGGCAGC | TCCGGCATTATTTCGCGGTA |
| 9. | *uidA* | TTGTCCAGTTGCAACCACCT | AGACTGTAACCACGCGTCTG |
| 10. | *uxuR* | AAATGCTTGATGTCACGCGG | CGTACTTCCACCAGCCCTTT |
| Investigated genes | | | |
| Number | Gene name | Forward Primer | Reverse Primer |
| 1. | *cpxA* | CCAAACCTGTACCGCCAGAT | CGCGAACAGATTTTCCGTCC |
| 2. | *dacA* | CGGTTCAGAGGCGAACTCTT | CTAACCTGGGGCTTCCGTTT |
| 3. | *deoB* | CTGCCAAATCTGACCCGTCT | CGATAACTTCAGCGTTGCCG |
| 4. | *dnaK* | ATGACCTGGGTGGTGGTACT | CGTTGGTTGCCAGAACTTCG |
| 5. | *dnaJ* | GCCGCTAAGCAAGATTATTACGA | CCGCGGGTCAGGTCGTCAAAAAA |
| 6. | *fabH* | GCGCACATCGTTGATGAGAC | AGGTTAGCCTGATGCGGAAC |

| | | | |
|---|---|---|---|
| 7. | *gmhB* | CATCCGCAGGGTAGTGTTGA | CGTGCTGACAAAAGCATCCC |
| 8. | *hldE* | TTGACGGCAACAATCAAGCG | GGTGATGACCAACGGTGTCT |
| 9. | *oxyR* | GCCAATATTCGTGATCTTGAGTA | CCAACCGCCTGTTTTAAAACTTT |
| 10. | *pgi* | AGCTCTGCGTCCGTACAAAA | CAAGAACAGCGTGGTTTCCG |
| 11. | *purA* | ACAACGCAGGCCATACTCTC | ACCGTTACCGATGATGCTGG |
| 12. | *rbfA* | CGTCATGTTTGACCACGCTG | TGCCGGAACTGACCTTCTTC |
| 13. | *rfaC (waaC)* | TGGGCGATGTTCTCCATACG | TCTGTGCGAACCCTTCTTCC |
| 14. | *rfaD* | GCGTCGCTTTCCATCTCAAC | CCACATAGACGAAGTCGCGT |
| 15. | *umuD* | GCCCGACGGTACAGCTTATT | ACACCAAAGACATCCAGCGT |
| 16. | *ydcX (ortT)* | TGCGGTTATGGCAGCAATCG | ATGTTGCCCCCACCAGAAAG |
| 17. | *yihE (srkA)* | TATTCTCTGGCGCGATGGTC | GCTCGGCTTTATCGCCATTG |

Table S2. Parameters for validation of the qPCR for each gene.

| Reference genes | | | | |
|---|---|---|---|---|
| Number | Gene | Slope | Efficiency | Efficiency [%] |
| 1. | *arcA* | -3,361 | 1,984 | 99,2 |
| 2. | *cysG* | -3,478 | 1,939 | 96,95 |
| 3. | *gyrA* | -3,725 | 1,856 | 92,8 |
| 4. | *hcaT* | -3,619 | 1,889 | 94,45 |
| 5. | *idnT* | -3,24 | 2,035 | 101,75 |
| 6. | *ihfB* | -3,325 | 1,999 | 99,95 |
| 7. | *rpoA* | -3,415 | 1,962 | 98,1 |
| 8. | *rssA* | -3,485 | 1,936 | 96,8 |
| 9. | *uidA* | -3,061 | 2,122 | 106,1 |
| 10. | *uxuR* | 3,48 | 1,936 | 96,8 |
| Investigated genes | | | | |
| Number | Gene | Slope | Efficiency | Efficiency [%] |
| 1. | *cpxA* | -3,492 | 1,934 | 96,7 |
| 2. | *dacA* | -3,292 | 2,013 | 100,65 |

| | | | | |
|---|---|---|---|---|
| 3. | *deoB* | -3,014 | 2,147 | 107,35 |
| 4. | *dnaK* | -3,397 | 1,97 | 98,5 |
| 5. | *dnaJ* | -3,918 | 1,8 | 90 |
| 6. | *fabH* | -3,58 | 1,903 | 95,15 |
| 7. | *gmhB* | -3,336 | 1,994 | 99,7 |
| 8. | *hldE* | -3,157 | 2,074 | 103,7 |
| 9. | *oxyR* | -3,901 | 1,804 | 90,2 |
| 10. | *pgi* | -3,461 | 1,945 | 97,25 |
| 11. | *purA* | -3,352 | 1,987 | 99,35 |
| 12. | *rbfA* | -3,369 | 1,981 | 99,05 |
| 13. | *rfaC (waaC)* | -3,498 | 1,983 | 0 |
| 14. | *rfaD* | -3,498 | 1,932 | 96,6 |
| 15. | *umuD* | -3,502 | 1,93 | 96,5 |
| 16. | *ydcX (ortT)* | -3,352 | 1,987 | 99,35 |
| 17. | *yihE (srkA)* | -3,438 | 1,954 | 97,7 |

## 8.5. Publication no. 5.

Kruszewska-Naczk *et al.*
*Chem. Biol. Technol. Agric.* (2024) 11:126
https://doi.org/10.1186/s40538-024-00658-x

Chemical and Biological Technologies in Agriculture

RESEARCH

Open Access

# Antibacterial blue light is a promising tool for inactivating *Escherichia coli* in the food sector due to its low risk of cross-stress tolerance

Beata Kruszewska-Naczk[1], Patrycja Pikulik-Arif[1], Mariusz Grinholc[1] and Aleksandra Rapacka-Zdonczyk[1*]

## Abstract

**Background** *Escherichia coli* is an integral part of the colonic microflora, though its pathogenic intestinal strains can contaminate animal and plant products and cause significant challenges in the food industry. Thermal processing is one of the most common methods used to preserve food. Nevertheless, non-thermal antibacterial methods, such as antibacterial blue light (aBL), are attracting more interest due to the growing demand for minimally processed products. Thus, the current study was aimed at assessment whether the risk of co-selection for these two food processing approaches exist.

**Results** The development of *E. coli* tolerance to both selective factors was observed after repeated exposure to sublethal doses of heat and aBL, and the observed adaptations were confirmed to be phenotypically stable. The results demonstrated that populations with increased tolerance to aBL also exhibited increased tolerance to temperature, while the sensitivity of temperature-tolerant populations to aBL did not change. We also identified 11 genes that could be involved in cross-stress tolerance. Neither adaptation changed the antibiotic sensitivity of the tolerant strains. Finally, short- and long-term pre-incubation at elevated temperatures significantly increased the tolerance of *E. coli* BW25113 to aBL.

**Conclusions** The results obtained clearly demonstrate that aBL may serve as a complementary approach in food industry lacking resistance development and exerting no impact on microbial drug susceptibility. Nevertheless, the phenomenon of cross-tolerance should be considered an issue when designing food processing including sequential use of aBL and high temperature.

**Keywords** Antimicrobial blue light, Co-selection, *Escherichia coli*

*Correspondence:
Aleksandra Rapacka-Zdonczyk
aleksandra.rapacka-zdonczyk@ug.edu.pl
Full list of author information is available at the end of the article

**Graphical Abstract**

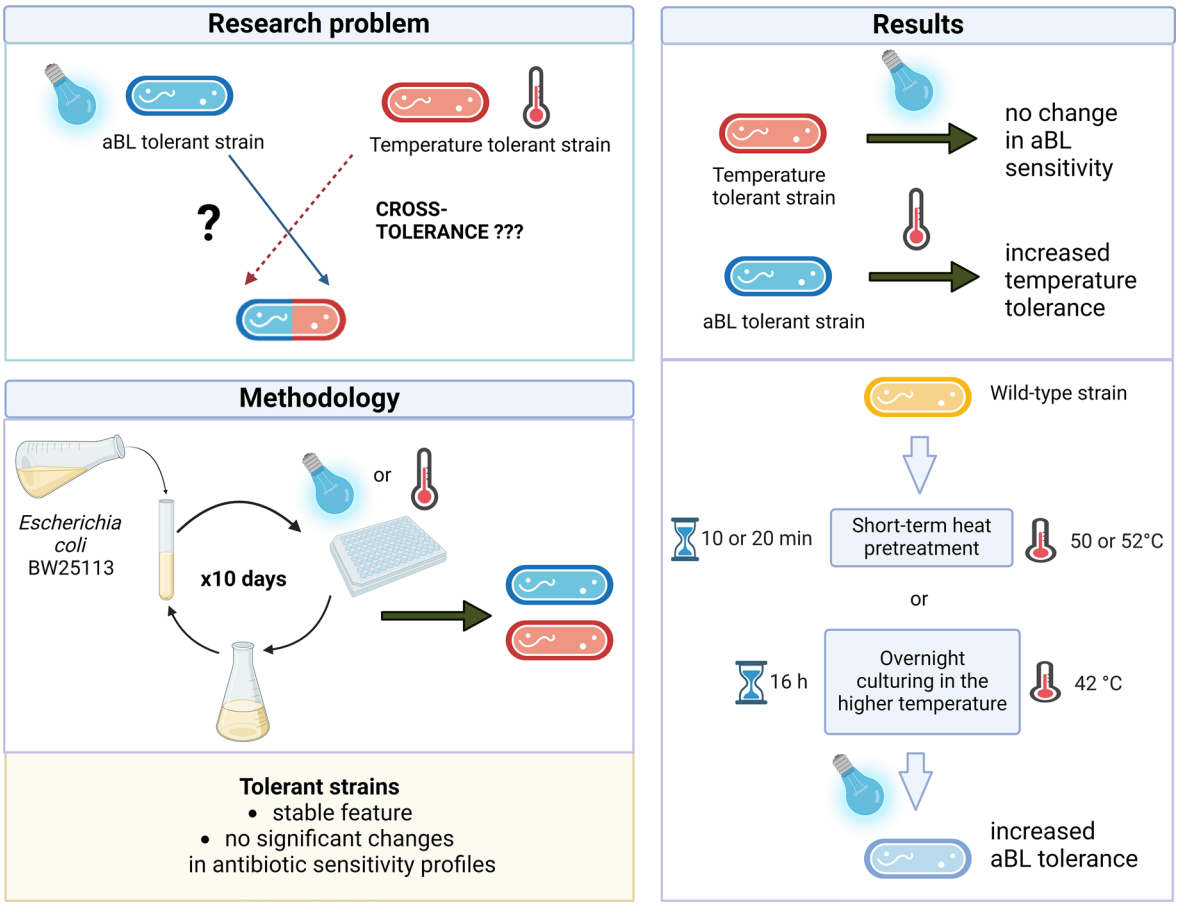


## Introduction

Foodborne diseases are a serious challenge to public health worldwide and are associated with significant morbidity and mortality. These diseases can lead to human suffering, hinder socioeconomic development, burden health systems and harm the national economy, tourism and trade. According to estimates, as many as 600 million people fall ill each year after eating contaminated food, resulting in 420,000 deaths. In low- and middle-income countries, where the problem is the most serious, expenditures related to the consumption of contaminated food reach 110 billion USD annually [1]. Foodborne pathogens are particularly dangerous for immunocompromised individuals, such as infants and small children, pregnant women, elderly people and people with immunodeficiencies. Statistics show that as many as 40% of cases occur in children under 5 years of age, even though these children constitute 9% of the world's population [1]. One of the most common bacterial pathogen that cause foodborne diseases is *E. coli*, which is the subject of current work [2].

Pathogenic strains (pathotypes) of *E. coli* can be found in various food products, including meat and animal products; plant products, such as fruits and vegetables, leaves, seeds and sprouts; and bakery products, such as flour and raw dough [3–5]. At each stage of the food production process, microorganisms encounter various selective pressure factors, which may negatively affect their growth and/or survival; however, these factors can lead to mutations that help bacteria adapt to unfavorable environmental conditions.

Thermal stress, which can be induced by high and low temperatures, is widely used in the food industry. High temperatures are used to disinfect food and production lines while low temperatures are most often used to extend the shelf life of food, after which food is still safe to eat [6]. Bacteria in composted food waste may be

exposed to temperatures between 40 and 70 °C depending on the stage of the process [7, 8].

As thermal food processing causes undesirable effects, such as changes in the taste, structure and appearance of some products and loss of food ingredients, minimal food processing is preferred; thus, researchers are searching for nonthermal bactericidal agents and methods with potential application in the food industry [9]. Promising modern technologies include high-pressure processing, pulsed electric field, cold plasma, and light-based technologies, such as antimicrobial blue light (aBL), which is the focus of this paper [10]. Many studies have confirmed the effectiveness of aBL in the eradication of numerous foodborne bacterial pathogens, such as *Bacillus cereus*, *Listeria monocytogenes*, *Staphylococcus aureus*, *Salmonella enterica*, *Shigella sonnei*, *Campylobacter jejuni* and *E. coli* [11–13]. Moreover, irradiation does not significantly affect the physicochemical quality of food products, i.e., color, pigment, antioxidant or vitamin content [14]. However, each methods used, or is likely to be used, introduces various stressors to foodborne pathogens, and research on bacterial responses to these alternative stressors is crucial to ensuring food safety. Furthermore, scientists dealing with this topic emphasize that further exploration of the antibacterial mechanism of phototreatment in food industry is needed [15]. The aim of the current work was to assess the risk of co-selection to aBL and thermal stress in *E. coli*. Co-selection studies help determine if exposure to one type of antimicrobial treatment, such as blue light, could potentially influence the resistance of microorganisms to other treatments like high temperatures. Understanding these dynamics is crucial for ensuring that food safety protocols effectively minimize the risk of microbial contamination and spoilage. Unfortunately, regular use of certain antimicrobial treatments can lead to tolerance among pathogens. By understanding co-selection mechanisms, food scientists can design treatment protocols that minimize the risk of developing resistant strains, thereby maintaining the efficacy of antimicrobial strategies over time. Finally, by preventing the spread of foodborne illnesses through effective antimicrobial strategies, the food industry plays a critical role in safeguarding public health. Co-selection studies are a key component in understanding how to best achieve this goal.

## Materials and methods

### Strains and culture conditions

Experiments were performed using *E. coli* BW25113 obtained from the Keio collection [16]. All of its variants were stored at − 80 °C with 20% glycerol and cultured in Luria–Bertani (LB) broth (BTL, Łódź, Poland) or LB agar medium (A&A, Gdansk, Poland) at 37 °C under aerobic conditions. Overnight cultures were prepared in an orbital incubator (Innova 40, Brunswick, Germany) at 150 rpm for 16–20 h.

In the analysis on the risk of tolerance development, and feature stability confirmation, the aBL and temperature-tolerant populations (day 10) were inoculated into LB media directly from frozen glycerol stocks for characterization. In experiments performed to evaluate the aBL and temperature sensitivity of *E. coli* (day 0), overnight cultures were inoculated from single colonies grown on LA plates using glycerol stocks frozen at − 80 °C.

Sixty-four aBL-hypersensitive mutants from the Keio collection were cultured in the presence of 15 µg/ml kanamycin [16]. The strains were stored in 96-deep-well plates filled with LB, and 15% glycerol medium was used for storage at − 80 °C. Before the cells were used, they were freshly stamped into new microtiter plates filled with LB medium and incubated overnight (16–20 h) in an orbital incubator at 150 rpm.

### Chemicals

Trimethoprim, ciprofloxacin, tigecycline, cefuroxime, ceftazidime, and piperacillin antibiotics were purchased from Sigma Aldrich (Darmstadt, Germany). Gentamycin and ampicillin were purchased from Carl Roth (Karlsruhe, Germany), while meropenem was purchased from Thermo Fisher Scientific (UK). Kanamycin sulfate was purchased from Gibco (Paisley, UK). All stock solutions at a concentration of 10 mg/l were stored at − 20 °C.

### Light source

Irradiation was performed using an LED light source emitting blue light ($\lambda_{max}$ 415 nm, irradiance 25 mW/cm$^2$; Cezos, Gdynia, Poland) [17].

### Determination of the temperature leading to *E. coli* BW25113 tolerance development

Overnight cultures in triplicate were adjusted to an optical density (OD) of 0.5 McF (approx. $5\times10^7$ CFU/ml). Aliquots (150 µl) were transferred to 1.5 ml tubes and incubated at 52 °C for 90 min in a TB-941 T/TB-941 U incubator (JW Electronic, Warsaw, Poland). Every 5 min, 10 µl aliquots were serially diluted and streaked horizontally on LB agar plates. After overnight incubation at 37 °C, the colonies were counted to estimate the survival rate and compared to that of the untreated cultures. For tolerance development analysis, a temperature dose leading to a decrease in the survival rate of 1.2 $\log_{10}$ CFU/ml was chosen (20 min of incubation at 52 °C).

#### Determination of the aBL dose leading to *E. coli* BW25113 tolerance development

The aBL dose used for tolerance analysis was determined according to our previously published work [18].

#### Determination of tolerance development following repeated sublethal exposure to aBL and temperature

Three biological replicates of aBL tolerance development were prepared exactly as described previously [17] with 10 days of sublethal exposure of 100 µl of overnight cultures to aBL (32.4 J/cm$^2$).

Temperature-tolerant strains were prepared as follows: overnight cultures of *E. coli* BW25113 in triplicate were diluted to an OD of 0.5 McF. Then, 1.5 ml aliquots were transferred to 1.5 ml Eppendorf tubes and incubated at 52 °C for 20 min. Following exposure, 10 µl aliquots of the incubated samples were collected to determine the survival rate. Sample aliquots of 50 µl were transferred to fresh LB medium (5 ml) for regrowth overnight. The next day, after 16–20 h of incubation, the treatment was repeated under the same conditions. The cycle of exposure—regrowth—exposure was repeated 10 times. Simultaneously, control samples were prepared in the same manner but without exposure to temperature or aBL.

Potential reductions in susceptibility to temperature and aBL were examined after the 5th and 10th consecutive cycles at higher doses of light (up to 86.4 J/cm$^2$) and compared to those of the control strain (day 0) and (day 10th).

#### Stability of the acquired tolerance to aBL or temperature

The experiments were performed using the samples that were taken from the 10th consecutive cycle of aBL or temperature treatment (the cycle in which a significant decrease in susceptibility was observed) and transferred to fresh LB medium and cultured overnight. The cycles of transfer—regrowth—transfer were repeated 5 times. After the 5th cycle, the cultures were diluted to an OD of 0.5 McF, and 100 µl of the bacterial suspensions were irradiated with 415 nm light at a dose up to 86.4 J/cm$^2$, or 150 µl of bacterial suspension was incubated at 52 °C for up to 90 min. The resulting suspensions were compared with the initial samples and with the untreated controls.

#### aBL and temperature sensitivity of *E. coli* BW25113

Analysis of aBL sensitivity was performed as described previously [18]. Different light doses ranging from 0 to 86.4 J/cm$^2$ were tested. To test temperature sensitivity, overnight cultures of temperature-tolerant populations (day 10) and controls (days 0 and 10) were diluted to an OD of 0.5 McF. A total of 150 µl of bacterial suspension was incubated at 50 °C, 52 °C, 54 °C, and 56 °C for up to 90 min, and 10 µl was collected every 5 min, diluted and streaked horizontally onto LB-agar plates to assess growth reduction. The experiments were performed in triplicate.

#### Assessment of the impact of short-term pre-incubation at increased temperatures on the sensitivity of *E. coli* BW25113 to aBL

Three overnight cultures of the *E. coli* BW25113 strain were diluted to an OD of 0.5 McF. Then, 350 µl aliquots were pre-incubated at 50 °C or 52 °C for 10 or 20 min in 1.5 ml Eppendorf tubes. Next, 100 µl of each sample was transferred to a 96-well plate, which was subsequently irradiated to assess the aBL sensitivity, diluted and incubated overnight at 37 °C, after which the surviving colonies were counted.

#### Assessment of the impact of long-term (overnight) incubation at increased temperatures on the sensitivity of *E. coli* BW25113 to aBL

Three cultures of *E. coli* BW25113 were incubated overnight in ThermoMixer C (Eppendorf, Hamburg, Germany) at 37 °C or 42 °C. Then, aBL sensitivity profiles were investigated as described previously.

#### Assessment of the sensitivity of 64-aBL-hypersensitive *E. coli* BW25113 single-gene mutants to increased temperature

Overnight cultures of single gene mutants maintained with kanamycin (15 mg/ml) and the wild-type strain were diluted 1:100 in LB media. The $OD_{600}$ of the initial cultures was measured using an EnVision Multilabel Plate Reader (PerkinElmer, USA). Then, the mutants were incubated for 16 h at 37 °C (control) or 40 °C in an orbital incubator (Innova 42, Brunswick, Germany) at 150 rpm, and the $OD_{600}$ was measured after 16 h. A heat shock temperature of 40 °C, which causes a greater than 50% reduction in the growth of the wild-type strain, was investigated. To determine growth defects, the $\Delta OD_{600}$ was calculated ($OD_{600,\ 16\ h}$–$OD_{600,\ 0\ h}$). The sensitivity of each mutant was calculated according to the following formula described by Krewing et al. [19]:

$$\begin{aligned}&\text{Grown defect [\%]}\\&= 100 - 100 \times OD_{wt} \times OD^{-1}_{wt,\ stressed}\\&\quad \times \left(OD_{mutant} \times OD^{-1}_{mutant,\ stressed}\right)^{-1}.\end{aligned}$$

### Antimicrobial susceptibility testing of aBL and temperature-tolerant strains

The MICs of trimethoprim, ciprofloxacin, tigecycline, cefuroxime, ceftazidime, piperacillin, gentamycin and meropenem were tested by the microbroth dilution method according to the European Committee for Antimicrobial Susceptibility Testing [20] for the temperature-tolerant strain (day 10), aBL-tolerant strain (day 10) and the control (day 0) and control (day 10) strains.

### Bioinformatics and statistical analysis

All the statistical analyses and figures were created using GraphPad Prism version 9.0 (GraphPad Software, Inc., CA, USA). The significant differences between the groups were calculated using two-way analysis of variance (ANOVA) with $P<0.05$ and Tukey's or Dunnett's multiple comparison tests. The graphic figures were prepared with the use of BioRender.com (accessed on 31 July 2024).

The experimental workflow is presented in Fig. 1.

## Results

### Establishment of $MDK_{99}$ conditions for assessing tolerance

The $MDK_{99}$ parameter should be determined to perform the tolerance study [21, 22]. This parameter demonstrates that the treatment conditions resulted in a reduction in cell viability of $<2$ $\log_{10}$. The determination of treatment doses leading to a 99% reduction in microbial viability must be determined to ensure a reliable experimental design, as sufficient number of cells of the treated bacterial population must remain alive for further analysis. After 20 min of incubation at 52 °C, a 1.2 CFU/ml reduction in the bacterial survival rate was observed. For aBL tolerance development, a light dose of 32.4 J/cm$^2$ was chosen, as described in our previous studies, and this dose also causes a 1.2 CFU/ml reduction in bacterial growth [18].

### Phenotypically stable temperature and aBL tolerance were observed after 5 cycles of selective pressure

Compared to the control passaged without selective pressure, significant differences in the bacterial survival rate

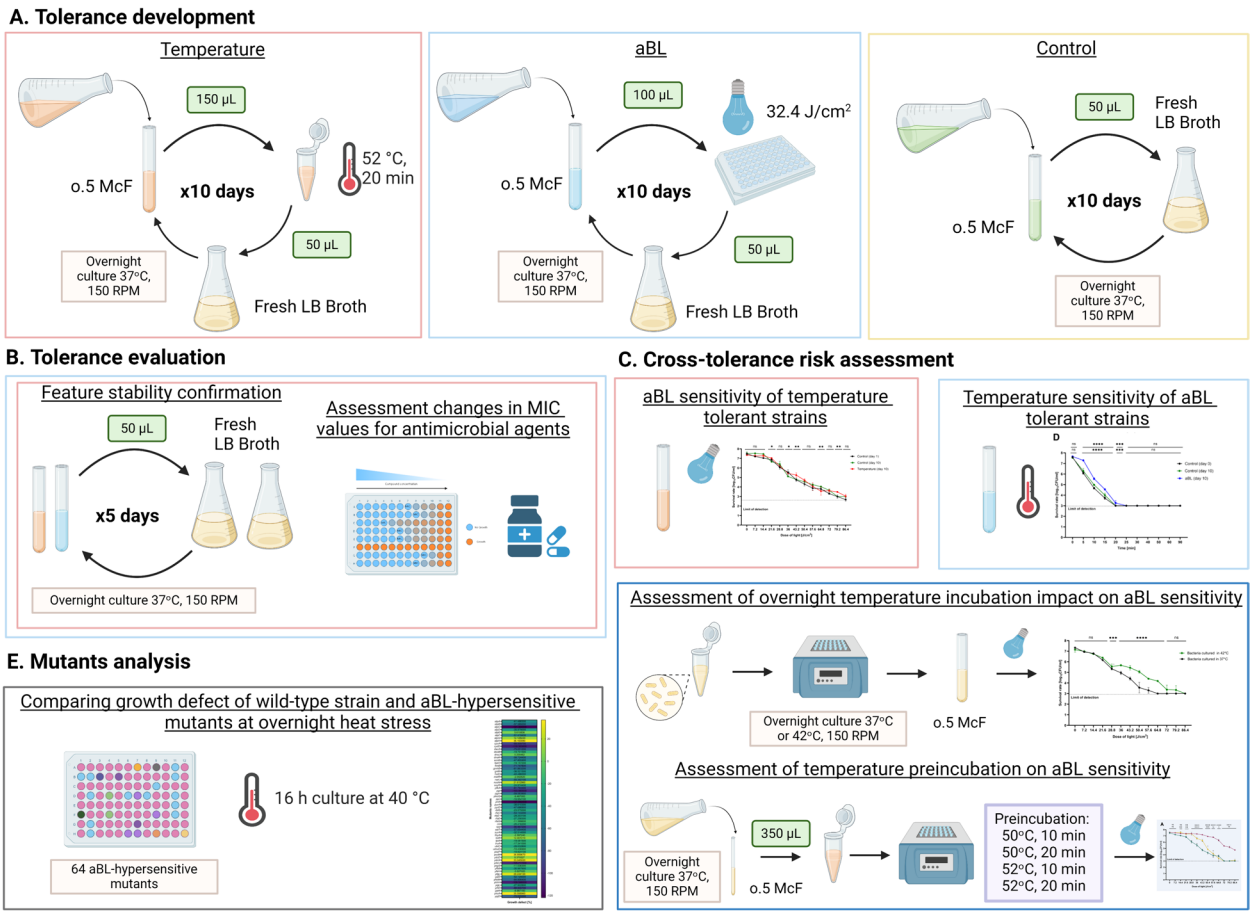


**Fig. 1** The experimental workflow

were observed starting on the 5th day of consecutive bacterial treatment. An increase in bacterial survival of up to 3.06 $\log_{10}$ CFU/ml was observed for the temperature treatment. Consecutive aBL pressure increased bacterial survival up to 2.74 $\log_{10}$ CFU/ml. This effect was also observed on the 10th day of bacterial treatment for both temperature and aBL treatment, causing an increase of up to 3.24 $\log_{10}$ CFU/ml in the survival rate (Fig. 2A, C).

The stability of the acquired adaptations was assessed by passaging strains from the 10th day of factor treatment for 5 subsequent cycles without selective pressure. This step was performed to assess whether the observed adaptations result from genetic alterations caused by repeated exposure to sublethal stressor doses or are a phenotypic change caused by temporary changes in the gene expression profile, which return to the original state after selective pressure is removed. After 5 cycles of incubation without selective factors, the sensitivity of the tolerant populations to temperature and aBL was investigated and compared to that of the tolerant populations from the 10th day of subsequent treatments. The results are presented in Fig. 2B, D. For the temperature test, a statistically significant reduction in bacterial survival of up to 0.55 $\log_{10}$ CFU/ml was observed in the passaged population without selective pressure in the 5th cycle compared to the initial culture from the 10th day. This may result from changes in gene expression profiles in response to a lack of selective pressure. However, the statistical significance remained the same for the difference between the tested population (day 10 + 5 passages) and the control (initial culture, day 10), suggesting that the acquired tolerance is stable.

No significant differences were observed between aBL (day 10) and aBL (day 10 + 5) (Fig. 2D), suggesting that the developed tolerance is caused mainly by stable genetic alterations due to multiple sublethal aBL irradiation cycles.

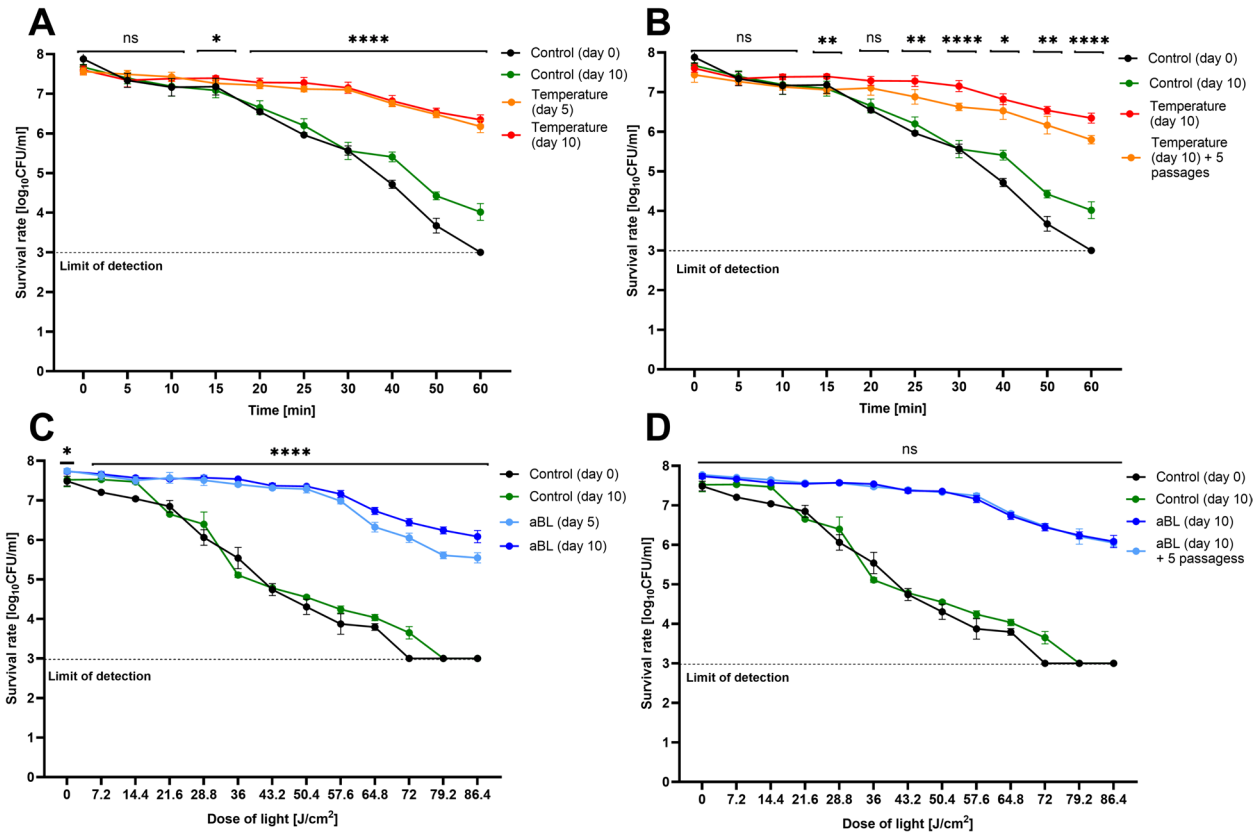


**Fig. 2** Temperature and aBL tolerance and stability. Response of *E. coli* populations to 52 °C. The survival rates of the control populations (days 0 and 10) and temperature-tolerant populations (day 5 and 10) were assessed (**A**). The stability of temperature tolerance after 5 passages without selective pressure (**B**). Response of *E. coli* populations to aBL. The survival rates of the control populations (days 0 and 10) and aBL-tolerant populations (day 5 and 10) were assessed (**C**). Stability of aBL tolerance after 5 passages without selective pressure (**D**). The plots present the reduction in $\log_{10}$ units of CFU/ml. The experiment was performed in biological triplicates. Statistical comparison between the tolerant population (day 10) and the control (day 10) (**A**, **C**) and between the tolerant population 10th day and passaged strains (**B**, **D**). Significance at the respective *P* values is marked with asterisks (ns $P > 0.05$; *$P < 0.05$; **$P < 0.01$; ***$P < 0.001$; ****$P \leq 0.0001$)

### Compared to the WT strain, the 52 °C temperature-tolerant strain is less sensitive to higher temperatures

After the *E. coli* population treated with a sublethal temperature was found to exhibit reduced sensitivity to heat stress, further studies were carried out to assess changes in sensitivity to different temperatures, i.e., 53 °C, 54 °C and 56 °C. The population from day 10 was used in this analysis because its tolerance level was constant and the accumulation of genetic changes resulting from prolonged selection pressure was potentially greater than that of other populations. The experimental results are presented in Fig. 3.

Compared to both control groups, the 52 °C-tolerant population showed significantly increased tolerance to all other tested temperatures (53 °C, 54 °C and 56 °C) (survival increased by $\leq$2.37, 2.18 and 3.05 $\log_{10}$, respectively) (Figs. 3A, 5B, C).

### The temperature-tolerant population does not exhibit increased tolerance to aBL

The obtained *E. coli* populations with stable temperature and aBL tolerance were used to assess the risk of co-selection. The first experiment was performed to determine the survival rate of the temperature-tolerant population under aBL stress conditions. The experimental results were compared with the results of the passaged control (day 10) and unpassaged control (day 0) for comparative analysis and are presented in Fig. 4A.

In Fig. 4A, the aBL sensitivity profiles of controls and temperature-tolerant population are compared. A statistically significant decrease in aBL sensitivity was observed for the temperature-tolerant population in comparison to the passaged control population with light doses of 21.6, 36, 43.2, 64.8, and 79.2 J/cm$^2$. This nonstable pattern of aBL sensitivity suggests that the temperature tolerance and aBL sensitivity are not correlated.

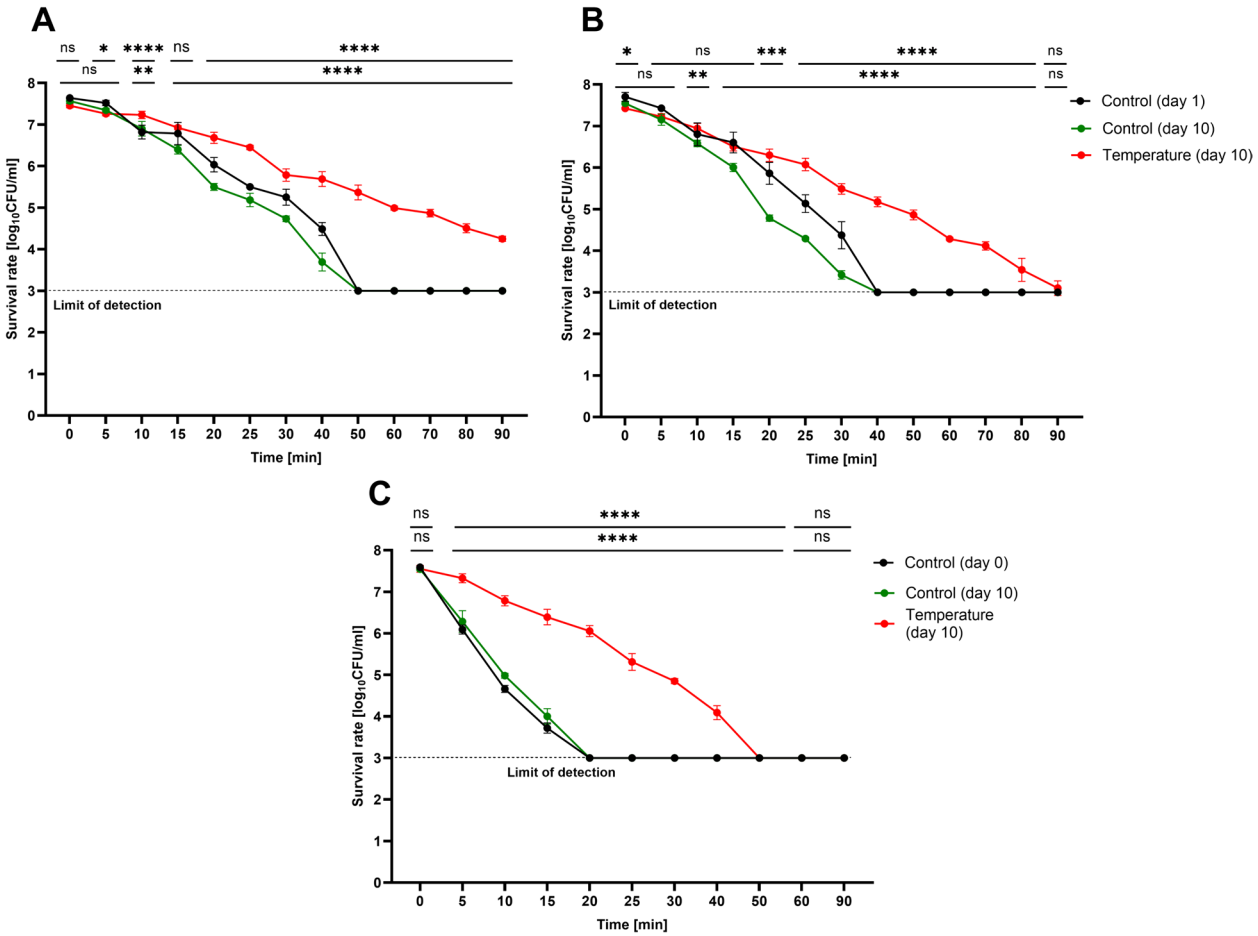


**Fig. 3** Temperature sensitivity profile of temperature-tolerant *E. coli*. **A** 53 °C, **B** 54 °C, **C** 56 °C. The plots present the reduction in $\log_{10}$ units of CFU/ml. The experiment was performed in biological triplicates. Statistical analysis between the temperature-tolerant strain (day 10) and the control strain (day 0) (upper asterisks) and between the temperature-tolerant strain (day 10) and the control strain (day 10) (lower asterisks). Significance at the respective *P* values is marked with asterisks (ns $P > 0.05$; *$P < 0.05$; **$P < 0.01$; ***$P < 0.001$; ****$P \leq 0.0001$)

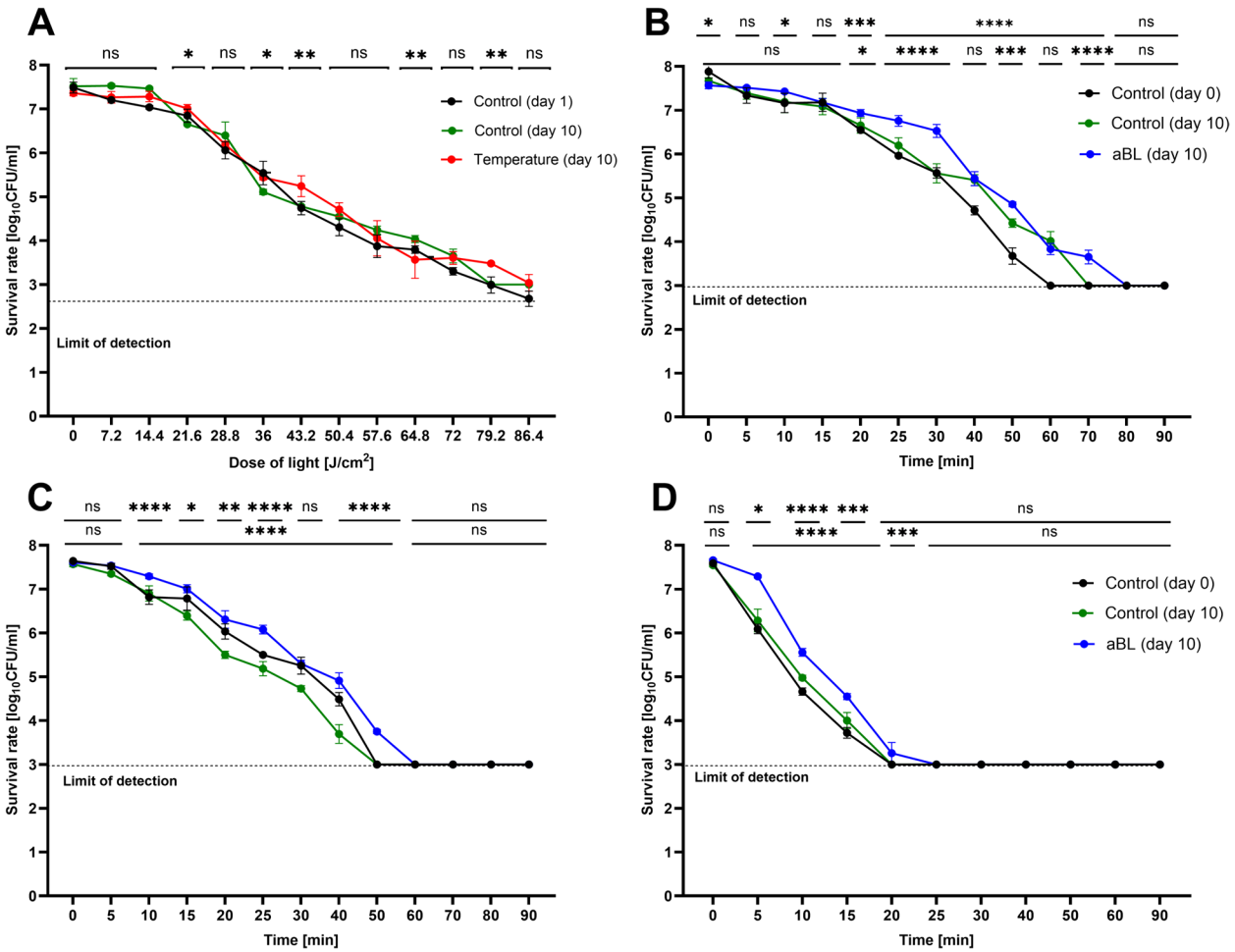


**Fig. 4** Co-selection studies. aBL sensitivity profile of the temperature-tolerant population and controls (**A**). Statistical comparison between the temperature-tolerant population and the control strain (day 10). Heat sensitivity profiles of the control (day 0), control (day 10) and aBL (day 10). **B** 52 °C, **C** 53 °C, **D** 56 °C. Statistical analysis between aBL (day 10th) and control (day 0)—upper asterisk and aBL (day 10th) and control (day 10th)—lower asterisk

### The aBL-tolerant population exhibits increased tolerance to elevated temperature

When higher temperatures (52 °C, 53 °C and 56 °C) were applied, significant differences in the average survival of the studied populations were observed. At all tested temperatures, the aBL-tolerant population exhibited greater mean survival rates than that of the passaged control group at some time points (survival increases of $\leq$0.97, 1.22, 0.64, and 1.01 $\log_{10}$) (Fig. 4B–D). However, it is important to emphasize that the temperature sensitivity of the aBL-tolerant strain did not reach the levels observed in the temperature-tolerant population.

The results obtained suggest that a co-selection phenomenon occurs in which acquired tolerance to aBL may confer a certain degree of cross-stress tolerance to temperature stress. Importantly, although co-selection occurs, the resulting temperature tolerance is significantly lower than that of populations selected for this feature.

The plots present the reduction in $\log_{10}$ units of CFU/ml. The experiment was performed in biological triplicates. Significance at the respective $P$ values is marked with asterisks (ns $P > 0.05$; *$P < 0.05$; **$P < 0.01$; ***$P < 0.001$; ****$P \leq 0.0001$). Statistical comparison between the temperature-tolerant population and the control population (day 10).

### Short-term pre-incubation at 50 °C increased *E. coli* tolerance to aBL

This experiment was performed to evaluate whether short-term thermal pre-incubation affects *E. coli* sensitivity to blue light treatment. In this study, *E. coli* were exposed to 50 °C or 52 °C for 10 or 20 min and then

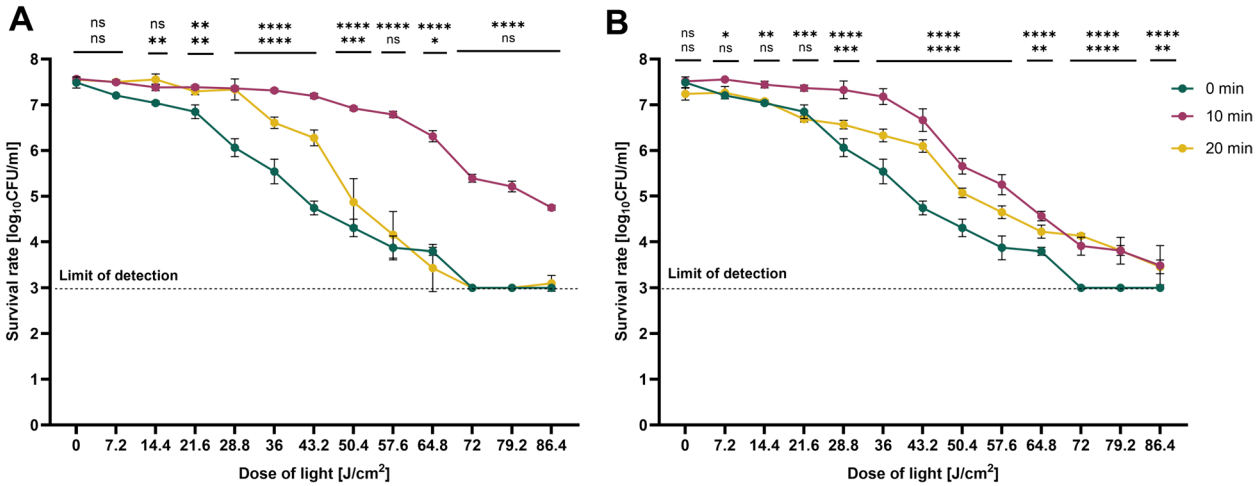


**Fig. 5** aBL sensitivity of temperature-pretreated bacteria. **A** 50 °C, **B** 52 °C. Statistical comparison between untreated and temperature-treated bacteria. The plots present the reduction in $\log_{10}$ units of CFU/ml. The experiment was performed in biological triplicates. Significance at the respective *P* values is marked with asterisks (ns $P > 0.05$; *$P < 0.05$; **$P < 0.01$; ***$P < 0.001$; ****$P \leq 0.0001$). The upper asterisk indicates 10 min of pretreatment, while the lower asterisk indicates 20 min of pretreatment

examined for their sensitivity to aBL in comparison to an untreated control (Fig. 5).

Under all conditions tested, populations subjected to short-term pre-incubation exhibited significantly reduced sensitivity to aBL. After pre-incubation at 50 °C, increases in survival of $\leq 2.55$ $\log_{10}$ and $\leq 1.50$ $\log_{10}$ were observed for exposure times of 10 min and 20 min, respectively. After pre-incubation at 52 °C, increases in survival of $\leq 2.07$ $\log_{10}$ and $\leq 1.32$ $\log_{10}$ were observed for exposure times of 10 and 20 min, respectively. These results indicate that at both temperatures, a shorter pre-incubation time (10 min) resulted in a greater increase in survival during light treatment, and the highest tolerance to aBL exposure was observed for the bacterial population exposed to a lower temperature (50 °C) for 10 min.

### Long-term incubation at 42 °C results in increased *E. coli* tolerance to aBL

The next experiment was performed to investigate whether long-term (overnight) culturing of *E. coli* at an elevated temperature (42 °C) affects its sensitivity to aBL. The aBL sensitivity profiles of bacteria cultured at 37 °C (optimal) and 42 °C were compared according to the results presented in Fig. 6. The population cultured at higher temperatures was less sensitive to aBL at light doses ranging from 36 to 64.8 J/cm$^2$ than the population grown at standard temperatures (survival increase of 0.58 to 1.19 $\log_{10}$). This observation confirms that the temperature significantly impacts the response of the tested bacterium to aBL treatment.

### Temperature and aBL adaptation mechanisms do not significantly affect the susceptibility of *E. coli* to antibiotics

This step was performed to assess whether the adaption of *E. coli* to aBL and increased temperature affects the susceptibility of *E. coli* to antimicrobial agents, which would support the hypothesis that genetic alterations occur during the development of tolerance. The MIC values are presented in Table 1. The most commonly reported change is a twofold increase in the MIC, and the greatest susceptibility (although still insignificant) was observed for ciprofloxacin upon the development of aBL tolerance. Nevertheless, the impact of tolerance development on drug susceptibility is limited because it results in a twofold increase in MICs and no change in the categorization of antimicrobial susceptibility.

### Cross-tolerance to heat and aBL can be regulated by certain genes

At the end of the studies, aBL-hypersensitive single-gene mutants of *E. coli* were cultured under heat shock conditions for 16 h; this was performed to assess the role of a single gene in bacterial survival at relatively high temperatures and the co-occurrence of aBL and temperature protection. The growth defect in comparison to the wild-type strain was observed only for 11 mutants lacking: ***atpE*** (ATP synthase Fo complex—subunit c), ***atpG*** (ATP synthase F1 complex subunit γ), ***atpH*** (ATP synthase F1 complex subunit δ), ***dnaJ*** (chaperone protein DnaJ), ***nuoN*** (NADH:quinone oxidoreductase subunit N), ***tolA*** (Tol–Pal system protein TolA), ***yccM*** (putative electron transport protein YccM), ***ydcE/pptA*** (tautomerase PptA),

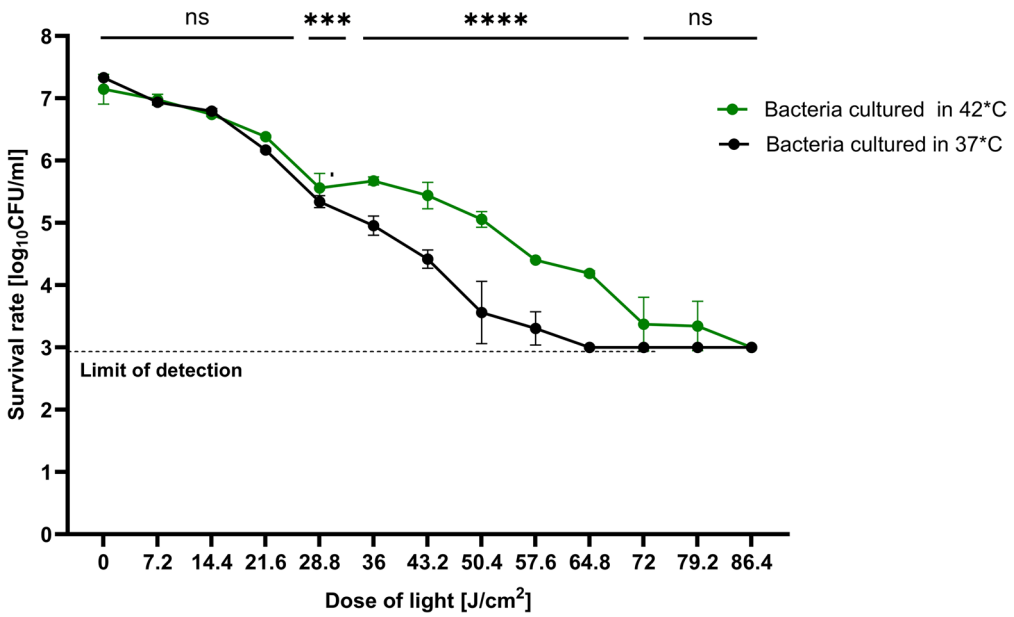


**Fig. 6** aBL sensitivity profiles of bacteria cultured at 37 °C and 42 °C. The plots present the reduction in $\log_{10}$ units of CFU/ml. The experiment was performed in biological triplicates. Significance at the respective *P* values is marked with asterisks (ns $P > 0.05$; *$P < 0.05$; **$P < 0.01$; ***$P < 0.001$; ****$P \leq 0.0001$)

**Table 1** Antimicrobial susceptibility testing

| Antibiotic | Strain | | | |
|---|---|---|---|---|
| | Control (day 0) | Control (day 10th) | Temperature tolerant (day 10th) | aBL tolerant (day 10th) |
| Ampicilin | 8 | 8 | 8 | 16↑ |
| Ciprofloksacin | 0.0078125 | 0.0078125 | 0.0078125 | 0.0625↑ |
| Ceftazydym | 0.5 | 1 ↑ | 1 ↑ | 1↑ |
| Cefuroxime | 8 | 8 | 8 | 8 |
| Gentamycin | 0.25 | 0.5 ↑ | 0.5 ↑ | 1↑ |
| Meropenem | 0.015625 | 0.03125 ↑ | 0.03125 ↑ | 0.0625↑ |
| Piperacillin | 1 | 2 ↑ | 2 ↑ | 2↑ |
| Tigecycline | 0.5 | 1 ↑ | 0.5 | 1↑ |
| Trimetoprim | 0.25 | 0.125 ↓ | 2 ↑ | 0.25 |

MICs of *E. coli*: control (day 0), control (day 10), temperature-tolerant population (day 10), and aBL-tolerant population (day 10). MIC values are presented in mg/l

***ydcX*** (orphan toxin OrtT), ***yfgL/bamB*** (outer membrane protein assembly factor BamB), ***yncA/mnaT*** (L-amino acid *N*-acyltransferase), while the most of proteins encoded by these genes are plasma membrane proteins (www.biocyc.org). Proteins encoded by these genes can play an important role in cellular protection against aBL and higher temperatures. For the remaining 53 mutants, growth defects under high temperature were not observed (according to the results presented in Fig. 7).

## Discussion

Thermal treatment is the most frequently used method in food processing and is performed to ensure food safety by eliminating pathogens [23]. Different microorganisms may have different sensitivities to heat stress. The term used to determine the thermal resistance of bacteria is the decimal reduction time (*D*-value), which corresponds to the time needed to reduce 90% of bacterial cells at a given temperature (a 1 $\log_{10}$ decrease in survival rate) [24]. The *E. coli* strain discussed in this paper is a relatively heat-sensitive bacterium. According to the literature,

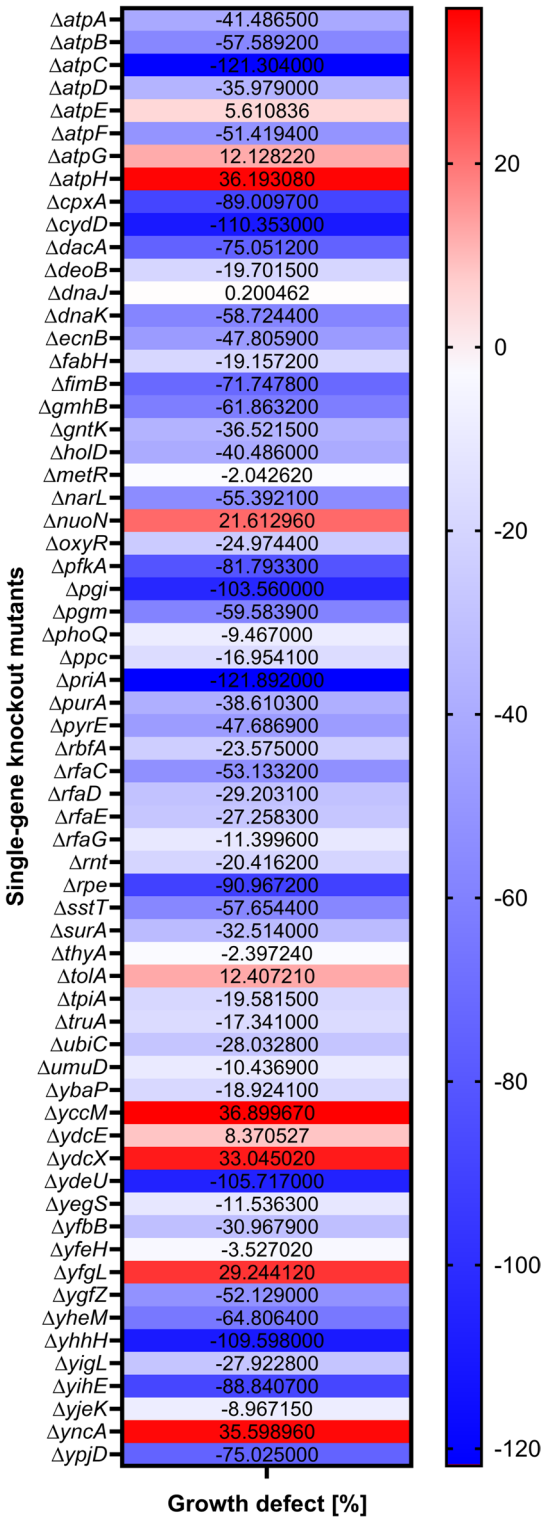


**Fig. 7** Growth defects of single-gene deletion mutants hypersensitive to aBL. The values are the means of five biological repetitions

the $D_{60°C}$ for *E. coli* K12 is approximately 0.1–0.3 min [25]; however, the development of tolerance may lead to a multiple increase in this value. For instance, highly heat-resistant *E. coli* strains isolated from a beef processing facility were characterized by $D_{60°C}$ values ranging from 15 to even 71 min [26]. Although much research has been conducted to understand the mechanisms by which heat treatment inactivates microorganisms, as in the case of aBL, this issue is not fully understood. It is believed that, similar to aBL, thermal stress has a broad spectrum of action and causes damage to many cellular structures; when the accumulation damages pass above a critical threshold, cellular death ultimately occurs [27]. Exposure to elevated temperatures induces significant morphological and structural changes in the outer membrane of gram-negative bacteria and leads to the loss of its lipopolysaccharide (LPS) component [28]. As a consequence, the permeability of the membrane is altered, leading to a loss of intracellular substances and disruption of osmotic and pH homeostasis [29–32]. Genetic material is also exposed to thermal damage. DNA is a cellular component with relatively high thermal stability, as temperatures close to 100 °C or higher are needed to denature DNA [33]. However, lower temperatures can also lead to damage, which mainly leads to an increased frequency of mutations [34]; these mutations can subsequently result in adaptation to thermal stress.

Recently, innovative approaches aimed at extending the shelf life of food products without the need for thermal treatment have been developed in the food industry. However, adapting these technologies to meet the requirements of sustainable and economic food preservation is challenging [35]. Therefore, light-emitting diode (LED)-based technologies are becoming increasingly desirable as environmentally friendly alternatives for the thermal sterilization of food [36]. The bactericidal effect of UV light is likely the best-tested thus far among these technologies. However, accidental exposure to this light poses serious health risks, leading to serious eye and skin diseases, hair loss, and an increased risk of skin cancer [37]. Therefore, aBL is attracting increased attention as an alternative that is safer for workers in industrial settings. The results of studies in animal models and volunteers suggest that exposure to blue light, at an effective antimicrobial dose, does not cause significant DNA damage to keratinocytes, inflammatory reactions or skin burns [38, 39]. The effectiveness of *E. coli* eradication using aBL has been demonstrated for nonpathogenic and pathogenic strains, including the seven main Shiga-like toxin-producing *E. coli* (STEC) pathotypes, which are among the most serious threats in the food industry [40, 41]. Promising in vitro research results have prompted many researchers to test the effects of blue

light on pathogens found directly in food products. It has been confirmed that aBL exhibits antimicrobial activity in milk and dairy products, which helps extend the shelf life of products without decreasing nutritional content [42–44]. Researchers have also demonstrated that aBL is effective in eliminating microorganisms and maintaining the sensory quality of various fruits and vegetables without significantly changing the composition of these products [10, 45]. Moreover, researchers have shown that LED light at a wavelength of 405 nm can improve the quality of stored strawberries by increasing the antioxidant activity of the enzymes within the fruit [46]. In the storage of cabbage, blue light contributed to increasing the levels of chlorophyll, polyphenols and vitamin C, which shows the potential of aBL to positively impact the appearance and nutritional value of food [47]. Furthermore, the effectiveness of aBL against pathogenic bacteria has also been demonstrated on materials such as stainless steel and polyethylene. These materials are often used in the food industry, serving as work surfaces and food packaging [48]. Less satisfactory results were obtained when the impact of aBL on meat, fish and seafood was examined. The observed decreases in bacterial survival were often sublethal, i.e., 1–2 $\log_{10}$ CFU/ml, which may result from limited light penetration due to the opacity and irregular surface of these products [12, 49–51]. This result indicates that aBL should be optimized for industrial applications to increase its effectiveness [49–51]. Photodynamic treatment opens up new possibilities for maintaining cleanliness and safety in the food industry. Nevertheless, bacteria may develop tolerance or resistance to many stress factors in addition to those used in food processing. In the environment, bacteria are exposed to different stressors (e.g., antibiotics, acids, organic solvents, heavy metals, and oxidative stress). Different environmental contaminants provide selective pressure for bacteria to mutate, evolve, and develop mechanisms to tolerate and resist such stressors [52]. It is essential to determine the factors that contribute the emergence of bacterial adaptation in environmental reservoirs, and studies of the co-selection phenomenon to other factors and/or to therapeutic approaches should also be performed. For instance, many studies indicate that bacteria gain cross-resistance to antibiotics, disinfectants, and heavy metals due to their antimicrobial properties [53–56]. Associations between specific patterns of antibiotic resistance and the levels or types of metal contamination suggest that several mechanisms underlie the co-selection process. These phenomena increase bacterial persistence and resistance and should be considered when developing strategies to reduce antimicrobial resistance [57]. Gram-negative bacteria, including *E. coli*, can adapt to many physical, chemical and environmental stressors, such as UV radiation [58], ionizing radiation [59], organic solvents [60], heavy metals [61], acids [62], antibiotics [63], aBL and aPDI [18, 64]. Ramteke [65] demonstrated that 90% of 448 coliform isolates were resistant to one or more antibiotics but showed tolerance to multiple metals. Rowe and Kirk [66] investigated the phenomenon of cross-protection in *E. coli* O157:H7 and found that salt or heat tolerance was increased when the bacteria were prestressed with acid, indicating that this procedure could affect food processing. Other studies have shown that adaptation to increased temperature often leads to a reduction in the sensitivity of microorganisms to other stressors, and vice versa. For example, Isohanni et al. [67] observed that *Arcobacter butzleri* (a pathogenic bacterium found in food) exhibited significantly reduced sensitivity to acidic conditions (pH 4.0) after a 2-h incubation at 48 °C. In addition, experiments conducted by Liao et al. [68] showed that exposure of some *Staphylococcus aureus* isolates from food to organic acids increases their tolerance to heat treatment. Bacterial co-selection for heat stress can be induced by factors other than acidic environments, such as nutrient deficiency, high salinity and ethanol. Jenkins et al. [69] showed that tolerance to heat (57 °C) increased in *E. coli* populations deprived of access to glucose or nitrogen. Similarly, Pumirat et al. [70] reported that the growth of *Burkholderia pseudomallei* on media rich in NaCl (150 and 300 mmol/l) significantly increased the survival of these bacteria when they were exposed to thermal stress (15 min at 50 °C). Yang et al. [71] reported a sevenfold increase in the survival rate of *Tetragenococcus halophilus* in response to ethanol exposure after prior exposure to high temperature (45 °C for 1.5 h). Moreover, research conducted by St. Denis et al. [72] has shown that the exposure of *Escherichia coli* to a sublethal dose of aPDI leads to significant changes in the levels of heat stress-related proteins. A sevenfold increase in the heat shock protein GroEL and a threefold increase in DnaK were observed. These results support the possibility of cross-adaptation to thermal stress and therapies based on the photodynamic mechanism, including aBL, which was examined in this study. Due to its antimicrobial properties, aBL could be considered as an advantageous tool in the prevention of foodborne illnesses. If this method were to be introduced to the food industry in the future, there is a risk that bacteria could be exposed to aBL (e.g. during surface disinfection) and then transferred to a food product that will be heat treated. It is also likely that bacteria that have already developed tolerance to heat stress could be exposed to aBL during food processing.

Our previously published studies [18, 64] revealed that sublethal aPDI and aBL treatment leads to tolerance development in *Staphylococcus aureus* and that sublethal

aBL treatment leads to tolerance development in *E. coli*, *Klebsiella pneumoniae* and *Pseudomonas aeruginosa*. The observed results suggest that the perceived accelerated mutation rate results directly from ROS-induced DNA damage, as evidenced in a previously published report [73]. Moreover, in another study, we performed screening analysis using the Keio knockout collection and identified 64 aBL-protective genes that could be involved in the development of tolerance or in *E. coli* [17]. Analogously, Murata et al. [74, 75] identified 72 thermotolerant genes in *E. coli* by screening the Keio collection grown at 47 °C. About 60% of mutants lacking genes involved in heat response were also $H_2O_2$ hypersensitive. In the present study, we cultured the selected aBL-hypersensitive single-gene mutants of *E. coli* under heat shock conditions to assess the role of a single gene in bacterial survival at high temperatures and risk of the co-selection of aBL and temperature. We observed growth defects in 11 of the 64 mutants lacking ***atpE***, ***atpG***, ***atpH*** (encoding ATP synthase subunits), ***dnaJ*** (encoding a chaperone protein), ***nuoN***, ***tolA***, ***yccM, ydcX***, ***yfgL/bamB*** (encoding plasma membrane proteins), ***ydcE/pptA*** and ***yncA/mnaT*** (enzymes). The presence of ATPase subunits and NADH: quinone oxidoreductase subunit N involved in ATP synthesis and coupled electron transport among the proteins encoded by deleted genes from mutants identified as co-sensitive to heat and aBL suggests that ATP is required in these two types of stress. One hypothesis could be that during stress all cellular repairs need energy, and the second hypothesis could be that due to the disruption of the cell membrane ATP is exposed to leakage and the lack of fully functional systems to restore ATP deficiencies causes greater sensitivity of bacteria to stress. Modification of the tRNA with a sulfur relay system encoded by *yccM* seems to be important in protection against heat and aBL. Murata et al. [75] confirmed that complementation of an appropriate single-gene mutant with *yccM* restored the insensitive phenotype, confirming the role of selected gene in the response to heat stress. Five of eleven genes encode proteins localized in the plasma membrane. In study by Ruiz et al. [76], it was observed that mutations in *yfgL* alter outer membrane permeability, which may contribute to greater sensitivity to membrane stress generated by heat and aBL treatments. TolA is also essential for outer membrane stability [77].

Therefore, proteins encoded by these genes can play an important role in cellular protection against aBL and higher temperatures and may be responsible for the cross-stress tolerance that was observed. These findings and insight into the function of the deleted genes suggest that heat stress contributes to cell membrane disruption and electron leakage, which can lead to ROS generation. This step is also present in the aBL mode of action, which partially explains that the same genes may be involved in the cellular response to heat and aBL and overexpression of shared protecting genes may lead to the risk of developing cross-stress tolerance to both stressors. Despite the similar effects of these two approaches, such as membrane disruption, ion and electron leakage, macromolecule damage resulting in bacterial death, heat stress and aBL have different initial cell killing strategies in which different genes are involved. According to current research, 53 of all 64 single-gene mutants hypersensitive to aBL were not hypersensitive to heat. The proposed mechanism of aBL and heat cross-stress tolerance is shown in Fig. 8.

Research has shown that populations that are tolerant to high temperatures do not exhibit different sensitivity profiles to aBL. In addition, aBL-tolerant populations were less sensitive to temperatures ranging from 52 to 56 °C. This result confirms that co-selection of thermal stress and aBL can occur with *E. coli*, but this process depends on the order of exposure to these selection factors. The results obtained suggest that a co-selection phenomenon occurs in which acquired tolerance to aBL may lead to cross-stress tolerance to temperature stress; however, the resulting temperature tolerance is significantly lower than that in a population selected for this feature. Fortunately, increased tolerance to temperature and aBL did not significantly affect the antibiotic sensitivity of the tolerant strains.

Our results indicate that both increased culture temperature (42 °C, 16–20 h) and short-term pre-incubation (50 °C or 52 °C, 10 or 20 min) at a high temperature affect the sensitivity of *E. coli* cultures to aBL. The aBL sensitivity profiles of bacteria cultured at 37 °C (optimal) and 42 °C were compared, and the population cultured at higher temperatures was less sensitive to aBL. Similarly, in the case of short-term pre-incubation, a significantly reduced sensitivity to aBL was observed for all tested parameters (50 °C or 52 °C; 10 min or 20 min), however, the greatest tolerance to aBL exposure was observed for the bacterial population exposed to shorter pre-incubation time (10 min, 50 °C). This is probably related to the heat shock response (HSR), which in *Escherichia coli* is a very rapid process involving the immediate transcription of heat shock proteins (HSPs) upon exposure to heat stress. The regulator of HSR (σ32 factor) is immediately stabilized and activated. Initiation of transcription of HSP genes takes place already in the first two minutes after exposure, and after five minutes of exposure, significant levels of mRNA for heat shock proteins can be detected. The HSPs' mRNA translation begins within 5–10 min. Which means that after 10–15 min, protective proteins accumulate in the cell

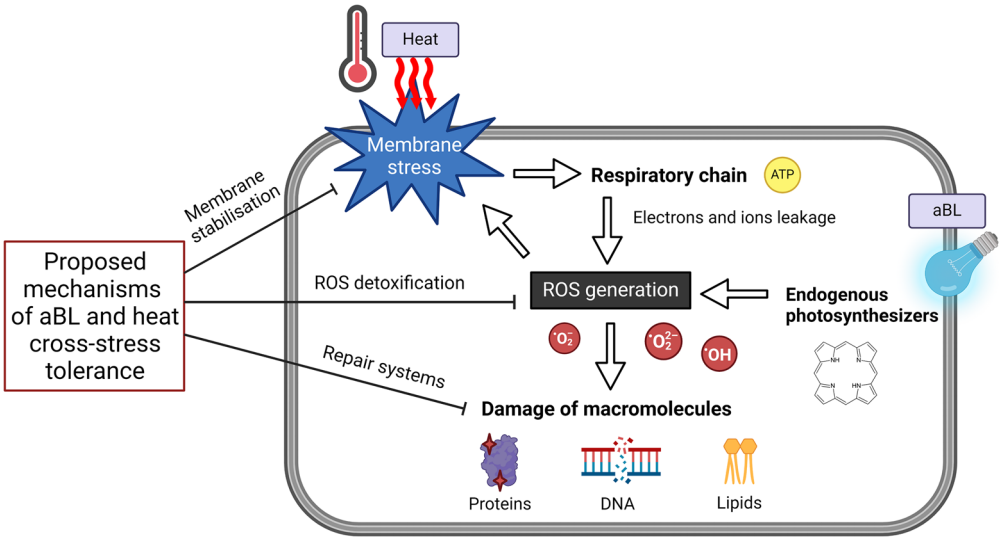


**Fig. 8** The proposed mechanism of aBL and heat cross-stress tolerance. aBL leads to the excitation of endogenous photosensitizers, which results in the generation of ROS causing membrane stress and affecting the respiratory chain. Heat stress leads to membrane destabilization and affects the respiratory chain, which leads to electron and ion leakage and consequently to generation of ROS. As a result of both aBL and heat stress, damage to cellular macromolecules accumulates, resulting in bacterial cell death. Possible mechanisms of cross-stress tolerance development may relate to membrane stabilization, ROS detoxification and activation of the macromolecule repair system. The figure is based on Murata et al. [75]

[78]. Most likely, 10 min of pre-exposure to elevated temperature was enough for *E. coli* cells to accumulate sufficient amounts of HSPs' mRNA and proteins in bacterial cells exposed to high temperature, which enabled increased tolerance to aBL. Apparently, as much as 20 min of exposure to pre-treatment with heat stress was less beneficial for the cells, perhaps it was associated with greater damage in the cell. Longer exposure to heat could also have caused that HSP proteins, instead of accumulating in the cell, were mostly already used in response to prolonged heat stress and in the case of aBL treatment there could have been significantly less of HSP accumulated in the cell.

Our result corresponds to the findings obtained by St. Denis et al. [72] for sublethal toluidine blue O-mediated (TBO-mediated) aPDI ($\lambda$ 635 nm) and pretreatment with heat (50 °C for 30 min). Short-term pre-incubation reduced *E. coli* sensitivity to TBO-mediated aPDI by 2 $\log_{10}$. The scientists also noted that protective responses, such as HSPs, were induced after TBO-aPDI treatment (GroEL increased sevenfold and DnaK threefold) [72]. The results obtained by Kitagawa et al. [79] suggest that small HSPs (IbpA and IbpB) is also involved in resistance to oxidative stress and heat. Moreover, research conducted by Bolean et al. [80] demonstrated that GroEL levels were increased following rose bengal-mediated (RB-mediated) aPDI of *Streptococcus mutans*. The expression of HSP after RB-aPDI was similar to that induced by osmotic stress (1 mol/l NaCl). HSR genes encode chaperones, proteases and other stress-related proteins that play important roles in cellular responses to stress associated with elevated temperatures and responses to several other environmental stresses, such as insufficient nutrients, DNA damage, oxidative stress and heavy metals [81].

## Conclusions

In conclusion, as in all studies on aBL conducted so far, bacteria did not develop resistance to this method, consistent with all studies on aBL conducted thus far. After repeated sublethal treatment with aBL, the drug susceptibility profile of the tolerant populations did not change significantly. Moreover, heat-tolerant strains can still be eradicated using aBL, and aBL is a safe method for the food sector, as many studies have indicated. The results obtained by our team do not invalidate the use of aBL in the food industry but indicate that researchers should consider adaptation or co-selection when establishing rules for the safe use of this method. Further research is needed on the long-term effects of aBL use and interactions with other stressors found in the food industry to develop protocols that ensure the greatest safety for consumers.

### Abbreviations

| | |
|---|---|
| 0.5 McF | McFarland standard |
| aBL | Antimicrobial blue light |
| aPDI | Antimicrobial photodynamic inactivation |
| CFU | Colony forming unit |

| | |
|---|---|
| HSP | Heat shock protein |
| HSR | Heat shock response |
| LB | Luria–Bertani medium |
| PS | Photosensitizer |
| RB | Rose Bengal |
| ROS | Reactive oxygen species |
| TBO | Toluidine blue O |

**Acknowledgements**
The authors thank the National BioResource Project (NBRP, NIG, Japan) for contributing to our work by providing us with *E. coli* BW25113 mutants from the Keio collection. The graphics were prepared with the use of BioRender.com (accessed on 31 July 2024).

**Author contributions**
Conceptualization was performed by A.R.-Z and B.K-N; data curation was performed by B.K. N.; formal analysis was performed by B.K.-N.; funding acquisition was performed by A.R.-Z.; investigation was performed by P.P and B.K.-N.; methodology was performed by A.R.-Z., B.K.-N.; project administration was performed by A.R.-Z.; resources were secured by A.R.-Z.; software was secured by B.K.-N.; supervision was performed by A.R.-Z. and M.G.; validation was performed by P.P, B.K.-N. and A.R.Z.; visualization was performed by B.K.-N.; writing (original draft) was performed by A.R-Z. and P.P and B.K.-N.; writing (review and editing) was performed by M.G.

**Funding**
This work was supported by the National Science Centre under Grant No. 2022/47/D/NZ7/01795 (A.R.-Z.).

**Data availability**
No datasets were generated or analysed during the current study.

## Declarations

**Competing interests**
The authors declare no competing interests.

**Author details**
[1]Laboratory of Photobiology and Molecular Diagnostics, Intercollegiate Faculty of Biotechnology, University of Gdansk and Medical University of Gdansk, Gdańsk, Poland.

Received: 18 June 2024 Accepted: 22 August 2024
Published online: 29 August 2024

**References**

1. World Health Organization. WHO estimates of the global burden of foodborne diseases: foodborne disease burden epidemiology reference group 2007–2015. 2015. https://iris.who.int/handle/10665/199350. Accessed 24 May 2024.
2. World Health Organization. Food safety. 2022. https://www.who.int/news-room/fact-sheets/detail/food-safety. Accessed 24 May 2024.
3. Kaper J, Nataro J, Mobley H. Pathogenic *Escherichia coli*. Nat Rev Microbiol. 2004;2(2):123–40. https://doi.org/10.1038/nrmicro818.
4. The European Food Safety Authority. Monitoring AMR in *Escherichia coli*. 2024. https://storymaps.arcgis.com/stories/788684f1e7cd48f09238101536577dc4. Accessed 24 May 2024.
5. Centers for Disease Control and Prevention. Reports of *E. coli* outbreak investigations from 2021. 2021. https://storymaps.arcgis.com/stories/788684f1e7cd48f09238101536577dc4. Accessed 24 May 2024.
6. Marmion M, Macori G, Ferone M, Whyte P, Scannell A. Survive and thrive: control mechanisms that facilitate bacterial adaptation to survive manufacturing-related stress. Int J Food Microbiol. 2022;368: 109612. https://doi.org/10.1016/j.ijfoodmicro.2022.109612.
7. Yousef A, Juneja V. Microbial stress adaptation and food safety. Boca Raton: CRC Press; 2002. https://doi.org/10.1201/9781420012828.
8. Lalremruati M, Devi A. Duration of composting and changes in temperature, pH and C/N ratio during composting: a review. Agric Rev. 2021. https://doi.org/10.18805/ag.R-2197.
9. Leistner L. Basic aspects of food preservation by hurdle technology. Int J Food Microbiol. 2000;55(1–3):181–6. https://doi.org/10.1016/S0168-1605(00)00161-6.
10. Hadi J, Wu S, Brightwell G. Antimicrobial blue light versus pathogenic bacteria: mechanism, application in the food industry, hurdle technologies and potential resistance. Foods. 2020;9(12):1895. https://doi.org/10.3390/foods9121895.
11. Bumah V, Masson-Meyers D, Enwemeka C. Blue 470 nm light suppresses the growth of *Salmonella enterica* and methicillin-resistant *Staphylococcus aureus* (MRSA) in vitro. Lasers Surg Med. 2015;47(7):595–601. https://doi.org/10.1002/lsm.22385.
12. Kim M, Adeline Ng B, Zwe Y, Yuk H. Photodynamic inactivation of *Salmonella enterica* Enteritidis by 405 ± 5-nm light-emitting diode and its application to control salmonellosis on cooked chicken. Food Control. 2017;82:305–15. https://doi.org/10.1016/J.FOODCONT.2017.06.040.
13. Meurer L, Payne W, Guffey J. Visible light as an inhibitor of *Campylobacter jejuni*. Int J Antimicrob Agents. 2020;55(1): 105818. https://doi.org/10.1016/j.ijantimicag.2019.09.022.
14. Kim MJ, Tang CH, Bang WS, Yuk HG. Antibacterial effect of 405±5 nm light emitting diode illumination against *Escherichia coli* O157: H7, *Listeria monocytogenes*, and *Salmonella* on the surface of fresh-cut mango and its influence on fruit quality. Int J Food Microbiol. 2017;244:82–9. https://doi.org/10.1016/j.ijfoodmicro.2016.12.023.
15. Sheng L, Li X, Wang L. Photodynamic inactivation in food systems: a review of its application, mechanisms, and future perspective. Trends Food Sci Technol. 2022;124:167–81. https://doi.org/10.1016/j.tifs.2022.04.001.
16. Baba T, Ara T, Hasegawa M, Takai Y, Okumura Y, Baba M, Datsenko KA, Tomita M, Wanner BL, Mori H. Construction of *Escherichia coli* K-12 in-frame, single-gene knockout mutants: the Keio collection. Mol Syst Biol. 2006;2(1):2006.0008. https://doi.org/10.1038/msb4100050.
17. Kruszewska-Naczk B, Grinholc M, Waleron K, Bandow JE, Rapacka-Zdończyk A. Can antimicrobial blue light contribute to resistance development? Genome-wide analysis revealed aBL-protective genes in *Escherichia coli*. Microbiol Spectm. 2024;12(1): e02490-23. https://doi.org/10.1128/spectrum.02490-23.
18. Rapacka-Zdonczyk A, Wozniak A, Kruszewska B, Waleron K, Grinholc M. Can Gram-negative bacteria develop resistance to antimicrobial blue light treatment? Int J Mol Sci. 2021;22(21):11579. https://doi.org/10.3390/ijms222111579.
19. Krewing M, Jarzina F, Dirks T, Schubert B, Benedikt J, Lackmann JW, Bandow JE. Plasma-sensitive *Escherichia coli* mutants reveal plasma resistance mechanisms. J R Soc Interface. 2019;16(152):20180846. https://doi.org/10.1098/rsif.2018.0846.
20. EUCAST, D. Determination of minimum inhibitory concentrations (MICs) of antibacterial agents by agar dilution. Clin Microbiol Infect. 2000;6(9):509–15.
21. Brauner A, Fridman O, Gefen O, Balaban NQ. Distinguishing between resistance, tolerance and persistence to antibiotic treatment. Nat Rev Microbiol. 2016;14(5):320–30. https://doi.org/10.1038/nrmicro.2016.34.
22. Brauner A, Shoresh N, Fridman O, Balaban NQ. An experimental framework for quantifying bacterial tolerance. Biophys J. 2017;112(12):2664–71. https://doi.org/10.1016/j.bpj.2017.05.014.
23. Sun DW. New technologies and quality issues. 2nd ed. Boca Raton: CRC Press; 2012. https://doi.org/10.1201/b12112.
24. Ball C. Short-time pasteurization of milk. Ind Eng Chem. 1943;35(1):71–84. https://doi.org/10.1021/ie50397a017.
25. Li H, Gänzle M. Some like it hot: heat resistance of *Escherichia coli* in food. Front Microbiol. 2016;7:1763. https://doi.org/10.3389/fmicb.2016.01763.
26. Dlusskaya E, McMullen L, Gänzle M. Characterization of an extremely heat-resistant *Escherichia coli* obtained from a beef processing facility. J Appl Microbiol. 2011;110(3):840–9. https://doi.org/10.1111/j.1365-2672.2011.04943.x.
27. Wang X, Zhou J. Response of foodborne pathogens to thermal processing. In: Stress responses of foodborne pathogens. Cham: Springer; 2022. p. 35–59. https://doi.org/10.1007/978-3-030-90578-1_2.
28. Katsui N, Tsuchido T, Hiramatsu R, Fujikawa S, Takano M, Shibasaki I. Heat-induced blebbing and vesiculation of the outer membrane of *Escherichia*

*coli*. J Bacteriol. 1982;151(3):1523–31. https://doi.org/10.1128/jb.151.3.1523-1531.1982.
29. Skinner F, Hugo W, Society for Applied Bacteriology, North West European Microbiological Group. Inhibition and inactivation of vegetative microbes. London: Academic Press; 1976.
30. Kramer B, Thielmann J. Monitoring the live to dead transition of bacteria during thermal stress by a multi-method approach. J Microbiol Methods. 2016;123:24–30. https://doi.org/10.1016/j.mimet.2016.02.009.
31. Leguérinel I, Spegagne I, Couvert O, Coroller L, Mafart P. Quantifying the effects of heating temperature, and combined effects of heating medium pH and recovery medium pH on the heat resistance of *Salmonella typhimurium*. Int J Food Microbiol. 2007;116(1):88–95. https://doi.org/10.1016/j.ijfoodmicro.2006.12.016.
32. Marcén M, Ruiz V, Serrano M, Condón S, Mañas P. Oxidative stress in *E. coli* cells upon exposure to heat treatments. Int J Food Microbiol. 2017;241:198–205. https://doi.org/10.1016/j.ijfoodmicro.2016.10.023.
33. Mackey B, Miles C, Parsons S, Seymour D. Thermal denaturation of whole cells and cell components of *Escherichia coli* examined by differential scanning calorimetry. J Gen Microbiol. 1991;137(10):2361–74. https://doi.org/10.1099/00221287-137-10-2361.
34. Zamenhof S. Gene unstabilization induced by heat and by nitrous acid. J Bacteriol. 1961;81(1):111–7. https://doi.org/10.1128/jb.81.1.111-117.1961.
35. Sampedro F, McAloon A, Yee W, Fan X, Geveke D. Cost analysis and environmental impact of pulsed electric fields and high pressure processing in comparison with thermal pasteurization. Food Bioprocess Technol. 2014;7(7):1928–37. https://doi.org/10.1007/s11947-014-1298-6.
36. Hyun J, Lee S. Blue light-emitting diodes as eco-friendly non-thermal technology in food preservation. Trends Food Sci Technol. 2020;105:284–95. https://doi.org/10.1016/J.TIFS.2020.09.008.
37. D'Orazio J, Jarrett S, Amaro-Ortiz A, Scott T. UV radiation and the skin. Int J Mol Sci. 2013;14(6):12222. https://doi.org/10.3390/IJMS140612222.
38. Dai T, Gupta A, Huang Y, Yin R, Murray C, Vrahas M, Sherwood M, Tegos G, Hamblin M. Blue light rescues mice from potentially fatal *Pseudomonas aeruginosa* burn infection: efficacy, safety, and mechanism of action. Antimicrob Agents Chemother. 2013;57(3):1238–45. https://doi.org/10.1128/AAC.01652-12.
39. Kleinpenning M, Smits T, Frunt M, van Erp P, van de Kerkhof P, Gerritsen R. Clinical and histological effects of blue light on normal skin. Photodermatol Photoimmunol Photomed. 2010;26(1):16–21. https://doi.org/10.1111/J.1600-0781.2009.00474.X.
40. Abana C, Brannon J, Ebbott R, Dunigan T, Guckes K, Fuseini H, Powers J, Rogers B, Hadjifrangiskou M. Characterization of blue light irradiation effects on pathogenic and nonpathogenic *Escherichia coli*. MicrobiologyOpen. 2017;6(4): e00466. https://doi.org/10.1002/mbo3.466.
41. Wu S, Ross C, Hadi J, Brightwell G. In vitro inactivation effect of blue light emitting diode (LED) on Shiga-toxin-producing *Escherichia coli* (STEC). Food Control. 2021;125: 107990. https://doi.org/10.1016/j.foodcont.2021.107990.
42. dos Anjos C, Sellera F, de Freitas L, Gargano R, Telles E, Freitas R, Baptista M, Ribeiro M, Lincopan N, Pogliani F, Sabino C. Inactivation of milk-borne pathogens by blue light exposure. J Dairy Sci. 2020;103(2):1261–8. https://doi.org/10.3168/JDS.2019-16758.
43. Hyun J, Lee S. Antibacterial effect and mechanisms of action of 460–470 nm light-emitting diode against *Listeria monocytogenes* and *Pseudomonas fluorescens* on the surface of packaged sliced cheese. Food Microbiol. 2020;86: 103314. https://doi.org/10.1016/j.fm.2019.103314.
44. Ricciardi E, Pedros-Garrido S, Papoutsis K, Lyng J, Conte A, Del Nobile M. Novel technologies for preserving ricotta cheese: effects of ultraviolet and near-ultraviolet-visible light. Foods. 2020;9(5):580. https://doi.org/10.3390/FOODS9050580.
45. Lena A, Marino M, Manzano M, Comuzzi C, Maifreni M. An overview of the application of blue light-emitting diodes as a non-thermic green technology for microbial inactivation in the food sector. Food Eng Rev. 2023;16(1):59–84. https://doi.org/10.1007/S12393-023-09355-1.
46. Xu X, Niu Y, Liang K, Wang J, Li X, Yang Y. Heat shock transcription factor δ32 is targeted for degradation via an ubiquitin-like protein ThiS in *Escherichia coli*. Biochem Biophys Res Commun. 2015;459(2):240–5. https://doi.org/10.1016/j.bbrc.2015.02.087.
47. Lee Y, Ha J, Oh J, Cho M. The effect of LED irradiation on the quality of cabbage stored at a low temperature. Food Sci Biotechnol. 2014;23(4):1087–93. https://doi.org/10.1007/s10068-014-0149-6.
48. Chen H, Cheng Y, Moraru CI. Blue 405 nm LED light effectively inactivates bacterial pathogens on substrates and packaging materials used in food processing. Sci Rep. 2023;13(1):15472. https://doi.org/10.1038/s41598-023-42347-z.
49. Gunther N, Phillips J, Sommers C. The effects of 405-nm visible light on the survival of *Campylobacter* on chicken skin and stainless steel. Foodborne Pathog Dis. 2016;13(5):245–50. https://doi.org/10.1089/FPD.2015.2084.
50. Li X, Kim MJ, Bang WS, Yuk HG. Anti-biofilm effect of 405-nm LEDs against *Listeria monocytogenes* in simulated ready-to-eat fresh salmon storage conditions. Food Control. 2018;84:513–21. https://doi.org/10.1016/J.FOODCONT.2017.09.006.
51. Shirai A, Yasutomo Y, Kanno Y. Effects of violet-blue light-emitting diode on controlling bacterial contamination in boiled young sardine. Biocontrol Sci. 2022;27(1):9–19. https://doi.org/10.4265/BIO.27.9.
52. Ashbolt NJ, Amézquita A, Backhaus T, Borriello P, Brandt KK, Collignon P, et al. Human health risk assessment (HHRA) for environmental development and transfer of antibiotic resistance. Environ Health Perspect. 2013;121(9):993–1001. https://doi.org/10.1289/ehp.1206316.
53. Puangseree J, Jeamsripong S, Prathan R, Pungpian C, Chuanchuen R. Resistance to widely-used disinfectants and heavy metals and cross resistance to antibiotics in *Escherichia coli* isolated from pigs, pork and pig carcass. Food Control. 2021;124: 107892. https://doi.org/10.1016/j.foodcont.2021.107892.
54. Pal C, Asiani K, Arya S, Rensing C, Stekel DJ, Larsson DJ, Hobman JL. Metal resistance and its association with antibiotic resistance. Adv Microb Physiol. 2017;70:261–313. https://doi.org/10.1016/bs.ampbs.2017.02.001.
55. Gnanadhas DP, Marathe SA, Chakravortty D. Biocides–resistance, cross-resistance mechanisms and assessment. Expert Opin Investig Drugs. 2013;22(2):191–206. https://doi.org/10.1517/13543784.2013.748035.
56. Baker-Austin C, Wright MS, Stepanauskas R, McArthur JV. Co-selection of antibiotic and metal resistance. Trends Microbiol. 2006;14(4):176–82. https://doi.org/10.1016/j.tim.2006.02.006.
57. Cantón R, Ruiz-Garbajosa P. Co-resistance: an opportunity for the bacteria and resistance genes. Curr Opin Pharmacol. 2011;11(5):477–85. https://doi.org/10.1016/j.coph.2011.07.007.
58. Witkin EM. Genetics of resistance to radiation in *Escherichia coli*. Genetics. 1947;32(3):221. https://doi.org/10.1093/genetics/32.3.221.
59. Harris DR, Pollock SV, Wood EA, Goiffon RJ, Klingele AJ, Cabot EL, et al. Directed evolution of ionizing radiation resistance in *Escherichia coli*. J Bacteriol. 2009;191(16):5240–52. https://doi.org/10.1128/jb.00502-09.
60. Aono R, Kobayashi H. Cell surface properties of organic solvent-tolerant mutants of *Escherichia coli* K-12. Appl Environ Microbiol. 1997;63(9):3637–42. https://doi.org/10.1128/aem.63.9.3637-3642.1997.
61. Gambushe SM, Zishiri OT, El Zowalaty ME. Review of *Escherichia coli* O157: H7 prevalence, pathogenicity, heavy metal and antimicrobial resistance, African perspective. Infect Drug Resist. 2022;15:4645–73. https://doi.org/10.2147/IDR.S365269.
62. Arnold CN, McElhanon J, Lee A, Leonhart R, Siegele DA. Global analysis of *Escherichia coli* gene expression during the acetate-induced acid tolerance response. J Bacteriol. 2001;183(7):2178–86. https://doi.org/10.1128/jb.183.7.2178-2186.2001.
63. Oliveira J, Reygaert WC. Gram negative bacteria. StatPearls. Treasure Island: StatPearls Publishing; 2022.
64. Rapacka-Zdonczyk A, Wozniak A, Pieranski M, Woziwodzka A, Bielawski KP, Grinholc M. Development of *Staphylococcus aureus* tolerance to antimicrobial photodynamic inactivation and antimicrobial blue light upon sub-lethal treatment. Sci Rep. 2019;9(1):1–18. https://doi.org/10.1038/s41598-019-45962-x.
65. Ramteke PW. Plasmid mediated co-transfer of antibiotic resistance and heavy metal tolerance in coliforms. Indian J Microbiol. 1997;37:177–82. https://doi.org/10.5897/AJMR12.1563.
66. Rowe MT, Kirk R. Investigation into the phenomenon of cross-protection in *Escherichia coli* O157: H7. Food Microbiol. 1999;16:157–64. https://doi.org/10.1006/fmic.1998.0229.
67. Isohanni P, Huehn S, Aho T, Alter T, Lyhs U. Heat stress adaptation induces cross-protection against lethal acid stress conditions in *Arcobacter butzleri* but not in *Campylobacter jejuni*. Food Microbiol. 2013;34(2):431–5. https://doi.org/10.1016/j.fm.2013.02.001.
68. Liao X, Chen X, Sant'Ana A, Feng J, Ding T. Pre-exposure of foodborne *Staphylococcus aureus* isolates to organic acids induces cross-adaptation

to mild heat. Microbiol Spectr. 2023;11(2): e03832-22. https://doi.org/10.1128/spectrum.03832-22.
69. Jenkins D, Schultz J, Matin A. Starvation-induced cross protection against heat or $H_2O_2$ challenge in *Escherichia coli*. J Bacteriol. 1988;170(9):3910–4. https://doi.org/10.1128/jb.170.9.3910-3914.1988.
70. Pumirat P, Vanaporn M, Boonyuen U, Indrawattana N, Rungruengkitkun A, Chantratita N. Effects of sodium chloride on heat resistance, oxidative susceptibility, motility, biofilm and plaque formation of *Burkholderia pseudomallei*. MicrobiologyOpen. 2017;6(4): e00493. https://doi.org/10.1002/mbo3.493.
71. Yang H, Yao S, Zhang M, Wu C. Heat adaptation induced cross protection against ethanol stress in *Tetragenococcus halophilus*: physiological characteristics and proteomic analysis. Front Microbiol. 2021;12: 686672. https://doi.org/10.3389/fmicb.2021.686672.
72. St. Denis T, Huang L, Dai T, Hamblin M. Analysis of the bacterial heat shock response to photodynamic therapy-mediated oxidative stress. Photochem Photobiol. 2011;87(3):707–13. https://doi.org/10.1111/j.1751-1097.2011.00902.x.
73. Grinholc M, Rodziewicz A, Forys K, Rapacka-Zdonczyk A, Kawiak A, Domachowska A, Golunski G, Wolz C, Mesak L, Becker K, Bielawski KP. Fine-tuning recA expression in *Staphylococcus aureus* for antimicrobial photoinactivation: importance of photo-induced DNA damage in the photoinactivation mechanism. Appl Microbiol Biotechnol. 2015;99(21):9161–76. https://doi.org/10.1007/s00253-015-6863-z.
74. Murata M, Fujimoto H, Nishimura K, Charoensuk K, Nagamitsu H, Raina S, Kosaka T, Oshima T, Ogasawara N, Yamada M. Molecular strategy for survival at a critical high temperature in *Eschierichia coli*. PLoS ONE. 2011;6(6): e20063. https://doi.org/10.1371/journal.pone.0020063.
75. Murata M, Ishii A, Fujimoto H, Nishimura K, Kosaka T, Mori H, Yamada M. Update of thermotolerant genes essential for survival at a critical high temperature in *Escherichia coli*. PLoS ONE. 2018;13(2): e0189487. https://doi.org/10.1371/journal.pone.0189487.
76. Ruiz N, Falcone B, Kahne D, Silhavy TJ. Chemical conditionality: a genetic strategy to probe organelle assembly. Cell. 2005;121(2):307–17. https://doi.org/10.1016/j.cell.2005.02.014.
77. Derouiche R, Gavioli M, Bénédetti H, Prilipov A, Lazdunski C, Lloubes R. TolA central domain interacts with *Escherichia coli* porins. EMBO J. 1996;15(23):6408–15. https://doi.org/10.1002/j.1460-2075.1996.tb01032.x.
78. Yura T, Nagai H, Mori H. Regulation of the heat-shock response in bacteria. Annu Rev Microbiol. 1993;47:321–51.
79. Kitagawa M, Matsumura Y, Tsuchido T. Small heat shock proteins, IbpA and IbpB, are involved in resistances to heat and superoxide stresses in *Escherichia coli*. FEMS Microbiol Lett. 2000;184(2):165–71. https://doi.org/10.1111/j.1574-6968.2000.tb09009.x.
80. Bolean M, Paulino TDP, Thedei G Jr, Ciancaglini P. Photodynamic therapy with rose bengal induces GroEL expression in *Streptococcus mutans*. Photomed Laser Surg. 2010;28(S1):S79. https://doi.org/10.1089/pho.2009.2635.
81. Gomes SL, Simão RDCG. Stress response: heat. In: Encyclopedia of microbiology. Amsterdam: Elsevier; 2009. p. 464–74.

## Publisher's Note

# 9. Statements of contributions

Gdańsk, 13.04.26

MSc Beata Kruszewska-Naczk

Laboratory of Photobiology and Molecular Diagnostics,

Intercollegiate Faculty of Biotechnology,

University of Gdansk and Medical University of Gdansk

Author contribution statement

I hereby declare my contribution to the following manuscript:

1) Kruszewska-Naczk, B., Burzyńska, N., Goik, D., Grinholc, M., Nakonieczna, J., Pawlik, N., Pierański, M. K., Woźniak-Pawlikowska, A., Rapacka-Zdończyk, A. & Dai, T. (2026). Mechanisms and determinants of bacterial susceptibility to antimicrobial Blue Light: from chromophores to transcriptomes. *Drug Resistance Updates*, 101391.

**Conceptualization, Writing - original draft - sections: Introduction, Genetic factors influencing bacterial susceptibility to aBL, Conclusions and future perspectives**

Beata Kruszewska-Naczk

2) Kruszewska-Naczk, B., Grinholc, M., Waleron, K., Bandow, J. E., & Rapacka-Zdończyk, A. (2024). Can antimicrobial blue light contribute to resistance development? Genome-wide analysis revealed aBL-protective genes in Escherichia coli. *Microbiology spectrum*, *12*(1), e02490-23. doi.org/10.1128/spectrum.02490-23

**Data curation, Formal analysis, Investigation, Methodology, Software, Validation, Visualization, Writing – original draft**

Beata Kruszewska-Naczk

3) Kruszewska-Naczk, B., Grinholc, M., & Rapacka-Zdonczyk, A. (2024). Mimicking the Effects of Antimicrobial Blue Light: Exploring Single Stressors and Their Impact on Microbial Growth. *Antioxidants*, *13*(12), 1583. doi.org/10.3390/antiox13121583

**Conceptualization, Data curation, Investigation, Methodology, Software, Validation, Writing - original draft, Formal analysis and Visualization - except mathematical analysis of the results performed by Anna Koelmer, M.A., a specialist biostatistician, as a paid service, from the Centre of Biostatistics and Bioinformatics Analysis, Medical University of Gdansk, Poland**

Beata Kruszewska-Naczk

Gdańsk, 13.04.26

MSc Beata Kruszewska-Naczk

Laboratory of Photobiology and Molecular Diagnostics,

Intercollegiate Faculty of Biotechnology,

University of Gdansk and Medical University of Gdansk

## Author contribution statement

I hereby declare my contribution to the following manuscript:

4) Kruszewska-Naczk, B., Grinholc, M., & Rapacka-Zdonczyk, A. (2025). Identification and validation of reference genes for quantitative gene expression analysis under 409 and 415 nm antimicrobial blue light treatment. *Frontiers in Molecular Biosciences*, *11*, 1467726. doi: 10.3389/fmolb.2024.1467726

**Conceptualization, Data curation, Formal Analysis, Funding acquisition, Investigation, Methodology, Project administration, Software, Validation, Visualization, Writing -original draft**

.....Beata Kruszewska-Naczk.....

5) Kruszewska-Naczk, B., Pikulik-Arif, P., Grinholc, M., & Rapacka-Zdonczyk, A. (2024). Antibacterial blue light is a promising tool for inactivating Escherichia coli in the food sector due to its low risk of cross-stress tolerance. *Chemical and Biological Technologies in Agriculture*, *11*(1), 126. doi.org/10.1186/s40538-024-00658-x

**Conceptualization, Investigation: Mutants Analyzing and Antimicrobial Susceptibility Testing, Bioinformatics and Statistical Analysis, Methodology, Software, Validation, Visualization, Data Curation, Formal Analysis, Writing - Original Draft**

.....Beata Kruszewska-Naczk.....

Gdańsk, 13.04.26

Dr Aleksandra Rapacka-Zdończyk

Laboratory of Photobiology and Molecular Diagnostics,

Intercollegiate Faculty of Biotechnology,

University of Gdansk and Medical University of Gdansk

## Author contribution statement

I hereby declare my contribution to the following manuscript:

1) Kruszewska-Naczk, B., Burzyńska, N., Goik, D., Grinholc, M., Nakonieczna, J., Pawlik, N., Pierański, M. K., Woźniak-Pawlikowska, A., Rapacka-Zdończyk, A. & Dai, T. (2026). Mechanisms and determinants of bacterial susceptibility to antimicrobial Blue Light: from chromophores to transcriptomes. *Drug Resistance Updates*, 101391.

**Conceptualization, Writing – review and editing, Writing - original draft - sections: Microbial determinants of susceptibility to aBL, Funding acquisition**

Rapacka - Zdończyk

2) Kruszewska-Naczk, B., Grinholc, M., Waleron, K., Bandow, J. E., & Rapacka-Zdończyk, A. (2024). Can antimicrobial blue light contribute to resistance development? Genome-wide analysis revealed aBL-protective genes in Escherichia coli. *Microbiology spectrum*, *12*(1), e02490-23. doi.org/10.1128/spectrum.02490-23

**Conceptualization, Funding acquisition, Methodology, Resources, Validation, Writing – original draft**

Rapacka - Zdończyk

3) Kruszewska-Naczk, B., Grinholc, M., & Rapacka-Zdonczyk, A. (2024). Mimicking the Effects of Antimicrobial Blue Light: Exploring Single Stressors and Their Impact on Microbial Growth. *Antioxidants*, *13*(12), 1583. doi.org/10.3390/antiox13121583

**Conceptualization, Methodology, Project administration, Resources, Supervision, Validation, Writing - original draft**

Rapacka - Zdończyk

Gdańsk, 13.04.26

Dr Aleksandra Rapacka-Zdończyk

Laboratory of Photobiology and Molecular Diagnostics,

Intercollegiate Faculty of Biotechnology,

University of Gdansk and Medical University of Gdansk

## Author contribution statement

I hereby declare my contribution to the following manuscript:

4) Kruszewska-Naczk, B., Grinholc, M., & Rapacka-Zdonczyk, A. (2025). Identification and validation of reference genes for quantitative gene expression analysis under 409 and 415 nm antimicrobial blue light treatment. *Frontiers in Molecular Biosciences*, *11*, 1467726. doi: 10.3389/fmolb.2024.1467726

**Funding acquisition, Methodology, Resources, Supervision, Validation, Writing –original draft.**

..... Rapacka - Zdończyk .....

5) Kruszewska-Naczk, B., Pikulik-Arif, P., Grinholc, M., & Rapacka-Zdonczyk, A. (2024). Antibacterial blue light is a promising tool for inactivating Escherichia coli in the food sector due to its low risk of cross-stress tolerance. *Chemical and Biological Technologies in Agriculture*, *11*(1), 126. doi.org/10.1186/s40538-024-00658-x

**Conceptualization, Funding acquisition, Methodology, Project administration, Resources, Supervision, Validation, Writing - original draft**

..... Rapacka - Zdończyk .....

Gdańsk, 13.04.26

Dr hab. Mariusz Grinholc prof. UG

Laboratory of Photobiology and Molecular Diagnostics,

Intercollegiate Faculty of Biotechnology,

University of Gdansk and Medical University of Gdansk

## Author contribution statement

I hereby declare my contribution to the following manuscript:

1) Kruszewska-Naczk, B., Burzyńska, N., Goik, D., Grinholc, M., Nakonieczna, J., Pawlik, N., Pierański, M. K., Woźniak-Pawlikowska, A., Rapacka-Zdończyk, A. & Dai, T. (2026). Mechanisms and determinants of bacterial susceptibility to antimicrobial Blue Light: from chromophores to transcriptomes. *Drug Resistance Updates*, 101391.

Writing – review and editing, Writing – original draft – sections: Environmental and physiological factors affecting aBL efficacy

.....

2) Kruszewska-Naczk, B., Grinholc, M., Waleron, K., Bandow, J. E., & Rapacka-Zdończyk, A. (2024). Can antimicrobial blue light contribute to resistance development? Genome-wide analysis revealed aBL-protective genes in *Escherichia coli*. *Microbiology spectrum*, *12*(1), e02490-23. doi.org/10.1128/spectrum.02490-23

Conceptualization, Methodology, Resources, Supervision, Writing – review and editing

.....

3) Kruszewska-Naczk, B., Grinholc, M., & Rapacka-Zdonczyk, A. (2024). Mimicking the Effects of Antimicrobial Blue Light: Exploring Single Stressors and Their Impact on Microbial Growth. *Antioxidants*, *13*(12), 1583. doi.org/10.3390/antiox13121583

Funding acquisition, Supervision, Writing – review and editing

.....

4) Kruszewska-Naczk, B., Grinholc, M., & Rapacka-Zdonczyk, A. (2025). Identification and validation of reference genes for quantitative gene expression analysis under 409 and 415 nm antimicrobial blue light treatment. *Frontiers in Molecular Biosciences*, *11*, 1467726. doi: 10.3389/fmolb.2024.1467726

Supervision, Writing – review and editing

.....

Gdańsk, 13.04.26

Dr hab. Mariusz Grinholc prof. UG

Laboratory of Photobiology and Molecular Diagnostics,

Intercollegiate Faculty of Biotechnology,

University of Gdansk and Medical University of Gdansk

## Author contribution statement

I hereby declare my contribution to the following manuscript:

5) Kruszewska-Naczk, B., Pikulik-Arif, P., Grinholc, M., & Rapacka-Zdonczyk, A. (2024). Antibacterial blue light is a promising tool for inactivating Escherichia coli in the food sector due to its low risk of cross-stress tolerance. *Chemical and Biological Technologies in Agriculture*, *11*(1), 126. doi.org/10.1186/s40538-024-00658-x

Supervision, Writing – review and editing

.....

Gdańsk, 13.04.26

Dr hab. Joanna Nakonieczna prof. UG

Laboratory of Photobiology and Molecular Diagnostics,

Intercollegiate Faculty of Biotechnology,

University of Gdansk and Medical University of Gdansk

**Author contribution statement**

I hereby declare my contribution to the following manuscript:

1) Kruszewska-Naczk, B., Burzyńska, N., Goik, D., Grinholc, M., Nakonieczna, J., Pawlik, N., Pierański, M. K., Woźniak-Pawlikowska, A., Rapacka-Zdończyk, A. & Dai, T. (2026). Mechanisms and determinants of bacterial susceptibility to antimicrobial Blue Light: from chromophores to transcriptomes. *Drug Resistance Updates*, 101391.

**Writing – original draft – sections: Molecular targets and lethal mechanisms of aBL**

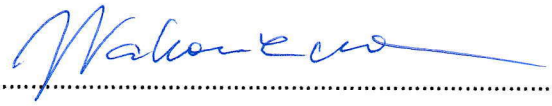

.....

Gdańsk, 13.04.26

MSc Dominika Goik

Laboratory of Photobiology and Molecular Diagnostics,

Intercollegiate Faculty of Biotechnology,

University of Gdansk and Medical University of Gdansk

**Author contribution statement**

I hereby declare my contribution to the following manuscript:

1) Kruszewska-Naczk, B., Burzyńska, N., Goik, D., Grinholc, M., Nakonieczna, J., Pawlik, N., Pierański, M. K., Woźniak-Pawlikowska, A., Rapacka-Zdończyk, A. & Dai, T. (2026). Mechanisms and determinants of bacterial susceptibility to antimicrobial Blue Light: from chromophores to transcriptomes. *Drug Resistance Updates*, 101391.

**Writing – original draft – sections: Transcriptomic responses to aBL-induced oxidative stress**

.....Goik Dominika.....

Gdańsk, 13.04.26

Dr. Agata Woźniak-Pawlikowska

Laboratory of Photobiology and Molecular Diagnostics,

Intercollegiate Faculty of Biotechnology,

University of Gdansk and Medical University of Gdansk

**Author contribution statement**

I hereby declare my contribution to the following manuscript:

1) Kruszewska-Naczk, B., Burzyńska, N., Goik, D., Grinholc, M., Nakonieczna, J., Pawlik, N., Pierański, M. K., Woźniak-Pawlikowska, A., Rapacka-Zdończyk, A. & Dai, T. (2026). Mechanisms and determinants of bacterial susceptibility to antimicrobial Blue Light: from chromophores to transcriptomes. *Drug Resistance Updates*, 101391.

**Visualization – preparing figures**

.....Agata Woźniak-Pawlikowska.....

Gdańsk, 13.04.26

MSc Natalia Burzyńska-Młotkowska

Laboratory of Photobiology and Molecular Diagnostics,

Intercollegiate Faculty of Biotechnology,

University of Gdansk and Medical University of Gdansk

**Author contribution statement**

I hereby declare my contribution to the following manuscript:

1) Kruszewska-Naczk, B., Burzyńska, N., Goik, D., Grinholc, M., Nakonieczna, J., Pawlik, N., Pierański, M. K., Woźniak-Pawlikowska, A., Rapacka-Zdończyk, A. & Dai, T. (2026). Mechanisms and determinants of bacterial susceptibility to antimicrobial Blue Light: from chromophores to transcriptomes. *Drug Resistance Updates*, 101391.

**Writing – original draft – sections: Endogenous porphyrins as primary photosensitizers in aBL**

Natalia Burzyńska-Młotkowska

Boston, 13.04.26

Tianhong Dai, PhD

Wellman Center for Photomedicine

Massachusetts General Hospital

Harvard Medical School, Boston

## Author contribution statement

I hereby declare my contribution to the following manuscript:

1) Kruszewska-Naczk, B., Burzyńska, N., Goik, D., Grinholc, M., Nakonieczna, J., Pawlik, N., Pierański, M. K., Woźniak-Pawlikowska, A., Rapacka-Zdończyk, A. & Dai, T. (2026). Mechanisms and determinants of bacterial susceptibility to antimicrobial Blue Light: from chromophores to transcriptomes. *Drug Resistance Updates*, 101391.

**Writing – review and editing** Tianhong Dai .....

Gdańsk, 13.04.26

Dr. Michał K. Pierański

Department of Pharmaceutical Technology and Biochemistry,

Faculty of Chemistry,

Gdansk University of Technology

## Author contribution statement

I hereby declare my contribution to the following manuscript:

1) Kruszewska-Naczk, B., Burzyńska, N., Goik, D., Grinholc, M., Nakonieczna, J., Pawlik, N., Pierański, M. K., Woźniak-Pawlikowska, A., Rapacka-Zdończyk, A. & Dai, T. (2026). Mechanisms and determinants of bacterial susceptibility to antimicrobial Blue Light: from chromophores to transcriptomes. *Drug Resistance Updates*, 101391.

Writing – original draft – sections: Susceptibility of *Streptococcus* and *Enterococcus* to aBL

13.04.2026 Michał Pierański

Gdańsk, 13.04.26

MSc Natalia Pawlik

Laboratory of Photobiology and Molecular Diagnostics,

Intercollegiate Faculty of Biotechnology,

University of Gdansk and Medical University of Gdansk

**Author contribution statement**

I hereby declare my contribution to the following manuscript:

1) Kruszewska-Naczk, B., Burzyńska, N., Goik, D., Grinholc, M., Nakonieczna, J., Pawlik, N., Pierański, M. K., Woźniak-Pawlikowska, A., Rapacka-Zdończyk, A. & Dai, T. (2026). Mechanisms and determinants of bacterial susceptibility to antimicrobial Blue Light: from chromophores to transcriptomes. *Drug Resistance Updates*, 101391.

**Writing – original draft – sections: Other endogenous photosensitizing chromophores**

Natalia Pawlik

MEDICAL
UNIVERSITY
OF GDAŃSK

www.mug.edu.pl
58 349 11 11
info@gumed.edu.pl
ul. M. Skłodowskiej-Curie 3a,
80-210 Gdańsk

GDAŃSK 13.04.2026

**Author contribution statement**

I hereby declare my contribution to the following manuscript:

1) Kruszewska-Naczk, B., Grinholc, M., Waleron, K., Bandow, J. E., & Rapacka-Zdończyk, A. (2024). Can antimicrobial blue light contribute to resistance development? Genome-wide analysis revealed aBL-protective genes in *Escherichia co*li. *Microbiology spectrum*, *12*(1), e02490-23. doi.org/10.1128/spectrum.02490-23

**I declare that my contribution to the creation of the above-mentioned publication includes:**

**Conceptualization, Writing – review and editing**

DEPARTMENT OF PHARMACEUTICAL MICROBIOLOGY, FACULTY OF PHARMACY
dr hab. Krzysztof Waleron | krzysztof.waleron@gumed.edu.pl |Al. Gen. J. Hallera 107, 80-416 Gdańsk

Bochum, 13.04.2026

Prof. Dr. Julia Elisabeth Bandow

Applied Microbiology, Faculty of Biology and Biotechnology

Ruhr University Bochum

Universitätsstraße, Bochum, Germany

**Author contribution statement**

I hereby declare my contribution to the following manuscript:

1) Kruszewska-Naczk, B., Grinholc, M., Waleron, K., Bandow, J. E., & Rapacka-Zdończyk, A. (2024). Can antimicrobial blue light contribute to resistance development? Genome-wide analysis revealed aBL-protective genes in *Escherichia coli*. *Microbiology spectrum*, *12*(1), e02490-23. doi.org/10.1128/spectrum.02490-23

**Methodology, Writing – review and editing**

Julia Bandow

Gdańsk, 13/04/2026

MSc Patrycja Pikulik-Arif

**Author contribution statement**

I hereby declare my contribution to the following manuscript:

5) Kruszewska-Naczk, B., Pikulik-Arif, P., Grinholc, M., & Rapacka-Zdonczyk, A. (2024). Antibacterial blue light is a promising tool for inactivating Escherichia coli in the food sector due to its low risk of cross-stress tolerance. *Chemical and Biological Technologies in Agriculture*, *11*(1), 126. doi.org/10.1186/s40538-024-00658-x

**Investigation: tolerance development and evaluation, long- and short-term preincubations, cross-tolerance experiments, Validation, Writing - original draft**

Patrycja Pikulik-Arif

# 10. List of references


1. Aminov, R. I. (2010). A brief history of the antibiotic era: lessons learned and challenges for the future. Frontiers in microbiology, 1, 134.

2. Anomaly, J. (2020). Antibiotics and animal agriculture: the need for global collective action. In Ethics and drug resistance: Collective responsibility for global public health (pp. 297-308). Cham: Springer International Publishing.

3. Ashkenazi, H., Malik, Z., Harth, Y., & Nitzan, Y. (2003). Eradication of Propionibacterium acnes by its endogenic porphyrins after illumination with high intensity blue light. FEMS Immunology & Medical Microbiology, 35(1), 17-24. https://doi.org/10.1016/s0928-8244(02)00423-6

4. Cieplik, F., Deng, D., Crielaard, W., Buchalla, W., Hellwig, E., Al-Ahmad, A., & Maisch, T. (2018). Antimicrobial photodynamic therapy – what we know and what we don't. Critical Reviews in Microbiology, 44(5), 571–589. https://doi.org/10.1080/1040841X.2018.1467876

5. Cong, X., Hillert, J., Krolla, P., & Schwartz, T. (2025). Cellular insights into reactive oxidative species (ROS) and bacterial stress responses induced by antimicrobial blue light (aBL) for inactivating antibiotic resistant bacteria (ARB) in wastewater. Science of the Total Environment, 1005, 180878. https://doi.org/10.1016/j.scitotenv.2025.180878

6. Dai, T., Gupta, A., Huang, Y. Y., Yin, R., Murray, C. K., Vrahas, M. S., ... & Hamblin, M. R. (2013). Blue light rescues mice from potentially fatal Pseudomonas aeruginosa burn infection: efficacy, safety, and mechanism of action. Antimicrobial agents and chemotherapy, 57(3), 1238-1245.

7. Das, M., Ojha, A. K., Dolma, K. G., Majumdar, T., Sarmah, P., Hazarika, S., ... & Ramamurthy, T. (2025). Monitoring the potential dissemination of antimicrobial resistance in foods, environment, and clinical samples: a one health prospective. Food Science and Biotechnology, 34(3), 803-813.

8. DeNegre, A. A., Ndeffo Mbah, M. L., Myers, K., & Fefferman, N. H. (2019). Emergence of antibiotic resistance in immunocompromised host populations: A case study of emerging antibiotic resistant tuberculosis in AIDS patients. PloS one, 14(2), e0212969.

9. Dos Anjos, C., Leanse, L. G., Ribeiro, M. S., Sellera, F. P., Dropa, M., Arana-Chavez, V. E., ... & Sabino, C. P. (2023). New insights into the bacterial targets of antimicrobial blue light. Microbiology Spectrum, 11(2), e02833-22.

10. Dos Anjos, C., Sellera, F. P., Ribeiro, M. S., Baptista, M. S., Pogliani, F. C., Lincopan, N., & Sabino, C. P. (2020a). Antimicrobial blue light and photodynamic therapy inhibit clinically relevant β-lactamases with extended-spectrum (ESBL) and carbapenemase activity. Photodiagnosis and Photodynamic Therapy, 32, 102086. https://doi.org/10.1016/j.pdpdt.2020.102086

11. Drug-resistant infections. A threat to our economic future. Washington DC: World Bank; 2017 (https://documents1.worldbank.org/curated/en/323311493396993758/pdf/final-report.pdf).

12. Ekici, G., & Dümen, E. (2019). Escherichia coli and food safety. In The universe of Escherichia coli. IntechOpen.

13. Fleming, A. (1929). On antibacterial action of culture of Penicillium, with special reference to their use in isolation of B. influenzae. Br. J. Exp. Pathol. 10, 226–236

14. Founou, L. L., Founou, R. C., & Essack, S. Y. (2016). Antibiotic resistance in the food chain: a developing country-perspective. Frontiers in microbiology, 7, 1881.

15. Grinholc, M., Rodziewicz, A., Forys, K., Rapacka-Zdonczyk, A., Kawiak, A., Domachowska, 1459 A., ... & Bielawski, K. P. (2015). Fine-tuning recA expression in Staphylococcus aureus for antimicrobial 1460 photoinactivation: importance of photo-induced DNA damage in the photoinactivation mechanism. Applied microbiology and biotechnology, 99, 9161-9176.

16. Hamblin, M. R., Viveiros, J., Yang, C., Ahmadi, A., Ganz, R. A., & Tolkoff, M. J. (2005). Helicobacter pylori accumulates photoactive porphyrins and is killed by visible light. Antimicrobial agents and chemotherapy, 49(7), 2822-2827. https://doi.org/10.1128/aac.49.7.2822-2827.2005

17. Han, X.M.; Hu, H.W.; Chen, Q.L.; Yang, L.Y.; Li, H.L.; Zhu, Y.G.; Li, X.Z.; Ma, Y.B. Antibiotic resistance genes and associated bacterial communities in agricultural soils amended with different sources of animal manures. Soil Biol. Biochem. 2018, 126, 91–102.

18. Hönigsmann, H. History of phototherapy in dermatology. Photochem Photobiol Sci 12, 16–21 (2013). https://doi.org/10.1039/c2pp25120e

19. Kim, M. J., & Yuk, H. G. (2017). Antibacterial mechanism of 405-nanometer light-emitting diode against Salmonella at refrigeration temperature. Applied and environmental microbiology, 83(5), 1562 e02582-16. https://doi.org/10.1128/aem.02582-16

20. Leanse, L. G., Dos Anjos, C., Mushtaq, S., & Dai, T. (2022). Antimicrobial blue light: A 'Magic Bullet'for the 21st century and beyond?. Advanced drug delivery reviews, 180, 114057. https://doi.org/10.1016/j.addr.2021.114057

21. Ma, J., Hiratsuka, T., Etoh, T., Akada, J., Fujishima, H., Shiraishi, N., ... & Inomata, M. (2018). Anti-proliferation effect of blue light-emitting diodes against antibiotic-resistant Helicobacter pylori. Journal of Gastroenterology and Hepatology, 33(8), 1492-1499. https://doi.org/10.1111/jgh.14066

22. Maćkiw, E., Stasiak, M., Kowalska, J., Kucharek, K., Korsak, D., & Postupolski, J. (2020). Occurrence and characteristics of Listeria monocytogenes in ready-to-eat meat products in Poland. Journal of food protection, 83(6), 1002-1009.

23. Moawad, A. A., Hotzel, H., Awad, O., Tomaso, H., Neubauer, H., Hafez, H. M., & El-Adawy, H. (2017). Occurrence of Salmonella enterica and Escherichia coli in raw chicken and beef meat in northern Egypt and dissemination of their antibiotic resistance markers. Gut pathogens, 9(1), 57.

24. Nikinmaa, S., Alapulli, H., Auvinen, P., Vaara, M., Rantala, J., Kankuri, E., ... & Pätilä, T. (2020). Dual-light photodynamic therapy administered daily provides a sustained antibacterial effect on biofilm and prevents Streptococcus mutans adaptation. PloS one, 15(5), e0232775.

25. Perreten, V., Schwarz, F., Cresta, L., Boeglin, M., Dasen, G., & Teuber, M. (1997). Antibiotic resistance spread in food. Nature, 389(6653), 801-802.

26. Pieranski, M., Sitkiewicz, I., & Grinholc, M. (2020). Increased photoinactivation stress tolerance of Streptococcus agalactiae upon consecutive sublethal phototreatments. Free Radical Biology and Medicine, 160, 657-669.

27. Rapacka-Zdonczyk, A., Wozniak, A., Pieranski, M., Woziwodzka, A., Bielawski, K. P., & Grinholc, M. (2019). Development of Staphylococcus aureus tolerance to antimicrobial photodynamic inactivation and antimicrobial blue light upon sub-lethal treatment. Scientific Reports, 9(1), 9423.

28. Rapacka-Zdonczyk, A., Wozniak, A., Kruszewska, B., Waleron, K., & Grinholc, M. (2021). Can gram-negative bacteria develop resistance to antimicrobial blue light treatment?. International Journal of Molecular Sciences, 22(21), 11579.

29. Rozman, U., Kranjec, K., Šeruga, A., Kramar, U., Vrbnjak, D., Lavrič, M., & Turk, S. Š. (2025). Impact of the COVID-19 pandemic on the consumption of antibiotics and the emergence of AMR: case study in a general hospital. Frontiers in Public Health, 13, 1584574.

30. Russell, C. D., Fairfield, C. J., Drake, T. M., Turtle, L., Seaton, R. A., Wootton, D. G., ... & Shears, R. K. (2021). Co-infections, secondary infections, and antimicrobial use in patients hospitalised with COVID-19 during the first pandemic wave from the ISARIC WHO CCP-UK study: a multicentre, prospective cohort study. The Lancet Microbe, 2(8), e354-e365.

31. Sołtysiuk, M., Przyborowska, P., Wiszniewska-Łaszczych, A. et al. Prevalence and antimicrobial resistance profile of Listeria spp. isolated from raw fish. BMC Vet Res 21, 333 (2025).

32. Wainwright, M., „Photodynamic antimicrobial chemotherapy (PACT)", J. Antimicrob. Chemother., t. 42, nr 1, ss. 13–28, 1998, doi: 10.1093/jac/42.1.13.

33. Wainwright, M., Maisch, T., Nonell, S., Plaetzer, K., Almeida, A., Tegos, G. P., & Hamblin, M. R. (2017). Photoantimicrobials—are we afraid of the light?. The Lancet Infectious Diseases, 17(2), e49-e55.

34. Wang, Y., Wang, Y., Wang, Y., Murray, C. K., Hamblin, M. R., Hooper, D. C., & Dai, T. (2017). Antimicrobial blue light inactivation of pathogenic microbes: State of the art. Drug Resistance Updates, 33, 1-22.

35. WHO (2025) Global antibiotic resistance surveillance report 2025: WHO Global Antimicrobial Resistance and Use Surveillance System (GLASS). Geneva: World Health Organization; 2025. Licence: CC BY-NC-SA 3.0 IGO.